

APPLICATION OF PLANT GROWTH PROMOTING RHIZOBACTERIA FOR THE IMPROVEMENT OF AGRICULTURAL PRODUCTIVITY



Claudia Petrillo

Dottorato in Biotecnologie
XXXIV ciclo



Università di Napoli Federico II



APPLICATION OF PLANT-GROWTH- PROMOTING RHIZOBACTERIA FOR THE IMPROVEMENT OF AGRICULTURAL PRODUCTIVITY

Claudia Petrillo

Dottorando: Claudia Petrillo

Relatore: Prof. Rachele Isticato

Coordinatore: Prof. Marco Moracci

Settore Scientifico Disciplinare BIO/19



INDEX

SUMMARY	8
RIASSUNTO	9
1. CHAPTER I – INTRODUCTION	12
1.1 Plant Growth Promoting Bacteria	13
1.2 Mode of action of PGPB	14
1.2.1 Direct plant growth mechanisms	14
1.2.1.1 Phosphate solubilization	14
1.2.1.2 Phytohormones production	15
1.2.1.3 Iron acquisition	16
1.2.1.4 Biological nitrogen fixation	16
1.2.2 Indirect plant growth mechanisms	16
1.2.2.1 Antibiotic synthesis	16
1.2.2.2 Production of cell wall degrading enzymes	17
1.3 Spore-forming PGPB as promising “plant probiotics”	17
1.4 <i>B. subtilis</i> sporulation	17
1.4.1 Morphological stages	18
1.4.2 Spore structure	19
1.5 The spore-based display system: a powerful biotechnological tool	20
1.5.1 Surface display on recombinant <i>B. subtilis</i> spores	22
1.5.2 Surface display on non-recombinant spores	22
1.5.3 Spores’ physicochemical properties	23
1.6 <i>Bacillus</i> spore as a platform to display molecules of agro-industrial interest	24
1.7 References	25

Part I - The spore-forming PGPB's potential in the agricultural field	32
CHAPTER II - Genomic and Physiological Characterization of <i>Bacilli</i> Isolated From Salt-Pans With Plant Growth Promoting Features	33
CHAPTER III - Plant Growth Promotion Function of <i>Bacillus</i> sp. Strains Isolated from Salt-Pan Rhizosphere and Their Biocontrol Potential against <i>Macrophomina phaseolina</i>	48
CHAPTER IV - Microbial consortia as a strategy to reduce drought stress in <i>Spinacia oleracea</i>	66
4.1 Abstract	66
4.2 Introduction	67
4.3 Materials and methods	68
4.3.1 Bacterial strains and growth conditions	68
4.3.2 Phenotypic characterization and growth conditions	69
4.3.3 Bioassays for PGP traits	69
4.3.3.1 Biofilm Production and Swarming Motility	69
4.3.3.2 Phosphate Solubilization	70
4.3.3.3 Indole-acetic Acid (IAA) Detection	70
4.3.3.4 Ammonia Production	70
4.3.3.5 Siderophores Production	71
4.3.3.6 Biosurfactants Production	71
4.3.3.7 Screening for hydrolytic enzymatic activity	71
4.3.4 Evaluation of potential biocontrol activity	72
4.3.5 Germination assay	73
4.3.6 Adhesion assay	73
4.3.7 Microbial compatibility <i>in vitro</i>	73

4.3.8 Statistical Analysis	74
4.4 Results and discussion	74
4.4.1 <i>In vitro</i> characterization of potential PGPB	74
4.4.2 Characterization of PGP traits under drought stress condition	76
4.4.3 Antagonistic Activity against <i>Spinacia oleracea</i> phytopathogens	76
4.4.4 Effects of seed-biopriming on <i>S. oleracea</i> germination <i>in vitro</i>	77
4.4.5 Effects of bacterial consortia on <i>S. oleracea</i> germination <i>in vitro</i>	79
4.5 Conclusions	80
4.6 Supplemental materials	82
4.7 Acknowledgements	82
4.8 Reference	83
CHAPTER V - <i>Myxococcus xanthus</i>' Frz chemosensory system	89
5.1 A potential PGPB: <i>M. xanthus</i>	89
5.2 Frz chemosensory system	90
5.3 HAMP domains	92
5.3.1 Role of the Frz HAMP domains in cluster formation	93
5.3.2 Role of the DNA Binding domain in cluster formation	93
5.4 Materials and methods	94
5.4.1 Bacterial Strains, Plasmids, and Growth	94
5.4.2 Proteins expression and purification	95
5.5 References	95
Part II The spore-based display system: a powerful biotechnological tool	98

CHAPTER VI - <i>Bacillus subtilis</i> builds structurally and functionally different spores in response to the temperature of growth	99
CHAPTER VII - The temperature of growth and sporulation modulates the efficiency of spore-display in <i>Bacillus subtilis</i>	111
Other collaborations	121
CHAPTER VIII - The power of two: An artificial microbial consortium for the conversion of inulin into Polyhydroxyalkanoates	122
CHAPTER IX – GENERAL CONCLUSIONS	131
<u>Appendix I</u> - Publications and Authors' Contributions	135
<u>Appendix II</u> - Participation to Congresses	139
<u>Appendix III</u> - Experiences in industry and foreign laboratories	140

SUMMARY

The dramatically growing world population has led to a considerable increase in the global demand for agricultural products: it is estimated that to meet worldwide food demand, food production must be doubled by 2050. This demand, together with the evidence that approximately half of the soil used for agricultural purposes is moderately or severely affected by degradation phenomena, such as erosion, salification, drought, acidification, or compaction, has pushed farmers towards an intensive agricultural practice. For instance, the use of chemical fertilizers and pesticides is exponentially increased over the last decades. Unfortunately, the continuous abuse is negatively impacting the well-being of man and the environment. Therefore, the great challenge is to develop an agro-industrial system that is committed to encouraging sustainable and eco-friendly strategies. One of the best approaches is the use of the phytomicrobiome, the so-called Plant-Growth-Promoting Bacteria (PGPB), beneficial soil microorganisms able to promote the well-being of plants through direct and/or indirect mechanisms, including nitrogen fixation, the solubilization of phosphate, the production of phytohormones, the mineralization of soil organic matter, as well as the inhibition of phytopathogens. However, to fully benefit from the action of PGPB, it is necessary to deeply understand the mechanisms through which they act, and to enhance them. In this framework fits my PhD Thesis, which aims at isolating, identifying, and characterizing -through the combination of *in vitro* and *in silico* techniques- new promising spore-forming PGPB to be exploited in the agricultural field. Their application in the form of consortia or functionalized spores has been investigated.

RIASSUNTO

L'incessante crescita della popolazione umana degli ultimi decenni ha comportato un notevole incremento della domanda di cibo a livello globale, che per poter essere soddisfatta necessita il raddoppio della produzione agricola entro il 2050. Questo, insieme all'evidenza che circa la metà del suolo utilizzato a scopo agricolo è moderatamente o gravemente affetto da degradazione dovuta a fenomeni quali erosione, salificazione, siccità, acidificazione, contaminazione o compattamento, ha spinto gli agricoltori verso una pratica di tipo intensivo basata sull'uso di elevate quantità di fertilizzanti e pesticidi chimici noti per essere dannosi per il benessere dell'uomo e dell'ambiente; infatti, non solo essi sono capaci di bio-accumularsi all'interno della catena alimentare, ma pongono anche a rischio gli insetti benefici e il microbiota che popolano il suolo, alterandone la fertilità e l'acidità. La grande sfida attuale è, dunque, sviluppare un sistema agro-industriale che si impegni a incentivare strategie sostenibili per limitare i danni ambientali, economici e sociali legati all'attuale pratica dell'agricoltura intensiva. Una delle strategie più accreditate è l'utilizzo del fitomicrobioma, in particolare dei cosiddetti *Plant-Growth-Promoting Bacteria* (PGPB), microrganismi benefici del suolo in grado di promuovere il benessere delle piante attraverso meccanismi diretti e/o indiretti, come la fissazione dell'azoto, la solubilizzazione del fosfato, la produzione di fitormoni, la mineralizzazione della materia organica, e ancora l'inibizione dei fitopatogeni. Per beneficiare al massimo dell'azione dei PGPB, è tuttavia necessario comprendere a fondo i meccanismi attraverso i quali essi agiscono, ed eventualmente potenziarli. All'interno di questo contesto si inserisce la mia Tesi di Dottorato, che attraverso l'integrazione di tecniche *in vitro* e *in silico*, mira a isolare, identificare e caratterizzare nuovi promettenti PGPB sporigeni da poter sfruttare sottoforma di consorzi o spore funzionalizzate. Il mio progetto di Tesi si suddivide in due parti principali.

Nella **Parte I** verranno descritti l'isolamento, l'identificazione e la caratterizzazione (*in vitro* e *in silico*) di batteri sporigeni del suolo prelevati da ambienti estremi quali le saline (**Capitolo II, III**). È noto, infatti, che l'elevata concentrazione di NaCl del suolo sia uno dei principali fattori limitanti la crescita delle piante: l'utilizzo di PGPB resistenti a tali condizioni di stress, favorirebbe certamente la crescita

delle stesse. In aggiunta, l'impiego di microorganismi in grado di produrre spore, come quelli appartenenti al genere *Bacillus*, gioverebbe ulteriormente a tale scopo. Le spore, infatti, recano diversi vantaggi utili sia per l'applicazione in campo, che per la produzione su scala industriale, poichè: i) la loro particolare struttura le rende resistenti a condizioni avverse come elevate temperature, stress meccanici e chimici; ii) sono sicure per l'uomo e l'ambiente; iii) possono essere conservate per lunghi periodi, facilitando la formulazione, la conservazione e il trasporto di eventuali prodotti commerciali; iv) la loro produzione è semplice ed economica. Alcuni dei microorganismi isolati hanno mostrato una notevole attività antifungina (**Capitolo III**). In particolare, il ceppo *B. vallismortis* RHFS10 è stato selezionato per la spiccata capacità di inibire la crescita del fitopatogeno della soia *Macrophomina phaseolina*. L'attività esibita *in vitro* è stata indagata e in parte attribuita a metaboliti secondari parzialmente purificati con tecniche di chimica analitica e identificati mediante spettrometria di massa. Nel **Capitolo IV**, in collaborazione con la ditta Agriges s.r.l., è stata eseguita una caratterizzazione preliminare di due *Bacilli* isolati dalle saline, *B. amyloliquefaciens* RHF6 e *B. vallismortis* RHFS10, e di alcuni ceppi della stessa ditta, in condizioni di stress da siccità. Lo scopo era quello di creare dei consorzi di PGPB capaci di alleviare *in vitro* lo stress idrico su piante di spinacio (*Spinacia oleracea*), scelto come organismo modello. I primi dati raccolti hanno evidenziato come il trattamento preliminare dei semi con alcuni dei ceppi utilizzati, e il loro rispettivo consorzio, abbia portato a miglioramenti della velocità e dell'efficienza di germinazione, e anche della lunghezza delle radichette primarie dei germogli, in condizioni standard. Il progetto è stato purtroppo rallentato dalla pandemia di Covid-19. Sarà necessario proseguire con le indagini per verificare che la capacità del migliore consorzio in condizioni standard, sia confermata anche in condizioni di stress idrico.

Il **Capitolo V** riporta la mia esperienza presso il “*Laboratoire de Chimie Bacterienne*” del CNRS di Marsiglia (Francia). In questa occasione ho imparato a coltivare e manipolare geneticamente il batterio Gram negativo del suolo *Myxococcus xanthus*, capace di formare corpi fruttiferi contenenti myxospore resistenti a condizioni estreme come l'essiccazione, le elevate temperature e l'irradiazione UV. I myxobatteri comprendono diverse specie di micropredatori di molti patogeni delle

piante; per questo motivo, il loro utilizzo come potenziali PGPB ha ricevuto recentemente una discreta attenzione. In questo periodo mi sono occupata dello studio del sistema chemotattico Frz o “frizzy”, che controlla la frequenza con la quale le cellule cambiano direzione per riorientarsi nell’ambiente su superfici solide.

La **Parte II** di questa Tesi si incentra sul sistema di *display* basato su spore di *B. subtilis*, come organismo modello. Esso, impiegato sia in forma ricombinante che non ricombinante, sfrutta tutte le caratteristiche vantaggiose delle spore precedentemente menzionate, e rappresenta un interessante strumento biotecnologico per la veicolazione di molecole eterologhe in diversi campi. In questa sezione sarà descritto come si è migliorata l’efficienza di *display*, sfruttando la temperatura di produzione delle spore (**Capitolo VII**). Infatti, è stato recentemente dimostrato che la struttura superficiale della spora di *B. subtilis*, principalmente coinvolta nel processo di *display*, cambia in relazione alla temperatura di sporulazione (**Capitolo VI**). L’idea proposta è quella di impiegare PGPB sporigeni come matrice per esporre molecole bioattive utilizzate in sostituzione di agenti chimici per la fertilità del suolo o per la protezione da fitopatogeni. In tal modo la produzione agricola beneficerebbe non solo della naturale azione dei PGPB, ma anche delle molecole che essi trasportano sulla loro superficie.

Nella sezione “**Altre collaborazioni**” è descritto il processo attraverso cui è stato sviluppato un consorzio batterico col fine di produrre bioplastiche nella forma di Polioidrossialcanoati (PHA), a partire da materiale di scarto agro-industriale, nel dettaglio l’inulina (**Capitolo VIII**), un polisaccaride di fruttosio di cui sono ricche le radici di molte piante, come il cardo o il carciofo, che spesso rappresentano uno scarto del processo industriale.

INTRODUCTION

CHAPTER I

1.1 Plant Growth Promoting Bacteria

In the past decades global population has been rising like never, reaching a value three times bigger than ever in human history. It has been estimated that by 2050, human population will grow up to 9 billion (Food and Agriculture Organization of the United Nations, 2017). To satisfy the rising food demand, farmers increased crop yields using massive amounts of chemical fertilizers and pesticides, which led to several negative consequences as the formation of stable phytopathogenic variants, the reduction of beneficial microorganisms, and the accumulation of toxic substances in the environment (Reddy et al., 2009; Pertot et al., 2017). Thus, researchers and industries are seeking more sustainable approaches to pesticides and fertilizers (Glick et al., 2007). A “green” alternative is the use of biofertilizers and biopesticides, usually defined as “substances containing living microorganisms, that when applied to the seed, the plant surface, or the soil, are able to colonize the rhizosphere and the plant, promoting the growth of the host by increasing the availability of primary nutrients or by inhibiting phytopathogens’ spread” (Vessey, 2003; Riaz et al., 2021). These microorganisms, capable of enhancing plant growth and protection from pests, are generally referred to as Plant Growth Promoting Bacteria (PGPB) (Fig. 1). Some of the most representative PGPB include *Azotobacter*, *Azospirillum*, *Acinetobacter*, *Agrobacterium*, *Arthrobacter*, *Bacillus*, *Burkholderia*, *Pseudomonas*, *Serratia*, *Streptomyces*, *Rhizobium*, *Bradyrhizobium*, *Mesorhizobium*, *Frankia*, and *Thiobacillus* (Wani and Gopalakrishnan, 2019).

To properly use PGPB in the “Green Revolution”, it is important to understand the mechanisms through which they influence and guarantee sustainable agriculture.

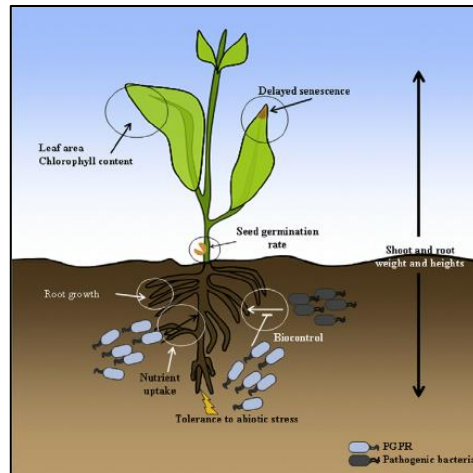


Figure 1 | Effects of PGPB on plant growth.

1.2 Mode of action of PGPB

The key role played by PGPB in plant growth enhancement is widely described (Vessey, 2003; Tilak et al., 2005). Beneficial microorganisms promote plant growth either directly or indirectly as shown in Fig. 2 (Swarnalakshmi et al., 2020). Direct methods include phosphorus solubilization; siderophore, and growth hormones production; nitrogen fixation (Fig. 2). These actions trigger morphological and physiological changes in plants, thus promoting plant growth. On the other hand, the indirect mechanisms comprise the production of low molecular weight compounds such as alcohols, ammonia, aldehydes, cyanogens, ketones, cell wall-degrading enzymes, and secondary bioactive metabolites with antagonistic traits and competition for nutrients (Fig.2) (Glick, 2012).

1.2.1 Direct plant growth mechanisms

1.2.1.1 Phosphate solubilization

Phosphorus (P) plays a key role in cell metabolism and signalling in plants (Vance et al., 2003). It can be present in the soil in an unavailable form bound with inorganic or organic molecules; in fact, only H_2PO_4^- and/or HPO_4^{2-} forms are usable by plants (Smyth et al., 2011).

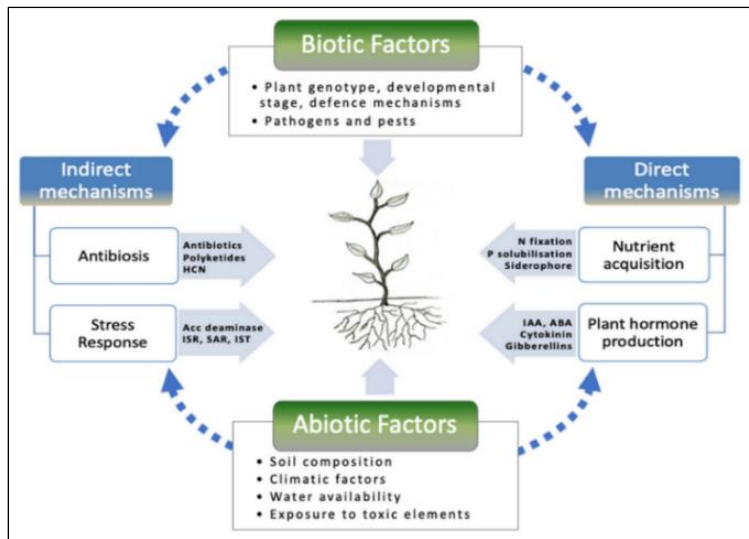


Figure 2 | Direct and indirect mechanisms of action exerted by PGPB.

Phosphate-solubilizing microorganisms can solubilize the phosphorous in free-living conditions and make it available to almost all types of crops. Some phosphorus-solubilizing bacterial genera are *Pseudomonas*, *Bacillus*, *Azotobacter*, *Agrobacterium*, *Rhizobium*, *Bradyrhizobium*, *Salmonella*, and *Thiobacillus* (Liu et al., 2012; Alori and Fawole, 2017). They mineralize phosphorus by several enzymes such as acid phosphatases, C-P lyase, D- α -glycerophosphate, phosphor hydrolases, phosphonoacetate hydrolase, and phytase (Gügi et al., 1991; Abd-Alla, 1994; Glick, 2012).

1.2.1.2 Phytohormones Production

Phytohormones are signal molecules produced by plants in a very low quantity, involved in the enhancement of growth, development, differentiation of cells, and in many other processes. They are also indirectly implicated in providing defence against pathogens and abiotic stresses such as salt stress, temperature, and drought (Egamberdieva et al., 2017). It has been demonstrated that PGPB in soil are capable of producing many hormones like auxins, gibberellins, cytokinins, ethylene and jasmonates involved in stimulating the division, elongation, and differentiation of cells (Bhardwaj et al., 2014), promoting seed germination, elongation of the stem, and flowering and also in

increasing the photosynthetic rate in plants (Khan et al., 2021). PGPB genera connected to the production of phytohormones are *Rhizobium*, *Herbaspirillum*, *Bacillus*, *Mesorhizobium*, *Pantoea*, *Arthrobacter*, *Pseudomonas*, *Bradyrhizobium*, *Rahnella*, *Enterobacter*, *Brevundimonas*, and *Burkholderia* (Orozco-Mosqueda et al., 2021).

1.2.1.3 Iron acquisition

Iron is another important nutritional element for plants' growth, used as a cofactor for proteins involved in metabolic processes such as respiration and photosynthesis. On earth, iron is mostly present in the ferric ionic form, not easily accessible for living beings (Ammari and Mengel, 2006). Nature has developed many strategies to cope with this issue: microbial siderophores is one of them. Siderophores are tiny peptides showing side chains and functional groups able to bind to ferric ions with high affinity (Moynié et al., 2019). Besides the biofertilizer activity, siderophores production is also implicated in biocontrol activity by depriving the pathogen from iron nutrition, as reported by several researchers (Kumar et al., 2017).

1.2.1.4 Biological nitrogen fixation

Nitrogen is necessary for the synthesis of amino acids, nucleotides, and mineral nutrients. However, as told for P and Fe, it is mostly available in the inaccessible form of N_2 , which both animals and plants cannot use (Petar and Normand, 2009). Impressively, many microorganisms, known as biological nitrogen-fixing bacteria (BNF), can help overcoming nitrogen deficiency. Indeed, they are able to fix the N_2 into available forms of nitrogen by utilizing energy in the form of ATP and convert it into nitrite, nitrate, and ammonia, which plants can easily assume (Soumare et al., 2020).

1.2.2 Indirect plant growth mechanisms

1.2.2.1 Antibiotic synthesis

Antibiotics are low molecular weight molecules generally produced as secondary metabolites by soil microorganisms, exhibiting biocidal or biostatic, target-specific activity on phytopathogens (Olanrewaju et al., 2017). For instance, *Bacillus spp.* are reported to produce many

antibiotics such as bacilysin, iturin, subtilosin, fengycin, bacillaene, phenazine-1-carboxylic acid, zwittermicin A, rhamnolipids, pyrrolnitrin, oomycin A etc. (Kundan et al., 2015). *P. aeruginosa* also produces phenazine, that damages lipids within the membrane of their targets, and also obstruct the electron transport in pathogens (Haas and Défago, 2005).

1.2.2.2 Production of cell wall degrading enzymes

Many PGPB are known to produce and release hydrolytic enzymes (e.g., proteases, cellulases, chitinase, lipases, xylanases, etc.) capable of degrading the cell wall of other organisms, such as pathogens, or other bacterial competitors in the soil, by changing their structural integrity, and in the end preventing their growth (Singh and Jha, 2017).

1.3 Spore-forming PGPB as promising “plant probiotics”

Among all the known PGPB genera, particular attention has been recently given to the spore-forming microorganisms as *Bacillus spp.*, that besides showing the general PGP features described above, exhibit a pool of unique traits that put them ahead. First, of great interest is their resistance to harsh environments and conditions, due to their capacity of producing spores that can survive at high temperatures and dehydration, thus making the formulation of a potential commercial product easier (Pesce et al., 2014). Moreover, they are efficient producers of a broad spectrum of secondary metabolites, can be easily genetically manipulated, and present a great ability to colonize plant surfaces (Kumar et al., 2011). The model of Gram-positive spore-forming bacteria certainly is *Bacillus subtilis*.

1.4 *B. subtilis* sporulation

B. subtilis is ubiquitous in nature and can effectively adapt to the changes of the environmental conditions (Tan and Ramamurthi, 2014), through many survival mechanisms like motility, competence, biofilm formation, or sporulation (Mirouze and Dubnau, 2013). The latter brings to the formation of an endospore, a quiescent cell highly resistant to starvation, high temperatures, ionizing radiations, mechanical abrasion,

chemical solvents, hydrolytic enzymes, desiccation, extreme pH, and antibiotics (Nicholson et al., 2000).

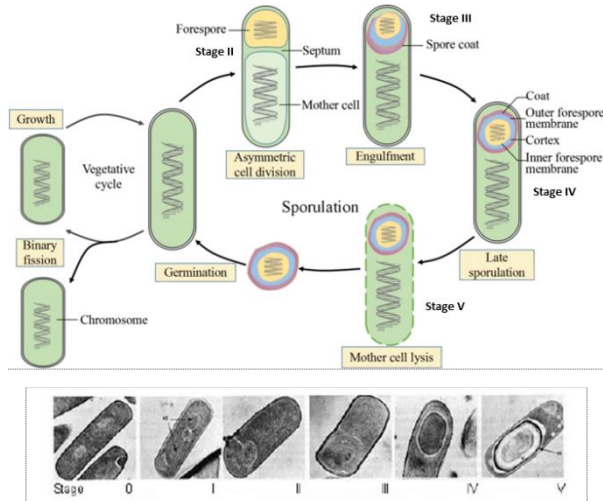


Figure 3 | The key stages of the sporulation cycle in *B. subtilis* (Lin et al., 2020). The inset shows electron micrographs of sporulating cells at each of the major stages.

Bacillus’ sporulation is a genetically highly controlled process that involves many morphological, biochemical, and physiological changes, leading to the development of two different, but genetically identical cells (Fig. 3): the mother cell and the forespore. This is possible due to different gene expression programs.

1.4.1 Morphological stages

The first morphological change of the sporulation process is the formation of a polar septum which forms two asymmetric compartments: the mother cell and the forespore (Fig. 3). The first one will nurture the spore until its development completes, and by the end of the process releases the mature spore by its own lysis. After the asymmetric cell division, the sporulation gene expression program splits and two distinct programs activate, one in each of the resulting cellular compartments. Soon after, the septum membrane migrates around the forespore, which after the completion of the process becomes a double membrane-bound structure, as a result of the engulfment process (Fig. 3). A series of protective layers are then synthesized in the mother cell

cytoplasm and assembled around the forming spore (Fig. 3, 4). The cortex is a modified peptidoglycan layer chemically different from that of the vegetative cells, deposited between the two membranes surrounding the forespore (Henriques and Moran, 2007). Meanwhile, the proteinaceous coat is deposited around the outer membrane. Two main coat layers can be observed by electron microscope analysis: a darkly stained outer coat, and a more lightly stained lamellar inner coat (Fig. 4). A third coat layer surrounds the spore: the *crust*, a glycoprotein layer composed of six proteins, whose architecture has not been cleared up yet (Bartels et al., 2019). The innermost part of the spore is the core which contains a partially dehydrated cytoplasm with a condensed and inactive chromosome (Fig. 4). The last stage of the sporulation process is the lysis of the mother cell, which releases the mature spore in the environment, where it can survive for a long time, continuously monitoring the environment, and waiting for the establishment of new favourable conditions. When this occurs, the spore can return to a vegetative state through the germination process (Fig. 3), which implies the spore core rehydration and the cracking of the spore protective layers, which will eventually release the nascent cell (Higgins and Dworkin, 2012).

1.4.2 Spore structure

As previously described, *B. subtilis* spore is made of a core surrounded by several protective layers: the inner membrane, the cortex, the outer membrane, and the coat (Fig.4). The core is the central part of the spore. It contains the spore cytoplasm with all the cellular components, such as cytoplasmic proteins, ribosomes, and DNA associated with a large amount of Small Acid Soluble Proteins (SASPs) which protect the DNA against many types of damage. The partially dehydrated core plays an important role in spore longevity, dormancy, and resistance (Setlow, 1994). The core is surrounded by the inner membrane, which exposes the germination receptors, and in turn is surrounded by the cortex, a modified peptidoglycan layer. The cortex is significant for the maintenance of spore core dehydration, resistance, and dormancy. The outer membrane, the second layer deriving from the engulfment process, has opposite polarity compared to the inner membrane. Finally, the outermost spore structure is the coat, mainly involved in spore resistance and germination, which apparently possesses

enzymatic functions that may permit interactions with other organisms in the environment.

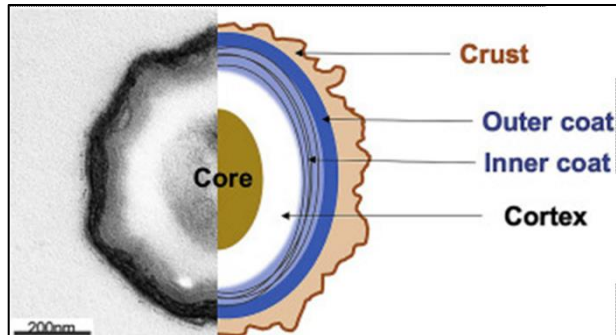


Figure 4 | *B. subtilis* spore structure. Left half, a micrograph taken by Transmission Electronic Microscopy (TEM).

The spore coat layer is an intricate web made of more than 80 proteins (Fig. 5), which are synthesized in the mother cell cytoplasm, and gradually moved to the forespore surface (Krajčiková et al., 2017) where are organized into three distinct layers: the inner coat, the outer coat, and the crust (Fig. 4). Out of the 80 coat proteins, the Cot proteins, identified so far, at least 20 have shown an enzymatic function: some of them guide the correct assembly of other coat components, by catalysing post-translational modifications; some others are involved in spore protection and germination.

1.5 The spore-based display system: a powerful biotechnological tool

The unique spore structure allowed to develop an innovative surface display system to vehicle heterologous proteins (Isticato et al., 2001). Surface display systems aimed at exhibiting biologically active molecules on phages, yeast, bacteria, or synthetic particles have been developed for environmental and biomedical purposes such as vaccine development, bioabsorbants, biocatalysts, and biosensors (Gouy et al., 2010; Chen et al., 2019).

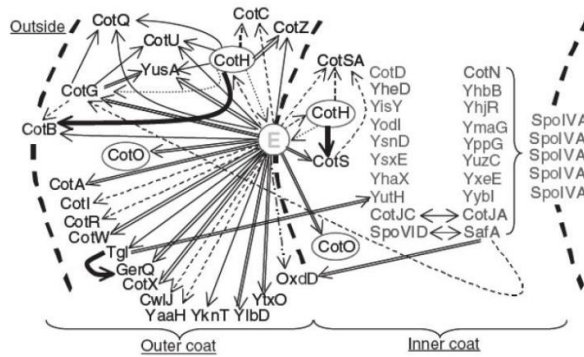


Figure 5 | Model of the coat protein interaction network (Kim et al., 2006).

Despite the promising results obtained, these technologies were not considered suitable for harsh industrial processes, especially for exposing enzymes sensitive to such conditions (Guoyan et al., 2019). In this framework, the proposal of bacterial spores as novel platforms for the display of heterologous antigens or enzymes looked like the answer (Isticato et al., 2001): the ability of bacterial spores to survive extreme environments and retain the capacity to sporulate and germinate make them suitable candidates for surface display technology (Isticato and Ricca, 2014; Isticato et al., 2020)). *B. subtilis* is the most used among the spore-forming bacterial species, due to its many advantages: it is classified as generally recognized as safe (GRAS), has poor nutritional requirements, and is considered the Gram-positive bacterial model (Chen et al., 2019). Moreover, a lot is known about its structure and physiology, indeed, among bacteria, the study of its genetic background is second only to *Escherichia coli* (Kunst et al., 1997). To expose heterologous proteins on the spore surface, two strategies have been developed (Fig. 6). Both exhibit many advantages over cell- or phage-based systems: the stability, safety, and amenability to laboratory manipulations of spores of several bacterial species, together with the lack of some constraints limiting the use of other systems. All of this makes the spore a highly efficient platform to display heterologous proteins.

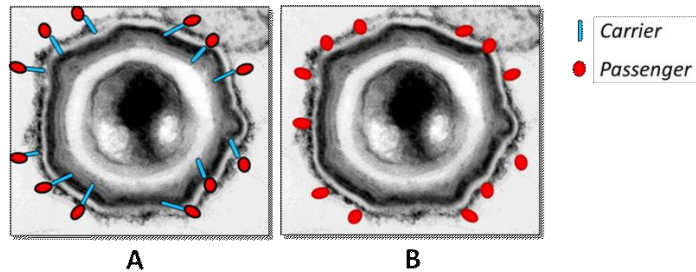


Figure 6 | Spore display system recombinant (A) and non-recombinant (B) approaches.

1.5.1 Surface display on recombinant *B. subtilis* spores

The extremely resistant structure of the spore coat clearly suggests the possibility of using its components as anchoring motifs for the expression of heterologous polypeptides on the spore surface. A genetic system to manipulate the coat of *B. subtilis* spores has been developed (Fig. 7A) (Isticato et al., 2001). The spore-based approach provides several advantages over other display systems, such as high stability even after prolonged storage, the possibility to display large multimeric proteins and the safety for human use. Attempts to expose heterologous proteins on the spore surface were focused mainly on CotB protein, selected for the surface location (Isticato et al., 2001), CotC and CotG, for the high relative abundance in spore coat layer (Mauriello et al., 2004).

1.5.2 Surface display on non-recombinant spores

The recombinant spore-based display system implies the genetic engineering of the host. This is a major drawback when the application of the display system is intended for the release into the environment of the recombinant host or is thought for human or animal use.

Serious concerns over the release of genetically modified microorganisms (GMOs) into nature, and their clearance from the host following oral delivery have been raised (Detmer and Glenting, 2006).

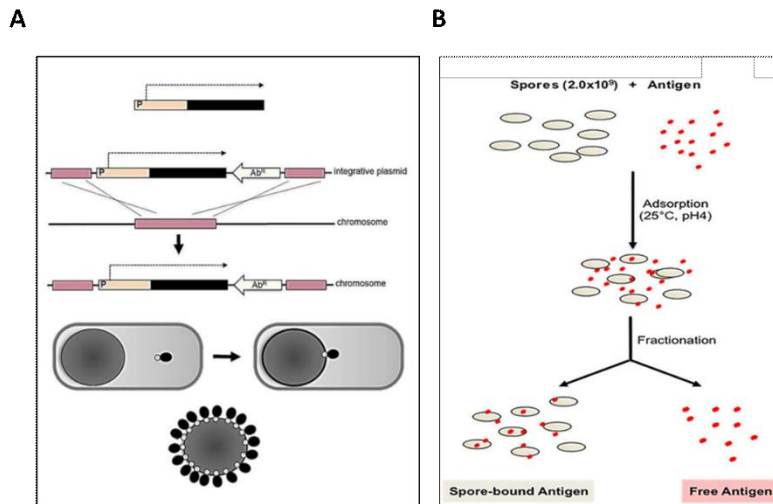


Figure 7 | A) *B. subtilis* coat engineering process in the recombinant display system approach; **B)** Schematic representation of a typical adsorption experiment. Purified spores were mixed with the purified antigen in 1X PBS buffer (pH 4.0) and incubated one hour at 25 °C. The sample mix was fractionated by centrifugation and fractions assayed independently.

To overcome this issue, a non-recombinant approach to expose heterologous proteins on the spore surface has been recently proposed (Fig. 7B). It has been demonstrated that adsorbed spores were shown able to induce specific and protective immune responses in mice immunized mucosally (Huang et al., 2010). Spore adsorption resulted more efficient when the pH of the binding buffer was acidic (pH 4) and less efficient or totally inhibited at pH values of 7 or 10 (Huang et al., 2010). Electrostatic and hydrophobic interactions between spores and antigen were suggested to drive the adsorption that was shown to be not dependent on specific spore coat components but rather due to the negatively charged and hydrophobic surface of the spore (Huang et al., 2010). In addition, the same study showed that killed or inactivated spores were equally effective as live spores in adsorbing the various antigens (Huang et al., 2010).

1.5.3 Spores' physicochemical properties

The spore surface' physicochemical properties have been addressed in different studies with different approaches. A first study showed that

spores of *B. subtilis* are negatively charged by time-resolved micropotentiometry (Kazakov et al., 2008). It has been shown that in an aqueous environment, spores behave like an almost infinite ionic reservoir and are able of accumulating billions of protons (approximately 2×10^{10} per spore) (Kazakov et al., 2008). The carboxyl groups were recognized as the main ionizable groups in the spore and according with the diffusion time analysis, it was found that proton diffusion is much lower in the spore core than within the coat and cortex (Kazakov et al., 2008). This implies the inner membrane to probably be a major permeability barrier for protons (Kazakov et al., 2008). The electrostatic forces' role in spore adhesion to a planar surface has been also addressed by studying spores of *B. thuringiensis* (Chung et al., 2010). By using combined atomic force microscopy (AFM)-scanning surface potential microscopy technique, the surface potentials of a spore and a mica surface were experimentally obtained (Chung et al., 2010): the surface charge density of the spores was estimated at $0.03 \mu\text{C}/\text{cm}^2$ at 20 % relative humidity and decreased with increasing humidity. The electrostatic force can be an important component in the adhesion between the spore and a planar surface (Chung et al., 2010).

1.6 *Bacillus* spore as a platform to display molecules of agro-industrial interest

One of the emerging application fields of the spore-display system is that of sustainable agriculture (Rostami et al., 2017). Replacing the current soil management strategies, mainly dependent on inorganic chemical-based fertilizers, and causing serious threats to human health and the environment, is a matter of main importance (Castaldi et al., 2021; Petrillo et al., 2021). To face two main problems obstructing plant growth, as the availability of nutrients and the defense against phytopathogens, the spore-based display system could represent a “green” answer.

B. subtilis spores are considered as safe live biocompatible carriers of bioactive molecules in soil that benefit from some advantages like low cost, safety, stability, easy preparation, and high resistance to harsh conditions. Applied to the field of our concern, microbial spores could be coated with molecules of agro-industrial interest. Agricultural enzymes, for example, are bioactive proteins used instead

of chemicals for food production and protection (Agricultural Enzymes Market Size, Share | Global Industry Report, 2022-2025). Unfortunately, these molecules are often unstable or easily degraded when in the agricultural environment. Active biomolecules stably carried on the spore surface, could be shielded from the external environmental conditions. Indeed, the advantage of this approach lies in the protection that the outermost layers of the spore structure offer to the heterologous molecules exposed (Sirec et al., 2012). Furthermore, a recent study has shown that proteins displayed by the non-recombinant approach are not exposed on the spore surface but rather localized at the level of the inner coat (Donadio et al., 2016). This internal localization probably contributes to the protection of the heterologous protein without interfering with its biological activity (Donadio et al., 2016). For this purpose, the adsorption of active biomolecules on the spore surface, could represent a reasonable eco-friendly solution. The chitinase ChiS from *B. pumilus* was successfully expressed on the spores of *B. subtilis* using CotG as a carrier protein by Rostami et al. (2017). The enzyme conserved its full activity and was able to efficiently inhibit the growth of the fungal phytopathogens *Rhizoctonia solani* and *Trichoderma harzianum*. On this path, many more enzymes like proteases, phosphatases, dehydrogenases, etc., could benefit from the spore display protection, and being efficiently applied to the agricultural field. The innovative idea this Thesis aims to shed the light on is the use of spore-forming PGPB as a matrix to expose agro-industrial molecules (functionalized PGPB). By doing so, crops would benefit not only from the natural action of PGPB, but also from the bioactive molecules brought upon their surface. Hence, as a powerful tool, *Bacillus* spore-based display system conceivably offers broad possibilities in its future.

1.7 References

Abd-Alla, M. h. (1994). Phosphatases and the utilization of organic phosphorus by *Rhizobium leguminosarum* biovar viceae. *Letters in Applied Microbiology* 18, 294–296. doi:10.1111/j.1472-765X.1994.tb00873.x.

Agricultural Enzymes Market Size, Share | Global Industry Report, 2022-2025 Available at: <https://www.grandviewresearch.com/industry-analysis/agricultural-enzymes-market> [Accessed November 29, 2021].

Alori, E. T., and Fawole, O. B. (2017). "Microbial Inoculants-Assisted Phytoremediation for Sustainable Soil Management," in *Phytoremediation: Management of Environmental Contaminants, Volume 5*, eds. A. A. Ansari, S. S. Gill, R. Gill, G. R. Lanza, and L. Newman (Cham: Springer International Publishing), 3–17. doi:10.1007/978-3-319-52381-1_1.

Ammari, T. G., and Mengel, K. (2006). Total soluble Fe in soil solutions of chemically different soils. doi:10.1016/J.GEODERMA.2006.06.013.

Bartels, J., Blüher, A., López Castellanos, S., Richter, M., Günther, M., and Mascher, T. (2019). The *Bacillus subtilis* endospore crust: protein interaction network, architecture and glycosylation state of a potential glycoprotein layer. *Mol Microbiol* 112, 1576–1592. doi:10.1111/mmi.14381.

Bhardwaj, D., Ansari, M. W., Sahoo, R. K., and Tuteja, N. (2014). Biofertilizers function as key player in sustainable agriculture by improving soil fertility, plant tolerance and crop productivity. *Microbial Cell Factories* 13, 66. doi:10.1186/1475-2859-13-66.

Castaldi, S., Petrillo, C., Donadio, G., Piazz, F. D., Cimmino, A., Masi, M., et al. (2021). Plant Growth Promotion Function of *Bacillus sp.* Strains Isolated from Salt-Pan Rhizosphere and Their Biocontrol Potential against *Macrophomina phaseolina*. *Int J Mol Sci* 22. doi:10.3390/ijms22073324.

Chen, T., Wang, K., Chi, X., Zhou, L., Li, J., Liu, L., et al. (2019). Construction of a bacterial surface display system based on outer membrane protein F. *Microbial Cell Factories* 18, 70. doi:10.1186/s12934-019-1120-2.

Detmer, A., and Glenting, J. (2006). Live bacterial vaccines--a review and identification of potential hazards. *Microb Cell Fact* 5, 23. doi:10.1186/1475-2859-5-23.

Donadio, G., Lanzilli, M., Sirec, T., Ricca, E., and Isticato, R. (2016). Localization of a red fluorescence protein adsorbed on wild type and mutant spores of *Bacillus subtilis*. *Microb Cell Fact* 15, 153. doi:10.1186/s12934-016-0551-2.

Egamberdieva, D., Wirth, S. J., Alqarawi, A. A., Abd_Allah, E. F., and Hashem, A. (2017). Phytohormones and Beneficial Microbes: Essential Components for Plants to Balance Stress and Fitness. *Frontiers in Microbiology* 8, 2104. doi:10.3389/fmicb.2017.02104.

Food and Agriculture Organization of the United Nations ed. (2017). *The future of food and agriculture: trends and challenges*. Rome: Food and Agriculture Organization of the United Nations.

- Glick, B. R. (2012). Plant growth-promoting bacteria: mechanisms and applications. *Scientifica (Cairo)* 2012, 963401. doi:10.6064/2012/963401.
- Glick, B. R., Cheng, Z., Czarny, J., and Duan, J. (2007). Promotion of plant growth by ACC deaminase-producing soil bacteria. *Eur J Plant Pathol* 119, 329–339. doi:10.1007/s10658-007-9162-4.
- Gouy, M., Guindon, S., and Gascuel, O. (2010). SeaView version 4: A multiplatform graphical user interface for sequence alignment and phylogenetic tree building. *Mol Biol Evol* 27, 221–224. doi:10.1093/molbev/msp259.
- Gügi, B., Orange, N., Hellio, F., Burini, J. F., Guillou, C., Leriche, F., et al. (1991). Effect of growth temperature on several exported enzyme activities in the psychrotrophic bacterium *Pseudomonas fluorescens*. *Journal of Bacteriology* 173, 3814–3820. doi:10.1128/jb.173.12.3814-3820.1991.
- Guoyan, Z., Yingfeng, A., Zayed, H. M., Qi, G., Yang, M., Jiao, Y., et al. (2019). *Bacillus subtilis* Spore Surface Display Technology: A Review of Its Development and Applications. 29, 179–190. doi:10.4014/jmb.1807.06066.
- Haas, D., and Défago, G. (2005). Haas D, Defago G.. Biological control of soil-borne pathogens by fluorescent *Pseudomonads*. *Nat Rev Microbiol* 3: 307–319. *Nature reviews. Microbiology* 3, 307–19. doi:10.1038/nrmicro1129.
- Henriques, A. O., and Moran, C. P. (2007). Structure, assembly, and function of the spore surface layers. *Annu Rev Microbiol* 61, 555–588. doi:10.1146/annurev.micro.61.080706.093224.
- Higgins, D., and Dworkin, J. (2012). Recent progress in *Bacillus subtilis* sporulation. *FEMS Microbiol Rev* 36, 131–148. doi:10.1111/j.1574-6976.2011.00310.x.
- Huang, J.-M., Hong, H. A., Van Tong, H., Hoang, T. H., Brisson, A., and Cutting, S. M. (2010). Mucosal delivery of antigens using adsorption to bacterial spores. *Vaccine* 28, 1021–1030. doi:10.1016/j.vaccine.2009.10.127.
- Isticato, R., Cangiano, G., Tran, H. T., Ciabattini, A., Medaglini, D., Oggioni, M. R., et al. (2001). Surface display of recombinant proteins on *Bacillus subtilis* spores. *J Bacteriol* 183, 6294–6301. doi:10.1128/JB.183.21.6294-6301.2001.
- Isticato, R., Lanzilli, M., Petrillo, C., Donadio, G., Baccigalupi, L., and Ricca, E. (2020). *Bacillus subtilis* builds structurally and functionally different spores in response to the temperature of growth. *Environmental Microbiology* 22, 170–182. doi:10.1111/1462-2920.14835.

Kazakov, S., Bonvouloir, E., and Gazaryan, I. (2008). Physicochemical Characterization of Natural Ionic Microreservoirs: *Bacillus subtilis* Dormant Spores. *J. Phys. Chem. B* 112, 2233–2244. doi:10.1021/jp077188u.

Khan, N., Ali, S., Shahid, M. A., Mustafa, A., Sayyed, R. Z., and Curá, J. A. (2021). Insights into the Interactions among Roots, Rhizosphere, and Rhizobacteria for Improving Plant Growth and Tolerance to Abiotic Stresses: A Review. *Cells* 10, 1551. doi:10.3390/cells10061551.

Kim, H., Hahn, M., Grabowski, P., McPherson, D. C., Otte, M. M., Wang, R., et al. (2006). The *Bacillus subtilis* spore coat protein interaction network. *Mol Microbiol* 59, 487–502. doi:10.1111/j.1365-2958.2005.04968.x.

Krajčiková, D., Forgáč, V., Szabo, A., and Barák, I. (2017). Exploring the interaction network of the *Bacillus subtilis* outer coat and crust proteins. *Microbiological Research* 204, 72–80. doi:10.1016/j.micres.2017.08.004.

Kumar, A., Prakash, A., and Johri, B. (2011). “*Bacillus* as PGPR in crop ecosystem. Bacteria in agrobiolgy: crop ecosystems,” in *Bacteria in agrobiolgy: Crop ecosystems* (Springer Berlin Heidelberg), 37–59.

Kundan, R., Pant, G., Jadon, N., and Agrawal, P. K. (2015). Plant Growth Promoting Rhizobacteria: Mechanism and Current Prospective. *J Fertil Pestic* 06. doi:10.4172/2471-2728.1000155.

Kunst, F., Ogasawara, N., Moszer, I., Albertini, A. M., Alloni, G., Azevedo, V., et al. (1997). The complete genome sequence of the Gram-positive bacterium *Bacillus subtilis*. *Nature* 390, 249–256. doi:10.1038/36786.

Lin, P., Yuan, H., Du, J., Liu, K., Liu, H., and Wang, T. (2020). Progress in research and application development of surface display technology using *Bacillus subtilis* spores. *Applied Microbiology and Biotechnology* 104. doi:10.1007/s00253-020-10348-x.

Liu, R., Dai, M., Wu, X., Li, M., and Liu, X. (2012). Suppression of the root-knot nematode [*Meloidogyne incognita* (Kofoid & White) Chitwood] on tomato by dual inoculation with arbuscular mycorrhizal fungi and plant growth-promoting rhizobacteria. *Mycorrhiza* 22, 289–296. doi:10.1007/s00572-011-0397-8.

Mauriello, E. M. F., Duc, L. H., Isticato, R., Cangiano, G., Hong, H. A., De Felice, M., et al. (2004). Display of heterologous antigens on the *Bacillus subtilis* spore coat using CotC as a fusion partner. *Vaccine* 22, 1177–1187. doi:10.1016/j.vaccine.2003.09.031.

Mirouze, N., and Dubnau, D. (2013). Chance and Necessity in *Bacillus subtilis* Development. *Microbiol Spectr* 1, 10.1128/microbiolspectrum.TBS-0004–2012. doi:10.1128/microbiolspectrum.TBS-0004-2012.

Moynié, L., Milenkovic, S., Mislin, G. L. A., Gasser, V., Malloci, G., Baco, E., et al. (2019). The complex of ferric-enterobactin with its transporter from *Pseudomonas aeruginosa* suggests a two-site model. *Nat Commun* 10, 3673. doi:10.1038/s41467-019-11508-y.

Nicholson, W. L., Munakata, N., Horneck, G., Melosh, H. J., and Setlow, P. (2000). Resistance of *Bacillus* endospores to extreme terrestrial and extraterrestrial environments. *Microbiol Mol Biol Rev* 64, 548–572. doi:10.1128/MMBR.64.3.548-572.2000.

Olanrewaju, O. S., Glick, B. R., and Babalola, O. O. (2017). Mechanisms of action of plant growth promoting bacteria. *World J Microbiol Biotechnol* 33, 197. doi:10.1007/s11274-017-2364-9.

Orozco-Mosqueda, Ma. del C., Flores, A., Rojas-Sánchez, B., Urtis-Flores, C. A., Morales-Cedeño, L. R., Valencia-Marin, M. F., et al. (2021). Plant Growth-Promoting Bacteria as Bioinoculants: Attributes and Challenges for Sustainable Crop Improvement. *Agronomy* 11, 1167. doi:10.3390/agronomy11061167.

Pertot, I., Caffi, T., Rossi, V., Mugnai, L., Hoffmann, C., Grando, M. S., et al. (2017). A critical review of plant protection tools for reducing pesticide use on grapevine and new perspectives for the implementation of IPM in viticulture. *Crop Protection* 97, 70–84. doi:10.1016/j.cropro.2016.11.025.

Pesce, G., Rusciano, G., Sasso, A., Isticato, R., Sirec, T., and Ricca, E. (2014). Surface charge and hydrodynamic coefficient measurements of *Bacillus subtilis* spore by optical tweezers. *Colloids Surf B Biointerfaces* 116, 568–575. doi:10.1016/j.colsurfb.2014.01.039.

Petar, P., and Normand, P. (2009). The root symbiosis between *Frankia* bacterium and actinorhizal plants. *Biofutur*, 26–29.

Petrillo, C., Castaldi, S., Lanzilli, M., Selci, M., Cordone, A., Giovannelli, D., et al. (2021). Genomic and Physiological Characterization of *Bacilli* Isolated From Salt-Pans With Plant Growth Promoting Features. *Front. Microbiol.* 12, 715678. doi:10.3389/fmicb.2021.715678.

Reddy, K. R. N., Reddy, C. S., and Muralidharan, K. (2009). Potential of botanical and biocontrol agents on growth and aflatoxin production by *Aspergillus flavus* infecting rice grains. *Food Control* 20, 173–178. doi:10.1016/j.foodcont.2008.03.009.

Riaz, U., Murtaza, G., Anum, W., Samreen, T., Sarfraz, M., and Nazir, M. Z. (2021). "Plant Growth-Promoting Rhizobacteria (PGPR) as Biofertilizers and Biopesticides," in *Microbiota and Biofertilizers: A Sustainable Continuum for Plant and Soil Health*, eds. K. R. Hakeem, G. H. Dar, M. A. Mehmood, and R. A. Bhat (Cham: Springer International Publishing), 181–196. doi:10.1007/978-3-030-48771-3_11.

Rostami, A., Hinc, K., Goshadrou, F., Shali, A., Bayat, M., Hassanzadeh, M., et al. (2017). Display of *B. pumilus* chitinase on the surface of *B. subtilis* spore as a potential biopesticide. *Pesticide Biochemistry and Physiology* 140, 17–23. doi:10.1016/j.pestbp.2017.05.008.

S., V. K., Menon, S., Agarwal, H., and Gopalakrishnan, D. (2017). Characterization and optimization of bacterium isolated from soil samples for the production of siderophores. *Resource-Efficient Technologies* 3, 434–439. doi:10.1016/j.reffit.2017.04.004.

Setlow, P. (1994). Mechanisms which contribute to the long-term survival of spores of *Bacillus* species. *Soc Appl Bacteriol Symp Ser* 23, 49S-60S. doi:10.1111/j.1365-2672.1994.tb04357.x.

Singh, R. P., and Jha, P. N. (2017). The PGPR *Stenotrophomonas maltophilia* SBP-9 Augments Resistance against Biotic and Abiotic Stress in Wheat Plants. *Front. Microbiol.* 8, 1945. doi:10.3389/fmicb.2017.01945.

Sirec, T., Strazzulli, A., Isticato, R., De Felice, M., Moracci, M., and Ricca, E. (2012). Adsorption of β -galactosidase of *Alicyclobacillus acidocaldarius* on wild type and mutant spores of *Bacillus subtilis*. *Microb Cell Fact* 11, 100. doi:10.1186/1475-2859-11-100.

Smyth, E. m., McCarthy, J., Nevin, R., Khan, M. r., Dow, J. m., O’Gara, F., et al. (2011). In vitro analyses are not reliable predictors of the plant growth promotion capability of bacteria; a *Pseudomonas fluorescens* strain that promotes the growth and yield of wheat. *Journal of Applied Microbiology* 111, 683–692. doi:10.1111/j.1365-2672.2011.05079.x.

Soumare, A., Diedhiou, A. G., Thuita, M., Hafidi, M., Ouhdouch, Y., Gopalakrishnan, S., et al. (2020). Exploiting Biological Nitrogen Fixation: A Route Towards a Sustainable Agriculture. *Plants (Basel)* 9, 1011. doi:10.3390/plants9081011.

Swarnalakshmi, K., Yadav, V., Tyagi, D., Dhar, D. W., Kannepalli, A., and Kumar, S. (2020). Significance of Plant Growth Promoting Rhizobacteria in Grain Legumes: Growth Promotion and Crop Production. *Plants* 9, 1596. doi:10.3390/plants9111596.

Tan, I. S., and Ramamurthi, K. S. (2014). Spore formation in *Bacillus subtilis*. *Environ Microbiol Rep* 6, 212–225. doi:10.1111/1758-2229.12130.

Tilak, K., Nandanavanam, R., Pal, K., De, R., Saxena, A., Nautiyal, C., et al. (2005). Diversity of plant growth and soil health supporting bacteria. *Current Science* 89.

Vance, C. P., Uhde-Stone, C., and Allan, D. L. (2003). Phosphorus acquisition and use: critical adaptations by plants for securing a nonrenewable resource. *New Phytologist* 157, 423–447. doi:10.1046/j.1469-8137.2003.00695.x.

Vessey, J. K. (2003). Plant growth promoting rhizobacteria as biofertilizers. *Plant and Soil* 255, 571–586. doi:10.1023/A:1026037216893.

Wani, S., and Gopalakrishnan, S. (2019). “Plant Growth-Promoting Microbes for Sustainable Agriculture,” in, 19–45. doi:10.1007/978-981-13-6790-8_2.

PART I

The spore-forming PGPB's potential in the agricultural field

CHAPTER II



Genomic and Physiological Characterization of Bacilli Isolated From Salt-Pans With Plant Growth Promoting Features

Claudia Petrillo^{1†}, Stefany Castaldi^{1†}, Mariamichela Lanzilli², Matteo Selci¹, Angelina Cordone¹, Donato Giovannelli^{1,3,4,5,6} and Rachele Isticato^{1,7*}

¹Department of Biology, University of Naples Federico II, Complesso Universitario Monte S. Angelo, Naples, Italy, ²Institute of Biomolecular Chemistry (ICB), CNR, Pozzuoli, Italy, ³National Research Council – Institute of Marine Biological Resources and Biotechnologies (CNR-IRBIM), Ancona, Italy, ⁴Department of Marine and Coastal Science, Rutgers University, New Brunswick, NJ, United States, ⁵Department of Marine Chemistry & Geochemistry, Woods Hole Oceanographic Institution, Woods Hole, MA, United States, ⁶Earth-Life Science Institute, Tokyo Institute of Technology, Tokyo, Japan, ⁷Interuniversity Center for Studies on Bioinspired Agro-Environmental Technology (BAT Center), Portici, Italy

OPEN ACCESS

Edited by:

Sukhwan Yoon,
Korea Advanced Institute of Science
and Technology, South Korea

Reviewed by:

Brent L. Nielsen,
Brigham Young University,
United States
Woo Jun Sul,
Chung-Ang University, South Korea

*Correspondence:

Rachele Isticato
isticato@unina.it

[†]These authors share first authorship

Specialty section:

This article was submitted to
Microbiological Chemistry and
Geomicrobiology,
a section of the journal
Frontiers in Microbiology

Received: 27 May 2021

Accepted: 10 August 2021

Published: 13 September 2021

Citation:

Petrillo C, Castaldi S, Lanzilli M,
Selci M, Cordone A,
Giovannelli D and Isticato R (2021)
Genomic and Physiological
Characterization of Bacilli Isolated
From Salt-Pans With Plant Growth
Promoting Features.
Front. Microbiol. 12:715678.
doi: 10.3389/fmicb.2021.715678

Massive application of chemical fertilizers and pesticides has been the main strategy used to cope with the rising crop demands in the last decades. The indiscriminate use of chemicals while providing a temporary solution to food demand has led to a decrease in crop productivity and an increase in the environmental impact of modern agriculture. A sustainable alternative to the use of agrochemicals is the use of microorganisms naturally capable of enhancing plant growth and protecting crops from pests known as Plant-Growth-Promoting Bacteria (PGPB). Aim of the present study was to isolate and characterize PGPB from salt-pans sand samples with activities associated to plant fitness increase. To survive high salinity, salt-tolerant microbes produce a broad range of compounds with heterogeneous biological activities that are potentially beneficial for plant growth. A total of 20 halophilic spore-forming bacteria have been screened *in vitro* for phyto-beneficial traits and compared with other two members of *Bacillus* genus recently isolated from the rhizosphere of the same collection site and characterized as potential biocontrol agents. Whole-genome analysis on seven selected strains confirmed the presence of numerous gene clusters with PGP and biocontrol functions and of novel secondary-metabolite biosynthetic genes, which could exert beneficial impacts on plant growth and protection. The predicted biocontrol potential was confirmed in dual culture assays against several phytopathogenic fungi and bacteria. Interestingly, the presence of predicted gene clusters with known biocontrol functions in some of the isolates was not predictive of the *in vitro* results, supporting the need of combining laboratory assays and genome mining in PGPB identification for future applications.

Keywords: spore-forming bacteria, biocontrol agents, halophiles, plant-growth-promoting bacteria, genome mining, Bacilli

INTRODUCTION

In the past decades, social concern about the environmental effects of the uncontrolled use of chemical pesticides, fertilizers, and herbicides in the agricultural field has risen considerably. The use of chemicals for the protection and enhancement of crops has led to several negative consequences: the formation of stable phytopathogenic variants, the reduction in the number of beneficial microorganisms, and the accumulation of toxic substances in soils and aquatic ecosystems (Reddy et al., 2009; Pertot et al., 2017). Given the increased global demand for crop production, researchers and industries are seeking new, more sustainable and greener approaches to pesticides and fertilizers (Glick et al., 2007). In this framework, the use of microorganisms known as Plant-Growth-Promoting Bacteria (PGPB) for crop production appears to be a promising alternative. PGPB improve crop fitness and yields both, through direct and indirect mechanisms. Direct mechanisms include the promotion of alternative nutrient uptake pathways, through the solubilization of phosphorus, the fixation of atmospheric nitrogen, the acquisition of iron by siderophores, and the production of growth hormones and molecules like vitamins, amino acids, and volatile compounds (Babalola, 2010). Indirect mechanisms instead, include the prevention or reduction of the damage induced by phytopathogens through the production of different classes of antimicrobial compounds such as hydrolytic enzymes that can lyse a portion of the cell wall of many pathogenic fungi (Jadhav et al., 2017).

The work presented here is part of a wide study aimed at identifying and selecting halophilic *Bacilli* with potential applications as biofertilizers or biocontrol agents. For this purpose, samples from the rhizosphere of the nurse plants *Juniperus sabina* and nearby soils were collected from salt-pans (Castaldi et al., 2021). Nurse plants, such as *J. sabina*, exert beneficial effects on their surrounding ecosystem, facilitating the growth and development of other plant species. This positive effect is in part due to the plant influence on the composition of soil microbial communities, generally selecting for microorganisms capable of mineralizing nutrients, enhancing soil fertility, and thus promoting plant growth and health (Hortal et al., 2013; Goberna et al., 2014; Rodríguez-Echeverría et al., 2016). For this reason, the nurse-plants rhizosphere and relative surrounding soil are a useful source of PGPB. In addition, bacteria growing in extreme environments, like salt-pans, have developed complex strategies to survive harsh conditions, which include the production of an array of diverse compounds, such as antioxidant pigments, lytic enzymes, and antimicrobial compounds, making them interesting biotechnological targets (Anwar et al., 2020). Among the PGPB, bacteria belonging to the *Bacillus* genus are of particular interest given their resistance to stressful environments and conditions due to their capacity of producing spores (Pesce et al., 2014), together with the ability to release a broad spectrum of secondary metabolites, the easy genetic manipulation, and the great ability to colonize plant surfaces (Kumar et al., 2011). In addition, the effectiveness of halo-tolerant *Bacillus* spp. to increase the growth of various crops under salt stress conditions has been

widely reported (Shultana et al., 2020). Recently, we have identified and characterized PGPB *Bacillus* strains isolated from the rhizosphere of *J. sabina* (Castaldi et al., 2021). The two strains, named as *Bacillus* sp. RHFS10 and *Bacillus* sp. RHFS18, emerged for their promising PGP traits. These strains produce siderophores and solubilize phosphorus, enhancing plant nutrients uptake, and secrete indoleacetic acid (IAA), a phytohormone playing a key role in both root and shoot development. Additionally, both isolates showed a strong biocontrol activity, inhibiting the fungal phytopathogen *Macrophomina phaseolina* growth (Castaldi et al., 2021).

Here, we present the results of the screening of 20 halophilic *Bacilli* isolated from salt-pan sand samples. All the strains were characterized for PGP traits and five strains emerged for their high potentiality as biofertilizers and biocontrol agents. Comparative genomic analysis of the five sand strains and the previously characterized rhizospheric strains RHFS10 and RHFS18 revealed the presence of known genes involved in plant growth promotion and protection, sustaining, in part, the activities observed *in vitro*. Overall, this work suggests a strategy for the selection of potential PGP candidates belonging to *Bacillus* genus using combined *in silico* and *in vitro* approaches.

MATERIALS AND METHODS

Isolation of Bacteria

Bacillus strains used in this study were isolated from sand samples collected in the proximity of *J. sabina* plants growing in the salt-pans of Formentera (Spain). Sand samples were heat-treated at 80°C, for 15 min to kill vegetative cells and select for spore-forming bacteria, and 1g of sample was suspended in 9 ml of TY broth (10 g/L tryptone, 5 g/L yeast extract, and 8 g/L NaCl) and 10-fold serial dilutions placed on TY plates (Cangiano et al., 2010). After 4–5 days of incubation at 30 ± 1°C, colonies were recovered and streaked on fresh TY plates, and pure cultures stored at –80°C into glycerol stocks (Giglio et al., 2011).

Phenotypic Characterization and Growth Conditions

The phenotypic variants of isolated strains were determined by visual inspection. The facultative anaerobic growth was determined using the AnaeroGen sachets (Unipath Inc., Nepean, Ontario, Canada) placed in a sealed jar with bacteria streaked on TY agar plates and incubated at 37°C for 3 days. To confirm the sporulation ability, the bacteria were grown in Difco sporulation medium (8 g/L Nutrient broth No. 4, 1 g/L KCl, 1 mM MgSO₄, 1 mM Ca(NO₃)₂, 10 μM MnCl₂, and 1 μM FeSO₄, Sigma-Aldrich, Germany) at 37°C for 30–48 h, and the presence of spores was checked by light microscopy. Salt, pH, and temperature tolerance were determined as follows: about 50 μl of culture of each isolate grown in TY broth for 6 h at 37°C (10⁷ cells/ml) were transferred to individual tubes containing 5 ml of TY broth with different pH (2.0, 4.0, 6.0, 7.0, 8.0, 10.0, and 12.0) or NaCl concentration (0, 5, 10, 13, 15, and 18%) and left to grow at 37°C with agitation (Cangiano et al., 2014). The temperature tolerance

of isolates was tested incubating the cultures at 37 (control), 4, 15, 25, 50, and 60°C. The growth (+) or no growth (-) in comparison with the controls after 24–48 h was recorded.

Plant Growth-Promoting Traits

Phosphate Solubilization

The phosphate solubilization activity was evaluated by spot inoculation of 3 μ l of the freshly grown bacterial culture (10^7 cells/ml) onto Pikovskaya's agar medium (Pikovskaya, 1948). The plates were incubated at 28°C for 10 days. The formation of transparent zones around the bacterial colonies indicates a positive result (Schoebitz et al., 2013).

Siderophores Production

The siderophores production was determined by the Chrome Azurol S (CAS) assay as described by Pérez-Miranda et al. (2007). Three milliliter of freshly-grown bacterial cultures was spot-inoculated on CAS agar plates and incubated at 28°C. The formation of a yellow-orange halo zone around the bacterial colony was a positive indicator of siderophore production and the halo zone diameters were measured after 4 days of incubation.

Indoleacetic Acid Detection

The indoleacetic acid production was measured as described by Etesami et al. (2014), with some modifications. Briefly, each strain was cultured in 10 ml of TY broth at 37°C for 4 days with shaking at 150 rpm. Following growth, 1 ml of bacteria supernatant was mixed with 2 ml of Salkowski reagent (0.5 M FeCl₃ in 35% HClO₄ solution), and the solution was vortexed and incubated at room temperature for 30 min. The formation of pink color was considered a positive reaction (Damodaran et al., 2013). Quantitative estimation of IAA (μ g/ml) was obtained by recording spectroscopic absorbance at 535 nm using a standard curve prepared separately with pure IAA (Sigma) in the range 0–100 μ g/ml (Gordon and Weber, 1951). Sterile TY medium was used as control.

Biofilm Production and Swarming Motility

To detect the ability to produce biofilm, bacterial isolates were grown in 24-well culture plates in TY broth for 48 h without agitation at 37°C in according to O'Toole (2011). Then, the supernatant was discarded, adhered cells were rinsed three times with distilled water and 1 ml of a 0.1% crystal violet (CV) solution was added to stain the adhered biomass. Plates were incubated for 30 min at room temperature, washed carefully three times with distilled water and patted dry. Dye attached to the wells was extracted with 1 ml of 70% ethanol and quantified at an absorbance of 570 nm. Data were normalized by total growth estimated by OD600 nm, and the experiment was performed in triplicate.

Swarming motility was tested according to the method adopted by Adler (1966). TY agar 0.7% plates were spot inoculated with 3 μ l of the freshly grown bacterial culture (10^7 cells/ml). After an overnight incubation at 37°C, the swarm diameters were measured.

Whole-Genome Sequencing of the Selected PGPB

DNA extraction was performed using the DNeasy PowerSoil kit (Qiagen, Hilden, Germany) according to the manufacturer's instructions. Genome sequencing was performed by MicrobesNG (Birmingham, United Kingdom) with the genomic DNA library prepared using the Nextera XT library prep kit (Illumina) following the manufacturer's protocol. Libraries were sequenced on the Illumina HiSeq using a 250 bp paired-end protocol. Reads were adapted and trimmed using Trimmomatic 0.30 with a sliding window quality cutoff of Q15 (Bolger et al., 2014) and the *de novo* genome assembly was carried out with SPAdes (version 3.7) via MicrobesNG. Genomes were annotated using Prokka (Seemann, 2014). Biosamples accession numbers for strains RHF6, RHF2, RHF6, RHF12, RHF15, RHS10, and RHF18 are, respectively: SAMN17389615, SAMN17389609, SAMN17389610, SAMN17389612, SAMN17389613, SAMN17389611, and SAMN17389614. MGS compliant details regarding each genome are available in the **Supplementary Table S1**.

Average Nucleotide Identity (ANI) values between the sequenced genomes and the closest bacterial species identified from the 16S rRNA phylogenetic analysis (see below) were obtained using the OrthoANI algorithm of EZBioCloud (Yoon et al., 2017). An ANI similarity of 95% was considered as a cut-off for species delineation.

Phylogenetic Analysis

The 16S rRNA genes were extracted from the sequenced genomes using Anvi'o v2.3.3 (Eren et al., 2021), and compared to 76 reference 16S rRNA genes from closely related strains identified using the Genome Taxonomy Database (GTDB)¹ taxonomy and retrieved from the NCBI database. All sequences were aligned using Seaview 4.4.0 software (Corrado et al., 2021), and the phylogenetic tree was constructed using the Maximum-likelihood algorithm with model GTR+I+G4. Statistical support was evaluated by the approximate likelihood-ratio test (aLRT) and is shown at the corresponding nodes of the tree. *Clostridium difficile* is used as an outgroup to root the tree.

Evaluation of Potential Biocontrol Activity

Isolated bacterial strains were tested *in vitro* for growth inhibitory activity against phytopathogenic fungi and bacteria are listed in **Table 1**. The phytopathogenic fungi are deposited in the fungal culture collection of the Plant Pathology Department of the University of Buenos Aires (FAUBA, Argentina) and were kindly supplied by Marcelo Anibal Carmona (Facultad de Agronomía, Cátedra de Fitopatología, Universidad de Buenos Aires, Buenos Aires, Argentina), except for *Stemphylium vesicarium*. All the fungi were stored on Potato Dextrose Agar (PDA) in Petri dishes. Dual-culture plate method was carried out to detect the antifungal activity in accordance with Xu and Kim (2014). Briefly, fungal plugs of 6 mm \times 6 mm diameter were placed at the center of PDA plates and 5 μ l of bacterial

¹<https://gtdb.ecogenomic.org>

TABLE 1 | List of the phytopathogenic fungi and bacteria used in this study.

Pathogen type	Species	Strain	Provenience	Host plant
Fungi	<i>Macrophomina phaseolina</i>	2,012,013-1	Argentine	Soy
	<i>Colletotrichum truncatum</i>	17-5-5	Argentine	Soy
	<i>Drechslera teres</i>	FT	Argentine	Barley
	<i>Cercospora nicotianae</i>	Ck_2017_B35	Bolivia	Soy
	<i>Stemphylium vesicarium</i>		Italy	Pear
Bacteria	<i>Pseudomonas tolaasii</i>	2,192	-	Mushroom
	<i>Pseudomonas syringae pv tabaci</i>	ICMP 2706	-	Tobacco
	<i>Pseudomonas syringae pv panici</i>	ICMP 3955	-	Rice
	<i>Pseudomonas caryophylli</i>	NCPBP349	Italy	Carnations
	<i>Pseudomonas syringae pv syringae</i>	B475	-	Mango
	<i>Pseudomonas syringae pv japonica</i>	ICMP 6305	-	Wheat
	<i>Pseudomonas syringae pv papulans</i>	Psp26	-	Apple

strains grown overnight in TY broth were placed on the opposite four sides of the plates 1.5 cm away from the fungal disc. This method was repeated for each fungus. Controls consisted of plates containing the fungal plugs alone. All plates were incubated at 28°C for 5–7 days. The antagonism activity against bacterial phytopathogens was performed as described in Li et al. (2020) with some modifications. Bacterial pathogens were streaked on TY plates and incubated at 25°C overnight. Single colonies were suspended in TY broth and incubated at 25°C. Approximately 1×10^{-6} CFU/ml were mixed with melted 0.8% TY agar medium before pouring plates. After solidification, 5 µl of bacterial isolates solution ($OD_{600} = 1.0$) was spot inoculated onto the plates and incubated at 28°C for 48 h, before measuring the diameters of inhibition halos. All experiments were performed in triplicate.

Identification of Biosynthetic Gene Clusters

Obtained genomes were analyzed by antiSMASH 5.0 (Blin et al., 2019) and BAGEL 4 (van Heel et al., 2018) to identify biosynthetic gene clusters (BCGs) of potential antimicrobial compounds such as non-ribosomal peptide synthetases (NRPSs), polyketide synthases (PKSs), post-translationally modified peptides (RiPPs), hybrid lipopeptides (NRPS-PKS) and bacteriocins. Biosynthetic Gene Clusters that shared less than 70% amino acid identity against known clusters were regarded as novel.

RESULTS AND DISCUSSION

Isolation and Characterization of Spore-Forming Plant-Growth-Promoting Bacteria

Spore-forming bacteria were specifically isolated from sand samples collected from gaps among nurse plants, belonging to the genus *J. sabina*, in salt-pans as described in the Materials and Methods section. Based on morphological characteristics, a total of 20 isolates were selected and preliminarily characterized for growth properties (Supplementary Table S2). All the strains can be classified as facultative anaerobic, mesophiles and moderate halophiles, excluding RHF5 strain, which survives up to 60°C and strain RHF6 unable to grow at temperature

and salt concentration higher than 37°C and 5% NaCl, respectively (Ventosa et al., 1998; Schiraldi and De Rosa, 2016).

To identify potential PGPB, the 20 strains were evaluated *in vitro* for physiological traits associated with plant growth enhancement and biocontrol ability (Table 2). Strain performance was compared with those of two promising PGPB, RHFS10, and RHFS18 strains, belonging to the *Bacillus* genus and isolated from *J. sabina* rhizosphere of the same collection site (Castaldi et al., 2021) and proposed as biocontrol agents for their antagonistic activity against the phytopathogen *M. phaseolina*. Most of the new strains displayed root-colonization phenotypes since able to surface spread by swarming and to form biofilms (Amaya-Gómez et al., 2020), while only five were found either positive to both solubilization of phosphate, indoleacetic acid (IAA), and siderophore production. Strains RHF6, RHF15, and RHF6 showed a better performance than when compared against the already characterized rhizobacteria strains RHFS10 and RHFS18, confirming that the microenvironments created under or nearby nurse shrubs are a promising source of PGPB (Rodríguez-Echeverría et al., 2016). All bacterial isolates were tested for *in vitro* activities of their extracellular hydrolytic enzymes (lipase, protease, amylase, xylanase, and cellulase) usually associated with biocontrol activity (Pal and McSpadden Gardener, 2006). As reported in Table 2, the highest hydrolytic activity was observed for RHF12, RHF15, and RHF6 strains, comparable with that exerted by rhizosphere strains RHFS10 and RHFS18.

Based on these results reported in Table 2, seven strains were selected for whole-genome sequencing analysis. All selected strains were able to solubilize phosphate with efficiency higher than the other ones and to produce Biofilm, IAA, and siderophores. Further, strains RHF12, RHF15, RHF6, and RHFS18 emerged for their strong hydrolytic potential, often associated to biocontrol activity (Castaldi et al., 2021), while strain RHF6 showed the ability to growth up to 13% NaCl, showing the best salt tolerance (Supplementary Table S2).

Genome Sequencing and Phylogenetic Analysis

The obtained genomes had coverage of ~30x, with a variable number of contigs between 40 and 1,105 for RHF15 and

TABLE 2 | Summary of plant growth-promoting and biocontrol traits exhibited by 20 spore-forming bacteria isolates.

Strain	PGPB activities					Hydrolytic activities				
	Biofilm (OD ₅₇₀)	Swarming	PVK	IAA (µg/ml)	Siderophores	Lipase	Protease	Amylase	Xylanase	CMC
RHF1	-	++	++	-	+	-	++	++	+	++
RHF2	0.2	+	+	18	+	-	+	+	+	+
RHF3	-	-	-	-	-	+	++	++	+	-
RHF4	-	+	-	-	+	+	++	++	-	+
RHF5	0.2	-	-	2	-	-	+	++	-	-
RHF6	0.3	+	++	31	++	-	+	+	+	++
RHF7	0.4	-	-	-	-	-	+	+	-	-
RHF8	0.6	++	-	6	-	-	++	++	++	-
RHF9	-	-	+	3.2	-	-	++	++	-	-
RHF10	-	-	-	4	-	-	++	+	+	+
RHF11	0.2	+	-	-	-	-	+	+	+	-
RHF12	0.7	++	+	25	++	-	++	++	++	++
RHF13	-	++	++	3	+	+	+	++	+	++
RHF14	-	-	-	-	-	+	+	+	+	-
RHF15	0.6	++	++	23	++	+	++	++	++	++
RHF16	-	-	-	-	-	+	+	+	-	-
RHF17	0.5	++	+	-	+	+	+	+	++	+
RHFB	0.3	+	++	32	++	++	++	++	++	+
RHFE	-	-	-	-	-	+	+	+	-	-
RHFL	0.3	-	-	-	-	-	+	+	-	-
RHFS10'	0.3	++	+	12	++	++	++	++	++	++
RHFS18'	0.5	+	+	12	++	+	++	++	++	++

No activity (-), halo or colony diameter <5 mm (+), halo or colony diameter ≥5 mm (++) , halo or colony diameter 10 mm (+++). Data are represented by means of at least three replicates ±SE at p ≤ 0.05 using LSD. The strains selected for further studies are indicated in bold. PVK, Pivovskaya; IAA, indoleacetic acid; and CMC, carboxymethylcellulose. ¹Available from Castaldi et al. (2021).

TABLE 3 | General features of the assembled genomes.

Analysis statistics	Strains						
	RHFB	RHF2	RHF6	RHF12	RHF15	RHFS10	RHFS18
Size (bp)	5,648,757	4,003,762	4,066,378	4,096,200	4,232,838	4,254,653	3,936,406
Number of contigs	158	52	156	280	40	46	1,105
Mean GC content (%)	40.57	43.74	46.3	44.01	43.39	43.95	46.14
CDS	5,413	3,988	3,901	3,997	4,282	4,182	3,87
N50	187,761	413,219	584,325	60,229	2,184,724	1,139,270	6,179
N75	82,022	306,766	292,476	34,071	1,049,735	348,257	3,118
L50	11	3	2	19	1	2	176
L75	21	6	4	42	2	4	397

RHFS18, respectively (Table 3). The genome of strain RHFS18 was particularly fragmented, and repeated sequencing of the same strain did not yield improved assembly suggesting that the results are not dependent on a low-quality sequencing library. The obtained genomes are approximately 4.0Mbp long except for RHFB's genome, being the longest (5.6Mbp) and the one with the highest number of predicted protein coding sequences compared to the others. Taxonomic identification of the strains was based on the phylogenetic analysis of the 16S rRNA sequence as well as the whole genome Average Nucleotide Identity. All the isolates were identified as members of the genus *Bacillus* (Figure 1) with six strains out of seven clustering into the same clade, and only strain RHFB falling in a different clade. The phylogenetic divergence observed for RHFB from the other strains agrees with the observed differences

in physiological traits for this strain (Supplementary Table S3). Since most *Bacillus* species are phylogenetically close, 16S rRNA analysis is not always exhaustive to obtain an unambiguous assignment (Rooney et al., 2009). To overcome this issue and classify the strains at the species level, whole genome ANI was used (Table 4). Strain RHFB exhibited 96.95% ANI against the genome of the closest relative *Brevibacterium frigoritolerans* and was therefore identified as a *B. frigoritolerans* species. Strain RHF2 was identified as *Bacillus subtilis*, based on 99.96% ANI score. Strains RHF6 and RHFS18 were classified as members of the *Bacillus amyloliquefaciens* species, exhibiting 99.26 and 98.36% ANI, respectively. Strain RHF12 was identified as *Bacillus halotolerans*, based on 98.04% ANI score, while RHF15 was classified as *Bacillus gibsonii*, showing 99.6% ANI score. As shown in Table 4, RHFB, RHF12, and RHFS18 strains were

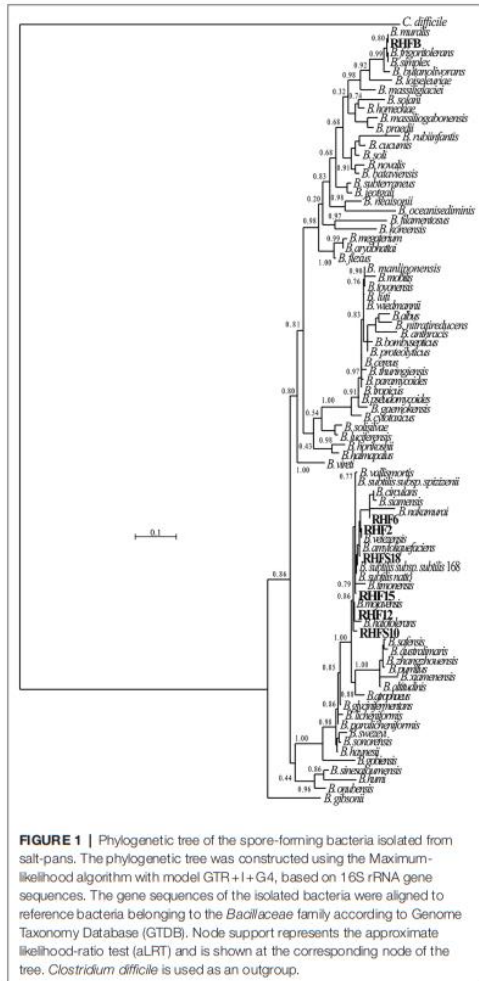


FIGURE 1 | Phylogenetic tree of the spore-forming bacteria isolated from salt-pans. The phylogenetic tree was constructed using the Maximum-likelihood algorithm with model GTR+I+G4, based on 16S rRNA gene sequences. The gene sequences of the isolated bacteria were aligned to reference bacteria belonging to the *Bacillaceae* family according to Genome Taxonomy Database (GTDB). Node support represents the approximate likelihood-ratio test (aLRT) and is shown at the corresponding node of the tree. *Clostridium difficile* is used as an outgroup.

univocally matched with the same species, while for RHF2, RHF6, and RHF15 strains the two analyses returned different results. This mismatch between the two methods of classification is due to the poor discrimination between closely related species of the *Bacillus* genus due to their high morphological, biochemical, and genetic similarities (Celandroni et al., 2019). Since taxonomy annotations based on genetic markers, such as the 16S rRNA gene, can give variable results depending on the strain, ANI-based classification has been preferred in this study when showing ANI scores $\geq 95\%$ (Jain et al., 2018). Based on this, RHF2, RHF6, and RHF15 were identified as

TABLE 4 | Classification of the seven selected strains.

	16S rRNA similarity	ANI (best score)
RHFB	<i>B. frigorigerans</i> (100%)	<i>B. frigorigerans</i> (96.95%)
RHF2	<i>B. velezensis</i> (99.87%)	<i>B. subtilis</i> 168 (99.96%)
RHF6	<i>B. velezensis</i> (100%)	<i>B. amyloliquefaciens</i> (99.26%)
RHF12	<i>B. halotolerans</i> (98.51%)	<i>B. halotolerans</i> (98.04%)
RHF15	<i>B. subtilis</i> (100%)	<i>B. gibsonii</i> (99.6%)
RHF10	<i>B. halotolerans</i> (97.5%)	<i>B. vallismortis</i> (93.48%)
RHF18	<i>B. amyloliquefaciens</i> (100%)	<i>B. amyloliquefaciens</i> (98.36%)

The 16S rRNA similarity and ANI score against the closest relative identified from the phylogenetic analysis are reported for each isolate.

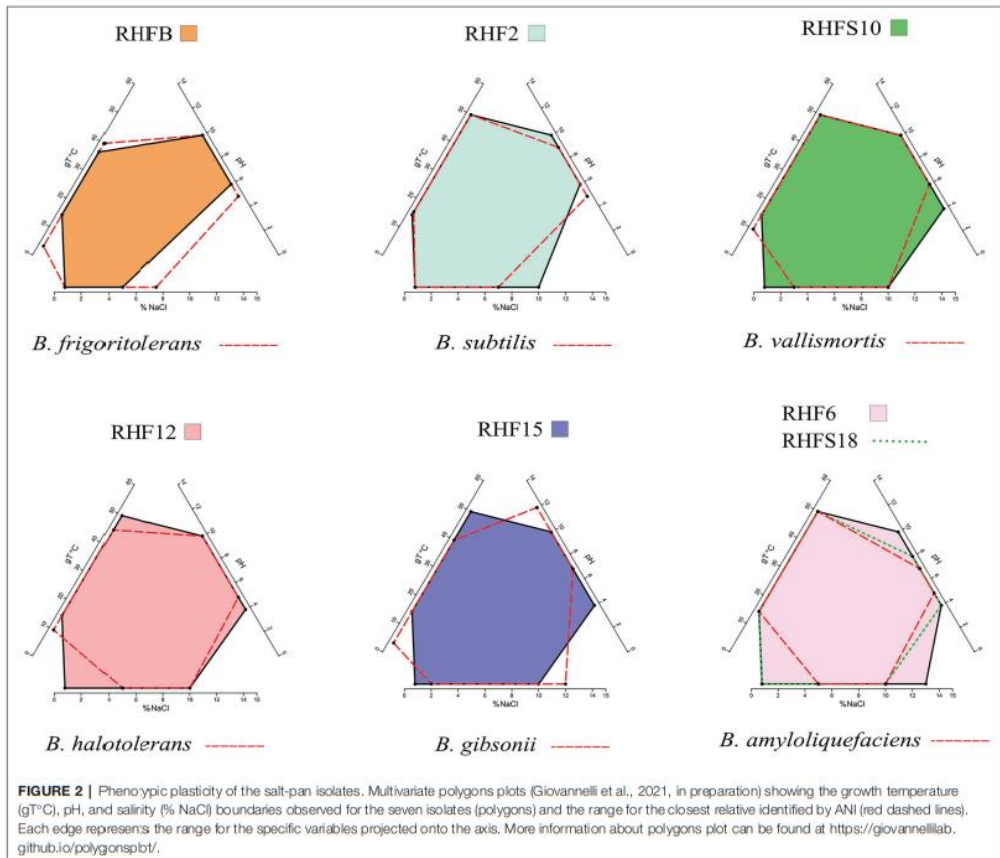
B. subtilis, *B. amyloliquefaciens*, and *B. gibsonii*, respectively (Table 4). Only strain RHF10 could not be classified at the species level due to the low ANI score (93.48%) when compared with the closest relative *Bacillus vallismortis* and it was classified as *Bacillus* sp. RHF10 (Table 3). Further analysis will be required to fill this classification gap.

Environmental Adaptation to Halophilic Conditions

The phenotypic plasticity of the salt-pans isolates was investigated by comparing their growth parameters against the closest *Bacillus* species identified by the ANI analysis (Table 4). Temperature, pH, and salinity ranges required for growth were evaluated. These parameters are useful to identify distinct phenotypic strategies used by microorganisms to better adapt to environmental conditions (Agrawal, 2001). As expected, taxonomically closer strains showed small differences when compared with each other or with their representative species (red dashed lines in Figure 2). As already highlighted by the phylogenetic analysis, *B. frigorigerans* RHF2 strain presented a diverging phenotype, especially considering the lower salt tolerance compared to the other isolates. Interestingly, some strains, like *B. halotolerans* RHF12, *B. gibsonii* RHF15, and *Bacillus* sp. RHF10, showed identical growth properties even though belonging to three different *Bacillus* species (Figure 2), while strains of the same species, like *B. amyloliquefaciens* RHF6 and RHF18, exhibited different adaptations to NaCl concentration and pH range. Moreover, *B. amyloliquefaciens* RHF6 like *B. subtilis* RHF2 were able to grow at higher salt concentrations than their representative species, suggesting an adaptive phenotypic variation to the high salinity condition of salt-pans.

Analysis of Potential PGP and Biocontrol Traits

To confirm the *in vitro* PGP characterization of the isolates, a prediction of the genes (Figure 3) and proteins (Table 5) involved in biocontrol activity and plant growth promotion was performed. The analyses identified genes that can be attributed to the strains ability to improve nutrient availability, suppress pathogenic fungi, and resist oxidative stress and quorum sensing in all analyzed genomes. For instance, the genome of most of the seven strains included the pyrroloquinolone quinone synthase (*pqq*) and the dependent glucose dehydrogenase (*gdh*)

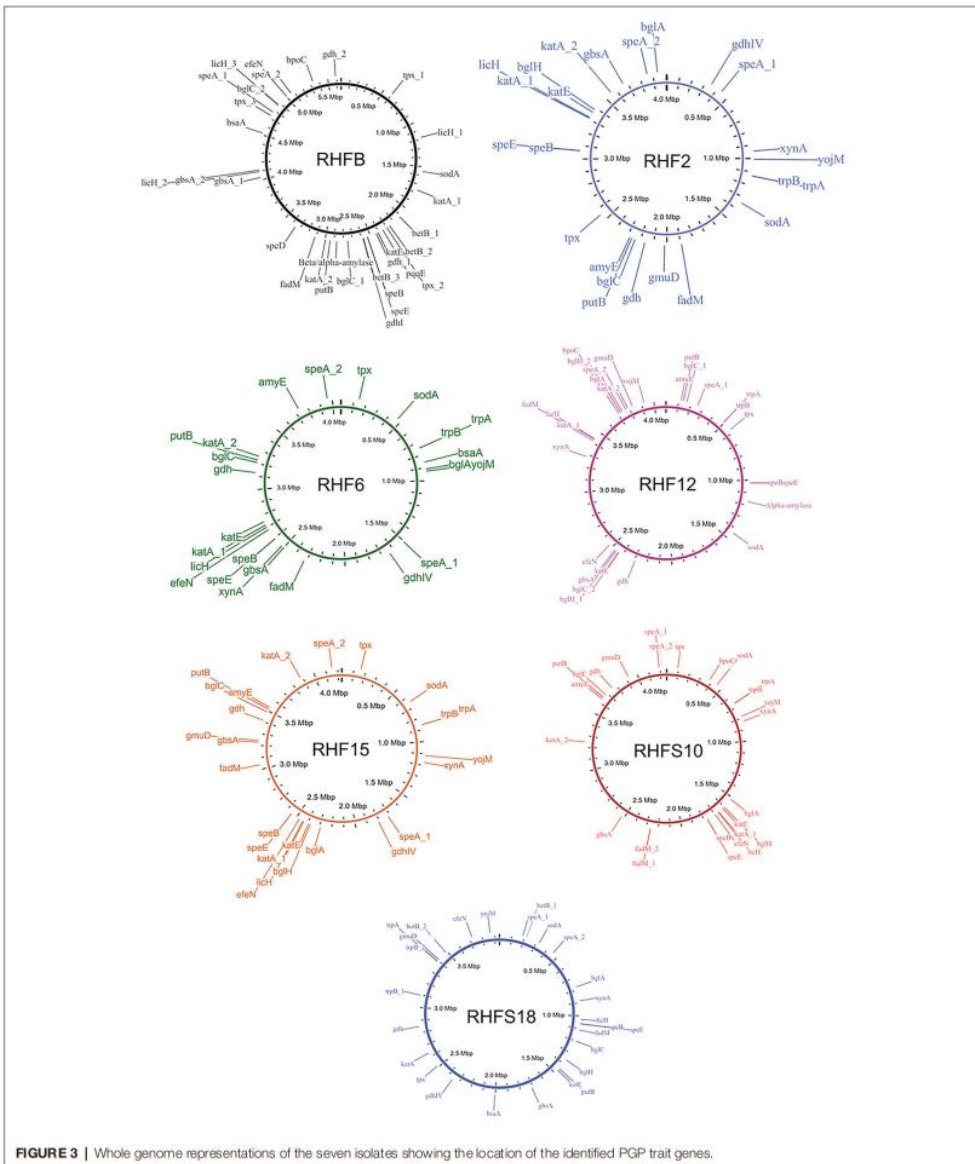


genes, involved in mineral phosphate solubilization as well as antifungal activities and systemic resistance induction. Interestingly, both isolates *B. amyloliquefaciens* RHF6 and RHFS18 did not carry the cofactor *pqq* gene cluster, suggesting that other mechanisms could co-exist (Table 2). IAA is one of the most common and effective plant-growth hormones. Besides plants, most rhizobacteria can produce and secrete IAA, increasing the growth and the yield of crops (Bursangiam et al., 2019). All the strains produced Tryptophan-2-monooxygenase and Indole-3-acetamide hydrolase, able to convert Tryptophan in Indole-3-acetamide and then in IAA, respectively (Bursangiam et al., 2019). The presence of other tryptophan synthases orthologs (subunits a and b) in all the analyzed genomes suggests alternative IAA biosynthesis pathways potentially involving different intermediates. This hypothesis is supported by the observation that *B. frigoritolerans* RHFB, one of the best IAA producers among the isolated PGPB, possessed the indole-3-pyruvate decarboxylase, a key enzyme

of another Trp-dependent pathway for IAA production (Sitbon et al., 2000).

All the strains were predicted to be potentially able to fix nitrogen and produce nitric oxide, both useful features in agricultural practices (Ahmad et al., 2013), and to synthesize polyamines, as spermidine and putrescine, and the ACC deaminase, involved in lateral root development and plant growth enhancement under abiotic stress (Xie et al., 2014; Gupta and Pandey, 2019).

As expected, the genome of all the halophilic *Bacillus* strains contained multiple genes involved in antioxidant response, such as peroxidases, catalases, superoxide dismutase, and glutathione peroxidase (Hassan et al., 2020; Figure 3; Table 5). Other enzymes involved in abiotic stress responses were identified in the strains, as the osmoprotectants choline dehydrogenase, betaine-aldehyde dehydrogenase, and proline dehydrogenase (Table 5). The predicted production of osmotically active metabolites, as well as ROS scavenging enzymes, reflects the



ability of the selected strains to survive in extreme environments, as salt-pans and to potentially alleviate abiotic stress in agricultural system.

Finally, all the isolates possessed in their genomes genes encoding for hydrolases involved in fungal cell-wall and starch degrading pathways, confirming the results obtained with the

TABLE 5 | Plant-Growth-Promoting traits-associated proteins identified in the proteome of the selected strains and their abundance.

PGP Trait	Protein	RHFB	RHF2	RHF6	RHF12	RHF15	RHFS10	RHFS18
Phosphate solubilization	Pyroloquinoline quinone	1	1	0	1	1	1	0
	Glucose 1-dehydrogenase	2	2	2	2	2	2	2
Nitrogen fixing	Nitrogenases	6	6	4	6	6	6	2
	Copper-containing nitrite reductase	1	2	1	3	2	2	1
Nitric oxide synthesis	Indole-3-pyruvate decarboxylase	1	0	0	0	0	0	0
	Tryptophan 2-monooxygenase	4	2	1	2	2	3	2
IAA biosynthesis	Tryptophan synthase (subunit a and b)	6	7	6	7	7	5	7
	Tryptophan aminotransferase	0	0	0	0	0	0	0
	Tryptophan decarboxylase	0	0	0	0	0	0	0
	Indole-3-acetamide hydrolase	0	0	0	0	0	0	0
	Arginine decarboxylase	3	2	2	2	2	2	2
Putrescine and Spermidine-related production	Agmatine ureohydrolase	1	1	1	1	1	1	2
	Ornithine decarboxylase	0	0	0	0	0	0	0
	SAM decarboxylase	1	1	1	1	1	2	1
	Spermidine synthase	1	1	1	1	1	1	1
ACC deaminase activity	ACC deaminase	2	2	3	1	2	1	3
	D-cysteine desulfhydrase	1	0	1	0	0	0	1
Antioxidant activity	Peroxidases	9	10	4	9	9	8	4
	Catalases	10	12	11	11	12	11	8
	Superoxide dismutase	7	5	5	6	5	5	5
	Glutathione peroxidase	1	1	1	1	2	1	1
	Glutathione reductase	0	0	0	0	0	0	0
	Glutathione S-transferase	2	5	2	2	5	2	3
Abiotic stress	Choline dehydrogenase	0	1	1	2	2	1	1
	Betaine-aldehyde dehydrogenase	5	2	2	2	2	2	2
	Proline dehydrogenase	2	3	2	2	2	2	2
	β -Glucosidase	1	3	2	5	3	3	3
	α -Glucosidase	3	4	4	3	4	4	2
Cell wall and degrading	Endo-1,4- β -xylanase	5	7	7	4	5	7	9
	Glucosylase	0	0	2	0	0	0	1
	α -Amylase	0	1	1	1	1	1	1
	Chitinase	1	0	0	0	0	1	1
	β -1,3-Glucanase	2	3	2	1	2	2	1
	Cellulase	0	3	2	3	3	4	2
	Protease	4	3	3	3	3	2	1

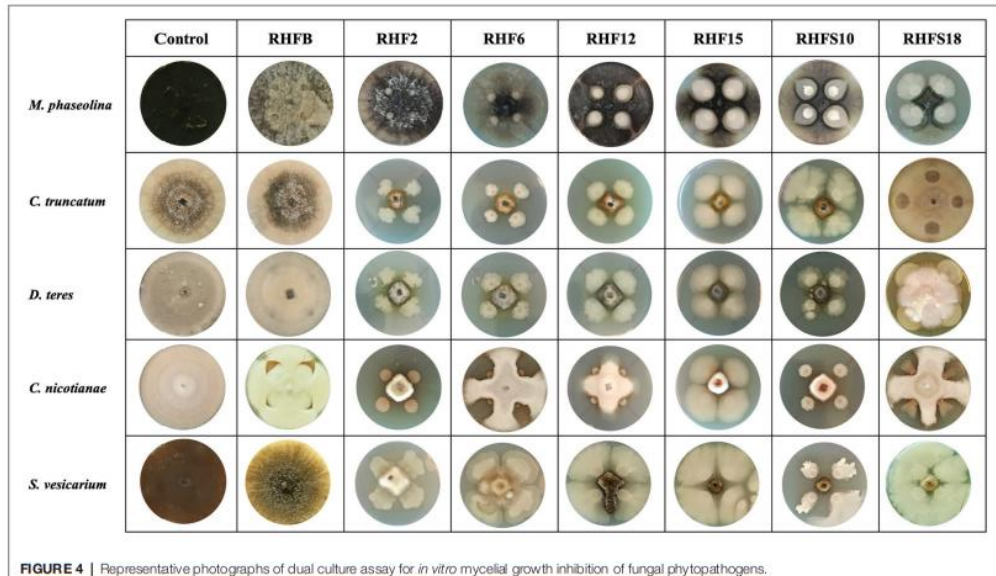
Only $\geq 40\%$ similarity scores were considered. IAA, indole-3-acetic acid; ACC, 1-aminocyclopropane-1-carboxylate.

in vitro analysis, except for strain *B. frigiditolerans* RHFB whose genome did not carry α -amylase or cellulase genes.

Antimicrobial Activity Screening

To verify the antagonistic potential that emerged from the genome-mining, the isolates were dually cultured with fungal and bacterial plant pathogens (see Table 1 for a list of the used phytopathogens). The results reveal that isolates inhibited plant pathogens growth on plates with different efficiency (Figure 4). Strains *B. subtilis* RHF2, *B. amyloliquefaciens* RHF6, and *Bacillus* sp.

RHFS10 showed a broad inhibitory spectrum, being able to antagonize both phytopathogenic fungi and bacteria, while *B. halotolerans* RHF12 and *B. amyloliquefaciens* RHFS18 exhibited an antimicrobial activity limited to fungi. The highest antagonistic activity was observed for strain *Bacillus* sp. RHFS10, capable of inhibiting the growth of most of the test pathogens, confirming its biocontrol potential already observed by Castaldi et al. (2021). Unexpectedly, *B. frigiditolerans* RHFB exhibited no activity at all. Nevertheless, in the last decade, this species has been identified as a potential insect pathogenic bacterial species, with nematocidal



activity (Selvakumar et al., 2011). The diversity observed in the antimicrobial activity against plant pathogens highlighted the phenotypic diversity of sand and rhizosphere isolated *Bacilli*, suggesting that in nature plant-associated bacteria may encounter different phytopathogens that may induce the acquisition of different antagonistic activity.

Genome Mining for Biosynthetic Gene Clusters

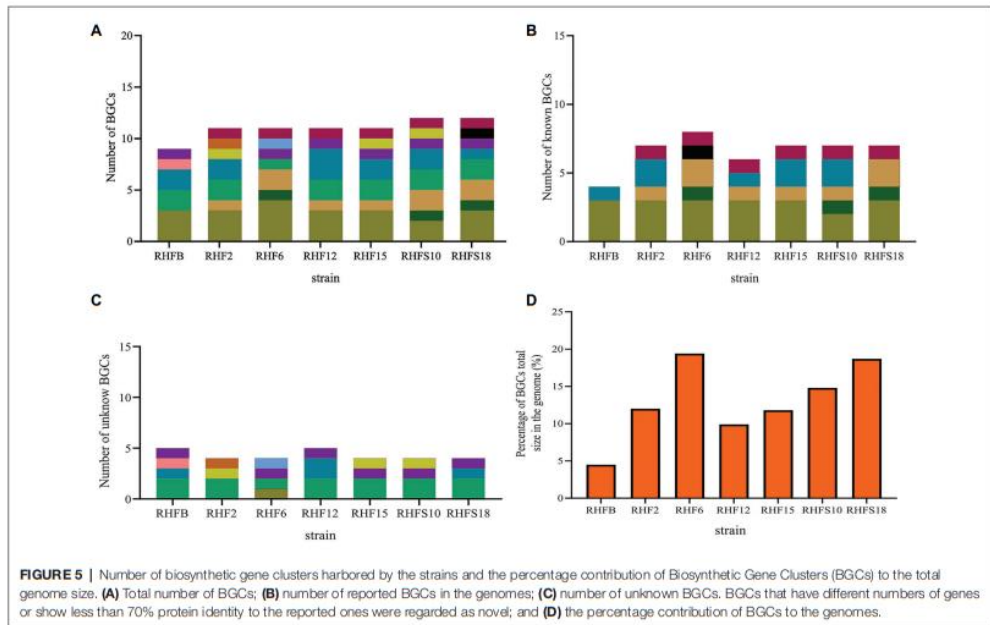
The biocontrol potential and the ability to enhance plant growth of PGPB are mostly attributed to their bioactive secondary metabolites. Proteins and metabolites released in the soil by PGPB, indeed, are implicated in root colonization, as well as in interactions with the plant immune response and the surrounding niche (Lugtenberg and Kamilova, 2009; Pieterse et al., 2014; Jamali et al., 2020). The strong antimicrobial activity of selected *Bacillus* strains is most likely due in part to the production of hydrolytic enzymes and siderophores observed in *in vitro* assays and confirmed by genome analysis (Tables 2 and 5). To better investigate this antagonistic activity, the biosynthetic potential of the halophilic PGPB was evaluated by using antiSMASH 6.0.0 to predict both characterized and unknown functioned secondary metabolites (Figure 5).

The bacterial isolates harbored BGCs coding for NRPSs, polyketide synthases (PKSs), post-translationally modified peptides (RiPPs), hybrid lipopeptides (NRPS-PKS; Figure 5A), and the majority of the BGCs are assigned to known products (Figure 5B; Supplementary Table S4). The unknown BGCs are type 3 polyketide synthase (T3PKS), RiPPs and terpenes (Figure 5C; Supplementary Table S4).

Novel Non-ribosomal Peptide Synthetases and Bacteriocins

NRPs are modular enzymes that synthesize secondary metabolites, some of which are known to be involved in plant disease control (Ongena and Jacques, 2008). Several bioactive compounds produced by *Bacillus* strains fit in this category, such as surfactin or fengycin (Keswani et al., 2020), both of them exhibiting antimicrobial activity potentially exploited for biocontrol in agriculture. We have identified one novel BGC belonging to the class of the NRPs from *B. amyloliquefaciens* RHF6 (Figure 6). This cluster of 66.3 Kb has six genes encoding 25 domains, which include six condensation (C) domains, seven adenylation (A) domains, one coenzyme A ligase (CAL) domain, two epimerization (E) domains, one thioesterase (TE) domain, one heterocyclization (Cy) domain and seven peptidyl carrier protein (PCP) domains. Among them, 24 domains are essential components of this cluster, and catalyze the incorporation of seven amino acids into the final product exhibiting the following sequence: D-Cys-Ser-Cys-Ala-Asn-D-Asn. This cluster shows no similarity to any known BGCs reported in the antiSMASH database (Supplementary Table S4). The single heterocyclization (C) domain in the first module of the BGC, could form a thiazoline ring from a residue of cystine (Cys). Interestingly, many antimicrobial drugs expose a thiazoline ring (Desai et al., 2016). This allows us to speculate on the potential antimicrobial activity of the compound produced by this novel BGC.

The seven genomes were also mined for potential novel bacteriocins BGCs using BAGEL4. Bacteriocins are ribosomally



B. amyloliquefaciens RHF6 (Cluster 7) BGC NRPs 66315 bp

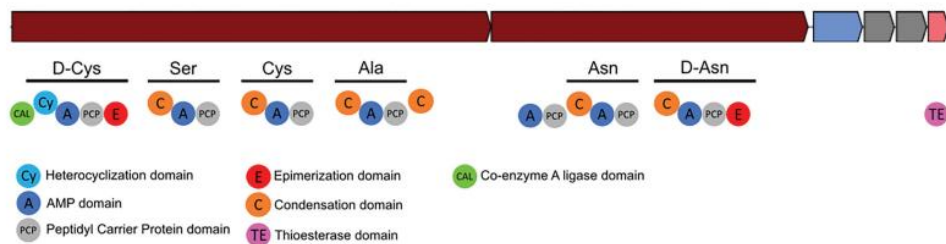


FIGURE 6 | Novel NRP Biosynthetic gene Clusters identified from the isolate *Bacillus amyloliquefaciens* RHF6.

synthesized antimicrobial peptides, generally active against bacteria closely related to producers (Cotter et al., 2013), and classified into three main classes: class I comprehends ribosomally produced and post-translationally modified peptides (RiPPs); class II unmodified peptides, and class III large antimicrobial peptides (Zhao and Kuipers, 2016). These molecules are directed against competitive microorganisms, and therefore generate a selective advantage for the producers. Generally, bacteriocins are highly specific against their target, although some might have a wider spectrum

(Jack et al., 1995). The analysis made using BAGEL4, returned 15 regions of interest (in contrast with the antiSMASH analysis which revealed a higher number of bacteriocins, **Supplementary Table S4**), even though only six of them could be classified as novel bacteriocins, sharing $\leq 70\%$ of similarity with known sequences from BAGEL4 database (**Figure 7**).

One orphan BGC of 27 genes is carried by both *B. amyloliquefaciens* RHF6 and RHFS18 strains (**Figures 7a.1,d.1**), although the core biosynthetic genes encode two different



precursor peptides of 40 and 29 amino acids, respectively, sharing 41.03 and 57.14% of similarity with ComX4 from the *B. subtilis* group. In particular, ComX4 belongs to the ComX subclass of RiPPs according to the BAGEL4 database, and it is part of a major quorum-sensing system that regulates the development of genetic competence (Okada et al., 2005) and the production of surfactins (Caulier et al., 2019). *Bacillus*

amyloliquefaciens RHF6 also harbors a BGC of 23 genes (Figure 7A-a.2), with the core biosynthetic gene encoding a 63-amino acids precursor peptide, showing a similarity of 36.51% compared to UviB, a class II bacteriocin first identified in the mobilizable plasmid pIP404, from *C. perfringens*, known to be bacteriocinogenic (Garnier and Cole, 1988). Interestingly, two different BGCs containing the same gene encoding for a

TABLE 6 | Antimicrobial activity of the seven selected strains against phytopathogenic fungi and bacteria.

Pathogen types	Species	RHFB	RHF2	RHF6	RHF12	RHF15	RHFS10	RHFS18
Fungi	<i>M. phaseolina</i>	-	-	-	+	++	+++	+++
	<i>C. truncatum</i>	-	-	+++	+++	+++	+++	+++
	<i>D. terreis</i>	-	-	+++	+++	+++	+++	+++
	<i>C. nicotianae</i>	-	+++	++	++	+++	+++	++
	<i>S. vesicarium</i>	-	++	+++	++	+++	+++	-
Bacteria	<i>P. tolaasii</i>	-	-	+	-	-	+	-
	<i>P. syringae</i> pv <i>tabaci</i>	-	++	++	-	-	+	-
	<i>P. syringae</i> pv <i>panici</i>	-	++	++	-	-	+	-
	<i>P. carliphilly</i>	-	-	-	-	+	+	-
	<i>P. syringae</i> pv <i>syringae</i>	-	+	+	-	-	++	-
	<i>P. syringae</i> pv <i>japonica</i>	-	++	++	-	-	+	-
	<i>P. syringae</i> pv <i>papularis</i>	-	-	-	-	-	-	++

No inhibition (-), inhibitory zone <5mm (+), inhibitory zone 5mm (++), and inhibitory zone >5mm (+++).

putative UviB-like bacteriocin, were found in strains *B. gibsonii* RHF15 (Figure 7B) and *B. amyloliquefaciens* RHFS18 (7D-d.1). Their precursor peptides share 42.1 and 33.4% similarity with UviB.

Finally, *Bacillus* sp. RHFS10 carries an orphan 28 genes BGC with a core biosynthetic gene encoding a 40-amino acids peptide sharing 35% of similarity with the competence pheromone of *B. subtilis* 168, a RiPP belonging to class I bacteriocins. *Bacillus* species are known to synthesize many well-studied bacteriocins, such as subtilin, ericin, paenibacillin, subtilosin, thuricin, and coagulin (Abriouel et al., 2011). Anyway, it is impossible to predict if the six compounds produced by strains *B. amyloliquefaciens* RHF6, and RHFS18, *B. gibsonii* RHF15 and *Bacillus* sp. RHFS10 actually have antimicrobial properties from genome sequence data only. Despite this, the antagonistic activity exerted by RHF6, RHF15, RHFS10, and RHFS18 strains observed previously in *in vitro* assays (Table 6) could be associated with these potential compounds. This will need to be validated by further experiments.

CONCLUSION

In a historic moment in which the increasing population coupled with land degradation aggravates crop production, the use of plant growth promoting bacteria to ensure agricultural productivity has a huge impact on our society. These soil microorganisms enhance plant performance and represent an eco-friendly alternative to chemical fertilizers and pesticides (Hashem et al., 2019). When applied directly to the soil, PGPB enhance plant growth by different action mechanisms such as the production of different phytohormones, accelerating the mineralization of organic matter and improving the bioavailability of the nutrients, and protecting plants from pests' damages. The beneficial activity exerted by PGPB is in part mediated by a broad spectrum of secondary metabolites and enzymes. For example, polyamines, such as spermidine, play important physiological and protective roles in plants, resulting in an increase in biomass, altered root architecture, and elevated photosynthetic capacity. Until recently, these key

metabolites were uncovered only by systematic investigation or by serendipity, often understating the PGPB potentiality during their screening. Many genes involved in PGP activity, in fact, could be silent under standard laboratory conditions, due to the absence of appropriate natural triggers or stress signals. More recently, the onset of the genomic era has facilitated the discovery of these ecologically important metabolites and novel strategies became available for PGPB characterization.

For example, genome mining allows to look over the whole genome of a PGPB strain and highlights genes encoding beneficial enzymes, involved in the enhancement of plant nutritional uptake or modulation of hormone levels, as well as for antimicrobial-encoding BGCs.

In this work, we have isolated soil halophilic *Bacilli* and performed their screening for PGP traits by using standard laboratory procedures and whole-genome analysis. *Bacilli* represent a significant fraction of the soil microbial community and some species are categorized as PGPB (Cazorla et al., 2007). They are also able to produce endospores, which besides enduring harsh environmental conditions fatal for other cell forms (Petrillo et al., 2020), permit easy formulation and storage of commercial PGPB-based products. In addition, salt-tolerant PGPB can easily withstand several abiotic stresses and ameliorate plant growth in degraded soil.

Seven *Bacillus* strains have been selected for *in vitro* PGP traits and identified at the species level by genome analysis. Based on genome mining, not only have we confirmed the beneficial activities PGP found by *in vitro* analysis, identifying the involved genes but also we have highlighted their strong potentiality by the discovery of novel biosynthesis gene clusters. Our results demonstrated that the genomic analyses, as genome mining, allow a full investigation of PGPB biosynthetic capacity for secondary metabolites and proteins and represent useful tools in the characterization of plant beneficial bacteria. Nevertheless, the divergences observed between the predicted biocontrol functions by found gene clusters and the results obtained by *in vitro* analysis, highlight the need of combining laboratory-assays and genome-mining in identification of new PGPB for future applications.

- Hashem, A., Tabassum, B., and Fathi Abd Allah, E. (2019). *Bacillus subtilis*: a plant-growth promoting rhizobacterium that also impacts biotic stress. *Saudi J. Biol. Sci.* 26, 1291–1297. doi: 10.1016/j.sjbs.2019.05.004
- Hassan, A. H. A., Alkhalifah, D. H. M., Al Yousef, S. A., Beemster, G. T. S., Mousa, A. S. M., Hozzein, W. N., et al. (2020). Salinity stress enhances the antioxidant capacity of *Bacillus* and *Planococcus* species isolated from saline lake environment. *Front. Microbiol.* 11:561816. doi: 10.3389/fmicb.2020.561816
- Hortal, J., Carrascal, L., Triantis, K., Thébaud, E., and Meiri, S. (2013). Species richness can decrease with altitude but not with habitat diversity. *Proc. Natl. Acad. Sci. U. S. A.* 110, E2149–E2150. doi: 10.1073/pnas.1301663110
- Jack, R. W., Tagg, J. R., and Ray, B. (1995). Bacteriocins of gram-positive bacteria. *Microbiol. Rev.* 59, 171–200. doi: 10.1128/mr.59.2.171-200.1995
- Jadhav, H., Shaikh, S., and Sayyed, R. (2017). "Role of hydrolytic enzymes of rhizoflora in biocontrol of fungal phytopathogens: an overview," in *Rhizotrophs: Plant Growth Promotion to Bioremediation*, ed. S. Mehnaz (Singapore: Springer Singapore) 183–203.
- Jain, C., Rodriguez-R, L. M., Philipp, A. M., Konstantinidis, K. T., and Aluru, S. (2018). High throughput ANI analysis of 90K prokaryotic genomes reveals clear species boundaries. *Nat. Commun.* 9:5114. doi: 10.1038/s41467-018-07641-9
- Jamali, H., Sharma, A., Roohi, and Srivastava, A. K. (2020). Biocontrol potential of *Bacillus subtilis* RH5 against sheath blight of rice caused by *Rhizoctonia solani*. *J. Basic Microbiol.* 60, 268–280. doi: 10.1002/jobm.201900347
- Keswani, C., Singh, H. B., Garcia-Estrada, C., Caradus, J., He, Y.-W., Mezaache-Aichour, S., et al. (2020). Antimicrobial secondary metabolites from agriculturally important bacteria as next-generation pesticides. *Appl. Microbiol. Biotechnol.* 104, 1013–1034. doi: 10.1007/s00253-019-10300-8
- Kumar, A., Prakash, A., and Johri, B. (2011). "Bacillus as PGPR in crop ecosystem," in *Bacteria in Agrobiology: Crop Ecosystems* (Springer Berlin Heidelberg), 37–59.
- Li, Z., Chakraborty, P., de Vries, R. H., Song, C., Zhao, X., Roelofs, G., et al. (2020). Characterization of two relaxinins belonging to a novel class of circular lipopeptides that act against gram-negative bacterial pathogens. *Environ. Microbiol.* 22, 5125–5136. doi: 10.1111/1462-2920.15145
- Lugtenberg, B., and Kamilova, F. (2009). Plant-growth-promoting rhizobacteria. *Annu. Rev. Microbiol.* 63, 541–556. doi: 10.1146/annurev.micro.62.081307.162918
- O'Toole, G. A. (2011). Microtiter dish biofilm formation assay. *J. Vis. Exp.* 30:2437. doi: 10.3791/2437
- Okada, M., Sato, I., Cho, S. J., Iwata, H., Nishio, T., Dubnau, D., et al. (2005). Structure of the *Bacillus subtilis* quorum-sensing peptide pheromone ComX. *Nat. Chem. Biol.* 1, 23–24. doi: 10.1038/nchembio709
- Ongena, M., and Jacques, P. (2008). Bacillus lipopeptides: versatile weapons for plant disease biocontrol. *Trends Microbiol.* 16, 115–125. doi: 10.1016/j.tim.2007.12.009
- Pal, K. K., and McSpadden Gardener, B. (2006). Biological control of plant pathogens. *Plant Health Instr.* 2, 1117–1142. doi: 10.1094/PHI-A-2006-1117-02
- Pérez-Miranda, S., Cabriol, N., George-Téllez, R., Zamudio-Rivera, L. S., and Fernández, F. J. (2007). O-CAS, a fast and universal method for siderophore detection. *J. Microbiol. Methods* 70, 127–131. doi: 10.1016/j.mimet.2007.03.023
- Pertout, L., Caffi, T., Rossi, V., Mugnai, L., Hoffmann, C., Grandi, M. S., et al. (2017). A critical review of plant protection tools for reducing pesticide use on grapevine and new perspectives for the implementation of IPM in viticulture. *Crop Prot.* 97, 70–84. doi: 10.1016/j.cropro.2016.11.025
- Pesce, G., Rusciano, G., Sasso, A., Istitico, R., Sirec, T., and Ricca, E. (2014). Surface charge and hydrodynamic coefficient measurements of *Bacillus subtilis* spore by optical tweezers. *Colloids Surf. B Biointerfaces* 116, 568–575. doi: 10.1016/j.colsurfb.2014.01.039
- Petrillo, C., Castaldi, S., Lanzilli, M., Saggese, A., Donadio, G., Baccigalupi, L., et al. (2020). The temperature of growth and sporulation modulates the efficiency of spore-display in *Bacillus subtilis*. *Microb. Cell Factories* 19:185. doi: 10.1186/s12934-020-01446-6
- Pieterse, C. M. J., Zamioudis, C., Berendsen, R. L., Weller, D. M., Van Wees, S. C. M., and Bakker, P. A. H. M. (2014). Induced systemic resistance by beneficial microbes. *Annu. Rev. Phytopathol.* 52, 347–375. doi: 10.1146/annurev-phyto-082712-102340
- Pikovskaya, R. I. (1948). Mobilization of phosphorus in soil in connection with the vital activity of some microbial species. *Mikrobiologiya* 17, 362–370.
- Reddy, K. R. N., Reddy, C. S., and Muralidharan, K. (2009). Potential of botanical and biocontrol agents on growth and aflatoxin production by *Aspergillus flavus* infecting rice grains. *Food Control* 20, 173–178. doi: 10.1016/j.foodcont.2008.03.009
- Rodriguez-Echeverria, S., Lozano, Y. M., and Bardgett, R. D. (2016). Influence of soil microbiota in nurse plant systems. *Funct. Ecol.* 30, 30–40. doi: 10.1111/1365-2435.12594
- Rooney, A. P., Price, N. P. J., Ehrhardt, C., Swezey, J. L., and Bannan, J. D. (2009). Phylogeny and molecular taxonomy of the *Bacillus subtilis* species complex and description of *Bacillus subtilis* subsp. inaequosorus subsp. nov. *Int. J. Syst. Evol. Microbiol.* 59, 2429–2436. doi: 10.1099/ijs.0.009126-0
- Schiraldi, C., and De Rosa, M. (2016). "Mesophilic organisms," in *Encyclopedia of Membranes*, eds. E. Drioli and L. Giorno (Berlin, Heidelberg: Springer Berlin Heidelberg), 1–2.
- Schoebitz, M., Ceballos, C., and Ciampi, L. (2013). Effect of immobilized phosphate solubilizing bacteria on wheat growth and phosphate uptake. *J. Soil Sci. Plant Nutr.* 13, 1–10. doi: 10.4067/S0718-95162013005000001
- Seemann, T. (2014). Prokka: rapid prokaryotic genome annotation. *Bioinformatics* 30, 2068–2069. doi: 10.1093/bioinformatics/btu153
- Selvakumar, G., Sushil, S. N., Stanley, J., Mohan, M., Deol, A., Rai, D., et al. (2011). *Brevibacterium frigoritolerans* a novel entomopathogen of *Anomala dimidiata* and *Holotrichia longipennis* (Scarabaeidae: Coleoptera). *Biocontrol Sci. Tech.* 21, 821–827. doi: 10.1080/09583157.2011.586021
- Shultana, R., Kee Zuan, A. T., Yusop, M. R., and Saud, H. M. (2020). Characterization of salt-tolerant plant growth-promoting rhizobacteria and the effect on growth and yield of saline-affected rice. *PLoS One* 15:e0238537. doi: 10.1371/journal.pone.0238537
- Sitbon, F., Astot, C., Edlund, A., Crozier, A., and Sandberg, G. (2000). The relative importance of tryptophan-dependent and tryptophan-independent biosynthesis of indole-3-acetic acid in tobacco during vegetative growth. *Planta* 211, 715–721. doi: 10.1007/s004250000338
- van Heel, A. J., de Jong, A., Song, C., Viel, J. H., Kok, J., and Kuipers, O. P. (2018). BAGEL4: a user-friendly web server to thoroughly mine RiPPs and bacteriocins. *Nucleic Acids Res.* 46, W278–W281. doi: 10.1093/nar/gky383
- Ventosa, A., Nieto, J. J., and Oren, A. (1998). Biology of moderately halophilic aerobic bacteria. *Microbiol. Mol. Biol. Rev.* 62, 504–544. doi: 10.1128/MMBR.62.2.504-544.1998
- Xie, S.-S., Wu, H.-J., Zang, H.-Y., Wu, L.-M., Zhu, Q.-Q., and Gao, X.-W. (2014). Plant growth promotion by spermidine-producing *Bacillus subtilis* OKB105. *Mol. Plant-Microbe Interact.* 27, 655–663. doi: 10.1094/MPMI-01-14-0010-R
- Xu, S. J., and Kim, B. S. (2014). Biocontrol of fusarium crown and root rot and promotion of growth of tomato by paenibacillus strains isolated from soil. *Mycobiology* 42, 158–166. doi: 10.5941/MYCO.2014.42.2.158
- Yoon, S.-H., Ha, S.-M., Lim, J., Kwon, S., and Chun, J. (2017). A large-scale evaluation of algorithms to calculate average nucleotide identity. *Antonie Van Leeuwenhoek* 110, 1281–1286. doi: 10.1007/s10482-017-0844-4
- Zhao, X., and Kuipers, O. P. (2016). Identification and classification of known and putative antimicrobial compounds produced by a wide variety of Bacillales species. *BMC Genomics* 17:882. doi: 10.1186/s12864-016-3224-y

Conflict of Interest: The authors declare that the research was conducted in the absence of any commercial or financial relationships that could be construed as a potential conflict of interest.

Publisher's Note: All claims expressed in this article are solely those of the authors and do not necessarily represent those of their affiliated organizations, or those of the publisher, the editors and the reviewers. Any product that may be evaluated in this article, or claim that may be made by its manufacturer, is not guaranteed or endorsed by the publisher.

Copyright © 2021 Petrillo, Castaldi, Lanzilli, Selci, Cordone, Giovannelli and Istitico. This is an open-access article distributed under the terms of the Creative Commons Attribution License (CC BY). The use, distribution or reproduction in other forums is permitted, provided the original author(s) and the copyright owner(s) are credited and that the original publication in this journal is cited, in accordance with accepted academic practice. No use, distribution or reproduction is permitted which does not comply with these terms.

DATA AVAILABILITY STATEMENT

The datasets presented in this study can be found in online repositories. The names of the repository/repositories and accession number(s) can be found in the article/**Supplementary Material**.

AUTHOR CONTRIBUTIONS

RI: conceptualization, supervision, project administration, and funding acquisition. SC and CP: methodology. SC, CP, ML, and MS: validation and formal analysis. SC, CP, and DG: investigation. SC, CP, MS, AC, and RI: data curation. RI, SC, CP, and DG: writing original draft preparation. All authors have read and agreed to the published version of the manuscript.

REFERENCES

- Abriouel, H., Franz, C. M. A. P., Ben Omar, N., and Gálvez, A. (2011). Diversity and applications of *Bacillus* bacteriocins. *FEMS Microbiol. Rev.* 35, 201–232. doi: 10.1111/j.1574-6976.2010.00244.x
- Agrawal, A. A. (2001). Phenotypic plasticity in the interactions and evolution of species. *Science* 294, 321–326. doi: 10.1126/science.1060701
- Ahmad, M., Zahir, Z. A., Khalid, M., Nazli, F., and Arshad, M. (2013). Efficacy of *Rhizobium* and *Pseudomonas* strains to improve physiology, ionic balance and quality of mung bean under salt-affected conditions on farmers' fields. *Plant Physiol. Biochem.* 63, 170–176. doi: 10.1016/j.plaphy.2012.11.024
- Adler, J. (1966). Chemotaxis in Bacteria. *Science* 153, 708–716. doi: 10.1126/science.153.3737.708
- Amaya-Gómez, C. V., Porcel, M., Mesa-Garriga, L., and Gómez-Álvarez, M. I. (2020). A framework for the selection of plant growth-promoting rhizobacteria based on bacterial competence mechanisms. *Appl. Environ. Microbiol.* 86, e00760–e00820. doi: 10.1128/AEM.00760-20
- Anwar, U. B., Zwar, I. P., and de Souza, A. O. (2020). "Chapter 12: Biomolecules produced by extremophiles microorganisms and recent discoveries," in *New and Future Developments in Microbial Biotechnology and Bioengineering*, ed. A. G. Rodrigues (Elsevier), 247–270.
- Babalola, O. O. (2010). Beneficial bacteria of agricultural importance. *Biotechnol. Lett.* 32, 1559–1570. doi: 10.1007/s10529-010-0347-0
- Blin, K., Shaw, S., Steinke, K., Villebro, R., Ziemert, N., Lee, S. Y., et al. (2019). antiSMASH 5.0: updates to the secondary metabolite genome mining pipeline. *Nucleic Acids Res.* 47, W81–W87. doi: 10.1093/nar/gkz310
- Bolger, A. M., Lohse, M., and Usadel, B. (2014). Trimmomatic: a flexible trimmer for Illumina sequence data. *Bioinformatics* 30, 2114–2120. doi: 10.1093/bioinformatics/btu170
- Bunsangiam, S., Sakpuntoon, V., Srisuk, N., Ohashi, T., Fujiyama, K., and Limtong, S. (2019). Biosynthetic pathway of indole-3-acetic acid in basidiomycetous yeast *rhodospiridiobolus* fuvalis. *Mycobiology* 47, 292–300. doi: 10.1080/12298093.2019.1638672
- Cangiano, G., Mazzone, A., Baccigalupi, L., Istitato, R., Eichenberger, P., De Felice, M., et al. (2010). Direct and indirect control of late sporulation genes by GerR of *Bacillus subtilis*. *J. Bacteriol.* 192, 3406–3413. doi: 10.1128/JB.00329-10
- Cangiano, G., Sirec, T., Panarella, C., Istitato, R., Baccigalupi, L., De Felice, M., et al. (2014). The *sps* gene products affect the germination, hydrophobicity, and protein adsorption of *Bacillus subtilis* spores. *Appl. Environ. Microbiol.* 80, 7293–7302. doi: 10.1128/AEM.02893-14
- Castaldi, S., Petrillo, C., Donadio, G., Piaz, F. D., Cimmino, A., Masi, M., et al. (2021). Plant growth promotion function of *Bacillus* sp. strains isolated from salt-pan rhizosphere and their biocontrol potential against macrophomina phaseolina. *Int. J. Mol. Sci.* 22:3324. doi: 10.3390/ijms22073324
- Cauler, S., Nannan, C., Gillis, A., Licciardi, F., Bragard, C., and Mahillon, J. (2019). Overview of the antimicrobial compounds produced by members of the *Bacillus subtilis* group. *Front. Microbiol.* 10:302. doi: 10.3389/fmicb.2019.00302

ACKNOWLEDGMENTS

We thank Marcelo Anibal Carmona (Facultad de Agronomía, Cátedra de Fitopatología, Universidad de Buenos Aires, Buenos Aires, Argentina) for supplying the phytopathogenic fungi (*M. phaseolina*, *C. truncatum*, *C. nicotianae*, and *D. teres*) used in this study.

SUPPLEMENTARY MATERIAL

The Supplementary Material for this article can be found online at: <https://www.frontiersin.org/articles/10.3389/fmicb.2021.715678/full#supplementary-material>

- Cazorla, F. M., Romero, D., Pérez-García, A., Lugtenberg, B. J. J., de Vicente, A., and Bloemberg, G. (2007). Isolation and characterization of antagonistic *Bacillus subtilis* strains from the avocado rhizosphere displaying biocontrol activity. *J. Appl. Microbiol.* 103, 1950–1959. doi: 10.1111/j.1365-2672.2007.03433.x
- Celandroni, F., Vecchione, A., Cara, A., Mazzantini, D., Lupetti, A., and Ghelardi, E. (2019). Identification of *Bacillus* species: implication on the quality of probiotic formulations. *PLoS One* 14:e0217021. doi: 10.1371/journal.pone.0217021
- Cotter, P. D., Ross, R. P., and Hill, C. (2013). Bacteriocins: a viable alternative to antibiotics? *Nat. Rev. Microbiol.* 11, 95–105. doi: 10.1038/nrmicro2937
- Corrado, I., Petrillo, C., Istitato, R., Casillo, A., Corsaro, M. M., Sanna, G., et al. (2021). The power of two: An artificial microbial consortium for the conversion of inulin into Polyhydroxyalkanoates. *Int. J. Biol. Macromol.* 189, 494–502. doi: 10.1016/j.ijbiomac.2021.08.123
- Damodaran, T., Sah, V., Rai, R. B., Sharma, D. K., Mishra, V. K., Jha, S. K., et al. (2013). Isolation of salt tolerant endophytic and rhizospheric bacteria by natural selection and screening for promising plant growth-promoting rhizobacteria (PGPR) and growth vigour in tomato under sodic environment. *Afr. J. Microbiol. Res.* 7, 5082–5089. doi: 10.5897/AJMR2013.6003
- Desai, N. C., Makwana, A. H., and Rajpara, K. M. (2016). Synthesis and study of 1,3,5-triazine based thiazole derivatives as antimicrobial agents. *J. Saudi Chem. Soc.* 20, S334–S341. doi: 10.1016/j.jscc.2012.12.004
- Eren, A. M., Kiehl, E., Shaiber, A., Veseli, I., Miller, S. E., Schechter, M. S., et al. (2021). Community-led, integrated, reproducible multi-omics with anvio. *Microbiol.* 6, 3–6. doi: 10.1038/s41564-020-00834-3
- Etesami, H., Mirsyed Hosseini, H., Alikhani, H. A., and Mohammadi, L. (2014). Bacterial biosynthesis of 1-amino-cyclopropane-1-carboxylate (ACC) deaminase and indole-3-acetic acid (IAA) as endophytic preferential selection traits by rice plant seedlings. *J. Plant Growth Regul.* 33, 654–670. doi: 10.1007/s00344-014-9415-3
- Garnier, T., and Cole, S. T. (1988). Complete nucleotide sequence and genetic organization of the bacteriocinogenic plasmid, pIP404, from *Clostridium perfringens*. *Plasmid* 19, 134–150. doi: 10.1016/0147-619X(88)90052-2
- Giglio, R., Fani, R., Istitato, R., De Felice, M., Ricca, E., and Baccigalupi, L. (2011). Organization and evolution of the *cotG* and *cotH* genes of *Bacillus subtilis*. *J. Bacteriol.* 193, 6664–6673. doi: 10.1128/JB.06121-11
- Glick, B. R., Cheng, Z., Czarny, J., and Duan, J. (2007). Promotion of plant growth by ACC deaminase-producing soil bacteria. *Eur. J. Plant Pathol.* 119, 329–339. doi: 10.1007/s10658-007-9162-4
- Goberna, M., García, C., and Verdú, M. (2014). A role for biotic filtering in driving phylogenetic clustering in soil bacterial communities. *Glob. Ecol. Biogeogr.* 23, 1346–1355. doi: 10.1111/geb.12227
- Gordon, S. A., and Weber, R. P. (1951). Colorimetric estimation of indoleacetic acid. *Plant Physiol.* 26, 192–195. doi: 10.1104/pp.26.1.192
- Gupta, S., and Pandey, S. (2019). ACC deaminase producing bacteria with multifarious plant growth promoting traits alleviates salinity stress in french bean (*Phaseolus vulgaris*) plants. *Front. Microbiol.* 10:1506. doi: 10.3389/fmicb.2019.01506

CHAPTER III



International Journal of
Molecular Sciences



Article

Plant Growth Promotion Function of *Bacillus* sp. Strains Isolated from Salt-Pan Rhizosphere and Their Biocontrol Potential against *Macrophomina phaseolina*

Stefany Castaldi¹, Claudia Petrillo¹, Giuliana Donadio², Fabrizio Dal Piaz³, Alessio Cimmino⁴, Marco Masi⁴, Antonio Evidente⁴ and Rachele Isticato^{1,*}

¹ Department of Biology, University of Naples Federico II, Complesso Universitario Monte S. Angelo, Via Cinthia 4, 80126 Naples, Italy; stefany.castaldi@unina.it (S.C.); claudia.petrillo@unina.it (C.P.)

² Department of Pharmacy, University of Salerno, 84084 Fisciano, Italy; gdonadio@unisa.it

³ Department of Medicine, Surgery and Dentistry, University of Salerno, Via Giovanni Paolo II, 84084 Fisciano, Italy; fdalpiaz@unisa.it

⁴ Department of Chemical Sciences, University of Naples Federico II, Complesso Universitario Monte S. Angelo, Via Cinthia 4, 80126 Naples, Italy; alessio.cimmino@unina.it (A.C.); marco.masi@unina.it (M.M.); evidente@unina.it (A.E.)

* Correspondence: isticato@unina.it; Tel.: +39-08-167-9038

Abstract: In recent decades, intensive crop management has involved excessive use of pesticides or fertilizers, compromising environmental integrity and public health. Accordingly, there has been worldwide pressure to find an eco-friendly and safe strategy to ensure agricultural productivity. Among alternative approaches, Plant Growth-Promoting (PGP) rhizobacteria are receiving increasing attention as suitable biocontrol agents against agricultural pests. In the present study, 22 spore-forming bacteria were selected among a salt-pan rhizobacteria collection for their PGP traits and their antagonistic activity against the plant pathogen fungus *Macrophomina phaseolina*. Based on the higher antifungal activity, strain RHFS10, identified as *Bacillus vallismortis*, was further examined and cell-free supernatant assays, column purification, and tandem mass spectrometry were employed to purify and preliminarily identify the antifungal metabolites. Interestingly, the minimum inhibitory concentration assessed for the fractions active against *M. phaseolina* was 10 times lower and more stable than the one estimated for the commercial fungicide pentachloronitrobenzene. These results suggest the use of *B. vallismortis* strain RHFS10 as a potential plant growth-promoting rhizobacteria as an alternative to chemical pesticides to efficiently control the phytopathogenic fungus *M. phaseolina*.

Keywords: plant growth-promoting bacteria; spore-forming bacteria; *Bacillus vallismortis*; *Macrophomina phaseolina*; phenotypic and genotypic characterization; biocontrol agents



Citation: Castaldi, S.; Petrillo, C.; Donadio, G.; Piaz, F.D.; Cimmino, A.; Masi, M.; Evidente, A.; Isticato, R. Plant Growth Promotion Function of *Bacillus* sp. Strains Isolated from Salt-Pan Rhizosphere and Their Biocontrol Potential against *Macrophomina phaseolina*. *Int. J. Mol. Sci.* **2021**, *22*, 3324. <https://doi.org/10.3390/ijms22073324>

Academic Editor: Hans-Peter Mock

Received: 8 February 2021

Accepted: 18 March 2021

Published: 24 March 2021

Publisher's Note: MDPI stays neutral with regard to jurisdictional claims in published maps and institutional affiliations.



Copyright: © 2021 by the authors. Licensee MDPI, Basel, Switzerland. This article is an open access article distributed under the terms and conditions of the Creative Commons Attribution (CC BY) license (<https://creativecommons.org/licenses/by/4.0/>).

1. Introduction

In the last century, the world population reached a size three times greater than any previous value across the whole history of humanity. To cope with the rising request for nutrients, such as those provided by wheat and rice, current agricultural practices are based on the wide use of chemical fertilizer and pesticides. As a result, agrochemical multinationals have gradually acquired the control of global food production and modern agriculture is increasingly diverging from the traditional model [1]. Additionally, the extensive use of synthetic agrochemicals has generated heavy environmental pollution and serious risk for human and animal health due to their translocation along the food chain [1,2]. The massive use of pesticides has also led to a gradual loss of protection efficiency due to new resistances acquired by pests, with a continuous increase in pesticide dosage [2,3]. A sustainable and safe strategy to ensure crop production is to substitute agrochemicals with Plant Growth-Promoting Rhizobacteria (PGPR) as agents stimulating plant growth and health [3–5]. These beneficial microbes not only play an important role

in increasing soil fertility but also enhance the growth and vigor of the plants—PGPRs, by colonizing the roots, may enhance nutrient uptake by nitrogen fixation or P solubilization [4], reduce abiotic stresses by biofilm production [5] or regulate plant hormone production [4]. Emerging evidence has shown that rich microflora of the rhizosphere can reduce plant disease through several antagonistic mechanisms such as competition, the production of cell-wall-degrading enzymes, (e.g., chitinase, glucanase, and protease) [6], volatile compounds and siderophores [7], antibiosis or the induction of plants' systemic resistance [8]. Replacing agrochemicals with the application of PGPRs may have both economic and environmental impacts, including relevant benefits such as rising yields, reduction in or elimination of chemical residues, limited or no development of resistance by pests and pathogens, employment of agricultural raw materials, and a low risk to non-target organisms, including pollinators. For this reason, intensive research on this group of microorganisms has been taking over to develop new biofertilizers and biocontrol agents.

In this contest, *Bacillus* genera include several exo- and endophytic bacteria species and plant growth-promoting (PGP) features have been associated with different strains [9,10]. In addition to the benefits shared with other PGPR, such as solubilization of soil P, enhancement of nitrogen fixation, and siderophore production, *Bacillus* spp. are suitable as biofertilizers because: (i) their application has little, if any, effect on the composition of the soil microbial communities, being common members of the plant root microflora [11]; (ii) these bacteria may form endospores, which can survive at high temperatures and dehydration, making the formulation of a commercial product easier [12]; (iii) some *Bacillus* PGPR strains have also been reported to perform well under different environmental conditions [13]. As biocontrol agents, *Bacillus* spp. exhibit both direct and indirect mechanisms to suppress diseases caused by pathogens. These bacteria secrete a vast range of secondary metabolites, such as cell-wall-degrading enzymes, and antioxidants that assist directly the plant in its defense against pathogen attack [14]. As an indirect mechanism, *Bacillus* spp. are able to induce the acquired systemic resistance of the colonized plant [8].

This manuscript describes the screening of 22 *Bacillus* strains isolated from samples of the rhizosphere of *Juniperus sabina* [15] collected from the National Park of Ses Salines d'Eivissa, Formentera (Spain), focused on finding a PGPR strain with antagonistic activity against the phytopathogenic fungus *Macrophomina phaseolina*.

M. phaseolina (Tassi) Goid is responsible for charcoal root rot, the most common and widely spread root disease affecting more than 500 cultivated and wild plant species. The fungus is distributed worldwide and prevalently in arid areas with low rainfall and high temperature where it can survive for up to 15 years in the soil as a saprophyte [16]. *M. phaseolina* generally affects the fibrovascular system of the roots and basal internodes producing black sclerotia, which allow the fungus survival after the plants rotted [16].

Each year, this fungus induces heavy damages in agrarian plants with a high world market value, such as soy, sunflower, leguminous, and corn [16]. Soybean grains, in particular, are globally utilized not only as foods but also as substrates for feeds, fuels, and bio-based materials [17]. Thus, many efforts are made for the control of *M. phaseolina* to reduce or avoid the loss of agricultural yields and the consequent economic damage.

Additionally, PGPRs have been evaluated as biocontrol agents against *M. phaseolina* and strains belonging to *Pseudomonas* and *Bacillus* genera showed the best performance. In a study carried out by Simonetti et al. [18], two strains, namely *Pseudomonas fluorescens* 9 and *Bacillus subtilis* 54, have been assayed for antifungal activity in combination with manganese phosphite or alone and shown to significantly reduced soybean disease severity induced by *M. phaseolina* compared to the untreated control.

Several studies are still in progress to identify the main antifungal metabolites produced by PGPRs and clarify their modes of action to achieve optimum disease control.

2. Results

2.1. Isolation and Screening of Plant Growth-Promoting Spore-Forming Rhizobacteria

Aerobic spore-forming bacteria were isolated from rhizosphere samples of *J. sabina* collected in Parque Natural de Ses Salines d'Eivissa, Formentera (Spain), as described in the Materials and Methods section. A preliminary characterization based on the bacterial morphology and growth properties has allowed the selection of 22 facultative anaerobic strains, mesophiles, which are able to grow at a different pH range (Table S1).

Analysis of the DNA sequence of the 16S rRNA gene of the 22 strains allowed the identification of all of them as belonging to the *Bacillus* genus (Table S2). In order to confirm the different species obtained by BlastN analysis (Table S2), a phylogenetic analysis (Figure 1) was performed by comparing the 16S sequences with respective type strains (\bar{T}) available at the NCBI Taxonomy database. The analysis corroborated the different *Bacillus* species by >0.90 bootstrap values. All isolates belong to species commonly considered as PGPR for their ability to colonize roots [11,19] and produce antimicrobial compounds [14,19].

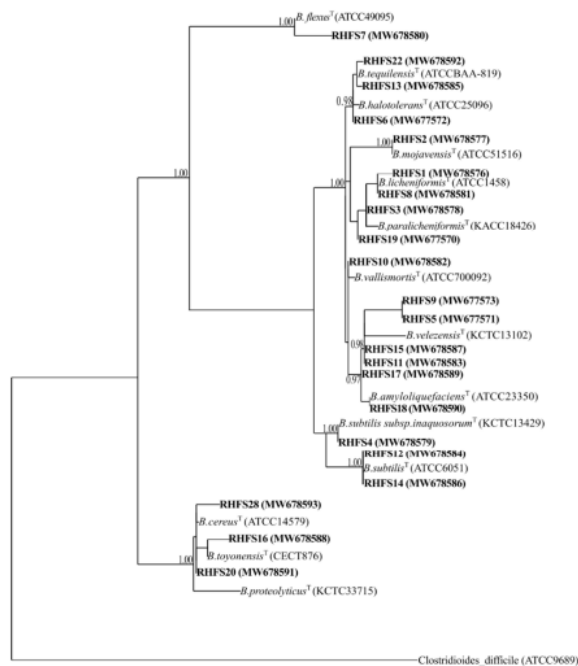


Figure 1. Phylogenetic tree of isolated rhizobacteria. The phylogenetic tree was constructed using the maximum-likelihood algorithm based on 16S rRNA gene sequences. The gene sequences of the isolated bacteria were aligned to the representative type strains (\bar{T}). The numbers in parentheses indicate the GenBank accession numbers. The percentage of replicate trees in which the associated taxa clustered together in the bootstrap test (1000 replicates) is shown next to the branches. The 16S rRNA sequence of *Clostridioides difficile* (ATCC9689) was used to assign an outgroup species.

The selected strains were analyzed for PGP traits by testing the presence of both fertilizing and biocontrol features. As summarized in Table 1, a high proportion was able to solubilize phosphate (Supplementary Figure S1), produce siderophores (Supplementary Figure S2) and indoleacetic acid, while only some of the strains were biosurfactant and biofilm producers and showed swarming motility.

Table 1. Summary of plant growth-promoting and biocontrol traits exhibited by 22 spore-forming bacteria isolates.

Strains Code	Biofertilizer Activities										Biocontrol Activities						
	Siderophores Production	PVK *	IAA *	Biofilm	Swarming	Protease Activity	Amylase Activity	Lipase Activity	Xylanase Activity	Cellulase Activity	Chitinase Activity	Catalase Activity					
RHFS1	+	-	-	+	+++	+++	+++	+	++	+	+++	+++					
RHFS2	-	++	+	+	+++	+++	+++	++	++	+	+++	-					
RHFS3	-	+	+	-	-	+++	+++	-	+++	+	+++	+++					
RHFS4	+	-	+	-	-	+++	+++	-	+	+	+++	+++					
RHFS5	+	-	+	-	-	+++	+++	-	+++	-	+++	+++					
RHFS6	-	+	++	-	-	+	-	+	+++	+	+++	+++					
RHFS7	-	+	++	-	-	+	-	+	+++	+	+++	+++					
RHFS8	++	-	-	-	+++	+++	+++	+	++	+	+++	+++					
RHFS9	+	-	-	+++	+++	+++	+++	++	+++	++	+++	+++					
RHFS10	+++	++	-	++	+++	+++	+++	++	+++	++	+++	+++					
RHFS11	-	+	+	-	-	+++	+++	+	+++	++	+++	+++					
RHFS12	-	+	+	+	-	-	+++	-	+++	++	+++	+++					
RHFS13	-	-	++	-	-	+++	+++	-	+++	++	+++	+++					
RHFS14	-	++	++	-	-	+	+	+	+++	+	+++	+++					
RHFS15	+	++	+++	+	-	++	++	+	+++	-	+++	+++					
RHFS16	+	+	++	+	-	++	++	-	+++	+	+++	+++					
RHFS17	+	++	++	+	++	+++	+++	++	+++	++	+++	+++					
RHFS18	+++	++	++	+++	++	+++	+++	++	+++	++	+++	+++					
RHFS19	++	++	+	++	++	+++	+++	++	+++	+	+++	+++					
RHFS20	+	-	+	-	-	+	+	-	++	+	+++	+++					
RHFS22	+	+	+	-	++	+++	+++	-	++	++	+++	+++					
RHFS28	-	-	-	-	-	+++	+++	-	++	++	+++	++					

+++; strong activity (formation halo ≥ 10 mm); ++; moderate activity (5 mm < halo < 10 mm); +; slight activity (halo < 5 mm); -; no activity; PVK *: Phosphate solubilization activity; IAA *: Indoleacetic acid.

Then, the potentiality as biocontrol agents of the 22 strains was tested analyzing their ability to secrete lytic enzymes (Supplementary Figure S3) [20]. As shown in Table 1, the number of protease and xylanase producers was the highest (over 90%) followed by amylase, chitinase and cellulase producers (over 80%), whereas less than 50% were lipase-producers (45%).

2.2. Antagonistic Activity of Spore-Forming Isolates against Fungal Plant Pathogen

The antagonistic activity of the 22 strains was examined against the phytopathogen *M. phaseolina* by dual-culture assay (Figure 2A).

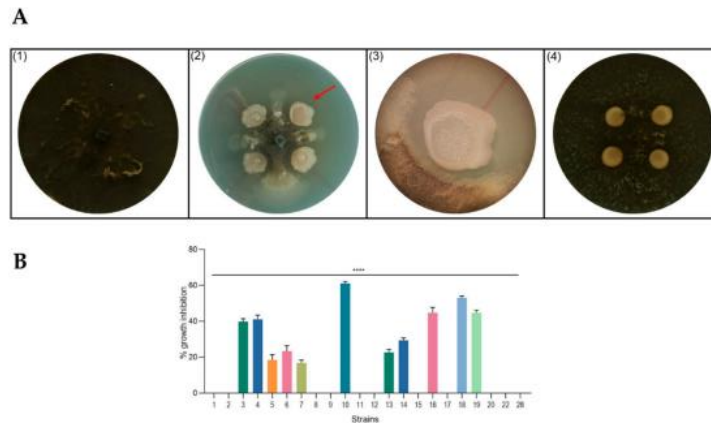


Figure 2. Antagonism assays in solid medium. **(A)** Representative photographs of dual-culture assay for in vitro inhibition of mycelial growth of *M. phaseolina* by isolated strains. (1) *M. phaseolina* (control plate); (2) example of active strain (RHFS10) against *M. phaseolina* growth; (3) images of interaction zone of RHFS10 strain and *M. phaseolina* acquired with a stereoscopic microscope (10× magnification); (4) example of inactive strain (RHFS28) against *M. phaseolina* growth; red arrow in panel 2 indicates the interaction zone magnified in panel 3. **(B)** Inhibition of fungal growth reported as the percentage reduction in the diameter of the fungal mycelia in the treated plate compared to that in the control plate. All experiments were performed in triplicate with three independent trials. Data are presented as means ± standard deviation ($n = 4$) compared to control *M. phaseolina* grown without bacteria. For comparative analysis of groups of data, one-way ANOVA was used and p values are presented in the figure: ****: extremely significant < 0.0001 .

Based on the size of the inhibition zone in dual-culture tests, some strains were found to be highly efficient against the fungal pathogen while others had limited or no antimicrobial activity (Figure 2B). For a more detailed analysis, the produced inhibition halos were observed under a stereomicroscope, highlighting agar-diffusible antifungal molecule production by the most active strains (Figure 2A, panel 3; Supplementary Figure S4).

Of all analyzed isolates, RHFS10 and RHFS18 proved to higher potentiality than PGPR, since they possess traits beneficial for both plant growth, such as the ability to solubilize phosphorus or produce siderophores, and show antagonistic ability against phytopathogens. For these reasons, both strains were selected for further experiments. Strain RHFS28, able to produce lytic enzymes but not showing antifungal activity, was selected as a negative control for the next experiments.

To assess the effect of the cell-free culture supernatants (CFSs) of RHFS10 and RHFS18 on mycelial growth, the CFSs at 24, 48, 72 and 96 h were collected and tested against *M. phaseolina*. The commercial fungicide pentachloronitrobenzene (PCNB) dissolved in toluene was used as a positive control and toluene alone was used as a negative control of

the experiments (Figure 3A). The antifungal activity increased proportionally with the growth time reaching a maximum after 72 h, specifically for the RHFS18 strain (Figure 3B). Based on the efficiency of inhibition, measured by the percentage of mycelial growth reduction, strain RHFS10 was chosen for further investigation.

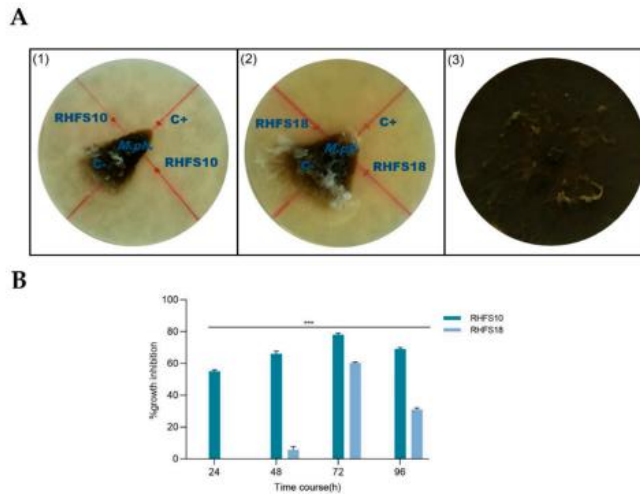


Figure 3. Antifungal activity of secreted metabolites by Plant Growth-Promoting Rhizobacteria (PGPR) strains. (A) Effects of the CSFs from RHFS10 (panel 1) and RHFS18 (panel 2) strains collected after 72 h of growth on the mycelial growth of *M. phaseolina* (panel 1). C+: Positive control, pentachloronitrobenzene; C−: Negative control, toluene. All experiments were performed in triplicate with three independent trials. (B) Antifungal activity of the Cell-Free Supernatants (CFS) of the two strains RHFS10 and RHFS18 collected from 24 to 96 h of growth. Percentage of fungal growth inhibition was reported as the percentage reduction in the diameter of the fungal mycelia compared to control plate (panel 3). Data are presented as means \pm standard deviation ($n = 3$). For comparative analysis of groups of data, one-way ANOVA was used and p values are presented in the figure: ***: extremely significant < 0.001 .

2.3. Characterization of Antifungal Metabolites

The stability of the antifungal metabolites secreted by RHFS10 was tested by incubating the CFS collected after 72 h (72-CFSs) with different proteolytic enzymes or organic solvents and then tested for inhibition of mycelial growth.

As shown in Figure 4A, the 72-CFS still had notable activity after incubation with organic solvents but decreased under the action of proteinase K or pepsin.

Thermostability was verified incubating the 72-CFS at increasing temperatures for 1 or 3 h. The results showed that treatments at 65 and 75 °C do not affect the inhibitory effect against *M. phaseolina*, while at 85 °C a reduction in the antifungal activity was observed (Figure 4B).

Finally, metabolites of the 72-CFSs were extracted with ethyl acetate at pH 2.0 and pH 7.0 and the two obtained phases were separated and tested against *M. phaseolina*. The results showed that the antifungal activity was mainly associated with the aqueous phase at pH 7.0 (data not shown). This data indicated a protein nature of the bioactive molecules in agreement with the protease sensitivity recorded in the previous tests.

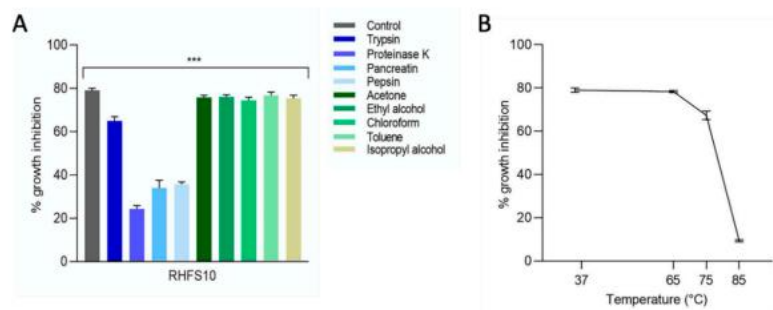


Figure 4. Stability of secreted antifungal metabolites. CFSs collected after 72 h (72-CFS) of RHFS10 was treated separately, with different enzymes and organic solvents (A) and incubated at increasing temperatures (37, 65, 75, and 85 °C) (B) and tested against *M. phaseolina*. All data represent the average of three separate experiments.

2.4. Purification of Antifungal Metabolites

To preliminarily identify the antifungal compounds released by the RHFS10 strain, 72-CFS was subjected to purification by two different steps. First, the 72-CFS was fractionated and the obtained fractions were tested against *M. phaseolina*. As shown in Figure 5A, the antifungal activity was observed in the fraction containing compounds with molecular weights between 10 and 50 kDa. In the second step of purification, the polypeptides present in 72-CFS were collected with ammonium sulfate, dialyzed to eliminate the polypeptides with a molecular weight lower than 10 kDa, and subjected to column chromatography. The three obtained fractions were tested against *M. phaseolina* and peaks 1 and 2 showed a wide zone of inhibition while no antagonistic activity was detected for the metabolites recovered in peak 3 (Figure 5B).

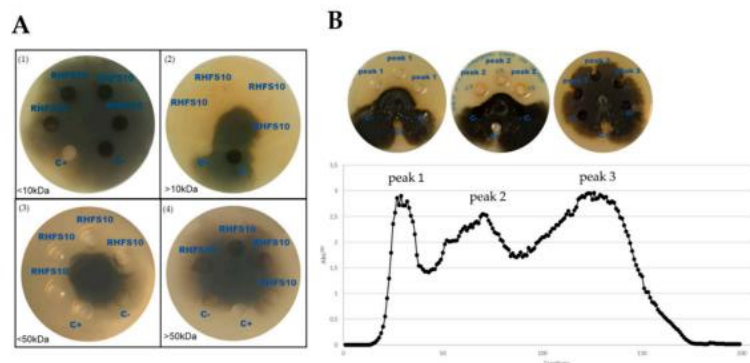


Figure 5. Antifungal activity of cell-free supernatant fractions of RHFS10. (A) 72-CFS was size-fractionated using 10, 30 kDa and 50 kDa cutoff spin columns, and the obtained fractions were tested against *M. phaseolina*. The results obtained with fractions <10 (1), >10 (2), <50 (3) and >50 kDa (4) are reported. C+: Positive control, pentachloronitrobenzene; C−: negative control, toluene; RHFS10: 0.1 mL of fractionated 72-CFS. (B) Elution profile of 72-CFS by fractionation on Sephadex G-50 fine column chromatography. The antagonist activity of the three recovered peaks (1 mg/dot) is reported in the upper part of the panel. All data represent the average of three separate experiments. ANOVA statistical analysis is extremely significant indicated— $p < 0.001$.

2.4.1. Minimum Inhibitory Concentration

Minimum inhibitory concentration (MIC) of the antifungal compounds presents in peaks 1 and 2 was determined, incubating decreasing concentrations of peaks 1 and 2 (Figure 6(A1,A2)) with *M. phaseolina* plugs. The antifungal efficiency of the compounds present in the peaks was compared to the commercial fungicide PCNB (Figure 6(A4)). The results obtained after 5 days of incubation clearly showed higher antifungal activity of peaks 1 and 2 than the fungicide PCNB. In particular, the deduced MIC for both peaks was 50 µg/mL, 10 times less than that deduced for PCNB (0.5 mg/mL). We also compared the stability of the antifungal activity over time. In this regard, the bioactive compounds present in peaks 1 and 2 perfectly retained their fungal growth inhibition for up to 14 days, while PCNB's efficiency decreased after a week. Peak 3 confirmed its inactivity (Figure 6 (A3)).

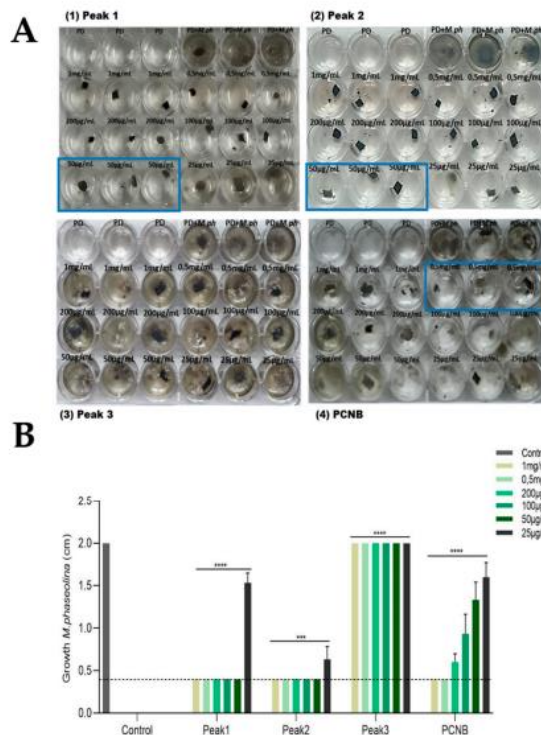


Figure 6. Minimum inhibitory concentrations of purified fractions of 72-CFS on fungal growth. (A) Minimum inhibitory concentration of the antifungal compound present in pick 1 (Panel 1), pick 2 (Panel 2) and pick 3 (Panel 3) of purified fractions of 72-CFS using a 24-well plate assay. The commercial fungicide pentachloronitrobenzene (PCNB) (Panel 4) was used as a reference. The tested concentrations are indicated. Fungal plugs incubated with only PD broth (PD + *M. phaseolina*) and the PD alone (PD) were used as a control. The blue lines represent the MICs of the tested samples. (B) Graphical representation of the MIC assay. The dotted line indicates the starting size (mm) of *M. phaseolina* plug (4 × 4 mm) at the beginning of the experiment. The results were obtained after 5 days of incubation at 28 °C. Data are presented as means ± standard deviation (*n* = 3 replication for each different concentration). ANOVA statistical analysis is extremely significant indicated—**** *p* < 0.0001 and *** *p* < 0.001.

2.4.2. Preliminary Identification of Bioactive Compounds

Finally, the three fractions were analyzed by liquid chromatography coupled with tandem mass spectrometry (LC–MS/MS). As shown in Table 2, several protease and lytic enzymes were identified in the two antifungal active peaks. Two different forms of subtilisin-like proteins were identified in peak 1, showing apparent molecular weights of 39 and 28 kDa and corresponding to the mature serine-protease and the proenzyme, respectively. Additionally, the glucuronoxylanase XynC was also detected. Both subtilisin-like protein forms were also present in peak 2, even if with a lower concentration, together with a B-glucanase, whereas peak 3 contains a metalloprotease and an alpha-amylase. As serine-proteases, beta-glucanase and glucuronoxylanase were demonstrated to act as antifungal agents [21,22], our results suggest that the activity of these secreted metabolites could be responsible, at least partially, for the antifungal action of RHFS10. To further corroborate this hypothesis, a mass spectrometry-based proteomic analysis on the previously described 72-CFSs of RHFS10 strain treated at increasing temperatures (cfr. 3.4) was performed. Again, the two forms of subtilisin and glucuronoxylanase XynC were identified in the samples retaining the antifungal activity. Interestingly, the two proteins were not detected in CFS from the negative control (RHFS28) when subjected to the same treatment. Although the genome of RHFS10 was in permanent draft stage (SAMN17389611), it allowed us to confirm the presence of all the purified protein genes, which when expressed could be involved in inhibiting fungal growth.

Table 2. The proteins identified on the three peaks are listed with their accession (AC) numbers and molecular weights.

Fractions	Mass (Da) ^a	Swiss Prot AC	Significant Sequences	Score	Description
Peak 1	47.924	XYNC_BACIU	18	1776	Glucuronoxylanase XynC OS = <i>Bacillus subtilis</i>
	39.483	SUBN_BACNA	5	1080	Subtilisin NAT OS = <i>Bacillus subtilis subsp. natto</i>
	27.42	SUBN_BACNA	5	865	Subtilisin NAT OS = <i>Bacillus subtilis subsp. natto</i>
	75.961	SACC_BACSU	1	795	Levanase OS = <i>Bacillus subtilis</i>
	38.141	PEL2_BACIU	3	566	Pectin lyase OS = <i>Bacillus subtilis</i>
Peak 2	27.365	GUB_BACAM	8	990	Beta-glucanase OS = <i>Bacillus amyloliquefaciens</i>
	39.483	SUBN_BACNA	5	800	Subtilisin NAT OS = <i>Bacillus subtilis subsp. natto</i>
	27.42	SUBN_BACNA	5	637	Subtilisin NAT OS = <i>Bacillus subtilis subsp. natto</i>
Peak 3	72.39	AMY_BACSU	1	41	Alpha-amylase OS = <i>Bacillus subtilis</i>
	34.106	MPR_BACSU	1	39	Extracellular metalloprotease OS = <i>Bacillus subtilis</i>

^a Molecular mass of the Swiss Prot sequence in the absence of molecule processing.

3. Discussion

Fungal pathogens represent one of the most common causes of plant disease and are responsible for losing a third of crops annually [23], causing economic loss and impacting global poverty. Among phytopathogenic fungi, *M. phaseolina* (Tassi) Goid is one of the most virulent and dangerous plant pathogens. The fungus is responsible for charcoal rot disease and for the consequent significant yield losses in major crops such as maize, sorghum, soybean, and common beans each year. The harmfulness of the pathogen is due to its ability to produce phytotoxins, to survive for a long time in the soil, and to target any stage of plant growth affecting seeds, seedlings, and adult plants [24]. The persistence of *M. phaseolina* in the soil and in turn its capacity to trigger plant infection depends on its ability to compete with other microorganisms of the rhizosphere—for example, competing for organic sources or host root colonization. For this reason, a growing number of studies have been focusing on the isolation and characterization of PGPRs able to limit *M. phaseolina* growth. PGPRs can not only colonize the rhizosphere improving plant growth by enhancing nutrient uptake or regulating plant hormone production, but can suppress a broad spectrum of phytopathogens, producing different antagonistic compounds or competing for nutrients.

In this contest, the focus of our research was to identify promising Bacilli rhizobacteria acting as biofertilizers and biocontrol agents against *M. phaseolina*. *Bacillus* species are a major type of rhizobacteria able to be beneficial to plants and to perform the same role as chemical fertilizers [25] and pesticides [26]. As PGPR, *Bacillus* spp. act both by

direct and indirect mechanisms, secreting phytohormones, antioxidants, solubilizing soil P, enhancing nitrogen fixation, or producing cell-wall-degrading enzymes and siderophores that promote plant growth and suppress the pathogens [27].

Moreover, the ability of the *Bacillus* spp. to produce endospores makes them more suitable candidates for PGPR-based commercial products since the resistance features of the spores can ensure the persistence of the bacteria during industrial processing and after their spread in the environment [12].

To this aim, spore-forming bacteria were isolated from salt-pan rhizosphere (Formentera, Spain) of the nurse plant *J. sabina*. As a nurse plant, *J. sabina* ensures a beneficial organization of plant communities and maintenance of biodiversity, particularly in harsh environments [28]. Growing evidence highlights that nurse plants alter the composition of soil bacterial communities, selecting microbiota that are more effective at nutrient mineralization and involved in plant growth-promoting mechanisms. Among isolates, 22 spore-forming bacteria strains were identified at a species level and first screened for their plant growth-promoting traits. More than 50% of the selected strains have shown to solubilize insoluble phosphates, to produce siderophores and secrete IAA, the main plant auxin able to regulate growth and developmental processes. These findings confirm that the rhizosphere of nurse plants is a useful source of PGPRs. Then, the biocontrol activity against the fungus *M. phaseolina* has been tested by dual-culture assay.

Among the 22 isolates, strain RHFS10, identified as *B. vallismortis*, showed the best performance for plant growth-promoting applications both as biofertilizer and biocontrol agents. The fungal growth inhibition revealed in the cell-free supernatant assay suggested the secretion of antifungal extracellular metabolites not induced by direct contact with the fungus. These data were in agreement with the stereoscopic observation of coculture experiments. Additionally, the antagonist activity of RHFS10 was not influenced by the bacterial growth stage, suggesting a constitutive production of the antimicrobial compounds.

Stability experiments revealed a thermostability of the antifungal compounds up to 75 °C and resistance to various organic solvents. Instead, the sensitivity to protease treatment as well as the association of the antifungal activity with the aqueous phase during the extraction with an organic solvent suggests a proteinaceous nature of the metabolites.

Purification experiments have associated the antifungal activity with metabolites with molecular weights between 10 and 50 kDa, while LC-MS/MS analysis revealed the presence of proteases and hydrolytic enzymes in the active fractions. In particular a glucuronoxylanase of 45 kDa and a homologous of the serine protease Subtilisin NAT from *B. subtilis* subsp. *natto* that could be directly implicated in the fungal growth inhibition. Both proteins were absent in the inactive peak, confirming their involvement in the observed antifungal activity.

There are, indeed, several functions ascribed to the release of these compounds during the stationary phase of growth. It is well known that during this very phase of their life cycle, bacteria generally release hydrolytic enzymes mainly involved in the cell wall turnover and nutritional functions, which in many cases show antimicrobial and/or antibiofilm activity [29]. Moreover, it has been lately reported that subtilisin-like proteases and glucuronoxylanases can digest fungal cell wall structural proteins [30], supporting our preliminary results. Recently, it has been shown that *B. subtilis natto* can use several fungal materials as a carbon source for growth, pointing out the role of constitutively secreted protease as a nutrient scavenger as well as a potent tool for fungal biocontrol [31].

A further important result is the higher efficiency of the purified antifungal metabolites than the commercial fungicide PCNB, used as a positive control in antagonism assays. The minimum inhibitory concentration assessed for the bacterial bioactive compounds against *M. phaseolina* growth (50 µg/mL) was 10 times lower than the one estimated for the commercial fungicide PCNB (0.5 mg/mL). Interestingly, the bacterial metabolites also appeared to be more stable over time—they retained their antifungal activity for up to two weeks, while PCNB registered an efficiency reduction after 6 days only. Hence, the purified

bacterial bioactive metabolites might be employed in lower concentrations, reaching a higher long term efficiency compared to chemical fungicides.

Altogether, these results suggest a strong antifungal effect of the protein compounds produced by the RHFS10 strain and a promising prospect for agricultural applications. The bacterial bioactive proteins could represent a valid sustainable eco-friendly fungicide and have potential as a biocontrol agent as an alternative to chemical pesticides.

Future studies will focus on the effect of the *M. phaseolina* on the expression of anti-fungal metabolites produced by RHFS10, to verify if the fungus itself may enhance the production of the bioactive compounds already detected in this study or, perhaps, trigger the expression of new metabolites. Other studies also need to optimize their large scale production and to find their best formulation for their application in field.

4. Materials and Methods

4.1. Isolation of Bacteria

Samples of the rhizosphere of *Juniperus sabina* plants were collected from the National Park of Ses Salines d'Eivissa, Formentera (Spain). To isolate rhizospheric bacteria, 1 g of roots samples was washed three times with 2 mL sterile distilled water to remove impurities, transferred into 9 mL $1 \times$ PBS, and vortexed. The selection of spore-forming strains was promoted through a heat pretreatment at 80 °C to kill all vegetative cells. In total, 1 mL of the mixture was inoculated into 9 mL of LB (8 g/L NaCl, 10 g/L tryptone, 5 g/L yeast extract), serially diluted up to 10^{-6} and 0.1 mL of each dilution were spread on LB agar plates. Plates were incubated at 30 ± 1 °C for 2–3 days. Pure cultures were obtained by serial subculturing. Glycerol stocks of the isolates were prepared and stored at -80 °C.

4.2. Growth Conditions

Each bacterial isolate was characterized by visual inspection for colony color and morphology, such as colony shape, size, margin and appearance. The ability to grow in facultative anaerobic conditions was determined using the AnaeroGen sachets (Unipath Inc., Nepean, ON, Canada) placed in a sealed jar with bacteria streaked on LB agar plates and incubated at 37 °C for 3–4 days. To determine the optimum growth conditions, the bacterial isolates were grown in LB agar at different pH (2.0, 4.0, 6.0, 7.0, 8.0, 10.0, 12.0) [32] and temperature (4, 15, 25, 37, 50, 60 °C) ranges [33]. Plates were incubated until the appearance of bacterial colonies.

4.3. Isolates Identification by PCR Amplification of 16S rRNA

Exponentially growing cells were used to extract chromosomal DNA using the DNeasy PowerSoil kit (Qiagen, Hilden, Germany) according to the manufacturer's instructions. 16S rRNA gene was PCR amplified by using chromosomal DNA as a template and oligonucleotides forward 8F (5'-AGTTTGATCCTGGCTCAG-3' annealing at position + 8/+ 28) and reverse 1517R (5'-ACGGCTACCTGTGTTACGACT-3' annealing at position + 1497/+ 1517). These two oligonucleotides were designed to amplify a 1500 bp DNA fragment and the reaction was carried out according to Grönemeyer et al. [34] in an Esco SwiftTM Max-Pro Thermal Cycler. The 1500 bp DNA amplified fragment was sequenced at the Bio-Fab research sequencing facility and analyzed using Basic Local Alignment Search Tool (BLAST). Phylogenetic analyses were carried out using Seaview 4.4.0 software package (<http://pbil.univ-lyon1.fr/software/seaview.html>, accessed on 7 January 2020) on 16S ribosomal RNA genes aligned using the Muscle algorithm. All 16S rRNA sequences were deposited in the NCBI Sequence Read Archive and identified with the accession number as shown in Table S1.

Phylogenetic reconstruction for nucleotide alignment was carried out using the maximum likelihood algorithm (PhyLM). The gene sequences of the isolated bacteria were aligned to the representative type strains (^T) belonging to the same species obtained from

BlastN analysis. The percentage of replicate trees in which the associated taxa clustered together in the bootstrap test (1000 replicates) is shown next to the branches.

4.4. *In Vitro* Screening for Plant Growth-Promoting (PGP) Traits

4.4.1. Phosphate Solubilization

The ability to solubilize inorganic phosphate was tested by growing the bacterial isolates on Pikovskaya agar (Oxoid Ltd., Hampshire, UK) dyed with bromophenol blue [35] for 10 days at 30 °C. The formation of more transparent zones around the bacterial colonies was indicative of inorganic phosphate solubilization on Pikovskaya agar.

4.4.2. Siderophore Production

To test siderophores production, 3 µL of overnight-grown culture in LB medium was spot-inoculated on iron-free S7 agar minimal medium. After 72 h of incubation at 28 °C, 10 mL of Chrome Azurol S (CAS) agar medium [36] was applied over agar plates containing cultivated microorganisms. Development of yellow-orange halo zone around bacterial spots was observed after 1 h of incubation.

4.4.3. Indole Acetic Acid Detection

To detect the IAA production, the bacteria were grown in LB broth for 72 h at 37 °C with shaking at 150 rpm. After, 2 mL of bacteria supernatant was mixed with 4 mL of Salkowski reagent (0.5 M FeCl₃ in 35% HClO₄ solution) and 2 drops of orthophosphoric acid, and was finally incubated for 30 min at 25 °C. The development of pink color indicates IAA production [37].

4.4.4. Biosurfactant Production

The bacterial strains were spot-inoculated on blood agar plates (BBL™ Trypticase™ Soy Agar (TSA II) with 5% Horse Blood) and after 72 h of incubation at 28 °C, the clear zone around the colonies indicates a positive result [38].

4.4.5. Swarming Motility

Bacterial isolates were analyzed for their swarming motility using LB with spot-inoculation on agar 0.7% and incubated at 37 °C overnight.

4.4.6. Biofilm Production

To evaluate the ability to produce biofilm, the isolates were separately grown in glass tubes in LB medium as described by Haney et al. (2018) [39]. Cultures were inoculated by adding 10 µL of an overnight culture of bacteria into 1 mL of sterile media, and the tubes were incubated statically at either 37 °C for 48 h.

4.5. Evaluation of Potential Biocontrol Features

4.5.1. Screening for Hydrolytic Enzymatic Activity

Twenty-two bacterial isolates were grown separately in 5 mL of LB broth at 37 °C overnight with shaking at 150 rpm. In total, 3 µL of each fresh bacterial culture was spot-inoculated on different assay plates to test hydrolytic enzyme activity. The protease activity was performed on Skimmed Milk Agar (SMA) [40] and the lipase activity on Tributylurea Agar medium [41]. After overnight at 37 °C, the formation of a clear halo around the colony was considered as positive production of these enzymes. To detect the amylase activity was used the method described by Sethi et al. (2013) [42] with Starch Agar plates. After the overnight incubation at 37 °C, the plates were flooded with iodine solution and the hydrolysis of starch was observed as a colorless zone with a violet background around grown colonies. For the detection of cellulase and xylanase activities, Xylanase Production Medium (XPM) agar plates were used with 0.5% xylan [43] (Megazyme) and a minimal medium with 0.5% carboxymethylcellulose (CMC) [44] as a sole carbon source. The plates were incubated at 37 °C for 3 days after which hydrolysis

zones were visualized by flooding the plates with 0.1% Congo Red for 15–20 min and then destained by washing twice with 1 M NaCl. Plates, where CMC and xylan were omitted, were used as nonsubstrate controls. Transparent hydrolytic zones around the colonies were considered positive. For the chitinase activity, the bacterial strains were spot-inoculated on colloidal chitin-containing medium plates [45]. After incubation at $25 \pm 2^\circ\text{C}$ for 2–3 days, the clear zones around or within the colonies are considered positive evidence. The catalase activity was checked qualitatively as described by Geetha et al. (2014) [46]. Three percent H_2O_2 was added (3–4 drops) on the colonies grown on LB agar plates; effervescences of O_2 released from the bacterial colonies indicate the positivity of catalase activity.

All experiments were performed in triplicate.

4.5.2. Dual-Culture Assay

The isolated strains were examined in vitro for antifungal activity against pathogenic fungus *M. phaseolina* (Tassi) Goid (ATCC[®] 64334TM). The fungus was obtained from infected soybean roots growing in Pergamino, Buenos Aires, Argentina, and it was maintained on Potato Dextrose Agar (PDA) in Petri dishes.

The in vitro antifungal bioassays were carried out based on the dual-culture method as previously described by Khamn et al. (2009) [47] with some modifications.

Fungal plugs of 6×6 mm diameter were placed at the center of PDA plates and $5 \mu\text{L}$ of bacteria strains overnight grown in LB broth was placed on the opposite four sides of the plates at 1.5 cm away from the fungal disc. Plates containing the fungal plugs without bacterial inoculation were used as control plates. All plates were incubated at 28°C for five days. The percentage of inhibition of the fungal growth was calculated using the following formula:

$$\% = [(Rc - Ri)/Rc] \times 100$$

where Rc is the radial growth of the test pathogen in the control plates (mm), and Ri is the radial growth of the test pathogen in the test plates (mm). The experiment was repeated thrice. Bacterial strains that showed an inhibition of the growth of pathogenic fungus were observed by stereoscopic microscope $10\times$ magnification.

4.5.3. Antifungal Assay of Cell-Free Supernatants (CFSs)

Bacteria were grown on LB at $28 \pm 2^\circ\text{C}$ and aliquots of the suspensions, collected at 24 h intervals for the first 96 h. Cells were removed by centrifugation ($7000 \times g$ for 30 min) and supernatants were filtered using $0.22 \mu\text{m}$ -pore-diameter membranes (Corning[®]) and concentrated 1:10. Then, $20 \mu\text{L}$ aliquots of sterilized supernatant samples were placed on the opposite four sides of the PDA plate at 1.5 cm from the fungal disc (6×6 mm diameter) of *M. phaseolina* [48]. As a positive control, fungicidal pentachloronitrobenzene $\geq 94\%$ (PCNB) (Sigma-Aldrich, Saint-Louis, MO, USA) dissolved in toluene was used. Toluene alone was used as a negative control. Plates were prepared in triplicate, incubated at 28°C for 5 days, and examined for zones of inhibition of grown colonies.

4.6. Extraction of Secondary Metabolites

The strains were grown in 300 mL of LB at $28 \pm 2^\circ\text{C}$ and for 72 h. The broth cultures were then centrifuged at $9000 \times g$ for 30 min at 4°C and filtered through a $0.22 \mu\text{m}$ syringe filter. The culture filtrate was extracted at pH7 and pH2 three times for each, mixed with an equal volume of EtOAc into the separating funnel, and shaken for complete extraction. The secondary compounds contained in the solvent phase were separated from the aqueous phase, dried with Na_2SO_4 , and evaporated under reduced pressure to yield the crude extracts. The crude extracts were dissolved in 1 mL 2% methanol at a final concentration of 5 mg/mL, the aqueous phase was concentrated 1:10. All fractions were tested against *M. phaseolina* on PDA plates and incubated at $28 \pm 2^\circ\text{C}$ for 5 days.

4.7. Stability of Antifungal Metabolites at Different Enzymes, Temperatures and Organic Solvent Conditions

In total, 100 µg/mL of enzymes (trypsin, proteinase K, pancreatin and pepsin) and 10% organic solvents (acetone, ethyl alcohol, chloroform, toluene and isopropyl alcohol) (see Figure 4) were added to 100 µL of culture supernatant. Enzyme-treated samples were incubated for 3 h at 37 °C (42 °C in the case of proteinase K) and the solvent-treated samples were incubated for 3 h at 25 °C and subsequently, 100 µL aliquots were tested for antifungal activity as described above. To assess the stability of the bioactive compounds at high temperatures, CSFs were incubated at 65, 75 and 80 °C for 1 or 3 h, and their activity toward *M. phaseolina* eventually tested.

4.8. Size-Fractionated Supernatants Tested for Antifungal Activity

RHFS10 strain was grown in 100 mL of LB broth for 72 h at 28 °C. The cultures were centrifuged at 7000× g for 30 min at 4 °C and the supernatants filter-sterilized with a 0.22 µm filter (Millipore, Bedford, MA, USA). The supernatants were size-fractionated (10, 30 and, 50 kDa cutoff spin column; Centricon, Millipore). Fractions were tested for antifungal activity and reported as a percentage of growth inhibition as described above.

4.9. LC-MS/MS Analyses

Protein extracts were electrophoretically separated on a 12.5% polyacrylamide gel, under denaturing conditions. Resulting lines were divided into 10 pieces, and each underwent trypsin in gel digestion procedure. NanoUPLC-hrMS/MS analyses of the resulting peptides mixtures were carried out on a Q-Exactive orbitrap mass spectrometer (Thermo Fisher Scientific, Waltham, MA, USA), coupled with a nanoUltimate300 UHPLC system (Thermo Fisher Scientific). Peptides separation was performed on a capillary EASY-Spray C18 column (0.075 × 100, 1.7 µm, Thermo Fisher Scientific) using aqueous 0.1% formic acid (A) and CH₃CN containing 0.1% formic acid (B) as mobile phases and a linear gradient from 3% to 30% of B in 60 min and a 300 nL min⁻¹ flow rate. Mass spectra were acquired over an *m/z* range from 350 to 1500. To achieve protein identification, MS and MS/MS data underwent Mascot software (Matrix Science, London, UK) analysis using the nonredundant Data Bank UniProtKB/Swiss-Prot (Release 2020_03). Parameter sets were: trypsin cleavage; carbamidomethylation of cysteine as a fixed modification and methionine oxidation as a variable modification; a maximum of two missed cleavages; false discovery rate (FDR), calculated by searching the decoy database, ≤0.05. A comparison between the proteins found in the different samples allowed discriminating those specifically expressed by the strains showing promising antifungal activity.

4.10. Detection of Antifungal Metabolites

RHFS10 strain was grown in 2 L of LB broth at 28 °C for 72 h with shaking at 150 rpm. The cells were removed by centrifugation (9000× g, 30 min) and the supernatant fluid was filter-sterilized using 0.22 µm-pore-diameter membranes. The antifungal activity of the preparation was determined against *M. phaseolina* using the cell-free supernatant assay described above. The culture filtrate (1800 mL) was precipitated with ammonium sulfate (66% w/v saturation) and stored overnight at 4 °C with shaking. The precipitate was removed by centrifugation (12,000× g, 20 min, 4 °C), resuspended in PBS 1× buffer (0.01 mol/L⁻¹, pH 6.5; 1/10 of the initial volume) and dialyzed against the same buffer for 48 h at 4 °C with several changes (dialysis tube, porosity 24, cutoff 12 kDa; Union Carbide Corporation, Danbury, CT, USA). The dialyzed precipitate was lyophilized, and the residue (483 mg) was dissolved in 6 mL ultrapure Milli-Q water and applied to a Sephadex G-50 fine column (Pharmacia, Uppsala, Sweden; 4.5 × 40 cm; flow rate 2.5 mL/min⁻¹). The column fractions (3 mL each) were collected in homogeneous groups according to the chromatogram obtained by monitoring proteins concentration at 280 nm [49]. Fractions were lyophilized, tested for antifungal activity (1 mg/dot) against *M. phaseolina*, and analyzed by SDS-PAGE. The SDS-PAGE was performed with 20 µg of total proteins, fractionated on 12.5% SDS polyacrylamide gels and stained by Brilliant Blue Coomassie.

Protein concentration was determined with the Bradford assay (Bio-Rad Protein Assay, Hercules, CA, USA; cat no. 500-0006) with bovine serum albumin used as standard.

4.11. Minimum Inhibitory Concentrations

The MIC determination was performed in 24-well culture plates according to the method described by Agrillo et al. (2019) [50] with some modification. The wells were prepared in triplicate for each concentration. The retentates (peaks 1, 2, and 3) containing the antifungal compounds were diluted separately at different concentrations (1 mg/mL; 0.5 mg/mL; 200 µg/mL; 100 µg/mL; 50 µg/mL and 25 µg/mL) in a volume of 500 µL of ultrapure Milli-Q water and were inoculated with 500 µL of *M. phaseolina* plugs (4 × 4 mm) resuspended in 2 × PD broth. As a control, 500 µL of *M. phaseolina* plugs (4 × 4 mm) were resuspended in 2 × PD broth diluted with 500 µL of ultrapure Milli-Q water. The retentates were compared with the fungicidal PCNB ≥94% (Sigma-Aldrich) at the same different concentrations. The plates were incubated at 28 °C for 5 days and the MIC was taken as the lowest concentration of antifungal agent at which there was no visible growth of the fungus after incubation. Finally, the percentage of inhibition of the fungal growth was calculated using the formula described above.

4.12. Whole-Genome Sequencing

The most promising bacterial strain, RHFS10, which showed outstanding biocontrol performance, was selected for whole-genome sequencing to obtain future relevant genetic information. DNA extraction was performed using the method described above. Genome sequencing was performed by MicrobesNG (Birmingham, UK) with the genomic DNA library prepared using the Nextera XT library prep kit (Illumina) following the manufacturer's protocol. Libraries were sequenced on the Illumina HiSeq using a 250 bp paired-end protocol. Reads were adapter trimmed using Trimmomatic 0.30 with a sliding window quality cutoff of Q15 [51] and de novo genome assembly was carried out with SPAdes (version 3.7) via MicrobesNG (University of Birmingham, Birmingham, UK).

4.13. Statistical Analysis

All the statistical analyses were performed using GraphPad Prism 8 software. Data were expressed as mean ± SEM. Differences among groups were compared by ANOVA or t-test as indicated in figure legends. Differences were considered statistically significant at $p < 0.05$.

Supplementary Materials: The following are available online at <https://www.mdpi.com/1422-0067/22/7/3324/s1>: Table S1. Preliminary characterization of spore-forming bacteria isolated from the rhizosphere of *J. sabina* plants. Table S2. 16S rRNA gene-based molecular identity of isolated spore-forming bacteria, their accession numbers, and strain identification is reported. Figure S1. Potential plant growth-promoting traits of selected bacterial isolates. Figure S2. Potential plant growth-promoting traits of selected bacterial isolates. Figure S3. Hydrolytic activities of selected bacterial isolates. Figure S4. Preliminary dual-culture assay.

Author Contributions: Conceptualization, R.I.; methodology, S.C., C.P., A.C., and G.D.; validation, and formal analysis, S.C. and G.D.; investigation, S.C., M.M. and F.D.P.; data curation, S.C., A.E. and R.I.; writing—original draft preparation, R.I., S.C., and C.P.; supervision, R.I.; project administration, R.I.; funding acquisition, R.I. All authors have read and agreed to the published version of the manuscript.

Funding: This work was supported by POR Campania FSE 2014-2020 ASSE III-Ob. Sp. 14 Az. 10.5.2-Avviso Pubblico "Dottorati di Ricerca con Caratterizzazione Industriale"—D.D.n.155 del 17.05.2018 CUP E66C18000900002 CML OP_7741 18062AP000000001.

Informational Review Board Statement: Not applicable.

Informed Consent Statement: Not applicable.

Data Availability Statement: Not applicable.

Acknowledgments: We thank Marcelo Anibal Carmona (Facultad de Agronomía, Cátedra de Fitopatología, Universidad de Buenos Aires, Buenos Aires, Argentina) to supply the strain of *Macrophomina phaseolina* used in this study.

Conflicts of Interest: The authors declare no conflict of interest.

References

1. Nicolopoulou-Stamati, P.; Maipas, S.; Kotampasi, C.; Stamatis, P.; Hens, L. Chemical Pesticides and Human Health: The Urgent Need for a New Concept in Agriculture. *Front. Public Health* **2006**, *4*, 148. [\[CrossRef\]](#)
2. Syed Ab Rahman, S.F.; Singh, E.; Pieterse, C.M.J.; Schenk, P.M. Emerging microbial biocontrol strategies for plant pathogens. *Plant Sci.* **2018**, *267*, 102–111. [\[CrossRef\]](#)
3. Cimmino, A.; Masi, M.; Evidente, M.; Superchi, S.; Evidente, A. Fungal phytotoxins with potential herbicidal activity: Chemical and biological characterization. *Nat. Prod. Rep.* **2015**, *32*, 1629–1653. [\[CrossRef\]](#)
4. Oleńska, E.; Malek, W.; Wójcik, M.; Swiecick, I.; Thijs, S.; Vangronsveld, J. Beneficial features of plant growth-promoting rhizobacteria for improving plant growth and health in challenging conditions: A methodical review. *Sci. Total Environ.* **2020**, *743*, 140682. [\[CrossRef\]](#) [\[PubMed\]](#)
5. Bhat, M.A.; Kumar, V.; Bhat, M.A.; Wani, I.A.; Dar, F.L.; Farooq, I.; Bhatti, F.; Koser, R.; Rahman, S.; Jan, A.T. Mechanistic Insights of the Interaction of Plant Growth-Promoting Rhizobacteria (PGPR) With Plant Roots Toward Enhancing Plant Productivity by Alleviating Salinity Stress. *Front. Microbiol.* **2020**, *11*, 1952. [\[CrossRef\]](#) [\[PubMed\]](#)
6. Pal, K.K.; McSpadden Gardener, B. Biological Control of Plant Pathogens. *Plant Health Instr.* **2006**, *36*, 37–45. [\[CrossRef\]](#)
7. Miljković, D.; Marinković, J.; Balešević-Tubić, S. The Significance of *Bacillus* spp. in Disease Suppression and Growth Promotion of Field and Vegetable Crops. *Microorganisms* **2020**, *7*, 1037. [\[CrossRef\]](#)
8. Meena, M.; Swapnil, P.; Divyanshu, K.; Kumar, S.; Harish; Tripathi, Y.N.; Zehra, A.; Marwal, A.; Upadhyay, R.S. PGPR-mediated induction of systemic resistance and physicochemical alterations in plants against the pathogens: Current perspectives. *J. Basic Microbiol.* **2020**, *60*, 828–861. [\[CrossRef\]](#)
9. Gamez, R.; Montes, M.; Ramirez, S.; Schnell, S.; Rodriguez, F. Screening, plant growth promotion and root colonization pattern of two rhizobacteria (*Pseudomonas fluorescens* Ps006 and *Bacillus amyloliquefaciens* Bs006) on banana cv. Williams (Musa acuminata Colla). *Microbiol. Res.* **2019**, *220*, 12–20. [\[CrossRef\]](#)
10. Tamošiūnė, I.; Staniene, G.; Haimi, P.; Stany, V.; Rugienius, R.; Baniulis, D. Endophytic *Bacillus* and *Pseudomonas* spp. Modulate Apple Shoot Growth, Cellular Redox Balance, and Protein Expression Under in Vitro Conditions. *Front. Plant Sci.* **2018**, *9*, 889. [\[CrossRef\]](#)
11. Rabbee, M.F.; Ali, M.S.; Choi, J.; Hwang, B.S.; Jeong, S.C.; Baek, K.H. *Bacillus velezensis*: A Valuable Member of Bioactive Molecules within Plant Microbiomes. *Molecules* **2019**, *24*, 1046. [\[CrossRef\]](#) [\[PubMed\]](#)
12. Pesce, G.; Rusciano, G.; Sasso, A.; Istitico, R.; Sirec, T.; Ricca, E. Surface charge and hydrodynamic coefficient measurements of *Bacillus subtilis* spore by optical tweezers. *Colloids Surf. B* **2014**, *116*, 568–575. [\[CrossRef\]](#) [\[PubMed\]](#)
13. Gardner, B.B.M. Ecology of *Bacillus* and *Paenibacillus* spp. in Agricultural System. *Phytopathology* **2004**, *94*, 1252–1258. [\[CrossRef\]](#)
14. Raaijmakers, J.M.; De Bruijn, L.; Nybroe, O.; Ongena, M. Natural functions of lipopeptides from *Bacillus* and *Pseudomonas*: More than surfactants and antibiotics. *FEMS Microbiol. Rev.* **2010**, *34*, 1037–1062. [\[CrossRef\]](#) [\[PubMed\]](#)
15. Rodrigue-Echeverria, S. Influence of soil microbiota in nurse plant systems. *Funct. Ecol.* **2015**, *30*, 30–40. [\[CrossRef\]](#)
16. Kaur, S.; Dhillon, G.S.; Brar, S.K.; Vallad, G.E.; Chand, R.; Chauhan, V.B. Emerging phytopathogen *Macrophomina phaseolina*: Biology, economic importance and current diagnostic trends. *CR Microbiol.* **2012**, *38*, 136–151. [\[CrossRef\]](#)
17. Pagano, M.C.; Miransari, M. The importance of soybean production worldwide. *Soybean Prod.* **2016**, *1*, 1–26. [\[CrossRef\]](#)
18. Simonetti, E.; Viso, N.P.; Montecchia, M.; Zilli, C.; Balestrasse, K.; Carmona, M. Evaluation of native bacteria and manganese phosphite for alternative control of charcoal root rot of soybean. *Microbiol. Res.* **2015**, *180*, 40–48. [\[CrossRef\]](#)
19. Bacher, R.; Rokem, J.S.; Ilangumaran, G.; Lamont, J.; Praslickova, D.; Ricci, E.; Subramanian, S.; Smith, D.L. Plant Growth-Promoting Rhizobacteria: Context, Mechanisms of Action, and Road map to Commercialization of Biostimulants for Sustainable Agriculture. *Front. Plant Sci.* **2018**, *9*, 1473. [\[CrossRef\]](#)
20. Jadhav, H.; Shaikh, S.S.; Sayyed, R. Role of Hydrolytic Enzymes of Rhizoflora in Biocontrol of Fungal Phytopathogens: An Overview. *Rhizotrophs Plant Growth Promot. Bioremed.* **2017**, *978*, 183–203. [\[CrossRef\]](#)
21. Hong, T.-T.; Meng, M. Biochemical characterization and antifungal activity of an endo-1,3-beta-glucanase of *Paenibacillus* sp. isolated from garden soil. *Appl. Microbiol. Biotechnol.* **2003**, *61*, 472–478. [\[CrossRef\]](#)
22. Tariq, M.; Noman, M.; Ahmed, T.; Hameed, A.; Manzoor, N.; Zafar, M. Antagonistic features displayed by Plant Growth Promoting Rhizobacteria (PGPR): A Review. *J. Plant Sci. Phytopathol.* **2017**, *1*, 38–43. [\[CrossRef\]](#)
23. Fisher, M.C.; Henk, D.A.; Briggs, C.J.; Brownstein, J.S.; Madoff, L.C.; McCraw, S.L.; Gurr, S.L. Emerging fungal threats to animal, plant and ecosystem health. *Nature* **2012**, *482*, 186–194. [\[CrossRef\]](#) [\[PubMed\]](#)
24. Masi, M.; Sautua, F.; Zatout, R.; Castaldi, S.; Arrico, L.; Istitico, R.; Peditelli, G.; Carmona, M.A.; Evidente, A. Phaseocyclopentenones A and B, Phytotoxic Penta- and Tetrasubstituted Cyclopentenones Produced by *Macrophomina phaseolina*, the Causal Agent of Charcoal Rot of Soybean in Argentina. *J. Nat. Prod.* **2021**, *84*, 459–465. [\[CrossRef\]](#) [\[PubMed\]](#)
25. Bhattacharyya, P.N.; Jha, D.K. Plant growth-promoting rhizobacteria (PGPR): Emergence in agriculture. *World J. Microbiol. Biotechnol.* **2012**, *28*, 1327–1350. [\[CrossRef\]](#) [\[PubMed\]](#)

26. Khan, N.; Martínez-Hidalgo, P.; Ice, T.A.; Maymon, M.; Humm, E.A.; Nejat, N.; Sanders, E.R.; Hirsch, A.M. Antifungal Activity of *Bacillus* Species Against *Fusarium* and Analysis of the Potential Mechanisms Used in Biocontrol. *Front. Microbiol.* **2018**, *320*, 175–189. [CrossRef] [PubMed]
27. Cazorla, F.M.; Romeo, D.; Pérez-García, A.; Lugtenberg, B.J.J.; De Vincente, A.; Bloemberg, G. Isolation and characterization of antagonistic *Bacillus subtilis* strains from the avocado rhizosphere displaying biocontrol activity. *J. Appl. Microbiol.* **2007**, *103*, 1950–1959. [CrossRef]
28. Taniguchi, T.; Usuki, H.; Kikuchi, J.; Hirobe, M.; Miki, N.; Fukuda, K.; Zhang, G.; Wang, L.; Yoshikawa, K.; Yamanaka, N. Colonization and community structure of root-associated microorganisms of *Sabina vulgaris* with soil depth in a semiarid desert ecosystem with shallow groundwater. *Mycorrhiza* **2012**, *22*, 419–428. [CrossRef]
29. Corvey, C.; Stein, T.; Düsterhus, S.; Karas, M.; Entian, K.-D. Activation of subtilin precursors by *Bacillus subtilis* extracellular serine proteases subtilisin (AprE), WprA, and Vpr. *Biochem. Biophys. Res. Commun.* **2003**, *304*, 48–54. [CrossRef]
30. Yan, L.; Qian, Y. Cloning and heterologous expression of SS10, a subtilisin-like protease displaying antifungal activity from *Trichoderma harzianum*. *FEMS Microbiol. Lett.* **2009**, *290*, 54–61. [CrossRef]
31. Schönbichler, A.; Díaz-Moreno, S.M.; Srivastava, V.; McKee, S.L. Exploring the Potential for Fungal Antagonism and Cell Wall Attack by *Bacillus subtilis* natto. *Front. Microbiol.* **2020**, *31*, 11–521. [CrossRef]
32. Cangiano, G.; Sirec, T.; Panarella, C.; Istitato, R.; Baccigalupi, L.; De Felice, M.; Ricca, E. The sps Gene Products Affect the Germination, Hydrophobicity, and Protein Adsorption of *Bacillus subtilis* Spores. *Appl. Environ. Microbiol.* **2014**, *80*, 7293–7302. [CrossRef] [PubMed]
33. Petrillo, C.; Castaldi, S.; Lanzilli, M.; Saggese, A.; Donadio, G.; Baccigalupi, L.; Ricca, E.; Istitato, R. The temperature of growth and sporulation modulates the efficiency of spore-display in *Bacillus subtilis*. *Microb. Cell Factories* **2020**, *19*, 185. [CrossRef] [PubMed]
34. Gronemeyer, J.L.; Burbano Roa, C.S.; Hurek, T.; Reinhold-Hurek, B. Isolation and characterization of root-associated bacteria from agricultural crops in the Kavango region of Namibia for Plant Growth Promoting Characteristics. *Plant Soil* **2012**, *71*, 566–571. [CrossRef]
35. Schoebitz, M.; Ceballos, C.; Ciampì, L. Effect of immobilized phosphate solubilizing bacteria on wheat growth and phosphate uptake. *J. Soil Sci. Plant Nutr.* **2013**, *12*, 1–10. [CrossRef]
36. Pérez-Miranda, S.; Cabirol, N.; George-Téllez, R.; Zamudio-Rivera, L.S.; Fernández, F.J. O-CAS, a fast and universal method for siderophore detection. *J. Microb. Methods* **2007**, *70*, 127–131. [CrossRef]
37. Damodaran, T.; Sah, V.; Nishra, V.K.; Jha, S.K.; Kannan, R. Isolation of salt tolerant endophytic and rhizospheric bacteria by natural selection and screening for promising plant growth-promoting rhizobacteria (PGPR) and growth vigour in tomato under sodic environment. *Afr. J. Microb. Res.* **2013**, *7*, 5082–5089. [CrossRef]
38. Sarwar, S.; Brader, G.; Corretto, E.; Aleti, G.; Abaidullah, M.; Sessitsch, A.; Hafeez, F.Y. Qualitative analysis of biosurfactants from *Bacillus* species exhibiting antifungal activity. *PLoS ONE* **2018**, *13*, e0198107. [CrossRef]
39. Haney, E.F.; Brito-Sánchez, Y.; Trimble, M.J.; Mansour, S.C.; Cherkasov, A.; Hancock, R.E.W. Computer-aided discovery of peptides that Effect of phosphate solubilizing *Pseudomonas putida* on the growth of maize and its survival in the rhizosphere specifically attack bacterial biofilms. *Sci. Rep.* **2018**, *8*, 1871. [CrossRef]
40. Morris, L.S.; Evans, J.; Marchesi, R. A robust plate assay for detection of extracellular microbial protease activity in metagenomic screens and pure cultures. *J. Microbiol. Methods* **2012**, *91*, 144–146. [CrossRef]
41. Parsad, M.P.; Manjunath, K. Effect of media and process parameters in the enhancement of extracellular lipase production by bacterial isolates from industrial effluents. *Int. J. Microbiol. Res.* **2012**, *4*, 308–311. [CrossRef]
42. Sethi, S.; Alariya, S.S.; Gupta, S.; Gupta, L.B. Amylase activity of a starch degrading bacteria isolated from soil. *Int. J. Curr. Microbiol. Appl. Sci.* **2019**, *8*, 659–671. [CrossRef]
43. Meddeb-Mouelhi, F.; Moisan, J.K.; Beauregard, M. A comparison of plate assay methods for detecting extracellular cellulase and xylanase activity. *Enzym. Microb. Technol.* **2014**, *66*, 16–19. [CrossRef]
44. Hankin, L.; Anagnostakis, S. Solid media containing carboxy methyl cellulose to detect CM cellulase activity of microorganisms. *Microbiology* **1977**, *98*, 109–115. [CrossRef]
45. Kuddus, S.M.; Ahmad, R.I.Z. Isolation of novel chitinolytic bacteria and production optimization of extracellular chitinase. *J. Genet. Eng. Biotechnol.* **2013**, *11*, 39–46. [CrossRef]
46. Geetha, K.; Venkatesham, E.V.; Hindumathi, A.; Bhadraiah, B. Isolation, screening and characterization of plant growth promoting bacteria and their effect on *Vigna Radia* (L.) R. Wilczek. *Int. J. Curr. Microbiol. Appl. Sci.* **2014**, *3*, 799–809. [CrossRef]
47. Khamna, S.; Yokota, A.; Lumyong, S. Actinomycetes isolated from medicinal plant rhizospheric soils: Diversity and screening of antifungal compounds, indole-3-acetic acid and siderophore production. *World J. Microbiol. Biotechnol.* **2009**, *25*, 649–655. [CrossRef]
48. Kumar, P.; Dubey, R.C.; Maheshwari, D.K. *Bacillus* strains isolated from rhizosphere showed plant growth promoting and antagonistic activity against phytopathogens. *Microbiol. Res.* **2012**, *8*, 493–499. [CrossRef]
49. Lavermicocca, P.; Lonigro, S.L.; Evidente, A.; Andolfi, A. Bacteriocin production by *Pseudomonas syringae* pv. *ciccaronei* NCPPB2355. Isolation and partial characterization of the antimicrobial compound. *J. Appl. Microbiol.* **2001**, *86*, 257–265. [CrossRef]

-
50. Agrillo, B.; Mirino, S.; Tatè, R.; Gratino, L.; Gogliettino, M.; Cocca, E.; Tabli, N.; Nabti, E.; Palmieri, G. An alternative biocontrol agent of soil-borne phytopathogens: A new antifungal compound produced by a plant growth promoting bacterium isolated from North Algeria. *Microbiol. Res.* **2019**, *221*, 60–69. [[CrossRef](#)]
 51. Bolger, A.M.; Lohse, M.; Usadel, B. Trimmomatic: A flexible trimmer for Illumina sequence data. *Bioinformatics* **2014**, *30*, 2114–2120. [[CrossRef](#)] [[PubMed](#)]

CHAPTER IV

Microbial consortia as a strategy to reduce drought stress in *Spinacia oleracea*

4.1 Abstract

Drought stress is considered one of the most severe abiotic stresses affecting soil fertility, plant health, and crop yield, considering that almost all agricultural lands are subjected to it. In addition, due to climate change, water shortage is destined to increase even further, becoming a serious threat to crop production. An efficient eco-friendly alternative to the polluting and soil-deteriorating chemical fertilizers, is the use of bioformulations of Plant-Growth-Promoting Bacteria (PGPB), either single or consortia. PGPB can promote plant fitness through direct and indirect approaches, involving the enhancement of nutrients uptake, the production of phytohormones, or the ability to inhibit phytopathogens' growth, thus strengthening plants' defences against biotic and abiotic stresses. The present study aims at constructing bacterial consortia exhibiting complementary PGP traits, to defend *Spinacia oleracea*'s seeds and seedlings from drought stress and promote their growth *in vitro*. Therefore, a characterization of six potential PGPB belonging to the *Bacillus*, *Azotobacter*, and *Pseudomonas* genera was performed under water-shortage condition and compared with two promising PGP-*Bacilli* recently isolated from salt-pans. To verify the bacterial PGP-potential, individual and consortia, a germination bioassay was performed using the seed-bioprimering method. Three bacterial strains identified as *B. amyloliquefaciens* RHF6, *B. amyloliquefaciens* LMG9814 and *B. sp.* AGS84 emerged as the most promising, positively affecting *S. oleracea*' seeds germination rate and efficiency, and promoting the seedlings' radical development, in standard conditions. Interestingly, out of the four consortia constructed according to the bacterial compatibility, the one made of strains RHF6, LMG9814 and AGS84 gave the best results, confirming the previous data. Although these preliminary results were encouraging, further analysis is required to confirm the outcome under drought stress and to improve this strategy, making it available for commercial use in the agro-industrial field.

4.2 Introduction

Plants generally undergo many abiotic stresses during their growth and development, including heat, drought, salinity and acidity, which directly and indirectly influence soil fertility, plant health and crop yield (Hanaka et al., 2021). Among these, drought is considered one of the most severe environmental stresses affecting agricultural productivity. It occurs due to temperature dynamics, light intensity, and low rainfall (Seleiman et al., 2021), and impacts all of the main agricultural lands (Sati et al., 2021). Indeed, it is well acknowledged that water plays a key role in most of plant's vital processes, being their body's fresh mass made of almost the 95 % of it (Abbasi and Abbasi, 2010). Drought stress negatively affects seed germination rate and efficiency, seedling growth, leaves' size, area and number; it limits the number of stomata and flowers, reduces roots' growth and elongation, and decreases plants' fresh and dry biomass (Ullah et al., 2019; Khan et al., 2021). Plants are normally able to defend themselves against numerous stress factors by several strategies, which imply different morphological and physiological responses (Hanaka et al., 2021). Therefore, plants may cope with water deficiency by producing osmoprotectants, shortening their life cycle, or by restarting their growth after the exposure to the abiotic stress (Fang and Xiong, 2015). Nevertheless, anthropogenic activities, together with the global warming led to an increased severity of droughts, imposing a serious threat on the agricultural productivity (Seleiman et al., 2021). Hence, plants defences may be not enough. Currently agriculture highly depends on chemical fertilizers, which expose the soil and the whole environment to deterioration (Kumar et al., 2011). For this reason, researchers and industries are seeking for greener and more sustainable approaches (Glick et al., 2007). One of the most promising solutions is represented by the skilful use of bioformulations, which may include the application of microorganisms inocula or the employment of natural metabolites acting as plants' growth enhancers (Vishwakarma et al., 2020; Oszust et al., 2021). A very common approach is the application of active microorganisms known as Plant Growth Promoting Bacteria (PGPB) (Niu et al., 2017). PGPB are microorganisms naturally capable of enhancing plants' growth by direct and indirect approaches, comprising the production of phyto-stimulant metabolites, the promotion of plants' nutrients up-take or the inhibition of pests (Castaldi et al., 2021; Petrillo et al., 2021). More importantly, they can arrange beneficial associations with the roots of plants to improve their growth and increase tolerance to abiotic stresses, such as water shortage (Vishwakarma et al., 2020). Recently,

importance has been given to the application of PGPB consortia, groups of bacteria exhibiting complementary features (Hanaka et al., 2021). Indeed, bacterial consortia were shown to have higher performances as compared to the inoculation of individual species (Baez-Rogelio et al., 2017) and were also shown to promote plant drought tolerance (Wang et al., 2012).

In the present study, a collection of six bacteria belonging to the genera *Bacillus*, *Azotobacter* and *Pseudomonas* was characterized for their PGP traits and biocontrol activity and compared with two recently isolated potential PGP- *Bacilli*, *B. amyloliquefaciens* strain RHF6 (Petrillo et al., 2021) and *B. vallismortis* strain RHFS10 (Castaldi et al., 2021), that emerged for their ability to endure abiotic stresses and inhibit phytopathogens' growth. The preliminary characterization was also performed under simulated drought stress and impressively, resulted in the enhancement of some PGP traits for many of the tested strains, according to the evidence that bacteria may respond to abiotic and biotic stresses by boosting their defence mechanisms. To confirm the bacterial strains PGP potential, their ability to promote *Spinacia oleracea* (Matador) germination was tested through a germination bioassay, performed using the seed-biopriming method, under standard condition. Spinach was selected as a model plant because it is one of the main vegetables sold as "ready-to-eat" bagged products and it is very sensitive to water stress (Bianchi et al., 2016). Three bacterial strains identified as *B. amyloliquefaciens* RHF6, *B. amyloliquefaciens* LMG9814 and *B. sp.* AGS84 emerged as the most promising, positively affecting *S. oleracea*' seeds germination rate and efficiency and promoting the seedlings' radical development. Moreover, out of the four consortia constructed according to the bacterial *in vitro* compatibility, the one made of strains RHF6, LMG9814 and AGS84 gave the best results, confirming the previous data.

Although the results obtained were encouraging, further analysis are required to validate and improve this strategy for a commercial use in the agro-industrial field of arid and semi-arid regions.

4.3 Materials and methods

4.3.1 Bacterial strains and growth conditions

The PGPB used in this study are listed in Table 1, grown on TY medium for routine use and pure cultures stored at -80°C into glycerol stocks (Giglio et al., 2011). Some of the strains are deposited in the culture

collection of Agriges s.r.l. (San Salvatore Telesino, Benevento, Italy) and were kindly supplied.

Table 1 | List of the bacterial strains used in this study.

Strain	Species	Source	Citation
RHF6	<i>B. amyloliquefaciens</i>	Sand (Spain)	Petrillo et al., 2021
RHFS10	<i>B. vallismortis</i>	Rhizosphere (Spain)	Castaldi et al., 2021
LS132	<i>A. chroococcum</i>	Rhizosphere (Italy)	Agriges collection
AGS172	<i>B. subtilis</i>	-	Agriges collection
LMG9814	<i>B. amyloliquefaciens</i>	Soil	Agriges collection
AGS84	<i>B. sp.</i>	Grape leaves	Agriges collection
AGS108	<i>B. amyloliquefaciens</i>	-	Agriges collection
AGS54	<i>P. fluorescens</i>	Sugar beet rhizosphere	Agriges collection

4.3.2 Phenotypic characterization and growth conditions

The phenotype of the bacterial strains was determined by visual inspection. The facultative anaerobic growth was determined using the AnaeroGen sachets (Unipath Inc., Nepean, Ontario, Canada) placed in a sealed jar with bacteria streaked on TY agar plates and incubated at 37 °C for 3 days. To confirm the sporulation ability, the bacterial strains were grown in Difco sporulation medium (DSM) (8 g/L Nutrient broth No. 4, 1 g/L KCl, 1 mM MgSO₄, 1 mM Ca(NO₃)₂, 10 µM MnCl₂, 1 µM FeSO₄, Sigma-Aldrich, Germany). The optimum growth conditions were determined by growing the strains in TY agar at different pH (2.0, 4.0, 6.0, 7.0, 8.0, 10.0, 12.0) (Cangiano et al., 2014), temperatures (4, 15, 25, 37, 50, 60 °C) (Petrillo et al., 2020) and PEG6000 (0, 5, 10, 15, 20 %) ranges.

4.3.3 Bioassays for PGP traits

The eight strains were characterized for their PGP traits as described below. When drought stress is simulated, 15% PEG6000 is supplemented to the media.

4.3.3.1 Biofilm Production and Swarming Motility

To investigate the capacity of producing biofilm, bacterial isolates were grown in 24-wells culture plates in TY broth for 48 h static conditions at 37 °C in accordance to O'Toole (2011). After that, the supernatant was discarded, adhered cells were rinsed three times with distilled water and 1 ml of a 0.1 % Crystal Violet (CV) solution was added to stain the adhered biomass. Plates were incubated for 30 min at room

temperature, carefully washed three times with distilled water and patted dry. Dye attached to the wells was extracted with 1 ml of 70 % ethanol and quantified at an absorbance of 570 nm. Data were normalized by total growth estimated by OD_{600nm} . The experiment was performed in triplicate. Swarming motility was assayed according to the method described by Adler (1966). TY agar 0.7 % plates were spot inoculated with 3 μ l of the freshly grown bacterial culture (10^7 CFU/ml). After an overnight incubation at 37 °C, the swarm diameters were measured.

4.3.3.2 Phosphate Solubilization

The microbial ability to solubilize phosphate was evaluated by spot inoculation of 3 μ l of a freshly grown bacterial culture (10^7 CFU/ml) onto Pikovaskya's agar medium (Pikovskaya, 1948). The plates were incubated at 28 °C for 10-15 days. A positive result is represented by the formation of transparent zones around the bacterial colonies (Schoebitz et al., 2013).

4.3.3.3 Indole-acetic Acid (IAA) Detection

The IAA production was measured as described by Etesami et al. (2013), with some modifications. Briefly, each strain was cultured in 10 ml of TY broth at 37 °C for 4 days with shaking at 150 rpm. Then, 1 ml of bacterial supernatant was mixed with 2 ml of Salkowski reagent (0.5 M $FeCl_3$ in 35 % $HClO_4$ solution), and the solution was vortexed and incubated at room temperature for 30 min. The formation of pink color represented a positive reaction (Damodaran et al., 2014). Quantitative estimation of IAA (μ g/ml) was achieved by recording spectroscopic absorbance at 535 nm using a standard curve prepared with pure IAA (Sigma) in the range 0–100 μ g/ml (Gordon and Weber, 1951). Sterile TY broth was used as control.

4.3.3.4 Ammonia production

To detect the production of ammonia, it was followed the method described by Bhattacharyya et al. (2020). The eight bacteria were grown in 4 % peptone broth and incubated for seven days at 30 °C. After that, to the bacterial suspension was added 0.5 ml of Nessler's reagent. The development of brown to yellow colour indicates ammonia production. The samples' absorbance was measured at 450 nm using a spectrophotometer. Quantitative estimation of the amount of ammonia production by the bacterial strains was performed comparing the results

with a standard curve generated using a standard ammonium sulphate solution.

4.3.3.5 Siderophores Production

The siderophores production was determined through the Chrome Azurol S (CAS) assay as described by Pérez-Miranda et al. (2007). 3 mL of freshly grown bacterial cultures were spot inoculated on CAS agar plates and incubated at 28 °C. The appearance of a yellow-orange halo zone around the bacterial colonies was a positive indicator of siderophores production and the halos' diameters were measured after 4 days of incubation.

4.3.3.6 Biosurfactants production

The bacterial isolates were spot inoculated on blood agar plates (BBL™ Trypticase™ Soy Agar (TSA II) supplemented with 5 % Horse Blood) and after 72 h of incubation at 28 °C, the clear zone around the colonies indicates a positive result (Sarwar et al., 2018).

4.3.3.7 Screening for hydrolytic enzymatic activity

The eight bacterial strains were grown separately in 5 mL of TY broth at 37 °C overnight with shaking at 150 rpm. 3 µL of each fresh bacterial culture was spot inoculated on plates containing different carbon sources, to test hydrolytic enzyme activity. The protease activity was assayed on Skimmed Milk Agar (SMA) (Morris et al., 2012). After an overnight incubation at 37 °C, the formation of a clear halo around the colonies was considered as positive activity. To detect the amylase activity, the method described by Alariya et al. (2013) with Starch Agar plates, was used. After the overnight incubation at 37 °C, the plates were flooded with iodine solution and the hydrolysis of starch was observed as a colourless zone around the colonies. To detect cellulase and xylanase activities, Xylanase Production Medium (XPM) agar plates with 0.5 % xylan (Megazyme) (Meddeb-Mouelhi et al., 2014) and a minimal medium with 0.5 % carboxymethylcellulose (CMC) (Hankin and Anagnostakis, 1977) as sole carbon sources, were used. The plates were incubated at 37 °C for 3 days after which hydrolysis zones were visualized by flooding the plates with 0.1 % Congo Red for 15–20 min and then destained by washing twice with 1 M NaCl. Plates, where CMC and xylan were omitted, were used as no substrate controls. Transparent hydrolytic zones around the colonies were considered positive.

To quantify the activity observed on plate, the ratio of the clear zone diameter to colony diameter was measured, assuming the largest ratio represents the highest activity. Hence, the following formula was applied:

$$\% \text{ Efficiency} = \frac{\text{total diameter} - \text{colony diameter}}{\text{colony diameter}} \times 100$$

All experiments were performed in triplicate.

4.3.4 Evaluation of potential biocontrol activity

The eight bacterial strains were tested *in vitro* for their biocontrol activity against spinach phytopathogenic fungi and bacteria listed in Table 5. *Colletotrichum truncatum* is deposited in the fungal culture collection of the Plant Pathology Department of the University of Buenos Aires (FAUBA, Argentina) and was kindly supplied by Marcelo Anibal Carmona (Facultad de Agronomía, Cátedra de Fitopatología, Universidad de Buenos Aires, Buenos Aires, Argentina). All the fungi were stored on Potato Dextrose Agar (PDA) in Petri dishes. A dual-culture assay method was performed to evaluate the antifungal activity in accordance with Xu and Kim (2014). In short, fungal plugs of 6 mm × 6 mm diameter were placed in the middle of PDA plates and 5 µl of bacterial cultures grown overnight in TY medium were spotted on the opposite four sides of the plates 1.5 cm away from the fungal disc. Negative controls consisted of plates containing the fungal plugs alone. All plates were incubated at 28 °C for 5–7 days. The antagonism activity against bacterial phytopathogens was carried out as described in Li et al. (2020) with some modifications. Bacterial pathogens were streaked on TY plates and incubated at 25 °C overnight. Single colonies were suspended in TY broth and incubated at 25 °C. Approximately 1 × 10⁻⁶ CFU/mL were mixed with melted 0.8 % TY agar before pouring the plates. After solidification, 5 µl of bacterial isolates solution (OD₆₀₀=1.0) was spot inoculated onto the plates and incubated at 28 °C for 48 h, before measuring the diameters of the inhibition halos. All experiments were performed in triplicate.

Table 2 | List of the phytopathogenic fungi and bacteria used in this study.

Pathogen type	Species	Strain	Provenience
Fungi	<i>Stemphylium vesicarium</i>		Italy
	<i>Colletotrichum truncatum</i>	17-5-5	Argentina
Bacteria	<i>Pseudomonas syringae pv tabaci</i>	ICMP 2706	-
	<i>Pseudomonas syringae pv panici</i>	ICMP 3955	-
	<i>Pseudomonas syringae pv syringae</i>	B475	-
	<i>Pseudomonas syringae pv japonica</i>	ICMP 6305	-
	<i>Pseudomonas syringae pv papulans</i>	Psp26	-

4.3.5 Germination assay

To test the ability of the microbial strains to promote seeds' germination, a modified method described by Wang et al. (2019) was performed. The bacterial strains were overnight cultured in TY medium at 37 ± 2 °C (25 ± 2 °C for strain AGS54). Then, the cells' concentration (CFU/mL) was determined by a Burkler chamber and diluted to 1×10^8 CFU/mL in 1X Phosphate-Buffered Saline (PBS). For the consortia, the dilutions of the single strains were mixed keeping a 1:1:1 ratio. *S. oleracea* (Matador) seeds were rapidly sterilized with 5 % H₂O₂ and rinsed with sterile deionized water. After that, 45 seeds were incubated with the proper bacterial dilution (single or consortium) for about 4 hours at room temperature, under stirred conditions to favor the bacterial adhesion to the seeds. Seeds treated with 1X PBS were used as control. The treated seeds were then spread on water agar (1.8 %) medium (WA) and incubated at 20 °C in dark conditions. Germination was defined as the appearance of radicles through the seed coat. The germination rate and efficiency were obtained from three independent experiments. To determine the seedlings' well-being, the length of primary roots was also measured by ImageJ software.

4.3.6 Adhesion assay

To evaluate bacterial adhesion onto *S. oleracea*'s seeds (each of the different treatments and the control), a modified method described by Hashmi et al. (2019), was performed. Three seeds were randomly collected to count bacterial cells adhering at their surface by flow cytometry. Seeds of each individual treatment were placed in sterile tubes containing 1 mL of sterile 1X PBS and vortexed vigorously for 1 min.

4.3.7 Microbial compatibility *in vitro*

To assess the ability of the eight strains to coexist, they were subjected to *in vitro* compatibility test using the agar diffusion assay as described by Tabacchioni et al. (2021), with minor modifications. A single colony of each strain was inoculated in TY medium and incubated at 37 ± 2 °C for ~ 18 h, 150 rpm. 100 µL of each strain were plated on TY agar medium, and 5 µL of the other strains were spotted on top of it. The plates were then incubated at 37 ± 2 °C. The microorganisms that overlap are considered compatible. On the other hand, when an inhibition halo appears, the two microorganisms are considered incompatible.

4.3.8 Statistical Analysis

All the statistical analyses were performed using GraphPad Prism 8 software. Data were expressed as mean \pm SEM. Differences among groups were compared by ANOVA or t-test as indicated in figure legends. Differences were considered statistically significant at $p < 0.05$.

4.4 Results and discussion

4.4.1 *In vitro* characterization of potential PGPB

The six bacterial strains of the collection listed in Table 1, were preliminarily characterized for growth properties (Supplementary Table S1) and compared with two *Bacilli* isolated from samples of sand and rhizosphere collected from salt-pans, strains RHF6 and RHFS10, recently emerged as promising PGPB (Castaldi et al., 2021; Petrillo et al., 2021). All the strains object of this study represent well-recognized PGPB genera, with more than the 70 % identified as members of the *Bacillus* genus, while strains LS132 and AGS54 were identified as the Gram-negative *A. chroococcum* and *P. fluorescens* (Table 1).

The eight strains can be classified as facultative anaerobic; almost all of them fit in the mesophiles group, except for strains LMG9814, AGS84 and AGS108 that can grow up to 60 °C and strain AGS54, which grows between 4 and 40 °C (Supplementary Table S1) (Schiraldi and De Rosa, 2016). In addition, to determine the tolerance to drought stress, the eight strains were grown in the presence of different PEG6000 concentrations (*Materials and methods*). The 60 % of the strains tolerate up to 15 % PEG6000; only strains AGS172, AGS84 and AGS54 survived up to 20 %. The strains used in this study seem to be moderately tolerant to the lack of moisture, proven by either the capacity

of growing in relatively high PEG6000 concentrations and the ability to survive at high temperatures. In fact, drought is strictly connected to the rising global warming: the higher temperatures promote evaporation, which in turn reduces surface water and dries out soils and vegetation (Drought and Climate Change, 2021). To compare the PGP potential of the six new strains to the already characterized *Bacilli*, strains RHF6 and RHFS10, their ability to produce growth hormones and siderophores, to solubilize phosphorous, and the capability of hydrolysing different polymers were assayed (Table 3). Most of the strains is potentially able to colonize root apparatus, since capable of surface spreading by swarming and to form biofilms (Amaya-Gómez et al., 2020), while only five were found positive to biosurfactants production. Strain AGS54 is the best IAA producer, followed by AGS84 and AGS172. On the other hand strain LS132 releases the highest amount of ammonia, as expected of an *Azotobacter* (Plunkett et al., 2020). As mentioned above, all the microorganisms were tested for their hydrolytic potential against different substrates (milk proteins, starch, xylan and cellulose). As shown in Table 3, the best hydrolytic activity, often connected to biocontrol (Pal and McSpadden Gardener, 2006), was registered for strains AGS172 and AGS84, comparable with that exerted by RHF6 and RHFS10; while LS132 strain, only exhibited proteolytic activity.

Table 3 | Summary of plant growth-promoting and biocontrol traits exhibited by the 8 bacterial strains.

Strain	PGP traits						HYDROLYTIC ACTIVITIES (%)			
	Swarming	PVK	IAA (µg/mL)	Ammonia production (mg/L)	Siderophores (%)	Biosurfactants	Protease	Amylase	Xylanase	CMC
RHF6 ¹	+	++	4.5	6.9	7.1	+	100	100	41.7	100
RHFS10 ²	+++	++	6.5	9.8	41.7	+	100	100	76.9	100
LS132	+	-	1.4	12.1	16.7	-	100	0	0	0
AGS172	+++	+	12.9	5.2	11.8	+	100	100	25	100
LMG9814	-	+	8.6	2.2	4.5	-	100	75	41.2	37.9
AGS84	+	+	17.2	4.1	7.1	-	100	20	100	100
AGS108	++	++	5.7	2.5	3.1	+	100	64.3	22.2	33.3
AGS54	-	++	24.1	2.7	47.1	+	100	4	0	47.8

No activity (-), halo or colony diameter < 5 mm (+), halo or colony diameter 10 mm (+++). Data are represented by means of at least three replicates ± SE at p ≤ 0.05 using LDS. PVK, Pikovskaya; IAA, indoleacetic acid; and CMC, carboxymethylcellulose. ¹ Available from Petrillo et al. (2021). ² Available from Castaldi et al. (2021).

Based on this preliminary characterization, it is possible to say that this bacterial collection has a strong PGPB potential *in vitro*.

4.4.2 Antagonistic activity against *Spinacia oleracea* phytopathogens

To verify if the bacterial strains, that already proved to possess many PGP traits *in vitro*, also exert an antagonistic activity against some *S. oleracea* phytopathogens (Koike et al., 2002; Liu et al., 2021), dual culture assays were performed between the PGPB and the pathogens listed in Table 2. The results revealed that the bacteria inhibit plant pathogens on plates with different efficiency (Fig. 1). Based on the size of the inhibition zone in dual culture tests, all the strains but LS132 showed a strong antifungal activity against *S. vesicarium* and *C. truncatum* (Fig.1; Table 4).

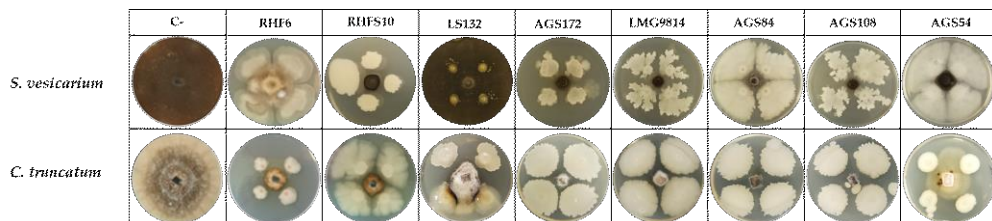


Figure 1 | Representative photographs of dual culture assay for in vitro mycelial growth inhibition of fungal phytopathogens.

In particular, it is possible to notice that *B. subtilis* strain AGS172 exhibited a broad spectrum of action against both fungal and bacterial pathogens (Table 4) comparable to the one already observed for strains RHF6 and RHFS10 (Petrillo et al., 2021); whereas strains *B. sp.* AGS84 and *B. amyloliquefaciens* AGS108 showed an inhibitory activity limited to the fungal pathogens. Unexpectedly, strain *A. chroococcum* LS132 showed any particular biocontrol activity.

Table 4 | Antimicrobial activity of the bacterial strains against phytopathogenic fungi and bacteria.

Pathogen type	Species	RHF6 ¹	RHFS10 ¹	LS132	AGS172	LMG9814	AGS84	AGS108	AGS54
Fungi	<i>S. vesicarium</i>	+++	+++	-	+++	+++	+++	+++	++
	<i>C. truncatum</i>	+++	+++	+	+++	+++	+++	+++	+
Bacteria	<i>P. syringae pv tabaci</i>	++	+	-	++	-	-	-	++
	<i>P. syringae pv panici</i>	++	+	-	-	-	-	-	-
	<i>P. syringae pv syringae</i>	+	++	-	+	++	++	-	+
	<i>P. syringae pv japonica</i>	++	+	-	++	-	-	++	-
	<i>P. syringae pv papulans</i>	-	-	-	+	+	+	-	+

No inhibition (-), inhibitory zone 5mm (+++). ¹ Available from Petrillo et al. (2021).

4.4.3 Characterization of PGP traits under drought stress condition

To fulfil the aim of this study, a further characterization of the bacterial strains was repeated under drought stress condition, in the presence of 15 % PEG6000. As expected, the results obtained this time were lower than the ones registered before (Table 5), on average.

Table 5 | Summary of plant growth-promoting and biocontrol traits exhibited by the 8 bacterial strains under drought stress.

Strain	PGPR traits					HYDROLYTIC ACTIVITIES			
	PVK	IAA ($\mu\text{g}/\text{mL}$)	Ammonia production (mg/l)	Siderophores (%)	Biosurfactants	Protease	Amylase	Xylanase	CMC
RHF6	+	4.2	1.3	3.5	++	0	0	0	0
RHFS10	+	18	0.0	25.0	+++	0	50	75	0
LS132	-	2.4	1.8	0	+	0	0	0	0
AGS172	+	5.2	1.7	5.2	++	100	50	75	0
LMG9814	-	3.5	0.8	3.2	++	100	66.7	0	0
AGS84	+	4.4	1.1	4.6	++	0	100	75	0
AGS108	+	2.3	0.6	3.5	+	100	75	75	0
AGS54	-	2.1	1.4	20.0	++	0	0	0	0

No activity (-), halo or colony diameter < 5 mm (+), halo or colony diameter 10 mm (+++). Data are represented by means of at least three replicates \pm SE at $p \leq 0.05$ using LDS. PVK, Pikovskaya; IAA, indoleacetic acid; and CMC, carboxymethylcellulose.

The most impressive loss was observed for the hydrolytic activities, cellulolytic activity on top of all. Strain RHF6 which exhibited one of the highest hydrolytic potentials, lost it completely, together with strains LS132 and AGS54. On the contrary, the xylanase activity exhibited by strains AGS172 and AGS108, and the amylase activity exhibited by strains AGS84 and AGS108 increased under drought-stress condition. This behaviour agrees with what has been recently stated by Bouskill et al. (2016). It was observed, indeed, that bacterial communities can respond to water stress by increasing the hydrolytic activity of classes of enzymes correlated to the metabolism of complex C-sources. The same tendency was observed for the IAA production shown by strains RHFS10 and LS132, which increased almost three and two times, respectively, reaching 18 and 2.4 $\mu\text{g}/\text{mL}$ (Table 5).

4.4.4 Effects of seed-bioprimering on *S. oleracea* germination *in vitro*

Once verified that the bacterial strains used in this study exhibited important PGP traits *in vitro* under standard and water-shortage

conditions, a germination bioassay was carried out to evaluate the effects of the potential PGPB, on the early vegetative growth stage of *S. oleracea* seedlings. *S. oleracea* was chosen as a model plant, due to its moisture-sensitiveness (Bianchi et al., 2016). To this aim, 45 seeds (per treatment) of *S. oleracea*, after being rapidly sterilized with 5 % H₂O₂ and rinsed with sterile deionized water, were incubated with a dilution of each one of the strains adjusted to 1 x 10⁸ CFU/mL with 1X PBS, for ~ 4 h at room temperature under stirred conditions to favor the bacterial adhesion to the seeds. Seeds treated with 1X PBS only, were used as control (*Material and methods*). Following the incubation, the seeds were spread on WA plates, and let germinate in the dark at 20 °C for about one week. Germination was defined as the appearance of radicles through the seed coat. In Fig.2A are reported the effects of *S. oleracea*'s seeds bio-priming. During the germination period, the number of germinated seeds was counted every day after incubation, to calculate the germination rate and efficiency (Fig.2B, 2D). To determine the seedlings' well-being, the length of primary roots was also measured (Fig.2C). As it is possible to observe, the bacterial strains affect seeds germination with different efficiency. Seed-bioprimering using strains RHF6, LMG9814 and AGS84 significantly improved seeds' germination rate and efficiency and produced the healthiest seedlings also, against the untreated control seeds (Fig. 2A); strain AGS108 also positively affected the seeds' germination. In particular, the longest radicle length (6.82 cm), and the highest germination rate and efficiency (Fig.2B, 2C, 2D) was recorded for seeds bioprimered with *B. amyloliquefaciens* strain RHF6. On the other hand, strains RHFS10, LS132, AGS172 and AGS54 -bioprimered seeds exhibited lower viability and vigor (Fig.2A).

A possible explanation for the best effects exerted by strains RHF6, LMG9814 and AGS84, could be a stronger adhesion of the bacterial cells to the seeds (Supplementary Figure S2). To evaluate this parameter, three bioprimered seeds were randomly collected to count bacterial cells adhering at their surface by flow cytometry as described in the *Materials and methods* section. Once again, strain RHF6 exhibited the best performance. Hence, we can say that the bacterial inoculation, in some cases, led to an acceleration of the radicle emergence (as for strains RHF6, LMG9814 and AGS84), and that it has a positive impact on radicle growth after its initial, rapid, protrusion from the seed.

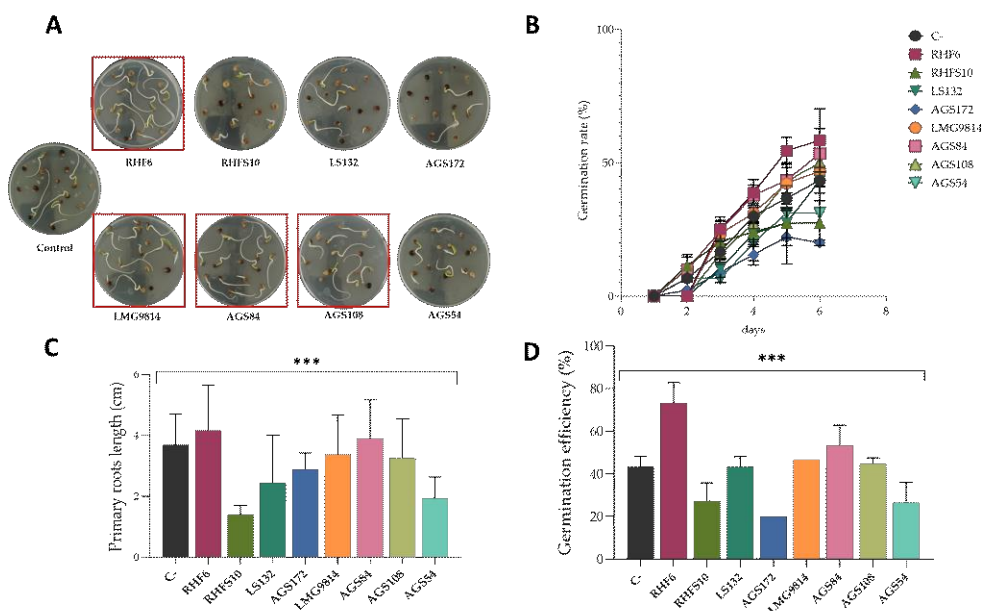


Figure 2 | A) Effects of seed-biopriming on *S. oleracea*. The red squares point out the treatments that gave the best results; **B)** Seeds germination rate (%) measured over a 6 days period; **C)** Measure of the seedlings' primary roots length by ImageJ software; **D)** Seeds germination efficiency measured over a 6 days period: the comparison between the number of total germinated seeds over the number of total seeds on each plate is reported in percentage. Data are presented as means \pm standard deviation ($n = 3$). For comparative analysis of groups of data, one-way ANOVA was used, and p values are presented in the figure: ***: extremely significant < 0.001 .

4.4.5 Effects of bacterial consortia on *S. oleracea* germination *in vitro*

A more recent strategy to increase plant growth, is the application of consortia of PGPB exhibiting complementary traits (Hanaka et al., 2021). Indeed, bacterial consortia were shown to have higher performances as compared to the inoculation of individual species (Baez-Rogelio et al., 2017). On the base of the results obtained for the *in vitro* bacterial compatibility assayed on Petri dishes and reported in Supplementary Table S3, four consortia named C1, C2, C3 and C4, were prepared out of the eight potential PGPB (Table 1). As described in the previous paragraph, a germination assay was performed to verify the action of the consortia on the germination phase of *S. oleracea* (Fig.3).

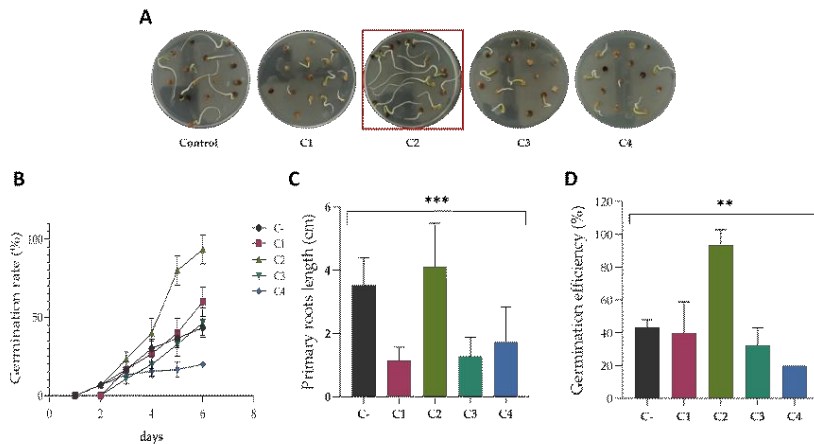


Figure 3 | A) Effects of seed-biopriming with the bacterial consortia on *S. oleracea*. The red square points out the consortium that gave the best results: C2; **B)** Seeds germination rate (%) measured over a 6 days period; **C)** Measure of the seedlings' primary roots length by ImageJ software; **D)** Seeds germination efficiency measured over a 6 days period: the comparison between the number of total germinated seeds over the number of total seeds on each plate is reported in percentage. C1: RHFS10, AGS172, AGS108; C2: RHF6, AGS84, LMG9814; C3: RHFS10, RHF6, AGS172; C4: RHFS10, AGS54, LS132. Data are presented as means \pm standard deviation (n = 3). For comparative analysis of groups of data, one-way ANOVA was used, and *p* values are presented in the figure: ***: extremely significant < 0.001; **: significant < 0.006.

This time the seeds were imbibed with the four cultures mixes (adjusted to 1×10^8 CFU/mL, maintaining a 1:1:1 ratio of the single microorganisms), and after that let germinate on WA plates. As previously described, the seedlings well-being was evaluated through several parameters (Fig.3B, 3C and 3D). Out of the four consortia, C2 made of strains RHF6, AGS84 and LMG9814, gave the best results, increasing the germination rate and efficiency up to ~100 %, and producing seedlings with the longest primary roots (6.96 cm) (Fig.3). Interestingly, the best consortium is the one bringing together the PGPB which showed the strongest effect when assayed individually (Fig.2). This outcome confirms the former results and allows to hypothesize a beneficial synergic action of the three strains in the consortium C2, at least looking at the germination efficiency.

4.5 Conclusions

The application of PGPB to the agricultural field is considered to have the potential for improving plant growth in extreme environments characterized by water shortage. Drought stress, indeed, is one of the main agricultural problems reducing crop yield in arid and semiarid

areas, and it is made even tougher by the rapid global warming, which brings longer drought periods, that severely damage food production in some countries (Seleiman et al., 2021). PGPB are known to enhance plant growth by several mechanisms including nitrogen fixation, phytohormone production (including auxins, cytokinins, and gibberellins), solubilization of mineral phosphates, and iron sequestration by siderophores production (Glick, 2012). Interestingly, many PGPB have been demonstrated to limit drought stress effects in plants, for example by reducing plant ethylene levels, a molecular stress marker, or by increasing their antioxidant potential (Mayak et al., 2004; Arshad et al., 2008). Anyway, the ability of bacteria to survive, and compete with the soil microflora, colonizing the rhizosphere remains a critical step for successful application (Bashan, 1998) especially in dry soils (van Meeteren et al., 2008). For these reasons, the application of drought tolerant PGPB may represent a valid strategy to deliver beneficial effects on plants. The present study aims at proposing new potential drought tolerant PGPB, which may be able to alleviate water-shortage induced stress on *S. oleracea* seedlings and plants. For this purpose, a collection of eight bacteria from the *Bacillus*, *Pseudomonas* and *Azotobacter* genera were preliminary characterized for their PGP traits as the ability to produce biofilm, growth hormones, siderophores or the capacity to surface-spread, and solubilize nutrients under standard and drought stress conditions (Table 3, 5). As hypothesized, the results obtained under simulated water-shortage were lower than the ones registered in optimal conditions (Table 5). The most impressive loss was observed for the hydrolytic activities, cellulolytic activity on top of all: strain RHF6 which exhibited one of the highest hydrolytic potentials, lost it completely. Interestingly, drought stress also triggered some of the bacterial features, such as the IAA production, which increased almost three and two times, compared to the standard condition, reaching 18 and 2.4 $\mu\text{g}/\text{mL}$ in strains RHFS10 and LS132, respectively (Table 5). The bacterial strains were also successfully tested for their biocontrol activity against some *S. oleracea*'s fungal and bacterial pathogens. All the strains but *A. chroococcum* LS132, exhibited inhibitory activity; strain *B. subtilis* AGS172 exhibited a broad spectrum of action against both fungal and bacterial pathogens (Table 6), showing a similar behaviour to the already characterized strains RHF6 and RHFS10, (Petrillo et al., 2021; Castaldi et al., 2021). Since seed germination is a critical step in plant growth as it controls seedling production and crop yield, to find approaches able to promote seed germination of economical-valuable crops is considered of great interest on global level (Makhaye et al., 2021). In this context, over the past

decades, inoculation of seeds with PGPB, has proved to be an efficient and “green” practice to increase plant tolerance over stresses, the durability of food production and reduce its ecological impact (Duhamel and Vandenkoornhuys, 2013; Gupta et al., 2015). This method is referred to as seed-biopriming (Mitra et al., 2021). This represents an effective method to introduce beneficial microbial inocula into the rhizosphere or soil, and improves the seed quality, germination, viability, by enhancing the production of regulatory substances, the uptake of nutrients, and protection from seed or soil-borne pathogens (Mitra et al., 2021). Hence, a germination bioassay was performed to evaluate the effects of the potential PGPB on the early vegetative growth stage of *S. oleracea* seedlings. *S. oleracea* was chosen as a model plant, due to its moisture-sensitiveness (Bianchi et al., 2016). The most promising strains were *B. amyloliquefaciens* RHF6, *B. amyloliquefaciens* LMG9814 and *B. sp.* AGS84, which significantly improved seeds’ germination rate and efficiency and produced the healthiest seedlings compared with the untreated seeds (Fig. 3). The beneficial effect, especially the one shown by strain RHF6, agrees with the stronger adhesion of the bacterial cells to the seed surface (Supplementary Figure S3). According to the *in vitro* compatibility, four consortia were prepared out of the eight bacterial strains. Again, the germination efficiency, rate and primary roots length were considered to determine the seedlings vigour (Fig.3). Interestingly, the best consortium (C2) is the one made of the three PGPB that exhibited the strongest beneficial effect on the germination, individually (Fig.2): strains RHF6, LMG9814 and AGS84. This outcome confirms the former results and allows to hypothesize a beneficial synergic action of the three strains in the consortium C2, at least for the germination efficiency.

Due to Covid-19 pandemic, this study hasn’t come to an end yet. Further experiments need to be performed to confirm the promising results reached so far.

4.6 Supplemental material

Supplementary Figures and Tables are available in **Appendix I**.

4.7 Acknowledgments

We thank Marcelo Anibal Carmona (Facultad de Agronomía, Cátedra de Fitopatología, Universidad de Buenos Aires, Buenos Aires, Argentina) to supply the strain of *Colletotrichum truncatum* used in this study.

4.8 References

- Abbasi, T., and Abbasi, S. A. (2010). Biomass energy and the environmental impacts associated with its production and utilization. *Renewable and Sustainable Energy Reviews* 14, 919–937. doi:10.1016/j.rser.2009.11.006.
- Adler, J. (1966). Chemotaxis in Bacteria. *Science* 153, 708–716. doi:10.1126/science.153.3737.708.
- Alariya, S. S., Sethi, S., Gupta, S., and Gupta, B. L. (2013). Amylase activity of a starch degrading bacteria isolated from soil. 10.
- Amaya-Gómez, C. V., Porcel, M., Mesa-Garriga, L., and Gómez-Álvarez, M. I. (2020). A Framework for the Selection of Plant Growth-Promoting Rhizobacteria Based on Bacterial Competence Mechanisms. *Appl Environ Microbiol* 86. doi:10.1128/AEM.00760-20.
- Arshad, M., Shaharoon, B., and Mahmood, T. (2008). Inoculation with *Pseudomonas spp.* Containing ACC-Deaminase Partially Eliminates the Effects of Drought Stress on Growth, Yield, and Ripening of Pea (*Pisum sativum L.*)*1 *1Project supported by the Higher Education Commission, Islamabad, Pakistan (No. PIN 041 211534 A-031). *Pedosphere* 18, 611–620. doi:10.1016/S1002-0160(08)60055-7.
- Baez-Rogelio, A., Morales-García, Y. E., Quintero-Hernández, V., and Muñoz-Rojas, J. (2017). Next generation of microbial inoculants for agriculture and bioremediation. *Microb Biotechnol* 10, 19–21. doi:10.1111/1751-7915.12448.
- Bashan, Y. (1998). Inoculants of plant growth-promoting bacteria for use in agriculture. *Biotechnology Advances* 16, 729–770. doi:10.1016/S0734-9750(98)00003-2.
- Bhattacharyya, C., Banerjee, S., Acharya, U., Mitra, A., Mallick, I., Haldar, A., et al. (2020). Evaluation of plant growth promotion properties and induction of antioxidative defense mechanism by tea rhizobacteria of Darjeeling, India. *Sci Rep* 10, 15536. doi:10.1038/s41598-020-72439-z.
- Bianchi, A., Masseroni, D., and Facchi, A. (2016). Modelling water requirements of greenhouse spinach for irrigation management purposes. *Hydrology Research* 48. doi:10.2166/nh.2016.079.
- Bouskill, N. J., Wood, T. E., Baran, R., Ye, Z., Bowen, B. P., Lim, H., et al. (2016). Belowground Response to Drought in a Tropical Forest Soil. I. Changes in Microbial Functional Potential and Metabolism. *Frontiers in Microbiology* 7, 525. doi:10.3389/fmicb.2016.00525.

Cangiano, G., Sirec, T., Panarella, C., Istatico, R., Baccigalupi, L., De Felice, M., et al. (2014). The sps Gene Products Affect the Germination, Hydrophobicity, and Protein Adsorption of *Bacillus subtilis* Spores. *Appl Environ Microbiol* 80, 7293–7302. doi:10.1128/AEM.02893-14.

Castaldi, S., Petrillo, C., Donadio, G., Piazz, F. D., Cimmino, A., Masi, M., et al. (2021). Plant Growth Promotion Function of *Bacillus* sp. Strains Isolated from Salt-Pan Rhizosphere and Their Biocontrol Potential against *Macrophomina phaseolina*. *Int J Mol Sci* 22. doi:10.3390/ijms22073324.

Damodaran, T., Rai, R. B., Jha, S. K., Kannan, R., Pandey, B. K., Sah, V., et al. (2014). Rhizosphere and endophytic bacteria for induction of salt tolerance in gladiolus grown in sodic soils. *Journal of Plant Interactions* 9, 577–584. doi:10.1080/17429145.2013.873958.

Drought and Climate Change (2021). *Center for Climate and Energy Solutions*. Available at: <https://www.c2es.org/content/drought-and-climate-change/> [Accessed December 3, 2021].

Duhamel, M., and Vandenkoornhuyse, P. (2013). Sustainable agriculture: possible trajectories from mutualistic symbiosis and plant neodomestication. *Trends Plant Sci* 18, 597–600. doi:10.1016/j.tplants.2013.08.010.

Etesami, H., Mirseyed, H., and Alikhani, H. (2013). In planta selection of plant growth promoting endophytic bacteria for rice (*Oryza sativa* L.). *Journal of soil science and plant nutrition* 14. doi:10.4067/S0718-95162014005000039.

Fang, Y., and Xiong, L. (2015). General mechanisms of drought response and their application in drought resistance improvement in plants. *Cell. Mol. Life Sci.* 72, 673–689. doi:10.1007/s00018-014-1767-0.

Giglio, R., Fani, R., Istatico, R., De Felice, M., Ricca, E., and Baccigalupi, L. (2011). Organization and Evolution of the cotG and cotH Genes of *Bacillus subtilis*. *Journal of bacteriology* 193, 6664–73. doi:10.1128/JB.06121-11.

Glick, B. R. (2012). Plant growth-promoting bacteria: mechanisms and applications. *Scientifica (Cairo)* 2012, 963401. doi:10.6064/2012/963401.

Glick, B. R., Cheng, Z., Czarny, J., and Duan, J. (2007). Promotion of plant growth by ACC deaminase-producing soil bacteria. *Eur J Plant Pathol* 119, 329–339. doi:10.1007/s10658-007-9162-4.

Gordon, S. A., and Weber, R. P. (1951). COLORIMETRIC ESTIMATION OF INDOLEACETIC ACID. *Plant Physiol* 26, 192–195.

- Gupta, G., Parihar, S., Ahirwar, N., Snehi, Dr. S. K., and Singh, V. (2015). Plant Growth Promoting Rhizobacteria (PGPR): Current and Future Prospects for Development of Sustainable Agriculture. *Microbial & Biochemical Technology* 7, 096–102.
- Hanaka, A., Ozimek, E., Reszczyńska, E., Jaroszuk-Ścisieł, J., and Stolarz, M. (2021). Plant Tolerance to Drought Stress in the Presence of Supporting Bacteria and Fungi: An Efficient Strategy in Horticulture. *Horticulturae* 7, 390. doi:10.3390/horticulturae7100390.
- Hankin, L., and Anagnostakis, S. L. (1977). Solid media containing carboxymethylcellulose to detect CX cellulose activity of micro-organisms. *J Gen Microbiol* 98, 109–115. doi:10.1099/00221287-98-1-109.
- Hashmi, I., Paul, C., Al-Dourobi, A., Sandoz, F., Deschamps, P., Junier, T., et al. (2019). Comparison of the plant growth-promotion performance of a consortium of *Bacilli* inoculated as endospores or as vegetative cells. *FEMS Microbiology Ecology* 95. doi:10.1093/femsec/fiz147.
- Khan, N., Ali, S., Shahid, M. A., Mustafa, A., Sayyed, R. Z., and Curá, J. A. (2021). Insights into the Interactions among Roots, Rhizosphere, and Rhizobacteria for Improving Plant Growth and Tolerance to Abiotic Stresses: A Review. *Cells* 10, 1551. doi:10.3390/cells10061551.
- Koike, S. T., Azad, H. R., and Cooksey, D. C. (2002). First Report of Bacterial Leaf Spot of Spinach Caused by a *Pseudomonas syringae* Pathovar in California. *Plant Dis* 86, 921. doi:10.1094/PDIS.2002.86.8.921A.
- Kumar, A., Prakash, A., and Johri, B. (2011). “*Bacillus* as PGPR in crop ecosystem. Bacteria in agrobiolgy: crop ecosystems,” in *Bacteria in agrobiolgy: Crop ecosystems* (Springer Berlin Heidelberg), 37–59.
- Li, Z., Chakraborty, P., de Vries, R. H., Song, C., Zhao, X., Roelfes, G., et al. (2020). Characterization of two relacidines belonging to a novel class of circular lipopeptides that act against Gram-negative bacterial pathogens. *Environ Microbiol* 22, 5125–5136. doi:10.1111/1462-2920.15145.
- Liu, B., Stein, L., Cochran, K., du Toit, L. J., Feng, C., and Correll, J. C. (2021). Three New Fungal Leaf Spot Diseases of Spinach in the United States and the Evaluation of Fungicide Efficacy for Disease Management. *Plant Dis* 105, 316–323. doi:10.1094/PDIS-04-20-0918-RE.
- Makhaye, G., Aremu, A. O., Gerrano, A. S., Tesfay, S., Du Plooy, C. P., and Amoo, S. O. (2021). Biopriming with Seaweed Extract and Microbial-Based Commercial Biostimulants Influences Seed Germination of Five *Abelmoschus esculentus* Genotypes. *Plants* 10, 1327. doi:10.3390/plants10071327.

- Mayak, S., Tirosh, T., and Glick, B. R. (2004). Plant growth-promoting bacteria that confer resistance to water stress in tomatoes and peppers. *Plant Science* 166, 525–530. doi:10.1016/j.plantsci.2003.10.025.
- Meddeb-Mouelhi, F., Moisan, J. K., and Beauregard, M. (2014). A comparison of plate assay methods for detecting extracellular cellulase and xylanase activity. *Enzyme Microb Technol* 66, 16–19. doi:10.1016/j.enzmictec.2014.07.004.
- Mitra, D., Mondal, R., Khoshru, B., Shadangi, S., Das Mohapatra, P. K., and Panneerselvam, P. (2021). Rhizobacteria mediated seed bio-priming triggers the resistance and plant growth for sustainable crop production. *Current Research in Microbial Sciences* 2, 100071. doi:10.1016/j.crmicr.2021.100071.
- Morris, L. S., Evans, J., and Marchesi, J. R. (2012). A robust plate assay for detection of extracellular microbial protease activity in metagenomic screens and pure cultures. *Journal of Microbiological Methods* 91, 144–146. doi:https://doi.org/10.1016/j.mimet.2012.08.006.
- Niu, X., Song, L., Xiao, Y., and Ge, W. (2017). Drought-Tolerant Plant Growth-Promoting Rhizobacteria Associated with Foxtail Millet in a Semi-arid Agroecosystem and Their Potential in Alleviating Drought Stress. *Front Microbiol* 8, 2580. doi:10.3389/fmicb.2017.02580.
- Oszust, K., Pylak, M., and Frąc, M. (2021). *Trichoderma*-Based Biopreparation with Prebiotics Supplementation for the Naturalization of Raspberry Plant Rhizosphere. *International Journal of Molecular Sciences* 22, 6356. doi:10.3390/ijms22126356.
- O'Toole, G. A. (2011). Microtiter Dish Biofilm Formation Assay. *J Vis Exp*, 2437. doi:10.3791/2437.
- Pal, K. K., and McSpadden Gardener, B. (2006). Biological Control of Plant Pathogens. *PHI*. doi:10.1094/PHI-A-2006-1117-02.
- Pérez-Miranda, S., Cabirol, N., George-Téllez, R., Zamudio-Rivera, L. S., and Fernández, F. J. (2007). O-CAS, a fast and universal method for siderophore detection. *J Microbiol Methods* 70, 127–131. doi:10.1016/j.mimet.2007.03.023.
- Petrillo, C., Castaldi, S., Lanzilli, M., Saggese, A., Donadio, G., Baccigalupi, L., et al. (2020). The temperature of growth and sporulation modulates the efficiency of spore-display in *Bacillus subtilis*. *Microb Cell Fact* 19, 185. doi:10.1186/s12934-020-01446-6.

Petrillo, C., Castaldi, S., Lanzilli, M., Selci, M., Cordone, A., Giovannelli, D., et al. (2021). Genomic and Physiological Characterization of *Bacilli* Isolated From Salt-Pans With Plant Growth Promoting Features. *Front. Microbiol.* 12, 715678. doi:10.3389/fmicb.2021.715678.

Plunkett, M. H., Knutson, C. M., and Barney, B. M. (2020). Key factors affecting ammonium production by an *Azotobacter vinelandii* strain deregulated for biological nitrogen fixation. *Microbial Cell Factories* 19, 107. doi:10.1186/s12934-020-01362-9.

Sarwar, A., Brader, G., Corretto, E., Aleti, G., Abaidullah, M., Sessitsch, A., et al. (2018). Qualitative analysis of biosurfactants from *Bacillus* species exhibiting antifungal activity. *PLoS One* 13, e0198107. doi:10.1371/journal.pone.0198107.

Sati, D., Pande, V., Pandey, S. C., and Samant, M. (2021). Recent Advances in PGPR and Molecular Mechanisms Involved in DroughtStress Tolerance. doi:10.20944/preprints202105.0331.v1.

Schiraldi, C., and De Rosa, M. (2016). "Mesophilic Organisms," in *Encyclopedia of Membranes*, eds. E. Drioli and L. Giorno (Berlin, Heidelberg: Springer Berlin Heidelberg), 1–2. doi:10.1007/978-3-642-40872-4_1610-2.

Schoebitz, M., Ceballos, C., and Ciamp, L. (2013). Effect of immobilized phosphate solubilizing bacteria on wheat growth and phosphate uptake. *Journal of soil science and plant nutrition* 13, 1–10. doi:10.4067/S0718-95162013005000001.

Seleiman, M. F., Al-Suhaibani, N., Ali, N., Akmal, M., Alotaibi, M., Refay, Y., et al. (2021). Drought Stress Impacts on Plants and Different Approaches to Alleviate Its Adverse Effects. *Plants (Basel)* 10, 259. doi:10.3390/plants10020259.

Tabacchioni, S., Passato, S., Ambrosino, P., Huang, L., Caldara, M., Cantale, C., et al. (2021). Identification of Beneficial Microbial Consortia and Bioactive Compounds with Potential as Plant Biostimulants for a Sustainable Agriculture. *Microorganisms* 9, 426. doi:10.3390/microorganisms9020426.

Ullah, A., Nisar, M., Ali, H., Hazrat, A., Hayat, K., Keerio, A. A., et al. (2019). Drought tolerance improvement in plants: an endophytic bacterial approach. *Appl Microbiol Biotechnol* 103, 7385–7397. doi:10.1007/s00253-019-10045-4.

van Meeteren, M. J. M., Tietema, A., van Loon, E. E., and Verstraten, J. M. (2008). Microbial dynamics and litter decomposition under a changed climate in a Dutch heathland. *Applied Soil Ecology* 38, 119–127. doi:10.1016/j.apsoil.2007.09.006.

Vishwakarma, K., Kumar, N., Shandilya, C., Mohapatra, S., Bhayana, S., and Varma, A. (2020). Revisiting Plant–Microbe Interactions and Microbial Consortia Application for Enhancing Sustainable Agriculture: A Review. *Frontiers in Microbiology* 11, 3195. doi:10.3389/fmicb.2020.560406.

Wang, C., Wu, B., and Jiang, K. (2019). Allelopathic effects of Canada goldenrod leaf extracts on the seed germination and seedling growth of lettuce reinforced under salt stress. *Ecotoxicology* 28, 103–116. doi:10.1007/s10646-018-2004-7.

Wang, C.-J., Yang, W., Wang, C., Gu, C., Niu, D.-D., Liu, H.-X., et al. (2012). Induction of drought tolerance in cucumber plants by a consortium of three plant growth-promoting rhizobacterium strains. *PLoS One* 7, e52565. doi:10.1371/journal.pone.0052565.

Xu, S. J., and Kim, B. S. (2014). Biocontrol of *Fusarium* crown and root rot and promotion of growth of tomato by *Paenibacillus* strains isolated from soil. *Mycobiology* 42, 158–166. doi:10.5941/MYCO.2014.42.2.158.

CHAPTER V

Myxococcus xanthus' Frz chemosensory system

5.1 A potential PGPB: *M. xanthus*

M. xanthus belongs to the *Myxococcales*, or myxobacteria, soil dwelling Gram-negative gliding bacteria that form fruiting bodies containing myxospores (Dawid, 2000) resistant to harsh conditions such as desiccation, high temperature, and UV irradiation (Reichenbach, 1999) (Fig.1).

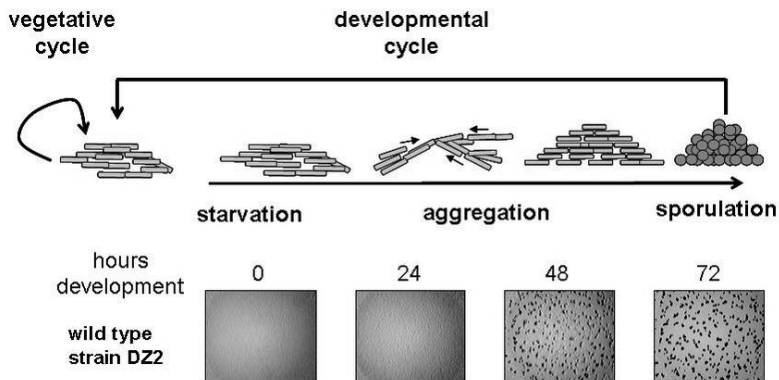


Figure 1 | *M. xanthus* life cycle.

Myxobacteria are found in both terrestrial soils and aquatic environments (Dawid, 2000), and besides fruiting bodies and spores formation (Curtis et al., 2007), show several complex social traits including cooperative swarming with two motility systems (Spormann, 1999), and group (or “wolf pack”) predation on both bacteria and fungi (Berleman et al., 2006) (Fig. 2). Myxobacteria embrace several species of micropredators that colonize soil and predate many microorganisms classified as plant pathogens (Adaikpoh et al., 2020); their predatory capabilities are ascribed to secreted hydrolytic enzymes and secondary metabolites with antimicrobial activity, which place the myxobacteria near or at the top of the microbial food chain (Konovalova et al., 2010).

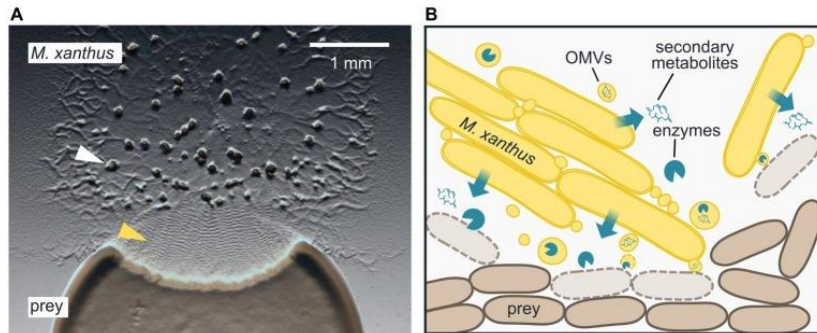


Figure 2 | Epibiotic predation by the myxobacterium *M. xanthus*. **A)** *M. xanthus* cells that are placed next to *E. coli* on a CF agar plate, which only provides a minimal amount of nutrients, expand radially using gliding motility, enter the prey colony, and lyse prey cells. Multicellular fruiting bodies (white arrowhead), in which *M. xanthus* cells differentiate into spores, start to emerge near the inoculation spot. Preying *M. xanthus* induces regular cell reversals, which appear as macroscopic ripples within the prey area (yellow arrowhead). The image was taken 2 days after the initial inoculation of predator and prey. **B)** *M. xanthus* secretes hydrolytic enzymes and secondary metabolites, which presumably kill and degrade prey cells for biomass acquisition. Outer membrane vesicles (OMVs) may contribute to the delivery of these lytic factors. *M. xanthus* cells typically move and prey in large clusters, but also individual cells can induce prey cell lysis.

This evidence indicates that myxobacteria may enhance plant health by inhibiting the growth of fungal and/or bacterial plant pathogens (Bull et al., 2002), acting as potential biocontrol agents by competition, antibiosis, and parasitism (Chet and Inbar, 1994).

5.2 Frz chemosensory system

At the CNRS of Marseille (France), I focused on one of the main chemosensory systems used by *M. xanthus*. The Frz (“frizzy”) chemosensory system controls the frequency at which cells change the direction of their movement on solid surfaces to reorient in the environment, analogously to controlled tumbles in *E. coli* (Blackhart and Zusman, 1985): this behavior allows cells to move towards favorable directions or away from toxic compounds. There is evidence that *M. xanthus* employs chemotaxis-like genes in its attack on prey cells (Berleman et al., 2008). In fact, myxobacteria use gliding motility (Spormann, 1999) to search the soil for preys and produce a wide range of antibiotics and lytic compounds that kill and decompose prey cells and break down complex polymers, thereby releasing substrates for growth (Sudo and Dworkin, 1972). In this contest, *M. xanthus*’ “frizzy” system seems to have a possible key role. It is known that the Frz system is activated by a variety of saturated fatty acids which trigger the

signal transduction pathway associated with chemotaxis in the microorganism. This system could probably respond to the plant signaling, attracting the myxobacteria to the roots, where they may act as biocontrol agents as previously explained.

In Fig. 3 is shown the Frz system organization. The Frz core is composed of a cytoplasmic Methyl-accepting Chemotaxis Proteins MCP (FrzCD), a CheA (FrzE) and a CheW (FrzA) (Sourjik and Berg, 2000) (Fig. 3B), encoded by a single operon (Fig. 3C). In the absence of any of these three proteins, cells display drastically reduced reversal frequencies and are no longer able to respond to isoamyl alcohol (IAA), a Frz activator (Sudo and Dworkin, 1972). The Frz system also includes a second CheW-like protein, FrzB, described as an accessory because while in its absence, cells show phenotypes similar to those caused by the deletion of core proteins, $\Delta frzB$ cells are still able to respond to IAA with increased reversal frequencies (Guzzo et al., 2015) (Fig. 3B).

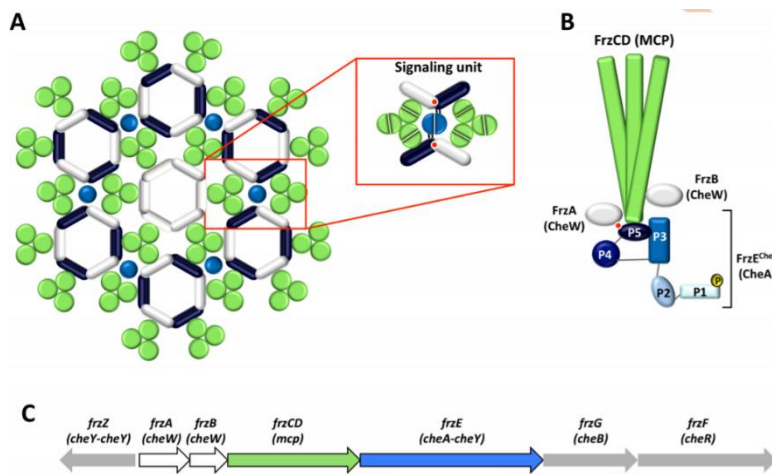


Figure 3 | Schematic representation of the supramolecular organization of Che proteins.

A) MCP form trimers of dimers (each dimer is shown as a green circle), which, in turn, form hexagons connected with rings composed of the CheA-P5 domain (dark blue bars) and CheW (white bars). The light blue circles represent the CheA-P4 domain and the red circles the interface between the β -strands 3 and 4 of subdomain 1 of CheA-P5 and the β -strands 4 and 5 of subdomain 2 of CheW. Rings containing six CheW proteins (shown at the center of the array) might serve to modulate the stability and activation of the system. A signaling unit is represented in the red box. **B)** FrzCD, FrzE, FrzA and FrzB proteins organization depicted by homology with Che proteins. **C)** Schematic representation of the *frz* operon.

In the Frz pathway, the FrzCD chemoreceptor activates the autophosphorylation of a CheA-CheY fusion, FrzE, which in turn phosphorylates the response regulator FrzZ (Guzzo et al., 2015). The system also possesses two CheW homologues (FrzA and FrzB), a

methyltransferase (FrzF) and methylesterase (FrzG). The chemoreceptor of the Frz pathway, FrzCD, lacks the transmembrane and periplasmic domains, which are replaced by a N-terminal domain of unknown function (Bustamante et al., 2004). When FrzCD was first localized in cells, it appeared organized in multiple dynamic cytoplasm clusters that aligned when cells made side-to-side contacts, which has been proposed to be part of a signaling process that synchronizes cell reversals (Mauriello et al., 2009). Furthermore, *M. xanthus* Frz system doesn't form clusters on the membrane, but directly on the bacterial chromosome. Clusters assembly is controlled by the chemoreceptor FrzCD, which binds to the DNA by a N-terminal domain carrying a positively charged eukaryotic histon-like tail (Parra et al., 2006). FrzCD appears to bind DNA in a non-sequence specific manner, thus, DNA-bound clusters do not occupy fixed localization sites but move across small areas on the nucleoid surface. While the binding of FrzCD to DNA is essential to target the Frz chemosensory system to the nucleoid, it is not sufficient for Frz cluster formation, as it requires downstream interactions with the FrzE kinase (Moine et al., 2017).

5.3 HAMP domains

An important question is how superficial receptors bring the signals across the cell membranes right into the cells. Bacteria and lower eukaryotes sense environmental stimuli through modular, dimeric transmembrane receptors, whose extra- and intracellular parts are often connected by a HAMP domain (Hulko et al., 2006). HAMP domains act as the signal relay modules in many receptors, physically bridging input and output components and transferring signals between them (Airola et al., 2013). HAMP domains were originally referred to as “linker regions” in histidine kinases and chemotaxis receptors, and subsequently named HAMP by Aravind and Ponting, (1999) for their occurrence in histidine kinases, adenylyl cyclases, methyl-accepting chemotaxis proteins, and phosphatases (Hulko et al., 2006). As mentioned above, *M. xanthus* Frz chemosensory system is made of several proteins encoded by a single operon. Among them FrzCD, a cytoplasmic MCP, represents the chemoreceptor of the pathway and controls Frz cluster assembly on the DNA. FrzCD contains two HAMP domains (Fig. 4), which most likely take part to the transduction of external stimuli, from the outside to the inside of the cell.

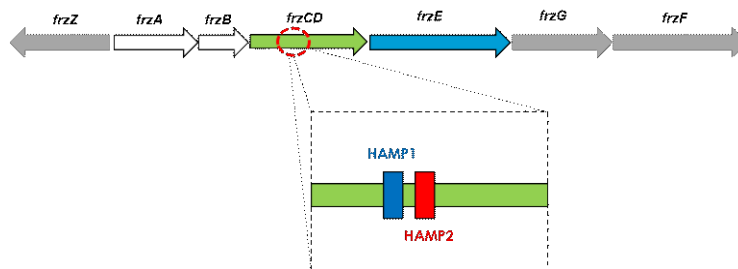


Figure 4 | Schematic representation of HAMP1 and HAMP2 domains in the *frzCD* gene sequence.

5.3.1 Role of the Frz HAMP domains in cluster formation

As demonstrated by Mauriello et al. (2009), Frz system chemoreceptor FrzCD is organized in multiple dynamic cytoplasm clusters that align when cells are side-by-side. This has been proposed to be involved in the process that controls cells reversals. As shown in Fig. 4 FrzCD is composed of two HAMP domains, which might be implicated. To investigate their involvement in clusters formation, *frzCD*^{Δhamp1} and *frzCD*^{Δhamp2} mutants were constructed as described in the *Materials and methods* section, bringing to the strains named EM777 and EM775, respectively. *frzCD* null mutant (EM410), and the double-mutant *frzCD*^{Δhamp1Δhamp2} (EM776) were already available in the lab. The mutants' motility and fruiting bodies formation were then analyzed by spotting fresh cultures onto CYE 0.5 % agar or CF 1.5 % agar, respectively, and observed by a binocular stereoscope after 48 °C incubation at 32 °C (data not shown).

5.3.2 Role of the DNA binding domain in cluster formation

Clusters assembly is generally guided by the interaction between FrzCD N-terminal domain and the DNA, in a non-sequence specific way (Parra et al., 2006). Surprisingly, in mutants carrying a lacking-DNA Binding Domain *frzCD*^{ΔDBD}, the protein is still able to form clusters, though smaller and less defined than wild type, that do not colocalize with the nucleoid (Fig. 5). The HAMP domains localized downstream the DNA Binding Domain (DBD), right after FrzCD N-terminal, could be implicated in the conservation of the interaction. To better understand this, HAMP truncated mutant proteins, FrzCD^{Δhamp1}, FrzCD^{Δhamp2}, FrzCD^{Δhamp1Δhamp2}, were expressed and purified together with the wild type FrzCD and the lacking DNA Binding Domain FrzCD^{ΔDBD}, used as positive and negative controls (Fig. 6). For this purpose, their capacity

to bind ssDNA was then investigated by Biolayer interferometry (BLItz) technique, useful for measuring interactions between proteins, peptides, nucleic acids, small molecules, and/or lipids in real time (data not shown).

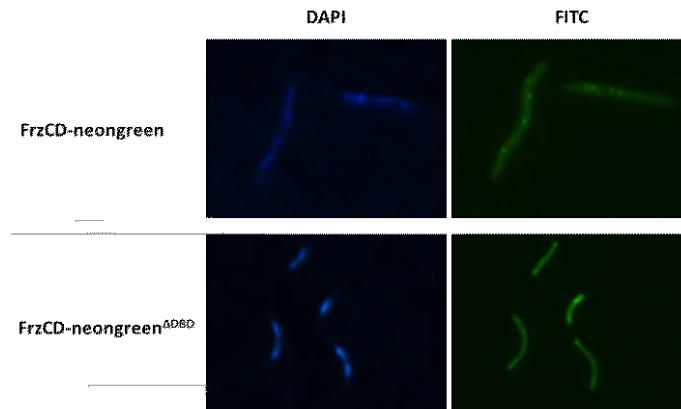


Figure 5 | Fluorescence microscopy analysis of the localization of FrzCD-neongreen and FrzCD-neongreen^{ΔDBD} in *M. xanthus* cells. DAPI (blue) and FITC (green) micrographs, acquired by an inverted Delta Vision optical sectioning microscope (Applied Precision) are shown.

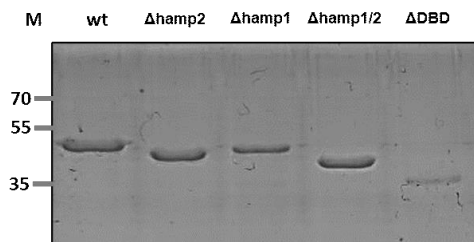


Figure 6 | SDS-PAGE of purified proteins. Lanes: 1) FrzCD (45.9 kDa); 2) FrzCD^{Δhamp2} (39.9 kDa); 3) FrzCD^{Δhamp1} (40.5 kDa); 4) FrzCD^{Δhamp1Δhamp2} (34.5 kDa); 5) FrzCD^{ΔDBD} (37.3 kDa). M: protein marker (kDa).

Unfortunately, due to COVID-19 pandemic I was unable to follow the successive analyses.

5.4 Materials and methods

5.4.1 Bacterial Strains, Plasmids, and Growth

M. xanthus strains were grown as described by Bustamante et al. (2004). *frzCD*^{Δhamp1} and *frzCD*^{Δhamp2} constructs were generated by overlap extension PCR and cloned into pBJ114 (Mauriello et al., 2009). The plasmid

obtained was used to electroporate wild type strain DZ2, yielding strains EM777 and EM775.

5.4.2 Proteins expression and purification

For the FrzCD^{Δhamp1}, FrzCD^{Δhamp2}, FrzCD^{Δhamp1Δhamp2}, FrzCD and FrzCD^{ΔDBD} production, cells of *E. coli* LB21 strains pEM663, pEM662, pEM658 and pEM414, bearing pMR3690 expression vector were grown for 3 h at 37 °C in 500 mL LB medium supplemented with 100 µg/mL Ampicillin and 0.5 mM IPTG to express the heterologous proteins. The His6-tagged proteins were then purified under native conditions by affinity chromatography and desalted using a Repligen's SpectraPor[®] membrane to remove high NaCl and imidazole concentrations.

5.5 References

Adaikpoh, B. I., Akbar, S., Albataineh, H., Misra, S. K., Sharp, J. S., and Stevens, D. C. (2020). Myxobacterial Response to Methyljasmonate Exposure Indicates Contribution to Plant Recruitment of Micropredators. *Frontiers in Microbiology* 11, 34. doi:10.3389/fmicb.2020.00034.

Airola, M. V., Sukomon, N., Samanta, D., Borbat, P. P., Freed, J. H., Watts, K. J., et al. (2013). HAMP Domain Conformers That Propagate Opposite Signals in Bacterial Chemoreceptors. *PLOS Biology* 11, e1001479. doi:10.1371/journal.pbio.1001479.

Aravind, L., and Ponting, C. P. (1999). The cytoplasmic helical linker domain of receptor histidine kinase and methyl-accepting proteins is common to many prokaryotic signalling proteins. *FEMS Microbiol Lett* 176, 111–116. doi:10.1111/j.1574-6968.1999.tb13650.x.

Berleman, J. E., Chumley, T., Cheung, P., and Kirby, J. R. (2006). Rippling Is a Predatory Behavior in *Myxococcus xanthus*. *J Bacteriol* 188, 5888–5895. doi:10.1128/JB.00559-06.

Berleman, J. E., Scott, J., Chumley, T., and Kirby, J. R. (2008). Predatation behavior in *Myxococcus xanthus*. *PNAS* 105, 17127–17132. doi:10.1073/pnas.0804387105.

Blackhart, B. D., and Zusman, D. R. (1985). “Frizzy” genes of *Myxococcus xanthus* are involved in control of frequency of reversal of gliding motility. *Proc Natl Acad Sci U S A* 82, 8767–8770. doi:10.1073/pnas.82.24.8767.

Bull, C. T., Shetty, K. G., and Subbarao, K. V. (2002). Interactions Between Myxobacteria, Plant Pathogenic Fungi, and Biocontrol Agents. *Plant Dis* 86, 889–896. doi:10.1094/PDIS.2002.86.8.889.

- Bustamante, V. H., Martínez-Flores, I., Vlamakis, H. C., and Zusman, D. R. (2004). Analysis of the Frz signal transduction system of *Myxococcus xanthus* shows the importance of the conserved C-terminal region of the cytoplasmic chemoreceptor FrzCD in sensing signals. *Mol Microbiol* 53, 1501–1513. doi:10.1111/j.1365-2958.2004.04221.x.
- Chet, I., and Inbar, J. (1994). Biological control of fungal pathogens. *Appl Biochem Biotechnol* 48, 37–43. doi:10.1007/BF02825358.
- Curtis, P. D., Taylor, R. G., Welch, R. D., and Shimkets, L. J. (2007). Spatial Organization of *Myxococcus xanthus* during Fruiting Body Formation. *J Bacteriol* 189, 9126–9130. doi:10.1128/JB.01008-07.
- Dawid, W. (2000). Biology and global distribution of myxobacteria in soils. *FEMS Microbiology Reviews* 24, 403–427. doi:10.1111/j.1574-6976.2000.tb00548.x.
- Guzzo, M., Agrebi, R., Espinosa, L., Baronian, G., Molle, V., Mauriello, E. M. F., et al. (2015). Evolution and Design Governing Signal Precision and Amplification in a Bacterial Chemosensory Pathway. *PLOS Genetics* 11, e1005460. doi:10.1371/journal.pgen.1005460.
- Hulko, M., Berndt, F., Gruber, M., Linder, J. U., Truffault, V., Schultz, A., et al. (2006). The HAMP domain structure implies helix rotation in transmembrane signaling. *Cell* 126, 929–940. doi:10.1016/j.cell.2006.06.058.
- Konovalova, A., Petters, T., and Søggaard-Andersen, L. (2010). Extracellular biology of *Myxococcus xanthus*. *FEMS Microbiology Reviews* 34, 89–106. doi:10.1111/j.1574-6976.2009.00194.x.
- Mauriello, E. M. F., Astling, D. P., Sliusarenko, O., and Zusman, D. R. (2009). Localization of a bacterial cytoplasmic receptor is dynamic and changes with cell-cell contacts. *Proc Natl Acad Sci U S A* 106, 4852–4857. doi:10.1073/pnas.0810583106.
- Moine, A., Espinosa, L., Martineau, E., Yaikhomba, M., Jazleena, P. J., Byrne, D., et al. (2017). The nucleoid as a scaffold for the assembly of bacterial signaling complexes. *PLOS Genetics* 13, e1007103. doi:10.1371/journal.pgen.1007103.
- Parra, M. A., Kerr, D., Fahy, D., Pouchnik, D. J., and Wyrick, J. J. (2006). Deciphering the Roles of the Histone H2B N-Terminal Domain in Genome-Wide Transcription. *Molecular and Cellular Biology* 26, 3842. doi:10.1128/MCB.26.10.3842-3852.2006.

Reichenbach, H. (1999). The ecology of the myxobacteria. *Environmental Microbiology* 1, 15–21. doi:10.1046/j.1462-2920.1999.00016.x.

Sasse, J., Martinoia, E., and Northen, T. (2018). Feed Your Friends: Do Plant Exudates Shape the Root Microbiome? *Trends Plant Sci* 23, 25–41. doi:10.1016/j.tplants.2017.09.003.

Sourjik, V., and Berg, H. C. (2000). Localization of components of the chemotaxis machinery of *Escherichia coli* using fluorescent protein fusions. *Mol Microbiol* 37, 740–751. doi:10.1046/j.1365-2958.2000.02044.x.

Spormann, A. M. (1999). Gliding motility in bacteria: insights from studies of *Myxococcus xanthus*. *Microbiol Mol Biol Rev* 63, 621–641. doi:10.1128/MMBR.63.3.621-641.1999.

Sudo, S., and Dworkin, M. (1972). Bacteriolytic Enzymes Produced by *Myxococcus xanthus*. *J Bacteriol* 110, 236–245.

PART II

The spore-based display system: a powerful biotechnological tool

CHAPTER VI

environmental
microbiology



Environmental Microbiology (2020) 22(1), 170–182

doi:10.1111/1462-2920.14835

Bacillus subtilis builds structurally and functionally different spores in response to the temperature of growth

Rachele Isticato ^{1*}, Mariamichela Lanzilli,^{1†}
Claudia Petrillo,¹ Giuliana Donadio,^{1‡}
Loredana Baccigalupi[‡] and Ezio Ricca¹

¹Department of Biology, Federico II University of Naples, Complesso Universitario di Monte Sant'Angelo, Via Cinthia, 80126 Naples, Italy.

²Department of Molecular Medicine and Medical Biotechnology, Federico II University of Naples, Complesso Universitario di Monte Sant'Angelo, Via Cinthia, 80126 Naples, Italy.

Summary

Bacterial spores are commonly isolated from a variety of different environments, including extreme habitats. Although it is well established that such ubiquitous distribution reflects the spore resistance properties, it is not clear whether the growing conditions affect the spore structure and function. We used *Bacillus subtilis* spores of similar age but produced at 25, 37, or 42°C to compare their surface structures and functional properties. Spores produced at the 25°C were more hydrophobic while those produced at 42°C contained more dipicolinic acid, and were more resistant to heat or lysozyme treatments. Electron microscopy analysis showed that while 25°C spores had a coat with a compact outer coat, not tightly attached to the inner coat, 42°C spores had a granular, not compact outer coat, reminiscent of the coat produced at 37°C by mutant spores lacking the protein CotG. Indeed, CotH and a series of CotH-dependent coat proteins including CotG were more abundantly extracted from the coat of 25 or 37°C than 42°C spores. Our data indicated that CotH is a heat-labile protein with a major regulatory role on coat formation when sporulation occurs

at low temperatures, suggesting that *B. subtilis* builds structurally and functionally different spores in response to the external conditions.

Introduction

Bacterial endospores (spores) are commonly isolated from a wide range of ecological niches, from soil to deep marine sediments, from the gastrointestinal tract of invertebrates and vertebrates to the rhizosphere of plants and to polluted environments (Nicholson *et al.*, 2000; Wömer *et al.*, 2019). Such ubiquitous distribution reflects both the metabolic dormancy of spores that do not require water and nutrients and also their structure, resistant to conditions that would not allow the survival of other cell forms (Setlow, 2006). The spore is structurally characterized by a dehydrated cytoplasm surrounded by several protective layers: a peptidoglycan-like cortex, that is a major factor in the resistance to heat (Nicholson *et al.*, 2000; Setlow, 2006) and a multi-layered coat, formed by over seventy different proteins and contributing to the resistance to chemicals, lytic enzymes and of the proper interaction of the spore with compounds that trigger germination (Henriques and Moran, 2007; Kailas *et al.*, 2011; McKenney *et al.*, 2013). Some spore former species, including *Bacillus anthracis*, *Bacillus cereus* and *Bacillus megaterium*, have an additional protective layer, the exosporium, a 'balloon-like' structure consisting of a paracrystalline basal layer and an external hair-like nap formed mainly by the collagen-like glycoprotein BclA (Henriques and Moran, 2007; McKenney *et al.*, 2013). In the model system for spore formers, *Bacillus subtilis*, the exosporium is not present but a crust, formed by proteins and glycoproteins, surrounds the coat and is the outermost spore layer (McKenney *et al.*, 2013).

The common isolation of live spores, able to germinate in response to the presence of nutrients originating vegetative cells, from highly diverse environments does not necessarily imply that these species are able to colonize all such habitats. In some cases, spores have been considered as tracers to estimate the gut transit time (Mir *et al.*, 1997), the microbial dispersal by ocean currents

Received 31 July, 2019; revised 16 October, 2019; accepted 17 October, 2019. *For correspondence. E-mail isticato@unina.it; Tel. (+39) 081 679038; Fax: (+39) 081 679233. †Present address: Institute of Biomolecular Chemistry, National Research Council of Italy, Pozzuoli, Naples, Italy ‡Present address: Department of Medicine, Surgery and Dentistry 'Scuola Medica Salernitana', University of Salerno, Fisciano, Italy

© 2019 Society for Applied Microbiology and John Wiley & Sons Ltd.

(Muller *et al.*, 2014) or the global microbial abundance in deep sediments (Wörmer *et al.*, 2019). However, spores of various species have been found able to germinate, proliferate and sporulate in the animal gut (Cutting, 2011), in the rhizosphere of plants (Timmusk *et al.*, 2011) and even in the deep marine sediments (Cupit *et al.*, 2018), pointing to a physiological role of spore formers in at least some of the analysed environments.

In laboratory conditions, *B. subtilis* spore dormancy, resistance and resilience is not fully acquired immediately upon their release by the sporulating cell but only few days after (Segev *et al.*, 2012; Camilleri *et al.*, 2019). Early released (young) spores have significant lower resistance to heat and chemicals than late released ones and can partially acquire such resistance properties during the maturation period through molecular changes that most likely involve the spore surface structures (Sanchez-Salas *et al.*, 2011).

A number of studies have shown that the temperature of growth and sporulation affects some spore properties, in particular the resistance to heat and chemicals both in *B. subtilis* (Palop *et al.*, 1995; Melly *et al.*, 2002) as well as in other *Bacillus* species (El-Bisi and Ordal, 1956; Warth, 1978). In *B. cereus*, the temperature of sporulation also alters the structure of the coat and of the exosporium (Bressuire-Isoard *et al.*, 2015). The regulatory coat protein CotE of *B. cereus* is more abundant in extracts from spores formed at 20°C than at 37°C, indicating that a high amount of that protein is required to maintain proper assembly of spore surface layers at low temperature and suggesting a complex relationship between the function of a spore regulatory protein and environmental factors during spore formation (Bressuire-Isoard *et al.*, 2015). However, as the temperature also affects the growth rate, the time of entry into the sporulation cycle and the time of spore formation, it cannot be excluded that the observed differences were at least in part due to the different age of the analysed spores.

To understand whether the environmental conditions affect the structure and the function of the forming spore, we used spores of a laboratory collection strain of the model organism *B. subtilis* produced at 25, 37 and 42°C. We first developed a method to collect spores of the same age grown at the three different temperatures and then analysed their structure and function. Our results

Effects of the temperature on *Bacillus subtilis* spores 171

point to the conclusion that *B. subtilis* builds different spore surfaces in response to the external temperature and indicate CotH, a previously identified spore coat protein with a regulatory role on at least nine other coat proteins, as a major regulator of coat formation at low temperatures.

Results and Discussion

Production of spores of similar age at 25, 37 and 42°C

Isogenic strains of *B. subtilis* carrying the gene coding for the green fluorescent protein (*gfp*) posed under the control of sporulation-specific promoters recognized by the RNA polymerase sigma factors σ^F (*spoIIQ* gene; Donadio *et al.*, 2016), σ^K (*gerE* gene; Donadio *et al.*, 2016) or σ^K acting in conjunction with GerE (*cotC* gene; Donadio *et al.*, 2016) were induced to sporulate in Difco Sporulation (DS) medium at 25, 37 and 42°C. Aliquots were collected at various times and analysed by fluorescence microscopy to assess the timing of appearance of the fluorescent signal at the various growth temperatures. In agreement with the literature data (Fujita and Losick, 2003), at 37°C fluorescence signals appeared 2, 5.5 or 7 h after the onset of sporulation when *gfp* expression was controlled, respectively, by the σ^F , σ^K or σ^K -GerE-dependent promoters (Table 1). With respect to cells growing at 37°C, production of fluorescent signals was delayed at 25°C and slightly accelerated at 42°C (Table 1). While the difference between the time of appearance of the fluorescence signal at 37 versus 42°C was only minimal and was not further considered in our study, a delay factor of 2.40 was calculated as the ratio between the hours needed to observe the appearance of fluorescent cells at 25 versus 37°C (Table 1).

As an additional approach, the *B. subtilis* strain PY79, isogenic to the strains used for the experiment of Table 1, was used to produce spores in DS medium at 25, 37 and 42°C. At different times during growth and sporulation aliquots were collected and analysed under the light microscope. For each time point cells and free spores of eight independent microscopy fields were counted and averaged. An amount of 85% of free spores was counted after 30 h at 37 and 42°C and after 69 h at 25°C (Supporting Information Figure S1), in good

Table 1. Time of appearance (hours after the onset of sporulation) of the fluorescence signal at the various temperatures.

Gene fusion	Transcriptional control	Temperature of growth			Delay factor 25°C/37°C	Delay factor (average)
		25°C	37°C	42°C		
P _{spoIIQ} ::gfp	σ^F	5.0	2.0	1.5	2.5	2.40
P _{gerE} ::gfp	σ^K	14.0	5.5	5.0	2.15	
P _{cotC} ::gfp	σ^K + GerE	18.0	7.0	7.0	2.57	

172 *R. Istitico et al.*

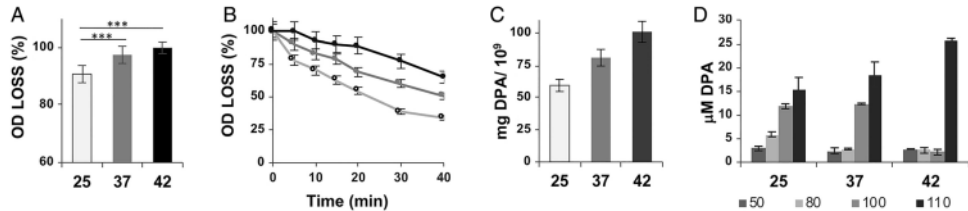


Fig. 1. Resistance of spores to lysozyme and heat. **A.** Spores formed at 25°C (white bar), 37°C (grey bar) and 42°C (black bar) were incubated with 50 mg ml⁻¹ of lysozyme and the percentage of loss of refraction measured. The results are the mean from six replicate experiments, each performed with an independently prepared spore suspension. Error bars represent standard deviations. Analysis of variance has been performed by unpaired two-tailed *t* test (****p* = 0.05). **B.** Spores formed at 25°C (white circles), 37°C (grey circles) and 42°C (black circles) were incubated at 100°C for 30 min. The data are the means of three independent experiments. **C.** DPA content of spores produced at 25°C (white bar), 37°C (dark-grey bar) and 42°C (black bar). **D.** DPA release (µM) from spores produced at 25, 37 and 42°C incubated at 50, 80, 100 and 110°C for 15 min.

agreement with the delay factor calculated in Table 1. Based on these, spores produced after 30 h at 37 and 42°C and after 69 h at 25°C were considered of similar age and used for all further experiments.

Functional analysis

Purified spores of similar age produced at the three different temperatures were analysed for their resistance properties, efficiency of germination and hydrophobicity. The temperature of growth and sporulation had small but statistically significant (*p* < 0.05) effects on the resistance to lysozyme digestion, with 25°C spores less resistant than those produced at 37 or 42°C (Fig. 1A). 25°C spores were also less resistant than 37°C spores, which in turn were less resistant than 42°C spores, after incubation at 100°C (Fig. 1B). The effect of the temperature on heat resistance was most likely mediated by the increased dipicolinic acid (DPA) content of spores (Fig. 1C) that caused a decrease of free water (Leguérinel *et al.*, 2007). The different resistance to heat of 25, 37 and 42°C

spores was also observed by measuring the amount of DPA released after a heat treatment. Next, 25°C spores released 5 µM of DPA after an incubation at 80°C, while the 37°C spores released DPA over the background level after an incubation at 100 and 42°C spores only released DPA after an incubation at 110°C (Fig. 1D).

The germination efficiency was measured by using either asparagine or alanine as germinants (Serrano *et al.*, 2005; Atluri *et al.*, 2006; Christie & Lowe, 2007). With asparagine, germination of 42°C spores (black symbols in Fig. 2A) was slower than that of 25 and 37°C spores (white and grey symbols, respectively, Fig. 2A). When alanine was used, the process was in general faster than with asparagine and 25°C spores (white symbols in Fig. 2B) were slightly faster than 37 and 42°C spores, that behaved similarly (Fig. 2B). Similar results were obtained by measuring germination by flow cytometry, as previously reported (Cangiano *et al.*, 2014; data not shown).

The effects of the temperature of growth and sporulation on the hydrophobicity of the spore surface were analysed by using the bacterial adherence To

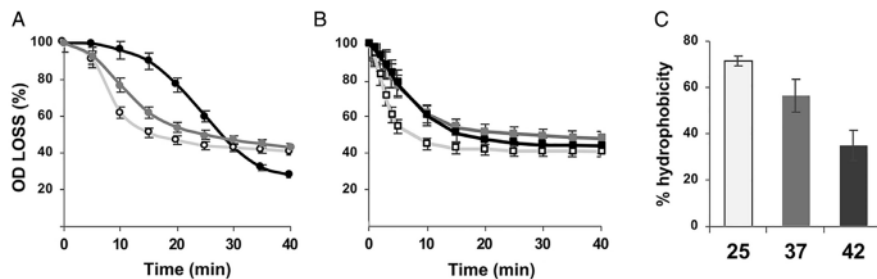


Fig. 2. Germination efficiency and spore relative hydrophobicity. Spore produced at 25°C (white symbols), 37°C (grey symbols) and 42°C (black symbols) were induced to germinate in response to asparagine (A) or to alanine (B). The percentage of germination was determined as OD₅₈₀ loss. Data are the means from three replicate experiments, each performed with an independently prepared spore suspension. Bars represent standard deviations. **C.** The percentage of hydrophobicity represents the proportion of spores in *n*-hexadecane after a separation into solvent and water phases. Each percentage is the mean from three replicate experiments, each performed with an independently prepared spore suspension. Error bars represent standard deviations.

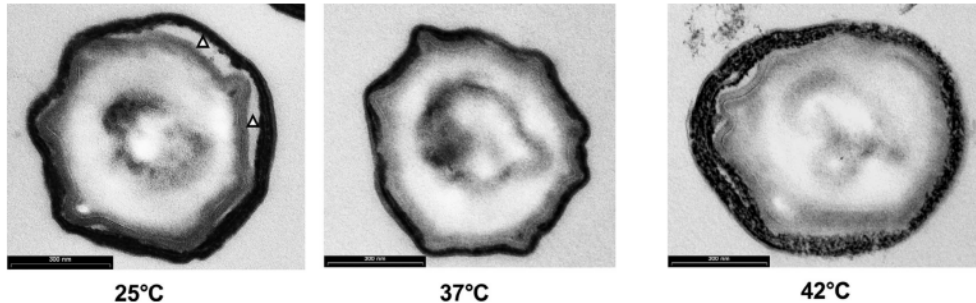


Fig. 3. Thin section transmission electron micrograph. Representative spore produced at 25, 37 or 42°C are reported. Triangles (left panel) point to sites of detachment between inner and outer coat. Bars correspond to 300 nm.

hydrocarbons (BATH) assay, based on the partitioning of spores between aqueous and hexadecane phases (Wienczek *et al.*, 1990). Spores produced at 42°C showed a lower relative hydrophobicity than those produced at 25 or 37°C (Fig. 2C).

All together results of Figs. 1 and 2 suggest that the temperature of growth and sporulation affects spore functions. Resistance to lysozyme and heat increases with the temperature of spore production, with 42°C spores more resistant than 37°C spores that in turn are more resistant than 25°C spores, while 25°C spores are slightly faster to respond to germinants and more hydrophobic than 37 and 42°C spores.

Structural analysis

A transmission electron microscopy (TEM) approach was used to compare the ultra-structure of spores prepared at 25, 37 and 42°C. As previously reported (McKenney *et al.*, 2013), unstained *B. subtilis* spores produced at 37°C showed a coat composed of a lamellar inner coat and a thick electron-dense outer coat (Fig. 3). The outermost structure of the *B. subtilis* coat, the crust, is only visible after a red-ruthenium staining (McKenney *et al.*, 2010) and, therefore, did not appear in our analysis. Over 40 spores of different sections were analysed for each temperature and about 80% of the analysed 25°C spores differed from 37°C spores and showed a lamellar, strongly electron-dense outer coat, partially detached from the inner coat (Fig. 3). A similar percentage of 42°C spores also differed from 37°C spores and showed a granular, not compact and thick outer coat (Fig. 3), reminiscent of the coat produced at 37°C by a *cotG* null mutant strain (Freitas *et al.*, 2019).

To further characterize the coat of spores produced at different temperatures, surface proteins were extracted by the SDS-dithiothreitol (DTT) treatment (Nicholson and

Setlow, 1990) and analysed by SDS-PAGE. As shown in Fig. 4A, the profile of proteins extracted from 25, 37 or 42°C spores showed several differences. In particular, the abundance of proteins of apparent molecular mass of 65, 30 and 22 kDa (indicated by the black arrows) decreased with the increase of temperature in a gradient-like manner (25 > 37 > 42). Other proteins of apparent molecular mass of 40 and 36 kDa (indicated by grey arrows) were abundantly extracted from 25°C spores and minimally extracted from 37°C spores (25 > 42 > 37). Other differences involved proteins extracted only from spores produced at one of the three temperatures (indicated by triangles).

To identify some of the proteins differentially represented in 25, 37 and 42°C spores a western blotting approach was followed by using a collection of antibodies previously raised against various spore coat proteins. Proteins of apparent molecular mass of 65 and 34 kDa were identified as CotB and CotG, respectively, and were both abundantly extracted from 25°C spores and were minimally extracted from 42°C spores (Fig. 4B). CotA was also extracted in slightly higher amounts at 25°C than 37 or 42°C but the differences were minimal (Fig. 4B). Other differentially expressed proteins were not recognized by any of the antibodies in our collection. Those indicated by the grey arrows in Fig. 4A were identified by N-terminal amino acid sequencing as CotQ (50 kDa) and CotS (40 kDa). Proteins indicated by the triangles in Fig. 4A were either not sufficiently abundant or not sufficiently resolved to be identified.

Assembly of CotH and other CotH-dependent proteins is controlled by the temperature

The proteins identified as differentially extracted from 25, 37 and 42°C spores, CotB, CotG, CotQ and CotS, are all known as dependent on the action of the

174 R. Isticato et al.

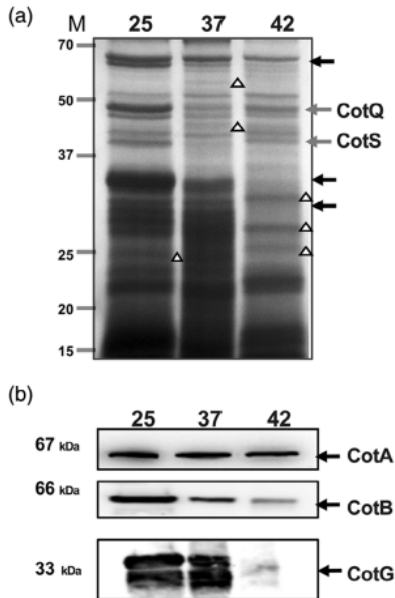


Fig. 4. Chromatographic profile of SDS-DTT extracted coat proteins. A. Proteins from spores prepared at 25, 37 or 42°C were analysed by SDS-PAGE. Arrows indicate proteins more abundantly extracted from 25°C spores than from 37 or 42°C (black arrows) or less abundant in 37°C spores than 25 or 42°C (grey arrows). Triangles indicate proteins only (or mostly) extracted from spores prepared at one of the three temperatures. M: Protein marker (kDa). B. Western blot analysis of proteins extracted from mature spores prepared at the three temperatures with anti-CotA, anti-CotB, anti-CotG antibodies.

regulatory protein CotH (Zilhao *et al.*, 2004; Kim *et al.*, 2006). Therefore, the presence of CotH in spores prepared at the three temperatures was evaluated by western blotting with anti-CotH antibody. As shown in Fig. 5A, CotH was abundantly extracted from 25°C spores while it was minimally extracted from 37 and 42°C spores. As CotH has been recently identified as an atypical protein kinase-like able to phosphorylate both CotB and CotG (Nguyen *et al.*, 2016), the kinase activity of CotH was assayed by western blotting in 25, 37 and 42°C spores with antibody specifically recognizing the phosphorylation consensus motif (pPKC-Ab). The western blot of Fig. 5B shows that the CotH kinase was active on CotB and CotG when sporulation had occurred at 25 or 37°C, while no activity was detected at 42°C even if some CotH protein was still present (Fig. 5A).

Based on the effects of the temperature on CotH, the abundance of other CotH-dependent proteins that were not resolved in the SDS-PAGE of Fig. 5A was analysed in 25, 37 and 42°C spores. As shown in Figs. 5C and 5D, CotC, CotU and CotZ were differentially extracted from

25, 37 and 42°C spores but while CotZ was more abundantly extracted from 25°C than from 37 or 42°C spores (Fig. 5C) following the same trend observed for CotB and CotG, all forms of CotC and CotU followed an opposite trend and were more abundantly extracted from 42 than from 37 or 25°C spores (Fig. 5D).

To analyse whether the observed different amount of CotH-dependent proteins was dependent on their extractability, spores expressing CotG and CotC fused to RFP or GFP (RH406 and DS127), respectively, were analysed by fluorescence microscopy (Donadio *et al.*, 2016). The highest fluorescent signal was observed around 25°C spores when the reporter proteins were fused to CotG (Fig. 6A) and around 42°C spores when GFP protein was fused to CotC (Fig. 6B). These results support the idea that the differences observed by western blot were due to different amounts of CotG and CotC present around the spores.

Results of Figs. 3–6 then suggest that the growth and sporulation temperature influence the ultrastructure and protein composition of the spore surface, in part through the action of the morphogenetic protein CotH.

CotH is a heat-labile protein

The abundance of CotH in 25°C spores (Fig. 5A) could be due to a high expression of the structural gene *cotH* at low temperatures or to a different stability of the protein at the various temperatures. To distinguish between these possibilities, *cotH* expression was analysed by using a previously characterized strain of *B. subtilis* (PY79) carrying a translational gene fusion between the *cotH* coding part and the *lacZ* gene of *Escherichia coli* (Baccigalupi *et al.*, 2004) and the *cotH*-driven β -galactosidase activity measured during sporulation at the three temperatures. The time-course experiment of Fig. 7A shows that *cotH* was expressed at different times at the three sporulation temperatures. In agreement with data of Table 1, *cotH* expression was delayed of a factor 2.4 with respect to the expression at 37°C while at 42°C it was slightly faster (Fig. 7A); however, the levels of expression were similar at the three temperatures, suggesting that similar level of CotH were produced at 25, 37 and 42°C.

The ScooP software (Pucci *et al.*, 2017) predicts the temperature-dependent stability of a monomer protein on the base of its structure and was used to analyse CotH. As the structure of the *B. subtilis* protein is not available, the *B. cereus* homolog (60% similarity) (Nguyen *et al.*, 2016) was used. The graph in Fig. 7B shows that the free energy (ΔG) associated with the CotH folding is lower at temperatures between 10 and 30°C, suggesting a major stability of the protein within this temperature range. To validate the *in silico* prediction, CotH of *B. subtilis* was overproduced in *E. coli* and purified by affinity

Effects of the temperature on *Bacillus subtilis* spores 175

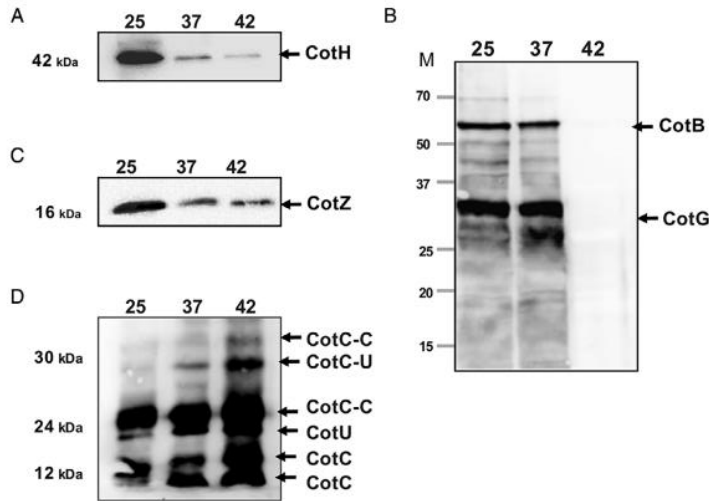


Fig. 5. Western blotting analysis of CotH and CotH-dependent proteins. Proteins extracted from spores prepared at the three temperatures were probed with anti-CotH (A), anti-PKC (B), anti-CotZ (C) or anti-CotC (D) antibodies. M: Protein marker (kDa). The various forms of CotC and CotU, all recognized by the same antibody (Isticato *et al.*, 2004) are indicated.

chromatography. The purified protein was incubated 30 min at 25, 37 or 42°C and the intrinsic fluorescence of the Trp residues measured by spectrofluorimetric analysis (Vivian and Callis, 2001). By this approach when the protein is properly folded the Trp residues are hidden and a high fluorescence intensity is expected. On the contrary, low fluorescence intensity is expected when the protein is unfolded and the Trp residues exposed to the

hydrophilic environment (Vivian and Callis, 2001). As shown in Fig. 7C, a decrease of fluorescent emission was observed raising the temperature of incubation of CotH. Results of Fig. 7 then indicate that CotH is produced at similar levels at 25, 37 and 42°C, and that the protein is more stable at low temperatures, suggesting that CotH is a heat-labile protein and explaining its higher abundance and activity at 25°C.

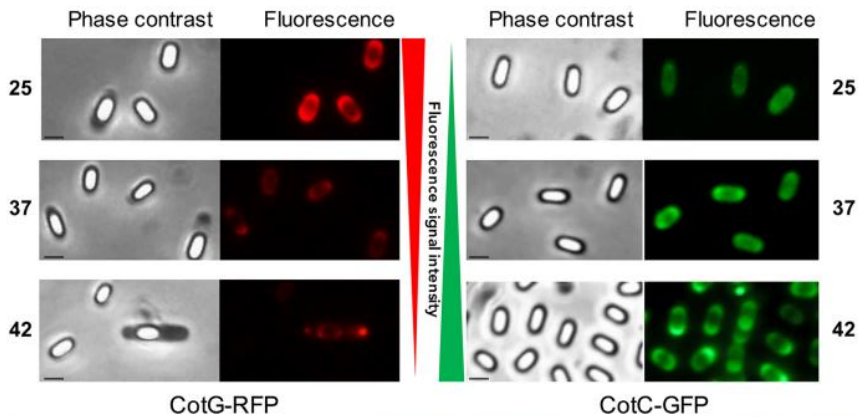


Fig. 6. Fluorescence microscopy analysis of spores expressing CotG-RFP and CotC-GFP and produced at different 25, 37 and 42°C. Phase-contrast and fluorescence images of spores of the RH406 (A) and DS127 (B) strains are shown. A representative microscopy field is reported for each temperature and strain. Scale bar 1 μm . The exposure time was the same for all samples with the same reporter gene. [Color figure can be viewed at wileyonlinelibrary.com]

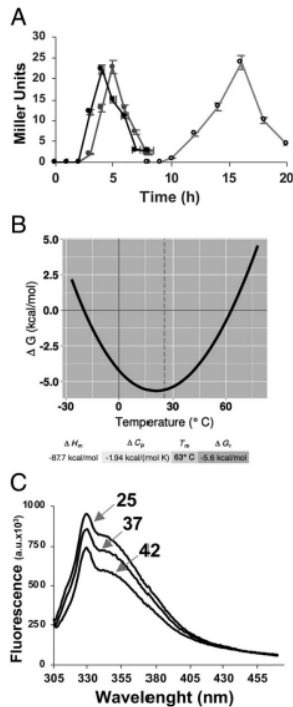


Fig. 7. Production and stability of CotH at 25, 37 and 42°C. A. Expression of a *cotH::lacZ* translational fusion (Baccigalupi et al., 2004) during sporulation at 25°C (white circles), 37°C (grey circles) and 42°C (black circles). Samples were collected at various times after the onset of sporulation. Enzyme activity is expressed in Miller units. The data are the means of two independent experiments. B. Stability curve of CotH in function of the temperature obtained by SCOP software (Pucci et al., 2017). C. CotH thermal stability monitored spectrofluorimetrically by Trp fluorescence. CotH emission was scanned after 30 min of incubation at 25, 37 and 42°C. For each temperature, the fluorescence emission of Trp was measured and normalized with the native protein. CotH concentration was 5 mmol l⁻¹ in PBS. Each spectrum was the average of three scans.

Spores lacking CotH are strongly defective when produced at low temperatures

Results of Figs. 5A, 5B and 7 propose CotH as a major regulator of coat formation at low temperatures of growth. To confirm this conclusion, a mutant strain not expressing CotH (Naclerio et al., 1996) was used to produce spores at 25, 37 and 42°C and to compare their structure and function. The mutant strain is not altered for its growth rate and sporulation efficiency (Naclerio et al., 1996), therefore spores were collected after 30 h (37 and 42°C) or 69 h (25°C), as defined for its isogenic parental strain, and used for functional analyses. Similar to wild-type

spores, also mutant spores produced at 25°C were less resistant to both lysozyme (Fig. 8A) and heat (Fig. 8B), but the effect was more severe than with the wild type (dashed bars in both panels).

Mutant spores produced at all three temperatures were less efficient to germinate than the isogenic wild-type spores with both asparagine (Fig. 8C) or alanine (Fig. 8D) as germination inducer. Comparing mutant (continuous lines in Figs. 8C and 8D) and wild type (dashed lines in Figs. 8C and 8D) spores, those produced at 25°C showed the biggest difference with both germinants.

Mutant spores produced at the three temperatures showed similar relative hydrophobicity (Fig. 8E), suggesting that the relative high hydrophobicity of wild-type spores produced at 25°C spores (Fig. 2C) was mostly due to CotH or CotH-dependent proteins.

Spores lacking CotH were also used for a structural analysis. As previously reported (Zilhao et al., 2004), *cotH* spores produced at 37°C showed an altered coat ultra-structure with both the inner and outer coat thinner than in wild-type spores and detached from each other (Fig. 9A). The same spores produced at 25°C showed a more severe alteration of both the inner and outer coat, which appeared to be amorphous and partially detached from the underlying cortex layer (Fig. 9A). At 42°C, the outer coat of *cotH* spores was thinner and less granular than wild-type spores produced at the same temperature (Fig. 9A).

Mutant spores were then used to extract and analyse by SDS-PAGE coat proteins. As shown in Fig. 9B and as previously reported for 37°C spores (Naclerio et al., 1996), the total number of proteins extracted from the *cotH* mutant was low compared with wild-type spores (see Fig. 4A). The profile of proteins extracted from 42°C spores was similar to that extracted from wild-type spores produced at the same temperature (see Fig. 4A). The profile of proteins extracted from mutant spores produced at 25°C showed two prominent proteins not present in the extracts of spores produced at 37 or 42°C (indicated by black arrows in Fig. 8B). These two proteins, identified by N-terminal amino acid sequencing as Mpr (33.7 kDa) and TasA (28.5 kDa), are known to be present in the core of the spore and their extraction by a coat-extraction treatment has been previously associated to a severely defective coat (Stöver and Driks, 1999).

Altogether results of Figs. 8 and 9 indicate that spores lacking CotH are strongly defective at 25°C and much less so at 42°C, in keeping with previous results indicating CotH as a major regulator of coat structure at low temperatures.

Conclusions

Main results of this manuscript are that *B. subtilis* builds structurally and functionally different spores in response

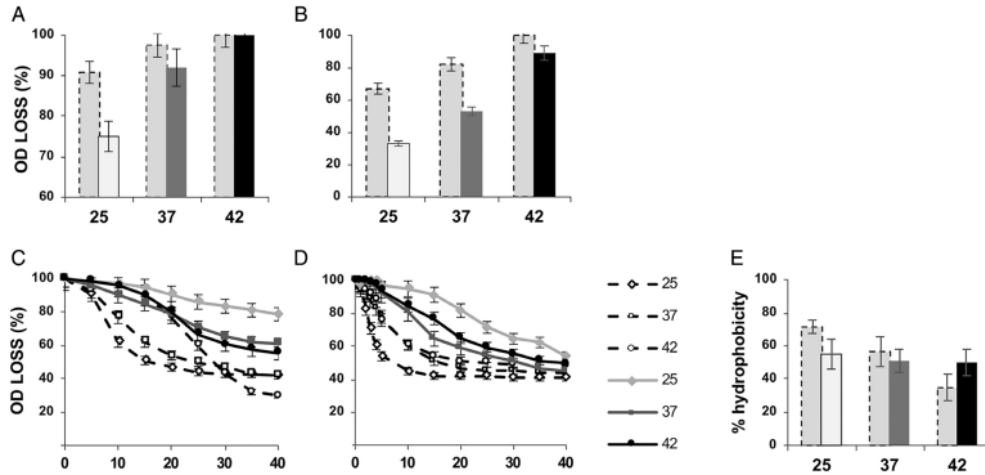


Fig. 8. Functional analysis of *cotH* mutant spores. Resistance to lysozyme digestion (A) and to heat (B) of spores produced at 25, 37 and 42°C of a wild type (dashed bars) and a *cotH* mutant (continuous bars). Germination in response to asparagine (C) or to alanine (D) of wild type (dashed lines) and *cotH* mutant (continuous lines) spores produced at 25°C (diamonds), 37°C (squares) and 42°C (circles). The percentage of germination was determined as OD₆₀₀ loss. Data are the means from three replicate experiments, each performed with an independently prepared spore suspension. Bars represent standard deviations. E. Percentage of hydrophobicity of wild type (dashed bars) and *cotH* mutant (continuous bars). Each percentage is the mean from three replicate experiments, each performed with an independently prepared spore suspension. Error bars represent standard deviations.

to the different environmental temperatures and that CotH is a heat-labile protein with a pivotal role in determining the outer coat protein composition at low temperatures.

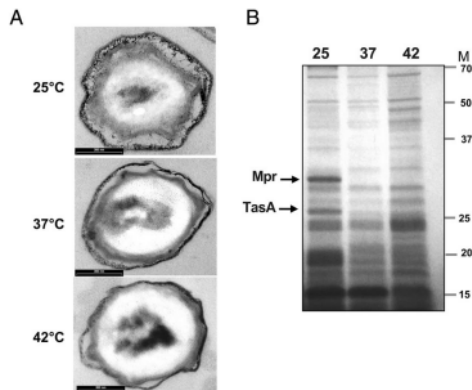


Fig. 9. Structural analysis of *cotH* mutant spores. A. Thin section transmission electron micrograph of *cotH* mutant spores produced at 25, 37 or 42°C. Bars correspond to 300 nm. B. SDS-PAGE profile of coat proteins extracted from *cotH* mutant spores. Arrows indicate proteins more abundantly extracted from 25°C spores than from 37 or 42°C identified by N-terminal amino acid sequencing. M: Protein marker (kDa).

Spores of the same age produced at 25, 37 or 42°C showed different functional and structural properties. In particular, compared with 37°C spores those produced at 25°C were less resistant to lysozyme and heat, slightly faster to germinate, more hydrophobic and showed a compact and lamellar outer coat, partially detached from the inner coat. Those produced at 42°C were, instead, more resistant to lysozyme and heat, slower to respond to asparagine as a germinant, less hydrophobic and showed a thick and apparently granular outer coat, reminiscent of the structure produced at 37°C by a mutant strain lacking CotG (Freitas *et al.*, 2019). The effects of the temperature on the spore relative hydrophobicity could be a consequence of the effects on CotG and CotZ. As both these proteins are major crust components (McKenney *et al.*, 2010), their amount affects crust composition which in turn affects the spore relative hydrophobicity (Shuster *et al.*, 2019).

Consistently with the ultrastructural analysis, the coat of spores produced at the three temperatures differed also in their protein composition, with several proteins that were extracted in different quantities from spores grown at 25, 37 or 42°C. Several of the proteins affected by the temperature belong to the group of CotH-dependent proteins and we observed that CotH is itself thermo-responsive. It is produced at the same levels at all tested temperatures but is heat labile and, therefore, more stable at low than at high temperatures.

CotH is known to have a regulatory role on the assembly of at least nine other coat proteins, including CotB, CotC, CotG, CotS, CotZ and CotQ (Kim *et al.*, 2006). CotH is an atypical kinase and performs its regulatory role on CotB and CotG by phosphorylating the serine residues present in the two coat proteins (Nguyen *et al.*, 2016). In agreement with the instability of CotH at high temperatures, we observed kinase activity only at 25 and 37°C while at 42°C no phosphorylation of CotB and CotG was detected. Based on this, we infer that the heat-labile kinase CotH phosphorylates CotB and CotG, allowing their coat assembly at 25 and 37°C, while at 42°C CotB–CotG are not phosphorylated and not assembled in the forming coat. It is noteworthy to observe that wild-type spores produced at 42°C do not contain CotG and have ultrastructural properties reminiscent of spores produced at 37°C by a CotG-lacking strain (Freitas *et al.*, 2019).

Other CotH-dependent proteins are not phosphorylated and therefore respond to CotH and to the temperature by different mechanisms. CotC and CotU, showed an opposite trend with respect to CotB–CotG and were extracted in higher amounts from 42°C spores than from 37 or 25°C. This observation is not surprising, since it has been previously reported (Saggese *et al.*, 2014) that in a CotH-lacking strain CotG has a negative effect on the coat assembly of CotC and CotU by a still unknown mechanism. Therefore, it is likely that the increase of CotC and CotU observed in 42°C spores was due to the absence of CotG. CotS assembly is also negatively affected by CotG when CotH is not present (Saggese *et al.*, 2014), and this is likely relevant for the observed CotS profile at the various temperatures.

As a working model for the temperature-dependent assembly of the outer coat we propose that at low temperatures CotH is abundant, active and able to efficiently phosphorylate CotB and CotG, thus allowing their coat assembly. In these conditions, the presence of CotG reduces by an unknown mechanism the amounts of CotC and CotU assembled in the outer coat. At high temperatures CotH becomes less active (or totally inactive), as a

consequence, CotG is less abundant or totally absent, and in these conditions the amounts of CotC and CotU assembled in the outer coat increase. In this way, CotH controls the switch from a CotB/CotG outer coat, which appears lamellar and highly electron dense, to a CotC/CotU outer coat that appears granular and thick.

In this still partial picture, many points remain to be elucidated, as the mechanism by which CotG plays a negative effect on CotC, CotU and CotS assembly, and the mechanism controlling CotS, CotQ and CotZ assembly. However, results so far obtained allow us to propose CotH as a major thermo-regulator of the *B. subtilis* spore surface.

Materials and methods

Bacterial strains, growth and sporulation

Bacillus subtilis strains used in this work are listed in the Table 2. Sporulation at 25, 37 and 42°C was induced by the exhaustion method in DS medium. Cell growth and sporulation induction were monitored by measuring the changes in optical density at 600 nm (OD₆₀₀) over time (Nicholson and Setlow, 1990). Fluorescence microscopy analyses were performed by collecting sporulating cells (500 µl) at various times during sporulation, re-suspending the sporangia in 50 µl of 1× PBS buffer and observing 5 µl with an Olympus BX51 fluorescence microscope using 100× objective UPlanF1. Phase-contrast and green fluorescent images were acquired as previously described (Donadio *et al.*, 2016). Cell growth and sporulation experiments to obtain spores of similar age were performed at least five times.

Purification of mature spores was performed by cold-water washing using overnight incubation in H₂O at 4°C to lyse residual sporangial cells. Spore purity was checked under optical microscope (Olympus BH-2 with 100× lenses) and was higher than 95% (Nicholson and Setlow, 1990). Spore counts were determined by direct counting with a Bürker chamber (Sigma, USA; BR719505) under an optical microscope (Olympus BH-2 with 40× lens).

Germination efficiency

Purified spores were heat activated as previously described (Cutting and Vander Horn, 1990) and diluted in 10 mM Tris–HCl (pH 8.0) buffer containing 1 mM glucose, 1 mM fructose, and 10 mM KCl. The germination was induced by adding 10 mM L-asparagine or 10 mM L-alanine and the assays were conducted in triplicate in 96-well plates incubated at 37°C measuring the optical density decrease at 580 nm in a microplates reader Biotek Synergy H4 (Cutting and Vander Horn, 1990).

Table 2. Bacterial strains.

	Strain	Genotype	Source
<i>Bacillus subtilis</i>	PY79	Wild type	Youngman <i>et al.</i> (1984)
	ER209	<i>cotH</i>	Naclerio <i>et al.</i> (1996)
	RH2466	<i>pspQ::gfp</i>	Donadio <i>et al.</i> (2016)
	RH2467	<i>pgfE::gfp</i>	Donadio <i>et al.</i> (2016)
	DS127	<i>cotC::gfp</i>	Donadio <i>et al.</i> (2016)
<i>Escherichia coli</i>	RH406	<i>cotG::rfp</i>	This study
	VS13	<i>cotH::his</i>	Isticato <i>et al.</i> (2015)
	GC237	<i>cotH::lacZ</i>	Baccigalupi <i>et al.</i> (2004)

Gemination was also monitored by cytofluorimetry as previously described (Cangiano *et al.*, 2014).

Lysozyme and heat resistance

Purified spores ($OD_{600} \sim 0.8$) were re-suspended in 10 mM Tris-HCl (pH 7.8) containing lysozyme (50 mg ml^{-1}) and the decrease in optical density was monitored at 595 nm for 30 min (Cutting and Vander Horn, 1990). Purified spores ($OD_{600} \sim 0.4$) were incubated at 100°C for 10 min. The decrease in optical density was monitored at 580 nm in 96-well plates using a microplates reader Biotek Synergy H4, with readings every 5 min for an hour (Cutting and Vander Horn, 1990). All experiments were conducted twice with two independently prepared batches of spores. All measurements were done in triplicate.

DPA content and DPA release

DPA concentration was measured as previously described (Abhyankar *et al.*, 2016). In brief, spore suspensions at an OD_{600} of 1.0 were washed twice in 50 mM KCl to remove readily exchangeable calcium, suspended in 1 ml of sterile Milli-Q water and subsequently autoclaved at 121°C for 30 min to induce the release of DPA. Then the samples were cooled on ice, centrifuged (10 min at 13 000g) and 0.8 ml of supernatant was transferred to new test tubes. Next, 0.2 ml of color reagent [$1\% \text{ Fe}(\text{NH}_4)_2(\text{SO}_4)_2 \cdot 6\text{H}_2\text{O}$ along with 1% ascorbic acid in 0.5 M acetate buffer of pH 5.5] was added to the supernatant. By measuring the absorbance at 440 nm, a standard curve was prepared for the concentration range of $100\text{--}10 \text{ mg l}^{-1}$. The OD_{440} of the samples was measured and the amounts of DPA/spores were calculated from the standard curve.

DPA release from heat-treated spores was monitored by measuring the emission at 545 nm of the fluorescent terbium-DPA complex as previously described (Jamroskovic *et al.*, 2016).

Suspension of 1.0×10^9 spores were incubated at 50, 80, 100 and 110°C for 15 min, then centrifuged (10 min at 13,000g) and the supernatant was transferred to 200 μl wells of a 96-well microtiter plate, in the presence of a freshly prepared solution of $30 \mu\text{M}$ TbCl_3 in 400 mM sodium acetate buffer, pH 5. The DPA content was measured following the formation of terbium³⁺-DPA complex in a microplates reader Synergy H4, BioTek, reading up to 1-h each 5 min ($\lambda_{\text{ex}} = 276$ and 545 nm). A sample containing $30 \mu\text{M}$ TbCl_3 was used as a blank while samples containing various concentrations of DPA without TbCl_3 were measured and their photoluminescence subtracted as background.

Effects of the temperature on *Bacillus subtilis* spores 179

Two independent experiments were carried out for each data point, and all measurements were done in duplicate.

Hydrophobicity assay

Spore relative hydrophobicity was evaluated by the BATH assay (Wiencek *et al.*, 1990). Briefly, 3.0 ml of water containing 1.5×10^8 spores produced at 25, 37 and 42°C was incubated for 15 min at 25°C . After incubation, 1.0 ml of hexadecane (Sigma-Aldrich) was added to each spore suspension, and the mixture was vortexed for 1 min in glass test tubes ($15 \times 100 \text{ mm}$). After 15 min, to allow the partition of the two phases, the aqueous phase was carefully collected with a Pasteur pipette, and the OD_{440} was measured. The spore relative hydrophobicity was calculated as

$$\text{Spore relative hydrophobicity} = \left(\frac{A_0 - A_f}{A_0} \right) \times 100.$$

where A_0 and A_f were the initial and final OD_{440} respectively.

Transmission electron microscopy

For thin sectioning TEM analysis, purified spores were processed as described previously [Freitas *et al.*, 2019] and imaged on a Philips EM 208S (FEI) microscope equipped with digital camera and Image Analysis Software.

Extraction of coat proteins and western blot analysis

Spore coat proteins were extracted from a suspension of spores by SDS-DTT or NaOH treatment (Isticato *et al.*, 2015). The concentration of extracted proteins was determined by using Bio-Rad DC protein assay kit (Bio-Rad), and 20 μg of total spore coat proteins were fractionated on 12.5% SDS polyacrylamide gels and staining by Brilliant Blue Coomassie or electro-transferred to nitrocellulose filters (Bio-Rad) for western blot analysis following standard procedures. CotH-, CotA-, CotC-, CotB-, CotG- (Isticato *et al.*, 2013) and Phospho-(Ser) PKC substrate-specific antibodies (Cell signal technology) were used at working dilutions of 1:150 for CotH detection, 1:7000 for CotA, CotC, CotB and CotG detection and 1:10 000 for PKC. Then a horseradish peroxidase-conjugated anti-rabbit secondary antibody was used (Santa Cruz). Western blot filters were visualized by the electro chemi luminescence method as specified by the manufacturer and processed to improve the contrast level using ChemidocXRS software (Bio-Rad).

180 R. Isticato et al.

Construction of *cotG::rfp* fusion

The coding sequence of *rfp* was polymerase chain reaction amplified using pRSET A-RFP plasmid DNA (Donadio *et al.*, 2016) as a template and synthetic oligonucleotides RFP-for (5'-GAATTCATGGCCTCCTCGG AGGAC-3') and RFP-rev (5'-GGTACCTTAGGCGCCGG TGGAG-3') to prime the reaction. The purified DNA fragment of 564 bp was digested with *EcoRI* and *KpnI* and cloned in frame to the 3' end of the *cotG* gene carried by the integrative vector pCotG-C (Iwanicki *et al.*, 2014), previously digested with the same restriction enzymes. The new plasmid was used to transform competent cells of strain PY79, yielding strain RH406 (*cotG::rfp*).

β -Galactosidase assay

Samples (1.0 ml each) of *cotH::lacZ*-bearing cells were collected during sporulation performed at 25, 37 and 42°C, centrifuged (10 min at 5000g) and the pellets assayed as previously described (Schaefer *et al.*, 2016) with some modifications. Briefly, 0.3 ml of a Z-Buffer solution (60 mM Na₂HPO₄ × 7H₂O, 40 mM NaH₂PO₄, 10 mM KCl, 1 mM MgSO₄ × 7H₂O, 166 μ l ml⁻¹ lysozyme, 50 mM β -mercaptoethanol) and 10 μ l of toluene, to permeabilize the cells, were added to the thawed pellets. After preincubation at 30°C for 15 min, 0.15 ml of each sample was transferred in 96 multiwells. The reaction starts adding 30 μ l of 4 mg ml⁻¹ ortho-Nitrophenyl- β -galactoside. The optical density was monitored at 420 and 595 nm in a microplates reader Biotek Synergy H4, reading every 2 minutes for the first 10 min and every 5 min for the 20 later min. The specific β -galactosidase activity was expressed in Miller units, calculated as follows:

$$\text{Miller Units} = \frac{1000 * (\text{OD}_{420} \text{ min}^{-1})}{\text{OD}_{595} * \text{volume used}}$$

where the kinetic OD₄₂₀ readings were converted into the slope of OD₄₂₀ over time (OD₄₂₀ min⁻¹).

Expression and purification of Coth

For Coth production, cells of *E. coli* strain VS13 (Isticato *et al.*, 2015), bearing pBAD-B expression vector (Life Technologies) carrying an in-frame fusion of the 5' end of the *cotH* coding region to six histidines, were grown for 18 h at 37°C in 100 ml of autoinduction medium to express the heterologous protein (Isticato *et al.*, 2015). The His6-tagged Coth protein was purified under native conditions using a His-Trap column as recommended by the manufacturer (GE Healthcare Life Science). Purified protein was desalted using a PD10 column

(GE Healthcare Life Science) to remove high NaCl and imidazole concentrations.

Spectrofluorometry

Purified Coth was dissolved in 1× PBS at a concentration of 5 μ mol l⁻¹. Fluorescence spectra were acquired after 30 min of incubation at 25, 37 and 42°C with a Fluoromax-4 fluorometer (Horiba, Edison, NJ) in 1 cm path length quartz cuvette. Samples were continuously stirred and allowed to equilibrate to each temperature before fluorescence readings were taken. Excitation wavelength of 295 nm was used to avoid the contribution from tyrosine residues. The excitation and emission band widths were set to 5 and 2.5 nm respectively. The emission spectra were recorded from 305 to 470. Each spectrum was the average of three scans (Jokiel *et al.*, 2005).

Acknowledgements

We thank Gianna Alleva for contribution to perform some of the experiments. This work was in part supported by a grant from the 'Programma per il finanziamento della ricerca di ateneo' grant number DR341 2016 to LB.

References

- Abhyankar, W.R., Kamphorst, K., Swarge, B.N., van Veen, H., van der Wel, N.N., Brul, S., *et al.* (2016) The influence of sporulation conditions on the spore coat protein composition of *Bacillus subtilis* spores. *Front Microbiol* **7**: 1636.
- Alturi, S., Ragkousi, K., Cortezzo, D.E., and Setlow, P. (2006) Cooperativity between different nutrient receptors in germination of spores of *Bacillus subtilis* and reduction of this cooperativity by alterations in the GerB receptor. *J Bacteriol* **188**: 28–36.
- Baccigalupi, L., Castaldo, G., Cangiano, G., Isticato, R., Marasco, R., De Felice, M., and Ricca, E. (2004) GerE-independent expression of *cotH* leads to CotC accumulation in the mother cell compartment during *Bacillus subtilis* sporulation. *Microbiology* **150**: 3441–3449.
- Bressuire-Isoard, C., Bomard, I., Henriques, A.O., Carlin, F., and Broussolle, V. (2015) Sporulation temperature reveals a requirement for CotE in the assembly of both the coat and exosporium layers of *Bacillus cereus* spores. *Appl Environ Microbiol* **82**: 232–243.
- Camilleri, E., Korza, G., Green, J., Yuan, J., Li, Y., Caimano, M.J., and Setlow, P. (2019) Properties of Aged Spores of *Bacillus subtilis*. *J Bacteriol* **201**: e00231–e00219.
- Cangiano, G., Sirec, T., Panarella, C., Isticato, R., Baccigalupi, L., De Felice, M., and Ricca, E. (2014) The *sps* gene products affect germination, hydrophobicity and protein adsorption of *Bacillus subtilis* spores. *Appl Environ Microbiol* **80**: 7293–7302.
- Christie, G., and Lowe, C.R. (2007) Role of chromosomal and plasmid-borne receptor homologues in the response

- of *Bacillus megaterium* QM B1551 spores to germinants. *J Bacteriol* **189**: 4375–4383.
- Cupit, C., Lomstein, B., and Kjeldsen, K. (2018) Contrasting community composition of endospores and vegetative Firmicutes in a marine sediment suggests both endo- and exogenous sources of endospore accumulation: Identity and origin of endospores in the seafloor. *Environ Microbiol Rep* **11**: 352–360.
- Cutting, S., and Vander Horn, P.B. (1990) Genetic analysis. In *Molecular Biological Methods for Bacillus*, Harwood, C., and Cutting, S. (eds). Chichester, UK: John Wiley and Sons, pp. 27–74.
- Cutting, S.M. (2011) *Bacillus* probiotics. *Food Microbiol* **28**: 214–220.
- Donadio, G., Lanzilli, M., Sirec, T., Ricca, E., and Isticato, R. (2016) Localization of a red fluorescence protein adsorbed on wild type and mutant spores of *Bacillus subtilis*. *Microb Cell Fact* **15**: 153.
- El-Bisi, H.M., and Ordal, Z.J. (1956) The effect of sporulation temperature on the thermal resistance of *Bacillus coagulans* var. *thermoacidurans*. *J Bacteriol* **71**: 10–16.
- Freitas, C., Plannic, J., Isticato, R., Pelosi, A., Zilhão, R., Serrano, M., et al. (2019) A protein phosphorylation module patterns the *Bacillus subtilis* spore outer coat. *bioRxiv* 469122. *Mol Microbiol*. <https://doi.org/10.1101/469122>.
- Fujita, M., and Losick, R. (2003) The master regulator for entry into sporulation in *Bacillus subtilis* becomes a cell-specific transcription factor after asymmetric division. *Genes Dev* **17**: 1166–1174.
- Henriques, A.O., and Moran, C.P., Jr. (2007) Structure, assembly, and function of the spore surface layers. *Annu Rev Microbiol* **61**: 555–588.
- Isticato, R., Esposito, G., Zilhão, R., Nolasco, S., Cangiano, G., De Felice, M., et al. (2004) Assembly of multiple CotC forms into the *Bacillus subtilis* spore coat. *J Bacteriol* **186**: 1129–1135.
- Isticato, R., Sirec, T., Giglio, R., Baccigalupi, L., Rusciano, G., Pesce, G., et al. (2013) Flexibility of the programme of spore coat formation in *Bacillus subtilis*: bypass of CotE requirement by over-production of CotH. *PLoS One* **8**: 10.1371.
- Isticato, R., Sirec, T., Vecchione, S., Crispino, A., Saggese, A., Baccigalupi, L., et al. (2015) The direct interaction between two morphogenetic proteins is essential for spore coat formation in *Bacillus subtilis*. *PLoS One* **10**: e0141040.
- Iwanicki, A., Piątek, I., Stasiłojć, M., Grela, A., Łęga, T., Obuchowski, M., and Hinc, K. (2014) A system of vectors for *Bacillus subtilis* spore surface display. *Microb Cell Fact* **13**: 30.
- Jamroskovic, J., Chromikova, Z., List, C., Bartova, B., Barak, I., and Bemier-Latmani, R. (2016) Variability in DPA and calcium content in the spores of *Clostridium* species. *Front Microbiol* **7**: 1791.
- Jokiel, M., Klajnert, B., and Bryszewska, M. (2005) Use of a spectrofluorimetric method to monitor changes of human serum albumin thermal stability in the presence of polyamidoamine dendrimers. *J Fluoresc* **16**: 149–152.
- Kailas, L., Terry, C., Abbot, N., Taylor, R., Mulin, N., Tzokov, S.B., et al. (2011) Surface architecture of endospores of the *Bacillus cereus/anthracis/thuringiensis* family at the subnanometer scale. *Proc Natl Acad Sci USA* **108**: 16014–16019.
- Kim, H., Hahn, M., Grabowski, P., McPherson, D.C., Otte, M. M., Wang, R., et al. (2006) The *Bacillus subtilis* spore coat protein interaction network. *Mol Microbiol* **59**: 487–502.
- Leguérinel, I., Couvert, O., and Mafart, P. (2007) Modelling the influence of the sporulation temperature upon the bacterial spore heat resistance, application to heating process calculation. *Int J Food Microbiol* **114**: 100–104.
- McKenney, P.T., Driks, A., and Eichenberger, P. (2013) The *Bacillus subtilis* endospore: assembly and functions of the multilayered coat. *Nat Rev Microbiol* **11**: 33–44.
- McKenney, P.T., Driks, A., Eskandarian, H.A., Grabowski, P., Guberman, J., Wang, K.H., et al. (2010) A distance-weighted interaction map reveals a previously uncharacterized layer of the *Bacillus subtilis* spore coat. *Curr Biol* **20**: 934–938.
- Melly, E., Cowan, A.E., and Setlow, P. (2002) Studies on the mechanism of killing of *Bacillus subtilis* spores by hydrogen peroxide. *J Appl Microbiol* **93**: 316–325.
- Mir, Z., Mir, P.S., Zaman, M.S., Selinger, L.B., McAllister, T. A., Yanke, L.J., and Cheng, K.-J. (1997) Use of *Bacillus stearothermophilus* spores as a marker for estimating digesta passage rate from the rumen in cattle. *Livestock Prod Sci* **47**: 231–234.
- Muller, A.L., de Rezende, J.R., Hubert, C.R.J., Kjeldsen, K. U., Lagkouvardos, I., Berry, D., et al. (2014) Endospores of thermophilic bacteria as tracers of microbial dispersal by ocean currents. *ISME J* **8**: 1153–1165.
- Naclerio, G., Baccigalupi, L., Zilhão, R., De Felice, M., and Ricca, E. (1996) *Bacillus subtilis* spore coat assembly requires *cotH* gene expression. *J Bacteriol* **178**: 4375–4380.
- Nguyen, K.B., Sreelatha, A., Durrant, E.S., Lopez-Garrido, J., Muszewska, A., Dudkiewicz, M., et al. (2016) Atypical spore coat protein kinases. *Proc Natl Acad Sci USA* **113**: E3482–E3491.
- Nicholson, W.L., Munakata, N., Homeck, G., Melosh, H.J., and Setlow, P. (2000) Resistance of *Bacillus* endospores to extreme terrestrial and extraterrestrial environments. *Microbiol Mol Biol Rev* **64**: 548–572.
- Nicholson, W.L., and Setlow, P. (1990) Sporulation, germination and outgrowth. In *Molecular Biological Methods for Bacillus*, Harwood, C., and Cutting, S. (eds). Chichester, UK: John Wiley and Sons, pp. 391–450.
- Palop, A., Raso, J., Condón, S., and Sala, F.J. (1995) Heat resistance of *Bacillus subtilis* and *Bacillus coagulans*: effect of sporulation temperature in foods with various acidulants. *J Bacteriol* **59**: 487–492.
- Pucci, F., Kwasiogroch, J.M., and Rooman, M. (2017) SCooP: an accurate and fast predictor of protein stability curves as a function of temperature. *Bioinformatics* **33**: 3415–3422.
- Saggese, A., Scamardella, V., Sirec, T., Cangiano, G., Isticato, R., Parè, F., et al. (2014) Antagonistic role of CotG and CotH on spore germination and coat formation in *Bacillus subtilis*. *PLoS One* **9**: e104900.
- Sanchez-Salas, J.L., Setlow, B., Zhang, P., Li, Y.Q., and Setlow, P. (2011) Maturation of released spores is necessary for acquisition of full spore heat resistance during *Bacillus subtilis* sporulation. *Appl Environ Microbiol* **77**: 6746–6754.

CHAPTER VII

Petrillo *et al. Microb Cell Fact* (2020) 19:185
<https://doi.org/10.1186/s12934-020-01446-6>

Microbial Cell Factories

RESEARCH

Open Access

The temperature of growth and sporulation modulates the efficiency of spore-display in *Bacillus subtilis*



Claudia Petrillo¹, Stefany Castaldi¹, Mariamichela Lanzilli^{1,3}, Anella Saggese¹, Giuliana Donadio^{1,4}, Loredana Baccigalupi², Ezio Ricca^{1*} and Rachele Isticato¹

Abstract

Background: Bacterial spores displaying heterologous antigens or enzymes have long been proposed as mucosal vaccines, functionalized probiotics or biocatalysts. Two main strategies have been developed to display heterologous molecules on the surface of *Bacillus subtilis* spores: (i) a recombinant approach, based on the construction of a gene fusion between a gene coding for a coat protein (carrier) and DNA coding for the protein to be displayed, and (ii) a non-recombinant approach, based on the spontaneous and stable adsorption of heterologous molecules on the spore surface. Both systems have advantages and drawbacks and the selection of one or the other depends on the protein to be displayed and on the final use of the activated spore. It has been recently shown that *B. subtilis* builds structurally and functionally different spores when grown at different temperatures; based on this finding *B. subtilis* spores prepared at 25, 37 or 42 °C were compared for their efficiency in displaying various model proteins by either the recombinant or the non-recombinant approach.

Results: Immune- and fluorescence-based assays were used to analyze the display of several model proteins on spores prepared at 25, 37 or 42 °C. Recombinant spores displayed different amounts of the same fusion protein in response to the temperature of spore production. In spores simultaneously displaying two fusion proteins, each of them was differentially displayed at the various temperatures. The display by the non-recombinant approach was only modestly affected by the temperature of spore production, with spores prepared at 37 or 42 °C slightly more efficient than 25 °C spores in adsorbing at least some of the model proteins tested.

Conclusion: Our results indicate that the temperature of spore production allows control of the display of heterologous proteins on spores and, therefore, that the spore-display strategy can be optimized for the specific final use of the activated spores by selecting the display approach, the carrier protein and the temperature of spore production.

Keywords: Display platform, Mucosal vaccines, *Bacillus subtilis*, Probiotics

Introduction

Endospores (spores) are quiescent cell forms produced by over 1000 bacterial species when the environmental conditions do not allow cell growth to continue [1].

In the spore form, these bacterial species can survive conditions, such as the prolonged absence of water and nutrients, the exposure to extremes of temperature and pH, to UV irradiations and to toxic chemicals, that would be lethal for other cell forms [2]. Although metabolically quiescent, the spore is able to sense the environment and respond to conditions that allow cell growth by germinating and generating a new vegetative cell [3]. Spore germination and resistance are in part due to the peculiar

*Correspondence: ericca@unina.it

¹ Department of Biology, Federico II University complesso universitario di Monte Sant'Angelo via Cinthia, 80126 Napoli, Italy
Full list of author information is available at the end of the article



© The Author(s) 2020. This article is licensed under a Creative Commons Attribution 4.0 International License, which permits use, sharing, adaptation, distribution and reproduction in any medium or format, as long as you give appropriate credit to the original author(s) and the source, provide a link to the Creative Commons licence, and indicate if changes were made. The images or other third party material in this article are included in the article's Creative Commons licence, unless indicated otherwise in a credit line to the material. If material is not included in the article's Creative Commons licence and your intended use is not permitted by statutory regulation or exceeds the permitted use, you will need to obtain permission directly from the copyright holder. To view a copy of this licence, visit <http://creativecommons.org/licenses/by/4.0/>. The Creative Commons Public Domain Dedication waiver (<http://creativecommons.org/publicdomain/zero/1.0/>) applies to the data made available in this article, unless otherwise stated in a credit line to the data.

structure of the spore, that has been studied in detail in *Bacillus subtilis*, the model system for spore formers [2, 4]. In *B. subtilis*, spores are formed by a partially dehydrated cytoplasm (core) surrounded by several protective layers: the thick peptidoglycan-like cortex, the multilayered, proteinaceous coat and the crust, the outermost layer formed of proteins and glycans [4]. In some species, including *B. anthracis*, *B. cereus* and *B. megaterium*, the outermost layer of the coat is the exosporium, a protective shell mainly made of glycoproteins [4].

The rigidity and compactness of the spore suggested the possibility of using this unusual cell as a platform to display heterologous proteins [5]. In a *proof-of-concept* work, the spore coat protein CotB of *B. subtilis* was used as a carrier to display the C fragment of the tetanus toxin (TTFC) of *Clostridium tetani* on the spore surface [5]. To this aim a genetic system was developed to generate gene fusions between the *cotB* gene and DNA coding for TTFC and to allow expression of the fusion during sporulation [5]. The mucosal administration of recombinant spores displaying TTFC was then shown protective against a challenge with the tetanus toxin and able to induce humoral and cellular immune responses [6, 7]. Over the years, the same approach has been used with other coat proteins as carriers and a variety of other heterologous proteins [8]. However, this display system has the drawback of generating recombinant spores, that in case of a field use could raise safety concerns [9]. To overcome this problem a non-recombinant display system based on the spontaneous and stable adsorption of heterologous proteins to bacterial spores has been also developed [10, 11]. Antigens and enzymes have been efficiently and stably adsorbed to spores [12, 13] and it has been proposed that the adsorption is due to the negative electric charge and the relative hydrophobicity of the spore surface [10, 14]. In addition, studies with *B. subtilis* and *B. megaterium* indicated that some proteins were able to infiltrate through "pores" of the outermost spore coat layers and localize in the inner coat of *B. subtilis* spores [15] or in the interspace between the exosporium and the outer coat in *B. megaterium* spores [16, 17].

The spore-display system by both the recombinant or non-recombinant approach, provides several advantages with respect to other display systems, such as a high stability even after a prolonged storage, the possibility of displaying large, multimeric proteins and the safety for a human use, demonstrated by the wide use of spores of some species as probiotics [18, 19]. Based on these, the activated spore has been proposed as a mucosal delivery system, as a vaccine vehicle, as a functionalized probiotic and as a platform to display enzymes [8, 20].

Both approaches are quite efficient, and it has been estimated that up to 3.0×10^3 heterologous molecules

can be displayed by each recombinant spore of *B. subtilis* [8, 21]. The efficiency of the non-recombinant approach can be higher than that measured for the recombinant system and depends on the heterologous protein and the *Bacillus* species used [12, 15, 16, 20]. In spite of the efficiency of these systems, the possibility to increase and/or control the number of heterologous proteins presented on the spore is an important achievement for the full exploitation of this biotechnology tool. In the case of a use as a vaccine vehicle, for example, an increased efficiency of display results in a higher dose of antigen delivered or reduced amounts of spores needed for the immunization.

Based on a recent report showing that *B. subtilis* builds spores with different structure when grown at 25, 37 or 42 °C [22], we investigated whether the efficiency of spore-display by both recombinant and non-recombinant approaches could be modulated by modifying the temperature of spore production.

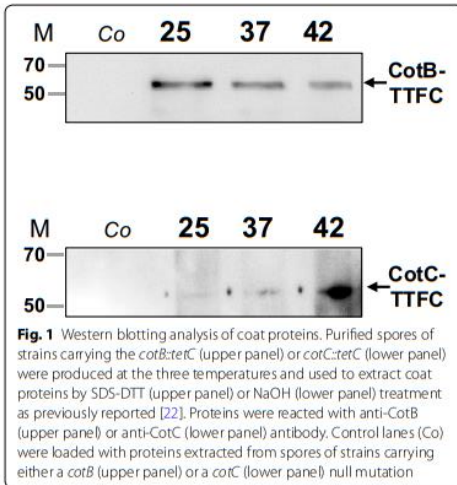
Results and discussion

Effects of the temperature on the recombinant display system

CotB, CotC and CotG are abundant coat proteins widely used as carriers to display heterologous proteins on the spore surface [8]. All three proteins have been recently found differentially represented in spores produced at 25, 37 or 42 °C, with CotB and CotG more abundant in spores prepared at 25 °C and CotC more abundant in 42 °C spores [22]. We used isogenic *B. subtilis* strains carrying DNA coding for the model antigen TTFC (*tetC*) fused to the gene coding for either CotB (*cotB*) [5] or CotC (*cotC*) [23] to evaluate the effect of the sporulation temperature on the fusion proteins. Spores of strains RH103 (*cotB::tetC*) and RH114 (*cotC::tetC*) were produced at 25, 37 and 42 °C and purified, as previously reported [22]. Surface proteins were extracted from RH103 and RH115 spores by the SDS-DTT or NaOH treatments, respectively and used for western blotting analysis with anti-CotB [5] or anti-CotC [23] antibodies.

As shown in Fig. 1, specific CotB-TTFC (upper panel) and CotC-TTFC (lower panel) signals were observed in all the samples but not in the negative controls, revealing that the temperature did not affect the self-assembly of the heterologous proteins around the spores. Moreover, we observed that the fusion protein CotB-TTFC was more represented in 25 °C spores than in 37 or 42 °C spores (upper panel), while the fusion CotC-TTFC showed the opposite trend (lower panel).

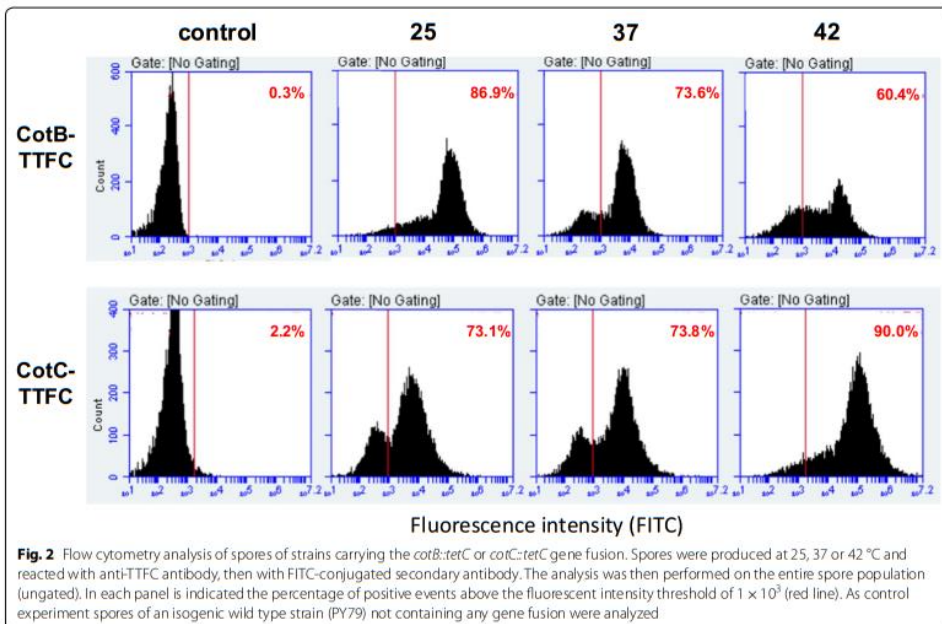
A flow cytometry approach was used to confirm and quantify the differences in the display of CotB-TTFC and CotC-TTFC at the various temperatures and evaluate their surface exposure. Spores of strains RH103



and RH114 were reacted with anti-TTFC [7] antibodies, then with fluorescently labeled secondary antibody

and analyzed by flow cytometry as previously reported [24]. The threshold of positive events was set at 1×10^3 fluorescence intensity and the percentages of fluorescent events for each temperature are indicated in red in each panel. The flow cytometry analysis indicated that CotB-TTFC was displayed with the highest efficiency in spores prepared at 25 °C (86.9% positive events) and that such efficiency decreased in 37 and 42 °C spores (Fig. 2). The efficiency of display was opposite with CotC-TTFC with the highest levels observed with 42 °C spores (90.0% of positive events) and lower levels with 37 and 25 °C spores (Fig. 2). In addition, the fluorescent intensity peak for CotB-TTFC was tenfold higher at 25 °C than at 42 °C while for CotC-TTFC was tenfold higher at 42 °C than at 25 °C, suggesting that the sporulation temperature affected not only the amount of assembled heterologous proteins but also their surface display.

Results of Figs. 1, 2 indicated, respectively, the amounts of fusion proteins extracted and exposed on the spore surface but did not allow to exclude that other amounts of each fusion were actually present (but not extracted or not exposed) on spores produced at different temperatures. To address this issue, we used different isogenic strains of *B. subtilis* RH238, carrying the Green Fluorescent Protein (GFP) fused to CotC [23], and RH296,



carrying the Red Fluorescent Protein (RFP) fused to CotG [22]. A fluorescence microscopy analysis on spores prepared at 25, 37 or 42 °C and the quantification of the fluorescence signals performed by the ImageJ software, as previously reported [24], indicated that the CotG-based fusion was more abundant at 25 °C, less abundant at 37 °C and almost undetectable at 42 °C while the CotC-based fusion showed an opposite pattern (Fig. 3).

Results of Fig. 3, confirming results of Figs. 1,2, allow to conclude that the CotB- and CotG-based fusions are efficiently displayed when spores are produced at 25 °C, while CotC-based fusions are better displayed when spores are produced at 42 °C and, therefore, that is possible to modulate the amount and the surface exposure of fusion proteins displayed on the spore by changing the temperature of spore production on the base of the carrier protein used for the display.

Effects of the temperature on recombinant spores displaying two fusion proteins

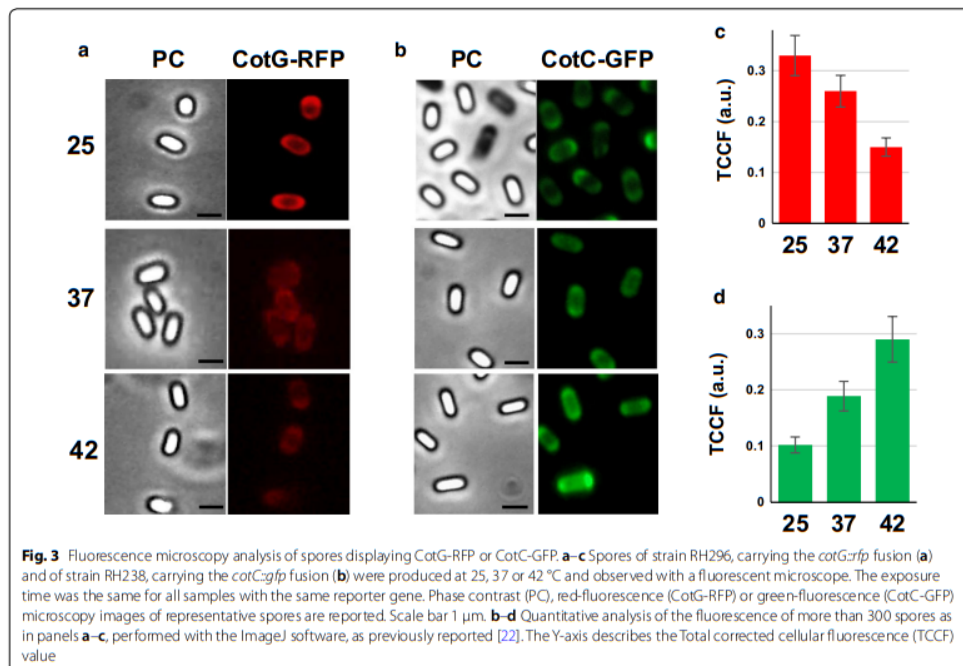
An extension of the recombinant spore-display technology is the use of spores carrying more than one heterologous protein. By chromosomal DNA-mediated

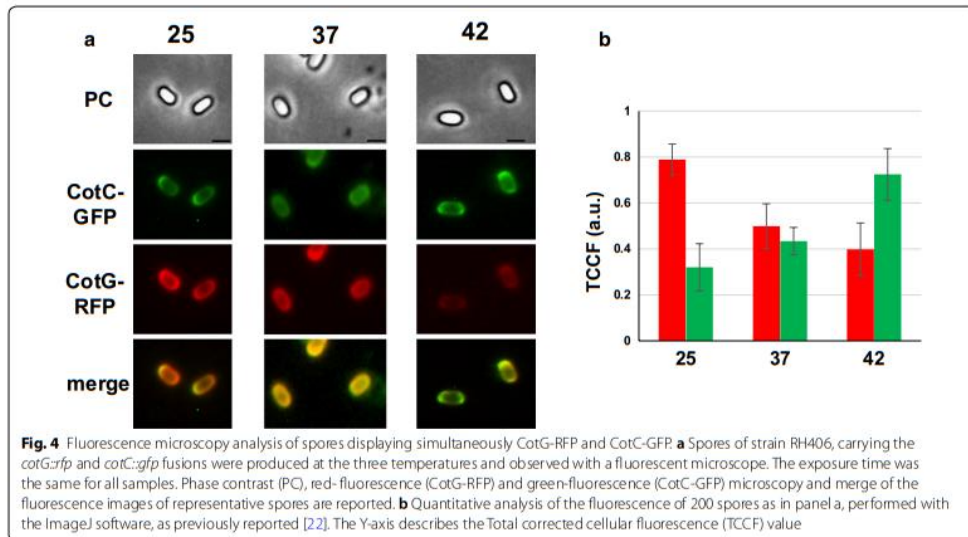
transformation [25], the gene fusion carried by strains RH238 (*cotC::gfp*) was moved into strain RH296 (*cotG::rfp*) obtaining strain RH406 that carried both fusions. As shown in Fig. 4, spores of strain RH406 presented both fluorescent proteins on their surfaces in similar amounts when spores were grown at 37 °C. When spores were produced at 25 °C the red fluorescent signal (CotG-RFP) was more abundant than the green one (CotC-GFP) that was instead predominant when spores were grown at 42 °C.

Results of Fig. 4 highlight an important improvement for the spore-display technology, showing that it is possible to produce spores that simultaneously display two heterologous proteins and to control which displayed protein has to be more abundantly represented by selecting the temperature of spore production.

Effects of the temperature on the non-recombinant display system

To evaluate the effects of the temperature on non-recombinant spore-display (adsorption) we used three model proteins: the pentapeptide HPHGH (herein PPT) of 0.77 kDa [26], the commercially available lysozyme

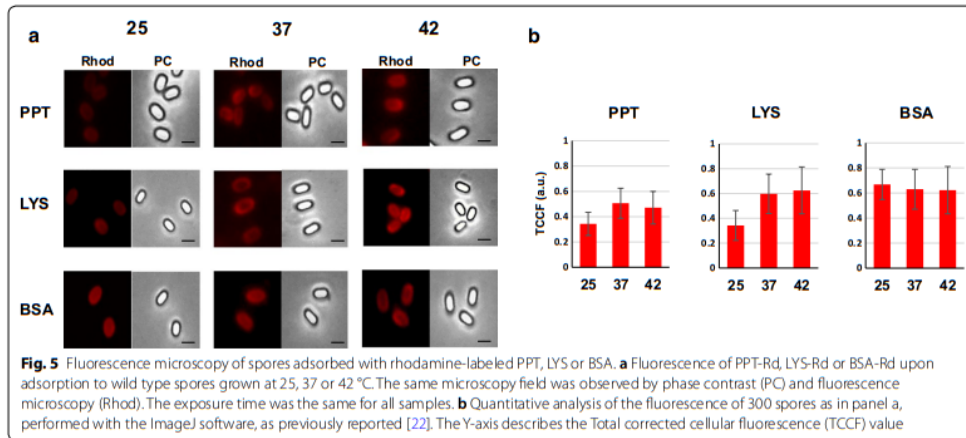




(herein LYS) of 14.4 kDa (Sigma) and the commercially available bovine serum albumin (herein BSA) of 66.4 kDa (New England-Biolabs). All three proteins were fluorescently labeled with rhodamine as previously described [26] and 10 mM of each model protein independently used for adsorption with 5.0×10^8 purified spores of the *B. subtilis* strains PY79 [27] produced at 25, 37 or 42 °C. The adsorption reactions were carried out for 1 h at 25 °C in 50 mM Sodium Citrate buffer, pH 4.0, as previously described [11]. Adsorbed spores were collected by centrifugation and analysed by fluorescence microscopy and flow cytometry, as previously described [24]. As shown in Fig. 5, all three proteins were adsorbed to the spores and the fluorescent signal distributed all around the spore surface. The relative fluorescence signals were analyzed by the ImageJ software (NIH), as previously reported [24]. Since the proteins were fluorescently tagged with rhodamine, an amine-specific label, the number of fluorophore molecules attached to each protein was different, impairing a comparison of fluorescence levels between different proteins. However, the analysis allowed to conclude that: (i) PPT adsorbed with similar efficiency to 37 °C and 42 °C and slightly less efficiently to 25 °C spores (37 = 42 > 25); ii) LYS had a pattern of adsorption similar to that described for PPT (37 = 42 > 25); and (iii) BSA adsorbed at similar levels to 25, 37 or 42 °C spores (25 = 37 = 42) (Fig. 5). Adsorbed spores were analyzed by flow cytometry and the percentage of positive-fluorescent events was obtained

as described for Fig. 2. This quantitative analysis performed in duplicate on 100,000 spores/each, confirmed the fluorescence microscopy results of Fig. 5, indicating that PPT was adsorbed much more efficiently at 37 or 42 °C, with respectively 75.95 and 77.80% positive events (p.e.) than at 25 °C (41.74% p.e.) (Fig. 6). A similar trend was observed with LYS, although the differences were smaller with 74.48, 82.15 and 90.44% p.e. at 25, 37 and 42 °C respectively, while no differences were observed with BSA with spores prepared at the three temperatures (Fig. 6).

Although the molecular mechanism of spore adsorption is not known in detail, it is likely that more factors are involved in the process. The negative electric charge and relative hydrophobicity of the spore surface have both been shown to influence the efficiency of adsorption [10, 14]. Since it has been previously reported that 25 °C spores are more hydrophobic than 37 and 42 °C spores [22], we hypothesized that the different relative hydrophobicity of spores could explain the reduced efficiency of adsorption of PPT and LYS to 25 °C spores. However, the GRAVY value, an estimation of protein hydrophobicity calculated by adding the hydropathy values of each amino acid residue of a protein and dividing by the number of residues in the protein [28], for PPT, LYS and BSA were -2.32, -0.15 and -0.45, respectively, with increasing positive values indicating an increasing hydrophobicity. Therefore, proteins with the least (PPT) and the highest (LYS) hydrophobicity value showed a similar



adsorption pattern (Figs. 5,6), making it unlikely that the hydrophobicity is a major determinant of the efficiency of adsorption, in our experiments. Other physical and chemical parameters of the heterologous proteins, including probably the size and the isoelectric point, have to be considered as they may mediate the ability of proteins to cross the outermost spore layers [15–17], resulting in relevant for the efficiency of the process.

Localization of proteins adsorbed on 25, 37 or 42 °C spores

A previous report showed that RFP when adsorbed to spores is able to cross the crust and the outer coat, localizing at the inner coat level [15]. In that study, the RFP fluorescence signal was localized by comparison with the signal due to GFP fused to proteins known to be localized in various spore coat layers [15]. A similar approach was used to evaluate whether the temperature of spore production also affected the localization of the adsorbed proteins within the coat. Since the high red fluorescence signal produced by rhodamine-labeled PPT, LYS or BSA overlapped (and caused interference) with the region of detection for the GFP signal, the localization assays were performed adsorbing RFP to spores carrying the *cotC::gfp* fusion [15] and prepared at 25, 37 or 42 °C.

As previously reported [15], in 37 °C spores the red fluorescence signal of RFP was internal to the green signal of CotC-GFP (Fig. 7). While RFP localization did not change with 25 °C spores, it was slightly altered with 42 °C spores where the RFP signal was external with respect to the CotC-GFP signal (Fig. 7). The different localization of RFP is most likely due to the different coat structure of spore produced at the various temperatures and indicates that the lamellar and highly

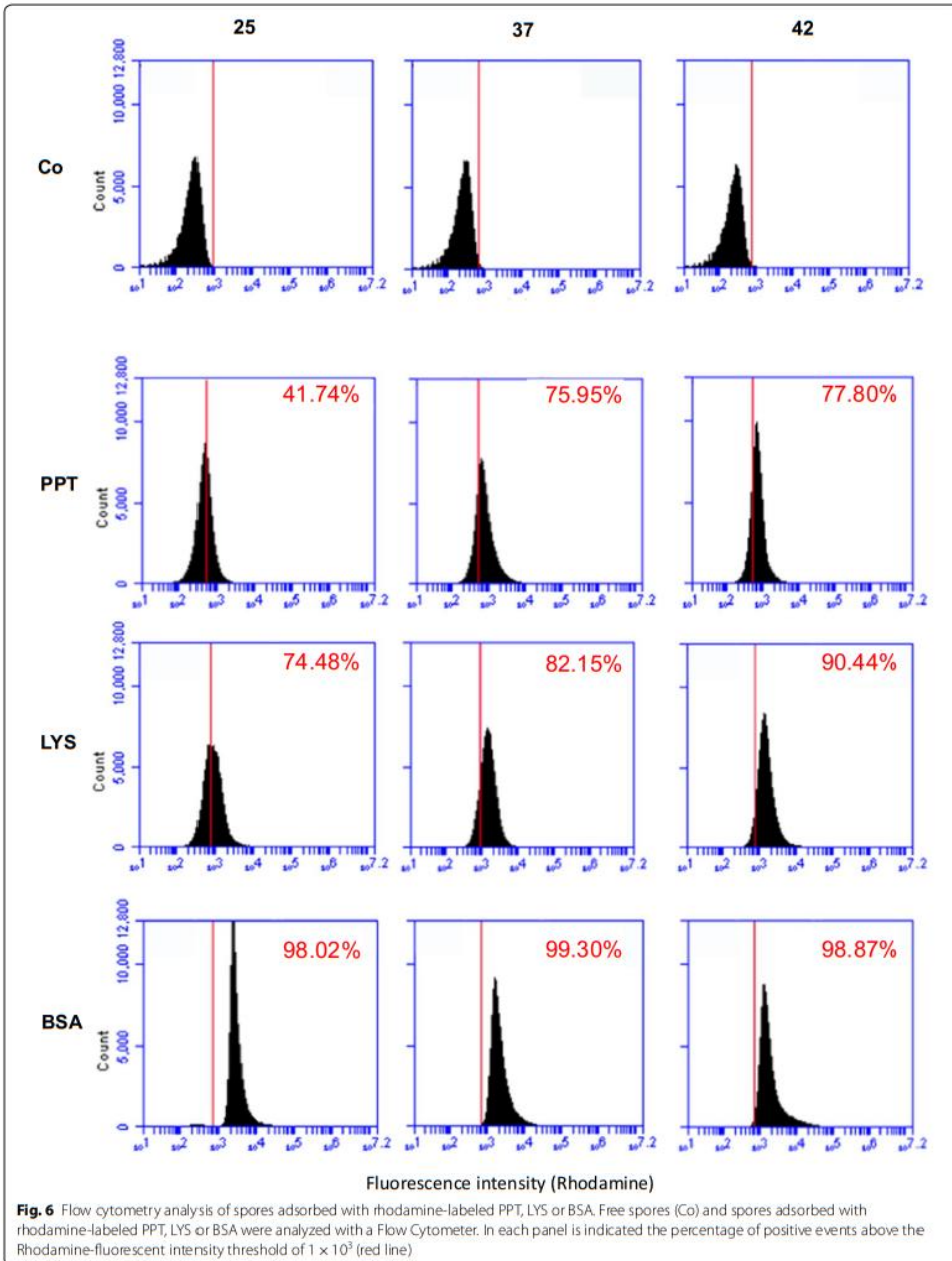
electron-dense outer coat (CotB-CotG rich) produced at low temperatures [22] is somehow a more permeable than the granular and thick coat (CotC rich) produced at 42 °C [22], at least with respect to RFP.

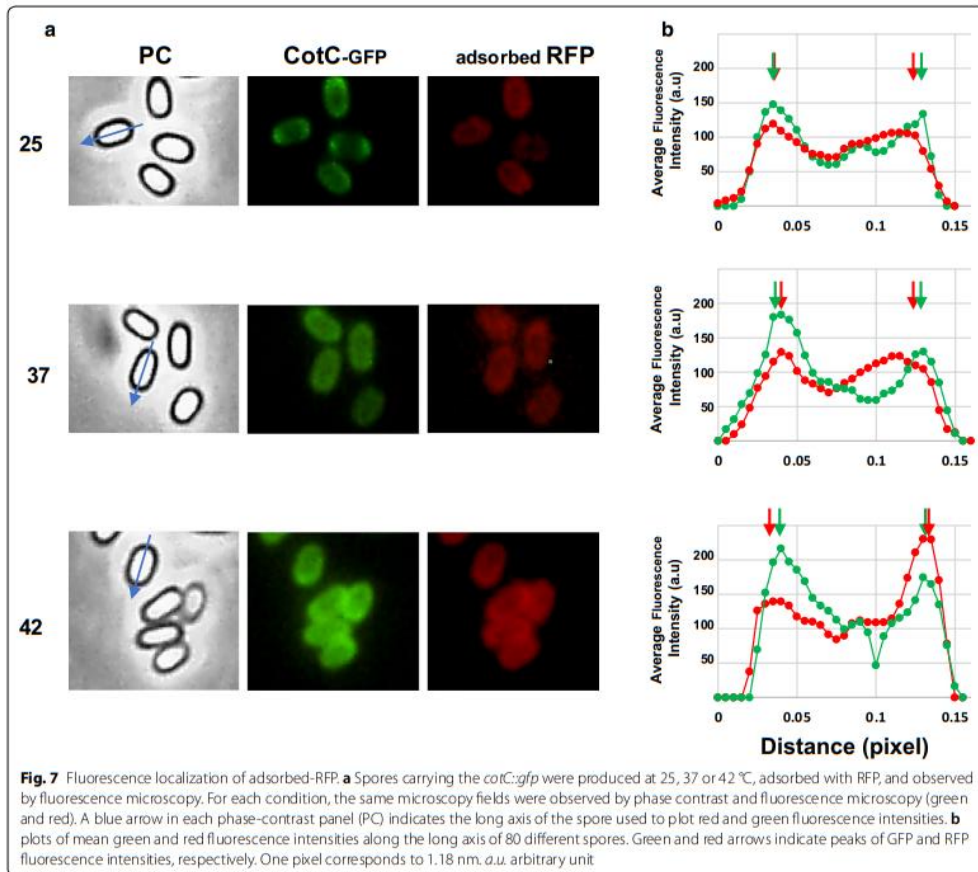
Conclusions

Main conclusion of this study is that the temperature of spore production affects the display of heterologous proteins on the spore surface:

- with the recombinant display the temperature modulates the amount and the surface exposure of the displayed proteins with CotB- and CotG-based fusions more efficient at low temperatures and CotC-based fusions are more efficient at high temperatures;
- when a recombinant spore carries two heterologous proteins each of them is differentially displayed at different temperatures on the base of the carrier used;
- with the non-recombinant display a modest effect is observed with small proteins (PPT and LYS) adsorbed more efficiently by 37 or 42 °C spores than by 25 °C spores;
- the localization of adsorbed RFP within the spore surface layers is modified by the temperature, indicating that spores produced at the low temperatures (CotB/CotG type coat) or at high temperature (CotC type coat) [22] have different adsorption properties.

Overall, this study indicates that the temperature of spore production is an essential parameter to be considered in the development of a spore-display system.





Materials and methods

Spore production, extraction of coat proteins and western blot analysis

Sporulation at 25, 37 and 42 °C was induced by the exhaustion method in Difco Sporulation (DS) medium as recently reported [24, 29]. Mature spores were purified by cold-water washing using overnight incubation in H₂O at 4 °C to lyse residual sporangial cells. Spore purity (higher than 95%) was checked under optical microscope.

Spore coat proteins were extracted from a suspension of spores by SDS-DTT or NaOH treatment [30]. The concentration of extracted proteins was determined by using Bio-Rad DC protein assay kit (Bio-Rad), and

20 µg of total spore coat proteins were fractionated on 12.5% SDS polyacrylamide gels and staining by Brilliant Blue Coomassie or electro-transferred to nitrocellulose filters (Bio-Rad) for western blot analysis following standard procedures. CotC- and CotB- substrate specific antibodies were used at working dilutions 1:7000 for CotC-TTFC and CotB-TTFC detection [5, 21]. Then, a horseradish peroxidase-conjugated antirabbit secondary antibody was used (Santa Cruz). Western blot filters were visualized by the electrochemiluminescence method as specified by the manufacturer and processed to improve the contrast level using ChemoDocXRS software (Bio-Rad).

The experiments have been repeated twice analyzing two distinct coat protein extractions.

Labeling with Rhodamine

2 mg/ml of pentapeptide HPHGH (PPT), commercially available lysozyme (LYS-Sigma), and bovine serum albumin (BSA-New England-Biolabs) were labeled with 50 μ l of Rhodamine B isothiocyanate (Sigma) (1 mg/ml in DMSO) as specified by the manufacturer. The protocol is based on the reaction between the isothiocyanate group of Rhodamine and epsilon-NH₂ of Lysine residues of the protein to be labeled in order to obtain a fluorescent complex. Final molar Rhodamine/Proteins ratio was 0.06 and the labeling reactions were performed pH 8.5. The labeling was followed by dialysis in 1 \times PBS to remove the unbound fluorescent excess and lyophilization.

Binding reaction

10 mM of PPT-Rd, LYS-Rd, BSA-Rd were added to a suspension of 5.0×10^8 wild type spores, produced at different temperatures, in 50 mM sodium citrate pH 4.5 in a final volume of 200 μ l. For the reaction with RFP, 1 μ g of purified protein was added to the suspension of 1.0×10^8 spores produced at different temperatures, in 1.5 M PBS pH 4.0 in a final volume of 200 μ l. After 1 h of incubation at 25 °C, the binding mixtures were washed and centrifuged (10 min at 13,000g) to fractionate adsorbed spores (pellet) from unbound protein (supernatant).

Flow cytometry

Recombinant spores expressing TTFC were analyzed by flow cytometry as previously described [31]. Briefly, 10^6 purified spores were incubated at room temperature for 30 min at room temperature in phosphate-buffered saline (PBS)-3% fetal bovine serum (FBS) prior to 1 h-incubation with anti-TTFC polyclonal antibodies diluted at 1:20 in 1 \times PBS-1%FBS. After three washes in 1 \times PBS, fluorescein isothiocyanate (FITC)-conjugated anti-rabbit immunoglobulin G (1:64; Sigma) was added and the mixture was incubated for 1 h at room temperature, followed by four washes in PBS.

For spores adsorbed with PPT-Rd, LYS-Rd and BSA-Rd, a total of 10^6 spores were resuspended in 0.5 ml of binding buffer and directly analyzed.

Flow cytometry analysis was performed by BD Accuri™ C6 Cytometer and BD Accuri™ C6 Software (BD Biosciences, Inc., Milan, Italy) collecting 100,000 events. Spore without the addition of primary and secondary antibodies or not adsorbed were used to measure the unspecific fluorescence, allowing to set the threshold of positive events at 1×10^3 fluorescence intensity. The experiments were repeated twice analyzing two independently prepared samples.

Fluorescence microscopy

10^5 adsorbed spores were resuspended in 50 μ l of binding buffer and observed with an Olympus BX51 fluorescence microscope fitted with a 100 \times objective UPlanF1 and U-MNG or U-MWIBBP cube-filters to detect the red and green fluorescence emission respectively. The exposure times are in the range between 500 and 1000 ms. Captured images were processed with Image Analysis Software (Olympus) for minor adjustments of brightness, contrast and color balance and for creation of merge images. For RFP adsorbed spores, the fluorescence intensities and the distance between two fluorescent peaks were measured using unadjusted merged images with Image J processing software (version 1.48, NIH) as previously described [15]. To obtain the total corrected cellular fluorescence (TCCF), an outline was drawn around several fluorescent spores and area, integrated density and the mean fluorescence measured, along with several adjacent background readings. The TCCF was calculated by subtracting the area of selected cell \times mean fluorescence of background readings to the integrated density.

Acknowledgements

Not applicable.

Authors' contributions

Ri, ER, LB, conceived and designed the experiments; CP, SC, carried out most of the experimental work; ML, AS, GD contributed to some of the experiments; Ri, ER, LB wrote and revised the manuscript. All authors read and approved the final manuscript.

Funding

No specific funds were receive to support this work.

Availability of data and materials

All data generated or analysed during this study are included in this published article and are available from the corresponding author on reasonable request.

Ethics approval and consent to participate

Not applicable.

Consent for publication

Not applicable.

Competing interests

The authors declare no competing interests.

Author details

¹ Department of Biology, Federico II University complesso universitario di Monte Sant' Angelo via Cinthia, 80126 Napoli, Italy. ² Department of Molecular Medicine and Medical Biotechnology, Federico II University of Naples, Napoli, Italy. ³ Present Address: Institute of Biomolecular Chemistry, National Research Council of Italy, Pozzuoli (Naples), Italy. ⁴ Present Address: Department of Medicine, Surgery and Dentistry 'Scuola Medica Salernitana', University of Salerno, Fisciano (SA), Italy.

Received: 31 July 2020 Accepted: 25 September 2020
Published online: 01 October 2020

References

1. Fritze D. Taxonomy and systematics of the aerobic endospore forming bacteria: *Bacillus* and related genera. In: Ricca E, Henriques AO, Cutting SM, editors. *Bacterial Spore Formers*. Norfolk: Horizon Bioscience; 2004. p. 17–34.
2. Driks A, Eichenberger P. The Spore Coat. *Microbiol Spectr*. 2016;4(2):R17–29.
3. Setlow P. Germination of spores of *Bacillus* species: what we know and do not know. *J Bacteriol*. 2014;196:1297–305.
4. McKenney PT, Driks A, Eichenberger P. The *Bacillus subtilis* endospore: assembly and functions of the multilayered coat. *Nat Rev Microbiol*. 2013;11:33–44.
5. Isticato R, Cangiano G, Tran TH, Ciabattini A, Medagliani D, Oggioni MR, De Felice M, Pozzi G, Ricca E. Surface display of recombinant proteins on *Bacillus subtilis* spores. *J Bacteriol*. 2001;183:6294–301.
6. Duc LH, Huynh HA, Fairweather N, Ricca E, Cutting SM. Bacterial spores as vaccine vehicles. *Infect Immun*. 2003;71:2810–8.
7. Mauriello EMF, Cangiano G, Maurano F, Saggese V, De Felice M, Rossi M, Ricca E. Germination-independent induction of cellular immune response by *Bacillus subtilis* spores displaying the C fragment of the Tetanus Toxin. *Vaccine*. 2007;25:788–93.
8. Isticato R, Ricca E. Spore surface display. *Microbiol Spectr*. 2014. <https://doi.org/10.1128/microbiol-spec-TBS-0011-2012>.
9. Detmer A, Glenting J. Live bacterial vaccines—a review and identification of potential hazards. *Microb Cell Fact*. 2006;5:23.
10. Huang JM, Hong HA, Van Tong H, Hoang TH, Brisson A, Cutting SM. Mucosal delivery of antigens using adsorption to bacterial spores. *Vaccine*. 2010;28:1021–30.
11. Sirec T, Strazzulli A, Isticato R, De Felice M, Moracci M, Ricca E. Adsorption of beta-galactosidase of *Alicyclobacillus acidocaldarius* on wild type and mutant spores of *Bacillus subtilis*. *Microb Cell Fact*. 2012;11:100.
12. Isticato R, Sirec T, Treppiccione L, Maurano F, De Felice M, Rossi M, Ricca E. Non-recombinant display of the B subunit of the heat labile toxin of *Escherichia coli* on wild type and mutant spores of *Bacillus subtilis*. *Microb Cell Fact*. 2013;12:98.
13. Matosovich R, Iacono R, Cangiano G, Cobucci-Ponzano B, Isticato R, Moracci M, Ricca E. Conversion of xylan by recyclable spores of *Bacillus subtilis* displaying thermophilic enzymes. *Microb Cell Fact*. 2017;16(1):218.
14. Pesce G, Rusciano G, Sirec T, Isticato R, Sasso A, Ricca E. Surface charge and hydrodynamic coefficient measurements of *Bacillus subtilis* spore by optical tweezers. *Colloids Surf B*. 2014;116:568–75.
15. Donadio G, Lanzilli M, Sirec T, Ricca E, Isticato R. Localization of a red fluorescence protein adsorbed on wild type and mutant spores of *Bacillus subtilis*. *Microb Cell Fact*. 2016;15:153.
16. Lanzilli M, Donadio G, Addevero R, Saggese A, Cangiano G, Baccigalupi L, Christie G, Ricca E, Isticato R. The exosporium of *Bacillus megaterium* QM B1551 is permeable to the Red Fluorescence Protein of the coral *Discosoma* sp. *Front Microbiology*. 2016;7:1572.
17. Lanzilli M, Donadio G, Fusco FA, Sarcinelli C, Limauro D, Ricca E, Isticato R. Display of the peroxiredoxin Bcp1 of *Sulfolobus solfataricus* on probiotic spores of *Bacillus megaterium*. *N Biotechnol*. 2018;46:38–44.
18. D'Arienzo R, Maurano F, Mazzarella G, Luongo D, Stefanile R, Ricca E, Rossi M. *Bacillus subtilis* spores reduce susceptibility to *Citrobacter rodentium*-mediated enteropathy in a mouse model. *Res Microbiol*. 2006;157:891–7.
19. Cutting SM. *Bacillus* probiotics. *Food Microbiol*. 2011;28:214–20.
20. Ricca E, Baccigalupi L, Cangiano G, De Felice M, Isticato R. Mucosal vaccine delivery by non-recombinant spores of *Bacillus subtilis*. *Microb Cell Fact*. 2014;13(1):115.
21. Mauriello EMF, Duc LH, Isticato R, Cangiano G, Hong HA, De Felice M, Ricca E, Cutting SM. Display of heterologous antigens on the *Bacillus subtilis* spore coat Using CotC as a fusion partner. *Vaccine*. 2004;22:1177–87.
22. Isticato R, Lanzilli M, Petrillo C, Donadio G, Baccigalupi L, Ricca E. *Bacillus subtilis* builds structurally and functionally different spores in response to the temperature of growth. *Environ Microbiol*. 2020;22(1):170–82.
23. Isticato R, Mase D, Mauriello EMF, De Felice M, Ricca E. Amino terminal fusion of heterologous proteins to CotC increases display efficiencies in the *Bacillus subtilis* spore system. *Biotechniques*. 2007;42:151–6.
24. Isticato R, Ricca E, Baccigalupi L. Spore adsorption as a nonrecombinant display system for enzymes and antigens. *J Vis Exp*. 2019;19:145.
25. Cutting S, Vander Horn PB. Genetic analysis in Molecular Biological Methods for *Bacillus*. Edited by Harwood C and Cutting S. Wiley, Chichester. 1990; pp. 27–74.
26. Donadio G, Di Martino R, Oliva R, Petraccone L, Del Vecchio P, Di Luccia B, Ricca E, Isticato R, Di Donato A, Notomista E. A new peptide-based fluorescent probe selective for zinc (II) and copper (II). *J Mater Chem B*. 2016;4:6979–88.
27. Youngman P, Perkins JB, Losick R. A novel method for the rapid cloning in *Escherichia coli* of *Bacillus subtilis* chromosomal DNA adjacent to Tn917 insertion. *Mol Gen Genet*. 1984;195:424–33.
28. Kyte J, Doolittle RF. A simple method for displaying the hydrophobic character of a protein. *J Mol Biol*. 1982;157:105–32.
29. Crescenzo R, Mazzoli A, Cancelliere R, Buccì A, Naclerio G, Baccigalupi L, Cutting SM, Ricca E, Iossa S. Beneficial effects of carotenoid-producing cells of *Bacillus indicus* HU16 in a rat model of diet-induced metabolic syndrome. *Beneficial Microbes*. 2017;8:823–31.
30. Isticato R, Sirec T, Giglio R, Crispino A, Baccigalupi L, Rusciano G, Pesce P, Zito G, Sasso A, De Felice M, Ricca E. Flexibility of the programme of spore coat formation in *Bacillus subtilis*: bypass of CotE requirement by overproduction of CotH. *PLoS ONE*. 2013;8(9):e74949.
31. Santos FDS, Mazzoli A, Maia AR, Saggese A, Isticato R, Leite F, Iossa S, Ricca E, Baccigalupi L. A probiotic treatment increases the immune response induced by the nasal delivery of spore-adsorbed TTFC. *Microb Cell Fact*. 2020;19:42.

Publisher's Note

Springer Nature remains neutral with regard to jurisdictional claims in published maps and institutional affiliations.

Ready to submit your research? Choose BMC and benefit from:

- fast, convenient online submission
- thorough peer review by experienced researchers in your field
- rapid publication on acceptance
- support for research data, including large and complex data types
- gold Open Access which fosters wider collaboration and increased citations
- maximum visibility for your research: over 100M website views per year

At BMC, research is always in progress.

Learn more biomedcentral.com/submissions



OTHER COLLABORATIONS

CHAPTER VIII

International Journal of Biological Macromolecules 189 (2021) 494–502



Contents lists available at ScienceDirect

International Journal of Biological Macromolecules

journal homepage: www.elsevier.com/locate/ijbiomac



The power of two: An artificial microbial consortium for the conversion of inulin into Polyhydroxyalkanoates

Iolanda Corrado^{a,1}, Claudia Petrillo^{b,1}, Rachele Istitico^b, Angela Casillo^a,
Maria Michela Corsaro^a, Giovanni Sannia^a, Cinzia Pezzella^{c,*}

^a Department of Chemical Sciences, University of Naples Federico II, Via Cinthia, 4-80126 Napoli, Italy

^b Department of Biology, University of Naples Federico II, Via Cinthia, 4-80126 Napoli, Italy

^c Department of Agricultural Sciences, University of Naples Federico II, Via Università, 100 80055 Portici, NA, Italy

ARTICLE INFO

Keywords

Artificial microbial consortium
Inulin
Central composite rotary design

ABSTRACT

One of the major issues for the microbial production of polyhydroxyalkanoates (PHA) is to secure renewable, non-food biomass feedstocks to feed the fermentation process. Inulin, a polydisperse fructan that accumulates as reserve polysaccharide in the roots of several low-requirement crops, has the potential to face this challenge.

In this work, a “substrate facilitator” microbial consortium was designed to address PHA production using inulin as feedstock. A microbial collection of *Bacillus* species was screened for efficient inulinase producer and the genome of the selected strain, RHF15, identified as *Bacillus gibsonii*, was analysed unravelling its wide catabolic potential. RHF15 was co-cultured with *Cupriavidus necator*, an established PHA producer, lacking the ability to metabolize inulin. A Central Composite Rotary Design (CCRD) was applied to optimise PHA synthesis from inulin by the designed artificial microbial consortium, assessing the impact of species inoculum ratio and inulin and N-source concentrations. In the optimized conditions, a maximum of 1.9 g L⁻¹ of Polyhydroxybutyrate (PHB), corresponding to ~80% (g_{polymer}/g_{CDSW}) polymer content was achieved. The investigated approach represents an effective process optimization method, potentially applicable to the production of PHA from other complex C-sources.

1. Introduction

The extensive worldwide use of plastic and the impact of its production chain have seriously harmed the environment, increasing the demand for fossil resources. Furthermore, plastic pollution of soil and water is urgently asking for biodegradable plastics.

Polyhydroxyalkanoates (PHAs) are a family of biodegradable polyesters produced by various microbial species for energy storage. Being produced from a renewable source, they have been proposed as a green alternative to traditional chemical plastics, including polyethylene (PE), polypropylene (PP), and polyethylene terephthalate (PET) [1]. Besides polyhydroxybutyrate (PHB), the best characterized member of PHA family, several hydroxyalkanoic acid monomers, differing in their chain length, have been identified so far, giving rise to different PHA copolymers with tunable properties [2].

The main limit for exploitation of PHA is related to their production cost, with the starting feedstocks accounting for more than the 50% of

the total. As a fact, the use of biomass and waste feedstocks has emerged as the main breakthrough for cost-effective PHA production, and, to this purpose, different lignocellulosic materials and food wastes have been tested [3,4]. To be considered as appropriate feedstocks for microbial synthesis of PHAs, the complex C-sources contained in raw materials require a preliminary catabolic step to be converted into suitable substrates for microbial PHA producers. The isolation of strains for direct high yield PHA synthesis from low-cost waste streams has been reported in few cases [1,5]. On the other hand, *in vivo* engineering approaches have been applied, focusing on the introduction of specific catabolic genes into native PHA producers or, *vice versa*, on the implementation of PHA-synthetic genes into non-native producers endowed with the ability to metabolize complex C-sources. Although effective on different waste materials, both the above-mentioned strategies are time-consuming and challenging [6].

The design and construction of artificial microbial consortia have opened a new perspective in this field. The production of several

* Corresponding author.

E-mail address: cpezzella@unina.it (C. Pezzella).

¹ Equally contributing authors

<https://doi.org/10.1016/j.ijbiomac.2021.08.123>

Received 5 May 2021; Received in revised form 16 August 2021; Accepted 16 August 2021

Available online 21 August 2021

0141-8130/© 2021 Elsevier B.V. All rights reserved.

microbial products by co-culture has been successfully reported, highlighting their advantages in terms of productivity and process economic over pure cultures [7]. Microbial consortia represent a valuable strategy to deal with the need to use complex C-sources that would be not metabolized by an individual species, and/or to relieve the negative effect of side products inhibiting one of the species of the consortium [8,9].

Co-culture based approaches have been applied to PHA synthesis [9]. Bhatia et al., (2018b) have co-cultured *Ralstonia eutropha* and *Bacillus subtilis*, respectively as PHA and invertase producers, to address PHA production from sucrose as substrate. These bacteria form a mutually beneficial symbiotic relationship, since glucose, fructose, and propionic acid produced by *B. subtilis* are efficiently converted into P(3HB-co-3HV) copolymer by *R. eutropha*. Simultaneous production of PHA and xanthan gum has been reported by a mixed culture of *Cupriavidus necator* and *Xanthomonas campestris* from palm oil [11]. Sawant et al. [12] have ascribed the increased efficiency in PHA production from lignocellulosic substrates by *Saccharophagus degradans* and *B. cereus* co-culture, to the occurrence of mutual communication and cooperative growth between the two bacteria. Finally, a mutually beneficial symbiotic relationship based on nutrient supply and detoxification, has been achieved by properly engineering *Escherichia coli* and *Pseudomonas malodoros* strains, during fermentation of mixed glucose and xylose substrates [13].

Inulin is a linear polysaccharide composed of β -2,1-linked D-fructose residues terminated by a glucose residue, accumulated as a reserve carbohydrate in the roots and tubers of various crops, such as chicory and dahlia and, more interestingly, in low-requirement crops, such as Jerusalem artichoke and *Cynara cardunculus* [14,15]. These inulin sources have a high potential for applications in biorefineries, being able to cope with drought, pests and diseases and growing well in marginal lands with little fertilizer applications [15]. Inulin hydrolysis into fermentable sugars, catalysed by microbial inulinases, is mandatory for its utilization as carbon and energy source in microbial processes. The synthesis of several microbial products has been reported from these inulin-rich biomasses [16–18], although PHA production is still less explored. In the reported examples, PHA production has been achieved by exploiting microbial inulinases in separate hydrolysis and fermentation (SHF) [19,20] and simultaneous saccharification and fermentation (SSF) processes [21], since no PHA-producing strain naturally endowed with the ability to hydrolyse inulin has been isolated so far.

C. necator is an established PHA producer, able to accumulate polymer with high productivity from fructose, however it lacks the hydrolytic enzymes necessary to convert inulin into fermentable sugars [21]. In this work, an artificial microbial consortium was designed to address PHA production from inulin, by complementing this *C. necator* enzymatic deficiency with a properly isolated inulin-hydrolysing microorganism. To this aim, a microbial collection of halophilic *Bacillus* species was screened for efficient inulinase producers. Halophilic bacteria are a useful source of enzymes suitable for industrial processes. To adapt to saline conditions, this group of microorganisms has developed different strategies, as the production of a large variety of extracellular hydrolytic enzymes. Moreover, these enzymes exhibit optimal activities at various ranges of salt concentration, pH and temperature, making them suitable to be used in many industrial processes [22].

A Central Composite Rotary Design (CCRD) was applied to optimise PHA synthesis from inulin by the designed artificial microbial consortium, assessing the impact of species inoculum ratio and inulin and N-source concentrations. The investigated approach represents an effective process optimization method, potentially applicable to the production of PHA from other complex C-sources.

2. Materials and methods

2.1. Microbial strains and culture conditions

Halophilic *Bacillus* sp. strains used in this work are listed in Table S1. Tryptone Yeast extract (TY) medium was used for *Bacillus* strains maintenance and pre-inoculum growth. Minimal medium (MM) supplemented with inulin 1% (w/v) was used for inulinase producers screening in liquid cultures [23]. *Bacillus* strains were grown at 37 °C with shaking (150 rpm).

C. necator DSM 428 strain was grown aerobically at 30 °C both in rich (Tryptic Soy Broth, TSB) and minimal medium (MM_{cn}) according to Budde, 2011 [23].

Powder inulin used in this study was a commercial mixture of chicory roots inulin provided by Sigma chemical as high purity grade substrate for *in vitro* assays (inulin from chicory, 9005-80-5, Sigma-aldrich) and a low purity grade inulin from chicory as carbon source for microbial growth (provided by Lineavi, Inulinpulver, Jeder Tag Ein Wohlfühltag).

2.2. Screening for inulinase producers

Iodine agar plate assay was used for screening on solid medium. Microorganisms were grown on MM supplemented with inulin 1% (w/v) agar plates for 24 h and then incubated in a close jar saturated of iodine vapours for 6 min at room temperature.

For screening in liquid medium, bacterial strains were grown in TY medium for 16 h and inoculated in MM+ Inulin 1% (w/v) at 0.4 OD₆₀₀/ml (250 mL Flasks with 25 mL of medium) for 30 h.

2.3. Inulinase enzymatic assay

The culture medium was centrifuged at 5000 g for 15 min and the supernatant was used as the inulinases source. Enzymatic activity was measured by the determination of reducing sugars released from inulin by DNS-method (Muller 1996) according to Corrado et al. (2021) [21]. One unit of the enzyme (inulinases or invertase activity) was defined as the amount of the enzyme which produces 1 μ mol of reducing sugars per minute. All the assays were carried out in duplicate.

2.4. Whole genomic annotation

The Rapid Annotation using Subsystems Technology (RAST) was applied to RHF15 genome, already available [24] for gene prediction and annotation [25,26]. CG View (Circular Genome Viewer) server 1.0 was used to construct a circular genome map of strain RHF15 [27].

2.5. Response surface methodology

A 2³ full factorial Central Composite Rotary Design (CCRD) was employed to find out the interactive effects of inulin, NH₄Cl concentration, bacteria strains inoculum concentration on both cell biomass production and PHA accumulation. CCRD was designed using Minitab 19 and resulted in 31 conditions with eight axial points and seven replicates at the center point (Table 1). The combination of predictor settings that optimized the fitted response was used to verify the model.

Experiments were performed at 20 ml scale in MM_{cn} at 30 °C for 96 h. The four components (Inulin, NH₄Cl, RHF15 and *C. necator*) were added to the media according to the designed values (Table 1). After 96 h cells were recovered by centrifugation (5500 g, 15 min) and lyophilized for CDW determination and PHA extraction. Regression analysis

Table 1
Optimization of growth variables for CDW production and PHA accumulation from co-cultures, using central composite rotatable design (CCRD).

Run	<i>C. necator</i> OD mL ⁻¹	RHF15 OD mL ⁻¹	NH ₄ Cl g L ⁻¹	Inulin g L ⁻¹	CDW g L ⁻¹	PHB %	U mL ⁻¹
1	0	0	0.5	10	0.0	0.0	0
2	0	0	0.5	30	0.0	0.0	0
3	0	0	2	10	0.0	0.0	0
4	0	0	2	30	0.0	0.0	0
5	0	0.2	0.5	10	0.8	0.0	6.8
6	0	0.2	0.5	30	0.9	0.0	13.4
7	0	0.2	2	10	1.3	0.0	2.0
8	0	0.2	2	30	1.5	0.0	22.7
9	0.2	0	0.5	10	0.3	12.4	0
10	0.2	0	0.5	30	0.6	28.2	0
11	0.2	0	2	10	0.2	5.2	0
12	0.2	0	2	30	0.4	16.5	0
13	0.2	0.2	0.5	10	1.4	58.4	3.2
14	0.2	0.2	0.5	30	2.1	68.7	13.3
15	0.2	0.2	2	10	1.5	31.2	2.1
16	0.2	0.2	2	30	1.9	42.5	1.9
17	0	0.1	1.25	20	1.3	0.0	5.3
18	0.1	0	1.25	20	0.4	7.9	0
19	0.1	0.1	1.25	20	1.5	14.7	3.5
20	0.1	0.1	1.25	20	1.7	19.0	3.3
21	0.1	0.1	1.25	20	1.5	21.2	3.3
22	0.1	0.1	1.25	20	1.4	19.9	2.7
23	0.1	0.1	1.25	20	1.6	17.8	4.1
24	0.1	0.1	1.25	20	1.7	20.3	3.3
25	0.1	0.1	1.25	20	1.6	17.9	3.3
26	0.3	0.1	1.25	20	2.0	59.7	2.3
27	0.1	0.3	1.25	20	1.1	18.2	5.1
28	0.1	0.1	0	20	0.9	34.4	3.2
29	0.1	0.1	2.75	20	0.6	16.7	8.32
30	0.1	0.1	1.25	40	1.3	23.0	13.3
31	0.1	0.1	1.25	0	0.0	5.7	1.2

using ANOVA was performed, and model fitting methods applied for data analysis. Contour and surface plots were created to visualize the interactive effects of all components on PHA accumulation.

2.6. Verification of the model for PHA production using inulin as carbon source

To validate the model a numerical optimization method via Minitab 19 was applied to predict the variables value. The high and low variables values were determined according to overlaid plots for all responses. Optimized conditions turn out to be 0.3 OD mL⁻¹ for bacteria inoculum, 2 g L⁻¹ of NH₄Cl and 30 g L⁻¹ of inulin. *Bacillus* strain and *C. necator* were co-cultured in MM_{C5} media at 20 mL scale up to 96 h. Samples were collected at 24 h intervals and analysed for biomass production (Cell Dry Weight, CDW) and PHA accumulation (% $g_{\text{polymer}}/g_{\text{CDW}}$). Concentration of glucose, fructose and residual inulin in the culture broth were assayed by D-fructose and D-glucose, and fructan assay kits (Megazyme).

2.7. PHA extraction and analysis

Polymer extraction was performed on lyophilized cells [21]. Gas chromatography mass spectrometry method (GC-MS) was used to analyse PHA production and composition as previously described by Vastano et al. (2015) [28].

2.8. NMR

¹H NMR spectrum of the extracted polymer was performed in CDCl₃: CD₃OD (1:1), at 298 K using a 600 MHz Bruker (Bruker Italia, Italy) instrument equipped with a cryogenic probe.

3. Results and discussion

3.1. Screening of halophilic bacteria for inulinase production

A halophilic bacteria collection was screened for the ability to produce inulinases (Table S1). All analysed microorganisms belong to a larger collection isolated from samples of sand and rhizosphere of *Juniperus sabina* collected from salt-pans [24,29]. The selected strains are facultative anaerobic belonging to the *Bacillus* genus, all classified as mesophiles-moderate halophilic bacteria, since able to grow at a temperature ranging from 15 °C to 50 °C and between 0.5 and 2.5 M of salt [30]. The 8 strains were chosen for their exoenzymatic activity profile, being able to hydrolyse substrates like cellulose, starch or xylan [24].

After the primary screening on agar, four strains were selected, based on the diameter of the hydrolytic zone. Once cultured in liquid medium,

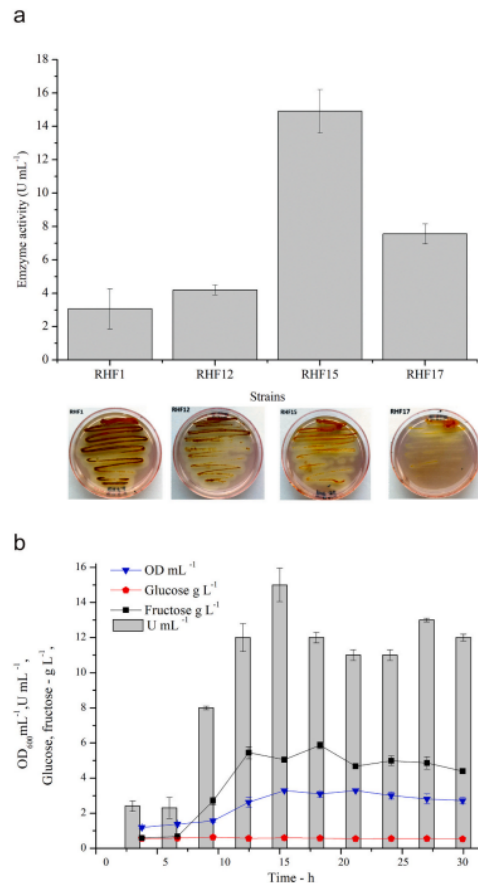


Fig. 1. Screening for inulinase producers. A) Maximum inulinase activity (U mL⁻¹) determined in liquid medium, for the strains selected from the first screening on solid medium (pictures below); B) Kinetic of growth, inulinase production and glucose and fructose consumption of the best inulinase producer, *B. gibsonii* RHF15, selected from the screening.

the strain RHF15, displayed the highest level of inulinase production, reaching up to 14 U mL^{-1} (Fig. 1) after 15 h, in line with the values reported for other inulinase producers [31]. The enzymatic activity was detected in the culture broth in the early stage of growth, probably as a result of inulin induction [31]. The inulinase/saccharase activity ratio, I/S, was equal to 2, indicating the prevalence of inulinase over invertase activity [32]. As a fact, the release of both glucose (the minority component of inulin) and fructose was recorded from the beginning of the process. Then, whilst glucose level remains almost neglectable, fructose concentration rises steeply up to 12 h, when it approaches a constant level in correspondence with the entry into the stationary growth phase. It is noteworthy that high inulinase activity levels were preserved in the culture broth even after prolonged stationary phase, representing an advantage for the exploitation of this strain as inulinase-producer in a properly designed artificial microbial consortium.

Based on these results, the strain RHF15, identified as *B. gibsonii*, was selected for further analysis.

3.2. Whole genome investigation of putative inulinase coding genes of the strain RHF15

The genome of strain RHF15 (Figure S2) was analysed by the RAST annotation server [25,26], revealing 100 RNAs and a total number of 4282 predicted protein-coding sequences (CDSs), where “Amino Acids and Derivatives” (17.4%) and “Carbohydrates” (14.4%) were the most represented subsystem features (Table S3). In order to identify proteins responsible for inulin hydrolysis, predicted amino acid sequences from Carbohydrates subsystem were analysed scanning for Carbohydrate-Active enZymes (CAZymes). CAZymes are a group of enzymes involved in carbohydrate metabolism, divided into classes according to their catalytic activity. The analysis revealed the presence of 129 CAZymes, including 16 Carbohydrate Esterases, 40 Glycoside Hydrolases (GH), 34 Glycosyl Transferases, 5 Polysaccharide Lyases and, 34 enzymes involved in Auxiliary Activities (Fig. 2A). The abundance of

hydrolytic enzymes belonging to different CAZY families, highlighted by this analysis, is in accordance with the wide hydrolytic abilities towards different substrates (xylan, cellulose, amylose, chitin) recently reported for this strain [24].

Among GH, the Glycoside Hydrolase Family 32 includes members of the β -fructosidase superfamily, able to hydrolyse non-reducing β -D fructosidic bonds releasing fructose [33] and for this reason, more attention was dedicated to this group of enzymes. Interestingly, 3 genes putatively coding for enzymes related to this family (Fig. 2B) have been identified. A multiple alignment of the deduced aminoacidic sequences with those of well-known GH32 hydrolases able to cleave inulin (Table S4) was performed using SeaView software [34] (Fig. S5), highlighting the typical highly conserved motifs of the GH32 family [35–37] in the selected RHF15 enzymes.

A blastP analysis of the aminoacidic sequences of the three putative inulinase coding genes was run against the NCBI database. The best hits were obtained with the levanasase SacC, the sucrose-6-phosphate hydrolase ScrB and the levaniobiose-producing levanasase LevB of *B. subtilis* with a sequence similarity score ranging between 99 and 100% (Table 2). *B. subtilis* levanasase SacC has been depicted as an exofructosidase, capable of hydrolysing both levan and inulin, leading to the production of free fructose [38]. Regarding ScrB, no data are available on the ability to hydrolyze inulin on behalf of this enzyme, whilst, from previous studies, it is known that *B. subtilis* LevB is an endolevanase that selectively cleaves the (β -2,6) fructosyl bonds and does not hydrolyse inulin [39]. Since the hydrolytic activity has been detected in the supernatant fraction, a predicted signal peptide in the primary structure of the SacC and ScrB homologous proteins has been searched using SignalP 3.0 Server [40]. The performed analysis allowed to identify the presence of a signal peptide (position 1–23) and a probable cleavage site (position 24–25) in SacC [41], whilst no significant result was obtained with ScrB, suggesting a cytoplasmic role of this enzyme. According to the collected information, the inulin hydrolytic activity associated with strain RHF15 is most likely due to the levanasase SacC homolog.

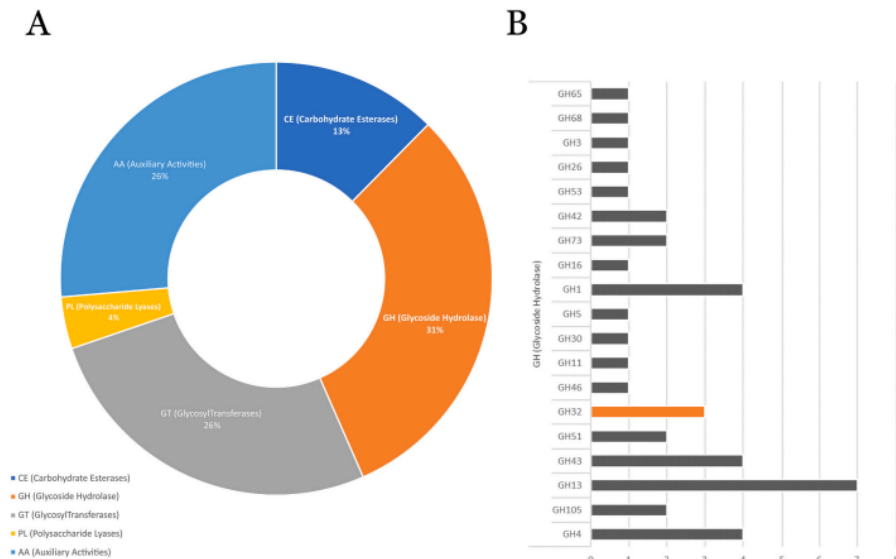


Fig. 2. Annotation of CAZymes in *B. gibsonii* RHF15 genome A) Distribution of CAZyme classes in strain RHF15. B) Distribution of CAZyme families in the GH class, and number of proteins belonging to each family.

Table 2

Summary of the blastP analysis run between the three selected enzymes of strain RHF15 (Query ID) and the NCBI database. Only the best hits are shown.

Query ID	Subject ID	Source	Type	Similarity (%)	Expect value	Bit score
33193_RHF15_00488	WP_153940225.1	<i>B. subtilis</i>	Levanase SacC	100.00	0.0	1399
33193_RHF15_02998	WP_106073378.1	<i>B. subtilis</i>	Levanbiose-producing levanase LevB	99.80	0.0	1062
33193_RHF15_02621	WP_072692791.1	<i>B. subtilis</i>	Sucrose-6-phosphate hydrolase ScrB	99.79	0.0	1005

3.3. Response surface design for optimization of PHA production from microbial co-culture

An artificial microbial co-culture able to utilize inulin as a carbon source for PHA production was designed exploiting the RHF15 strain and *C. necator* as inulinase and PHA producers, respectively.

No genes coding for essential proteins in the PHA biosynthesis (PhbA, β -ketothiolase, PhbB, acetoacetyl coenzyme A reductase; and PhbC, Polyhydroxyalkanoate-synthase) were identified in the genome of the RHF15.

A Central Composite Rotary Design (CCRD) was used to explore the effectiveness in PHA production of the co-culture as a function of inulin and NH_4Cl concentrations as well as of the inoculum amount of each strain. The design resulted in 31 experiments (Table 1).

Cell dry weight (CDW g L^{-1}) and PHA content (PHA %) were assumed as the parameters influenced by the four independent variables. Biomass production and PHA accumulation were determined after 96 h. Inulinase activity was also assayed in culture supernatants at the end of the process (Table 1). The experimental results were fitted with a second order polynomial equations:

$$\text{PHA} \% = -10.59 + 53.1^*A + 116.7^*B - 1.03^*C + 0.79^*D + 207^*A^2 - 383.2^*B^2 + 2.12^*C^2 - 0.02^*D^2 + 866^*A^*B - 60.3^*A^*C + 3.04^*A^*D - 28.9^*B^*C - 0.35^*B^*D - 0.03^*C^*D$$

$$\text{CDW g L}^{-1} = -1.234 + 0.69^*A + 11.22^*B - 1.05^*C + 0.09^*D + 3.57^*A^2 - 39.72^*B^2 - 0.38^*C^2 - 0.002^*D^2 + 4.89^*A^*B - 1.14^*A^*C + 0.086^*A^*D + 0.99^*B^*C + 0.06^*B^*D - 0.002^*C^*D$$

being A) *C. necator* inoculum concentration (OD mL^{-1}); B) RHF15 inoculum concentration (OD mL^{-1}); C) NH_4Cl concentration (g L^{-1}); D) inulin concentration (g L^{-1}).

The significance of the models is depicted by F-value of 30.15 and 60.08 for both CDW and PHA, respectively. Analysis of variance (ANOVA) was used to determine the influence and the significance of the independent variables on the dependent responses (Table 3). The significance of model terms is defined by their P values, where only the

terms with a Prob > F lower than 0.05 are considered significant.

In this work, the P value for model terms A, B, D, B^2 , C^2 , D^2 and A, B, C, D, AB, AC, AD, BC, B^2 , C^2 was found to be lower than 0.05, therefore they are significant terms for both CDW production and PHA accumulation, respectively (Table 3). Conversely the model terms C, AB, AC, AD, BC, BD, CD, A^2 and BD, CD, C^2 with a P value higher than 0.05 are not significant for both CDW and PHA, respectively.

The goodness of fit is confirmed by R^2 , that reflects a good co-relation between actual and predicted value. The value of R^2 , adjusted R^2 and predicted R^2 are 0.96, 0.93, 0.76 for CDW production and 0.98, 0.96, 0.89 for PHA accumulation. The difference less than 0.2 between adjusted R^2 and predicted R^2 further validates the model.

Lack of fit-F value of the quadratic model proves the co-relation between response variables and independent factors. The Lack of fit-F value for both CDW production and PHA production is 3.59 and 3.51, respectively. The non-significant value justifies the fitness of the model.

The significance of interactive model terms for PHA production is depicted by contour plot and relative three-dimensional surface plots presented in Fig. 3. 3D graphs displayed the effect of the interaction between RHF15: *C. necator*, NH_4Cl : *C. necator*, NH_4Cl : RHF15 and Inulin: *C. necator* on the dependent variable PHA accumulation. The combined effect of variables was studied keeping the following mid-values: 0.15 OD mL^{-1} inoculum concentration for both bacterial strains, 20 g L^{-1} inulin and 1.7 g L^{-1} NH_4Cl . It is evident from the plot that PHA production reaches a maximum with the increase of the concentration of both bacterial species (Fig. 3, Panel A). Furthermore, for *C. necator* inoculum in the range 0.2–0.3 OD mL^{-1} , PHA production holds at ~70% with NH_4Cl concentration below 1 g L^{-1} (Fig. 3, Panel B). From the interactive plot NH_4Cl : RHF15, it is evident that a positive effect on polymer production is linked to an increase of RHF15 inoculum together with a decrease of NH_4Cl (Fig. 3, Panel C). This phenomenon can be due to the negative effect of NH_4Cl on inulinase production. As a fact, in the co-culture system, high concentration of NH_4Cl seems to negatively affect the production of inulinases (compare runs 14 and 16). Conversely, in the absence of *C. necator*, a higher NH_4Cl amount seems to promote inulinase production (runs 6 and 8) (Table 2). Thus, a major contribution of RHF15 to the co-culture seems to be required to promote

Table 3

Analysis of variance (ANOVA) and regression analysis of quadratic model for the growth optimization (a, Sum of Squares SS; b, Degree of Freedom DF; c, Mean Square, MS; *, significant model terms with a P value lower than 0.05).

Source	ANOVA						Regression Analysis			
	CDW g L^{-1}			PHB %			CDW g L^{-1}		PHB %	
	SS ^a	DF ^b	p Value Prob>F	SS ^a	DF ^b	p Value Prob>F	MS ^c	F Value	MS ^c	F Value
Model	12.8991	14	<0.0001*	10.2645	14	<0.0001*	0.9214	30.15	733.18	60.08
<i>C. necator</i> (A)	0.7506	1	<0.0001*	5274.3	1	<0.0001*	0.7506	24.56	5274.3	432.20
RHF15(B)	0.6856	1	<0.0001*	765.4	1	<0.0001*	0.6856	22.44	765.4	62.72
NH_4Cl (C)	0.0204	1	0.425	618.3	1	<0.0001*	0.0204	0.67	618.3	50.66
Inulin(D)	0.8447	1	<0.0001*	396.6	1	<0.0001*	0.8447	27.65	396.6	30.29
AB	0.0383	1	0.279	1200.0	1	<0.0001*	0.0383	1.25	1200.0	98.33
AC	0.1161	1	0.069	327.6	1	<0.0001*	0.1161	3.80	327.6	26.84
AD	0.1195	1	0.065	148.1	1	0.003	0.1195	3.91	148.1	12.14
BC	0.0889	1	0.107	75.3	1	0.024	0.0889	2.91	75.3	6.17
BD	0.0514	1	0.213	1.9	1	0.697	0.0514	1.68	1.9	0.16
CD	0.0052	1	0.687	0.8	1	0.803	0.0052	0.17	0.8	0.06
A^2	0.0211	1	0.418	70.9	1	0.028	0.0211	0.69	70.9	5.81
B^2	2.6100	1	<0.0001*	242.9	1	<0.0001*	2.6100	85.42	242.9	19.9
C^2	1.0093	1	<0.0001*	31.6	1	0.127	1.0093	33.03	31.6	2.59
D^2	1.2465	1	<0.0001*	72.1	1	0.027	1.2465	40.80	72.1	2.55

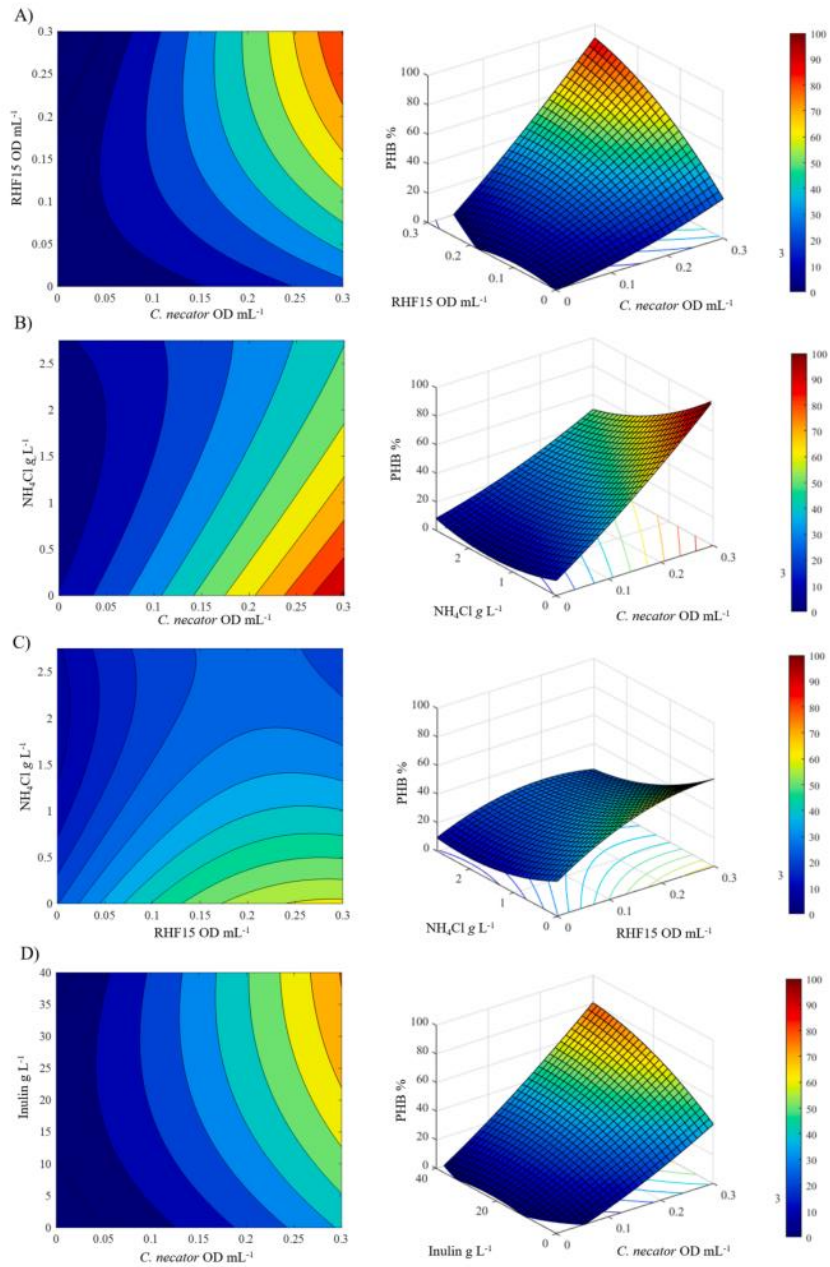


Fig. 3. Contour and 3D surface plots for the significant interactive model terms for PHA production. A) RHF15: *C. necator*; B) NH_4Cl : *C. necator*; C) NH_4Cl : RHF15; D) Inulin: *C. necator*.

PHA accumulation. Interestingly, at the temperature chosen for the microbial consortium (30 °C), RHF15 assured high level of inulinase activity production, comparable with the values obtained in the screening conditions (37 °C).

As for the interactive effect inulin: *C. necator*, their concomitant increase positively affects polymer production, assuring up to 70% PHA content at more than 20 g L⁻¹ inulin together with more than 0.25 OD mL⁻¹ *C. necator* (Fig. 3, Panel D).

To validate the models and define the variable values that allow obtaining up to 2 g L⁻¹ of CDW and up to 80% of PHA accumulation, overlaid contour plots were constructed (Fig. 4). In the plot each set of contours defines the boundaries of acceptable response values. The solid contour line and the dotted one correspond to the lower and the upper bounds respectively, whilst the white portion in the plot represents the acceptable range wherein the possible combination of parameter settings can be obtained. In the case study, two overlaid contour plots were considered: *C. necator*: NH₄Cl and *C. necator*: RHF15.

From the first plot (Fig. 4A) the optimal solutions are defined by 0.1–0.3 OD mL⁻¹ for *C. necator* and a wide range of NH₄Cl concentrations, being RHF15 and inulin at the mid value, 0.15 OD mL⁻¹ and 20 g L⁻¹ respectively). At low concentrations of NH₄Cl, a PHA content higher than 20% can be obtained at low inoculum concentration, whilst when the N-source is increased, it is necessary to increase the inoculum. From the overlaid plot RHF15: *C. necator* (Fig. 4B) it is evident that at low RHF15 inoculum it is necessary to increase the *C. necator* concentration at least to 0.25 OD mL⁻¹ to obtain more than 1 g L⁻¹ CDW together with a minimum of 20% PHA. On the other hand, the increase in RHF15 inoculum allows to reduce the contribution of *C. necator* to be in the acceptable range.

The possible combination settings were used as starting values for the numerical optimization of the models. The inoculum concentration of bacterial strains was set to 0.3 OD mL⁻¹, NH₄Cl was set in the range 1.5–2 g L⁻¹, and a concentration of inulin higher than 20 g L⁻¹ was chosen.

The optimum variable values were 0.3 OD mL⁻¹ for inoculum, 2 g L⁻¹ of NH₄Cl and 30 g L⁻¹ of inulin. The result obtained using predicted response verified the model with a degree of accuracy higher than 95%. In the optimum conditions, up to 2.4 g L⁻¹ of CDW and 75% of PHA production were achieved.

The composition of the polymers produced in all the conditions explored in the CCRD design was determined by GC-MS analysis, and revealed the presence of 3-hydroxybutyrate (3HB) as the only component.

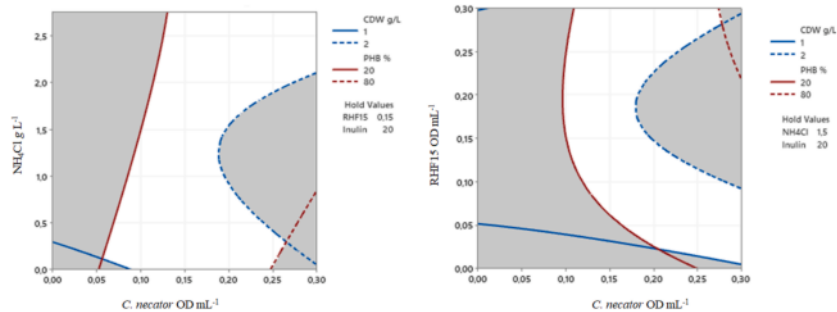


Fig. 4. Overlaid contour plots A) *C. necator*: NH₄Cl; B) *C. necator*: RHF15. The solid contour line and the dotted one correspond to the lower and the upper bounds respectively; the white portion represents the acceptable range (1–2 g L⁻¹ for CDW, 20–80% PHB) wherein the possible combination of parameter settings can be obtained.

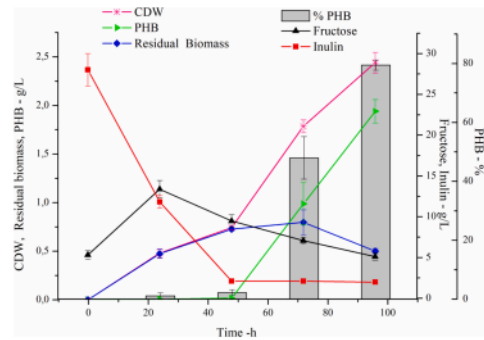


Fig. 5. Inulin conversion into PHA by the artificial microbial consortium. Kinetic profiles of CDW, g L⁻¹; PHB, g L⁻¹; Residual Biomass, g L⁻¹; Fructose, g L⁻¹; Inulin, g L⁻¹ in the optimized conditions for the co-culture.

3.4. Kinetics of polymer production

Fig. 5 displays the kinetics of PHB production in the optimized conditions defined for the artificial microbial consortium. An increase in cell biomass was observed in the earlier phase, whilst polymer synthesis started only after 48 h. From this point onward, the cellular growth slowed down and PHA production sharply increased reaching up to 1.9 g L⁻¹ at 96 h, corresponding to a polymer accumulation ($Y_{P/X}$) of 78.8% and a productivity of 0.02 g L⁻¹ h⁻¹. The efficiency of the mutual species interaction is visible from the profiles of C-sources consumption. Inulin concentration dropped rapidly in the first 24 h and, concomitantly fructose concentration increased, indicating an efficient polysaccharide conversion into fermentable sugars, in accordance with inulinase production in the early growth phase, observed for RHF15 strain. After 48 h, almost all the inulin was consumed, whilst fructose was available at high level (~10 g L⁻¹), thus assuring the carbon source excess necessary for polymer accumulation. At the end of the process, 93% of inulin was converted, with yield coefficients $Y_{P/S} = 0.07$ and $Y_{X/S} = 0.09$. No residual glucose was detected in the culture broth, indicating its consumption by the co-culture. Although glucose is the minority monomer in inulin (about 3 g L⁻¹ estimated from the total hydrolysis of 30 g L⁻¹ inulin), its release promoted the growth of RHF15, being *C. necator* DSM 428 not able to metabolize glucose [42], thus leaving a higher amount of fructose available for PHB production.

Table 4

Comparison of processes for PHA production from inulin-based substrates. SHF (Separated Hydrolysis and Fermentation), SSF (Simultaneous Saccharification and Fermentation).

Process	Substrate	Strain	CDW g L ⁻¹	PHB g L ⁻¹	Y _{P/X} (%)	Productivity, g L ⁻¹ h ⁻¹	Ref.
Microbial co-culture (Shake flasks)	Inulin from chicory roots	<i>C. necator</i> 428 and <i>B. gibsonii</i> RHF15	2.4	1.9	79	0.02	This work
SHF (Shake flasks)	Inulin from Jerusalem artichoke tubers	<i>C. necator</i> 4058	7.7	4	52	0.07	Koutinas, 2013
SHF (Bioreactor)	Inulin from chicory roots	<i>C. necator</i> 428	11.0	7.3	66	0.062	Haas, 2015
		<i>C. necator</i> 531	3.5	1.6	45	0.016	
		<i>C. necator</i> 545	14.0	11.0	78	0.15	
SHF	Inulin from chicory roots	<i>C. necator</i> 428	3.2	2.0	62	0.02	Corrado, 2021
SSF (Shake flasks)		<i>C. necator</i> 428	3.9	3.2	82	0.03	

Finally, the purity of the extracted polymer was checked by ¹H NMR. The spectrum confirmed the presence of the characteristic signals attributable to the homopolymer polyhydroxybutyrate [43] (Fig. S6).

The use of inulin-rich biomass for PHA production has been reported in Separated Hydrolysis and Fermentation (SHF) processes using various fungal inulinase mixtures and different *C. necator* strains (Table 4). In these examples, the PHB volumetric productivities refer only to the fermentation process and do not take into account the overall process time, including also the production of the enzyme and the inulin hydrolysis steps. Recently, the efficiency of a Simultaneous Saccharification and Fermentation (SSF) process for one-step inulin hydrolysis by a *Penicillium lanosoceruleum* inulinase mixture and PHA production by *C. necator* H16 has been demonstrated, with a PHB productivity of 0.03 g L⁻¹ h⁻¹ [21]. Although leading to a slightly reduced productivity if compared to the SSF reported by Corrado et al. (2021), the process with the co-culture is carried out in “one-pot”, allowing to reduce the overall production time by skipping the enzyme production step.

To our knowledge, this is the first example of the use of a “substrate-facilitator” [7] microbial consortium for PHA production from inulin. A similar strategy has been applied by Bhatia et al., (2018b) to a different substrate, saccharose, co-culturing *R. eutropha* 5119 strain with the sucrose hydrolysing *B. subtilis*. Interestingly, in this example, the synthesis of a P(3HB-co-3 HV) copolymer has been reported, thanks to the supplying of the required precursor (propionate) from *B. subtilis* [10]. Despite the similarity of the microbial species involved as well as of the supplied carbon sources, it is worth noting that differences in metabolic profiles of each strain of the consortium, their mutual interactions, together with the applied experimental conditions (concentration of the C and N sources, ratio between the two strains) might translate into substantial variation in polymer composition.

Noteworthy, besides the PHB-containing cells, about 12 U mL⁻¹ of inulinase activity were detected in the supernatant of the co-culture system developed in this work, leading to envisage the possibility to recover these enzymes as extracellular co-products of the process, enhancing its overall cost-competitiveness [2,44,45].

In conclusion, several engineering strategies have been applied for the designing of consolidated bioprocesses involving strains able to convert complex substrates into different microbial products [4,6]. The use of artificial consortia, although still less explored, allows to overcome the need for strain engineering, providing that the compatibility of the consortium members has been verified. The results of this work add a piece of knowledge in this field, providing an optimized process based on an artificial microbial consortium for inulin conversion into PHA.

4. Conclusions

A “substrate facilitator” microbial consortium, composed of the inulin-hydrolysing *B. gibsonii* strain RHF15 and the PHA-producer *C. necator*, was designed to address polymer production from inulin. The RHF15 strain was isolated from the screening of a halophilic microbial collection for its ability to produce inulinase, and its genome

investigated, highlighting its hydrolytic potential.

The co-culture performances were optimized through response surface methodology, achieving a maximum of 1.9 g L⁻¹ of PHB, corresponding to ~80% (g_{polymer}/g_{CDW}) polymer content.

The applied methodology can be extended to other complex carbon sources, exploiting the reservoir of hydrolytic activities discovered in RHF15 genome combined with other PHA producing strains with different substrate preferences.

CRedit authorship contribution statement

Iolanda Corrado: Methodology, Validation, Investigation; **Claudia Petrillo:** Investigation, Formal Analysis; **Rachele Istitico:** Conceptualization, Writing original draft; **Angela Casillo:** Investigation; **Maria Michela Corsaro:** Validation; **Giovanni Sannia:** Funding acquisition, **Cinzia Pezella:** Conceptualization, Writing original draft, Writing - Review & Editing, Supervision.

Acknowledgments

This work was supported by grants from PRIN: PROGETTI DI RICERCA DI RILEVANTE INTERESSE NAZIONALE – Bando 2017. “CARDoon valorisation by InTeGrated biorefinery (CARDIGAN)” (COD. 2017KBTK93). Iolanda Corrado acknowledges Università degli Studi di Napoli Federico II for doctoral fellowships.

Appendix A. Supplementary data

Supplementary data to this article can be found online at <https://doi.org/10.1016/j.ijbiomac.2021.08.123>.

References

- [1] D. Tan, Y. Wang, Y. Tong, G.Q. Chen, Grand challenges for industrializing polyhydroxyalkanoates (PHAs), Trends Biotechnol. 1–11 (2021), <https://doi.org/10.1016/j.tibtech.2020.11.010>.
- [2] R. Turco, G. Santagata, I. Corrado, et al., In vivo and post-synthesis strategies to enhance the properties of PHB-based materials: a review, Front. Bioeng. Biotechnol. 8 (2021), <https://doi.org/10.3389/fbioe.2020.619266>.
- [3] F.A. El-malek, H. Khairy, A. Farag, S. Omar, The sustainability of microbial bioplastics, production and applications, Int. J. Biol. Macromol. 157 (2020) 319–328, <https://doi.org/10.1016/j.ijbiomac.2020.04.076>.
- [4] R. Sirohi, J. Prakash Pandey, V. Kumar Gaur, et al., Critical overview of biomass feedstocks as sustainable substrates for the production of polyhydroxybutyrate (PHB), Bioresour. Technol. 311 (2020), 123536, <https://doi.org/10.1016/j.biortech.2020.123536>.
- [5] D. Bustamante, S. Segarra, M. Tortajada, et al., In silico prospection of microorganisms to produce polyhydroxyalkanoate from whey: *calobacter segnis* DSM 29236 as a suitable industrial strain, Microb. Biotechnol. 12 (2019) 487–501, <https://doi.org/10.1111/1751-7915.13371>.
- [6] L. Favaro, M. Basaglia, S. Casella, Improving polyhydroxyalkanoate production from inexpensive carbon sources by genetic approaches: a review, Biofuels Bioprod. Biorefin. 13 (2019) 208–227, <https://doi.org/10.1002/bbb.1944>.
- [7] S.K. Bhatia, R.K. Bhatia, Y.K. Choi, et al., Biotechnological potential of microbial consortia and future perspectives, Crit. Rev. Biotechnol. 38 (2018) 1209–1229, <https://doi.org/10.1080/07388551.2018.1471445>.

- [8] M. Diender, I. Parera Olm, D.Z. Sousa, Synthetic co-cultures: novel avenues for bio-based processes, *Curr. Opin. Biotechnol.* 67 (2021) 72–79, <https://doi.org/10.1016/j.copbio.2021.01.006>.
- [9] M. Ai, Y. Zhu, X. Jia, Recent advances in constructing artificial microbial consortia for the production of medium-chain-length polyhydroxyalkanoates, *World J. Microbiol. Biotechnol.* 37 (2021) 1–14, <https://doi.org/10.1007/s11274-020-02986-0>.
- [10] S.K. Bhatia, J.J. Yoon, H.J. Kim, et al., Engineering of artificial microbial consortia of *Ralstonia eutropha* and *Bacillus subtilis* for poly(3-hydroxybutyrate-co-3-hydroxyvalerate) copolymer production from sugarcane sugar without precursor feeding, *Bioresour. Technol.* 257 (2018) 92–101, <https://doi.org/10.1016/j.biortech.2018.02.056>.
- [11] P.R. Rodrigues, D.J. Assis, J.L. Druzian, Simultaneous production of polyhydroxyalkanoate and xanthan gum: from axenic to mixed cultivation, *Bioresour. Technol.* 283 (2019) 332–339, <https://doi.org/10.1016/j.biortech.2019.03.095>.
- [12] S.S. Sawant, B.K. Salunke, L.E. Taylor, B.S. Kim, Enhanced agarose and xylan degradation for production of polyhydroxyalkanoates by co-culture of marine bacterium, *Saccharophagus degradans* and its contaminant, *Bacillus Cereus*, *Appl. Sci.* 7 (2017), <https://doi.org/10.3390/app7030225>.
- [13] Y. Liu, S. Yang, X. Jia, Construction of a “nutrition supply–detoxification” coculture consortium for medium-chain-length polyhydroxyalkanoate production with a glucose–xylose mixture, *J. Ind. Microbiol. Biotechnol.* 47 (2020) 343–354, <https://doi.org/10.1007/s10295-020-02267-7>.
- [14] S.R. Hughes, N. Qureshi, J.C. López-Núñez, et al., Utilization of inulin-containing waste in industrial fermentations to produce biofuels and bio-based chemicals, *World J. Microbiol. Biotechnol.* 33 (2017) 1–15, <https://doi.org/10.1007/s11274-017-2241-6>.
- [15] O.K.K. Bedzo, M. Mandegari, J.F. Görgens, Techno-economic analysis of inulinoligosaccharides, protein, and biofuel co-production from Jerusalem artichoke tubers: a biorefinery approach, *Biofuels Bioprod. Biorefin.* 14 (2020) 776–793, <https://doi.org/10.1002/bbb.2105>.
- [16] H.Y. Choi, H.K. Ryu, K.M. Park, et al., Direct lactic acid fermentation of Jerusalem artichoke tuber extract using *Lactobacillus paracasei* without acidic or enzymatic inulin hydrolysis, *Bioresour. Technol.* 114 (2012) 745–747, <https://doi.org/10.1016/j.biortech.2012.03.075>.
- [17] M.M. Khatun, C.G. Liu, X.Q. Zhao, et al., Consolidated ethanol production from Jerusalem artichoke tubers at elevated temperature by *Saccharomyces cerevisiae* engineered with inulinase expression through cell surface display, *J. Ind. Microbiol. Biotechnol.* 44 (2017) 295–301, <https://doi.org/10.1007/s10295-016-1881-0>.
- [18] Y. Qiu, Y. Zhang, Y. Zhu, et al., Improving poly-(γ -glutamic acid) production from a glutamic acid-independent strain from inulin substrate by consolidated bioprocessing, *Bioprocess Biosyst. Eng.* 42 (2019) 1711–1720, <https://doi.org/10.1007/s00449-019-02167-w>.
- [19] A.A. Koutinas, L.L. Garcia, N. Kopsahelis, et al., Production of fermentation feedstock from Jerusalem artichoke tubers and its potential for polyhydroxybutyrate synthesis, *Waste Biomass Valoriz.* 4 (2013) 359–370, <https://doi.org/10.1007/s12649-012-9154-2>.
- [20] C. Haas, V. Steinwandter, E.D. De Apodaca, et al., Production of PHB from chicory roots - comparison of three cupriavidus necator strains, *Chem. Biochem. Eng. Q.* 29 (2015) 99–112, <https://doi.org/10.1525/CABEQ.2014.2250>.
- [21] I. Corrado, N. Cascelli, G. Ntasi, et al., Optimization of inulin hydrolysis by *penicillium lanosocoeruleum* inulinases and efficient conversion into polyhydroxyalkanoates, *Front. Bioeng. Biotechnol.* 9 (2021) 1–17, <https://doi.org/10.3389/fbioe.2021.616908>.
- [22] M.de L. Moreno, D. Pérez, M.T. García, E. Mellado, Halophilic bacteria as a source of novel hydrolytic enzymes, *Life* 3 (2013) 38–51, <https://doi.org/10.3390/life3010038>.
- [23] C.F. Budde, S.L. Riedel, F. Hübner, et al., Growth and polyhydroxybutyrate production by *Ralstonia eutropha* in emulsified plant oil medium, *Appl. Microbiol. Biotechnol.* 89 (2011) 1611–1619, <https://doi.org/10.1007/s00253-011-3102-0>.
- [24] C. Pettilo, S. Castaldi, M. Seki, D. Giovannelli, R. Istitico, Genomic Mining of Halophilic Bacilli Exhibiting Promising Plant Growth-Promoting and Biocontrol Potentials, 2021, <https://doi.org/10.1101/2021.05.17.444429> bioRxiv.
- [25] R.K. Aziz, D. Bartek, A.A. Best, et al., The RAST server: rapid annotations using subsystems technology, *BMC Genomics* 9 (2008) 75, <https://doi.org/10.1186/1471-2164-9-75>.
- [26] R. Overbeek, R. Olson, G.D. Pusch, et al., The SEED and the rapid annotation of microbial genomes using subsystems technology (RAST), *Nucleic Acids Res.* 42 (2014) D206–D214, <https://doi.org/10.1093/nar/gkt11226>.
- [27] P. Stothard, D.S. Wishart, Circular genome visualization and exploration using CGView, *Bioinformatics* 21 (2004) 537–539, <https://doi.org/10.1093/bioinformatics/btd054>.
- [28] M. Vastano, A. Casillo, M.M. Conaro, et al., Production of medium chain length polyhydroxyalkanoates from waste oils by recombinant *Escherichia coli*, *Eng. Life Sci.* 15 (2015), <https://doi.org/10.1002/elsc.201500022>.
- [29] S. Castaldi, C. Pettilo, G. Donadio, et al., Plant growth promotion function of *Bacillus* sp. strains isolated from salt-pan rhizosphere and their biocontrol potential against *Macrophomina phaseolina*, *Int. J. Mol. Sci.* 22 (2021), <https://doi.org/10.3390/ijms22073324>.
- [30] D.J. Kushner, *Microbial Life in Extreme Environments*, 1978.
- [31] R.S. Singh, K. Chauhan, J.F. Kennedy, A panorama of bacterial inulinases: production, purification, characterization and industrial applications, *Int. J. Biol. Macromol.* 96 (2017) 312–322, <https://doi.org/10.1016/j.jbiomac.2016.12.004>.
- [32] R.S. Singh, R.P. Singh, Production of fructooligosaccharides from inulin by endoinulinases and their prebiotic potential, *Food Technol. Biotechnol.* 48 (2010) 435–450.
- [33] R. Barrangou, E. Altermann, R. Hutkins, et al., Functional and comparative genomic analyses of an operon involved in fructooligosaccharide utilization by *Lactobacillus acidophilus*, *Proc. Natl. Acad. Sci.* 100 (2003) 8957–8962, <https://doi.org/10.1073/pnas.1332765100>.
- [34] M. Gouy, S. Guindon, O. Gascuel, SeaView version 4: a multiplatform graphical user interface for sequence alignment and phylogenetic tree building, *Mol. Biol. Evol.* 27 (2009) 221–224, <https://doi.org/10.1093/molbev/msp259>.
- [35] W. Lammens, K. Le Roy, L. Schroeven, et al., Structural insights into glycoside hydrolase family 32 and 68 enzymes: functional implications, *J. Exp. Bot.* 60 (2009) 727–740, <https://doi.org/10.1093/jxb/er333>.
- [36] V.A. Reddy, F. Maley, Identification of an active-site residue in yeast invertase by affinity labeling and site-directed mutagenesis, *J. Biol. Chem.* 265 (1990) 10817–10820.
- [37] T. Pons, D.G. Naumoff, C. Martínez-Fleites, L. Hernández, Three acidic residues are at the active site of a beta-propeller architecture in glycoside hydrolase families 32, 43, 62, and 68, *Proteins* 54 (2004) 424–432, <https://doi.org/10.1002/prot.10604>.
- [38] I. Martin, M. Debarbouille, A. Klier, G. Rapoport, Induction and metabolic regulation of levansucrase synthesis in *Bacillus subtilis*, *J. Bacteriol.* 171 (1989) 1885–1892, <https://doi.org/10.1128/jb.171.4.1885-1892.1989>.
- [39] S.L. Jensen, M.B. Diemer, M. Lundmark, et al., Levansucrose from *Bacillus subtilis* hydrolyses β -2,6 fucosyl bonds in bacterial levans and in grass fructans, *Int. J. Biol. Macromol.* 85 (2016) 514–521, <https://doi.org/10.1016/j.jbiomac.2016.01.008>.
- [40] J.D. Bendtsen, H. Nielsen, G. von Heijne, S. Brunak, Improved prediction of signal peptides: SignalP 3.0, *J. Mol. Biol.* 340 (2004) 783–795, <https://doi.org/10.1016/j.jmb.2004.05.028>.
- [41] H. Tjalsma, A. Bolhuis, J.D. Jongbloed, et al., Signal peptide-dependent protein transport in *Bacillus subtilis*: a genome-based survey of the secretome, *Microbiol. Mol. Biol. Rev.* 64 (2000) 515–547, <https://doi.org/10.1128/mmlr.64.3.515-547.2000>.
- [42] C. Azubuike, M. Edwards, A. Gatehouse, T.P. Howard, Data Driven Modelling of a Chemically Defined Growth Medium for *Cupriavidus necator* H16, 2019, <https://doi.org/10.1101/548891> bioRxiv 548891.
- [43] D. Sabarinathan, S.P. Chandrika, P. Venkatraman, et al., Production of polyhydroxybutyrate (PHB) from pseudomonas plecoglossicida and its application towards cancer detection, *Inf. Med. Unlocked* 11 (2018) 61–67, <https://doi.org/10.1016/j.imu.2018.04.009>.
- [44] P. Kumar, B.S. Kim, Valorization of polyhydroxyalkanoates production process by co-synthesis of value-added products, *Bioresour. Technol.* 269 (2018) 544–556, <https://doi.org/10.1016/j.biortech.2018.08.120>.
- [45] Assis D. de Jesus, J. Santos, C.S. de Jesus, et al., Valorization of crude glycerol based on biological processes for accumulation of lipophilic compounds, *Int. J. Biol. Macromol.* 129 (2019) 728–736, <https://doi.org/10.1016/j.jbiomac.2019.02.077>.

GENERAL CONCLUSIONS

CHAPTER IX

The employment of plant-beneficial soil microorganisms known as PGPB to the agricultural field, is receiving increasing attention for their biotechnological potential as alternatives to chemicals. Among soil microorganisms, spore-forming bacteria such as *Bacillus* and *Myxococcus*, are catching researchers' interest. Due to their low-cost production, easy manipulation, safety, and high resistance to harsh conditions, spore-forming bacteria present undoubted advantages in the development of new eco-friendly fertilizers and pesticides formulations.

In this framework, our findings highlighted the value of the extreme environments such as salt-pans, as remarkable reservoirs of biotechnological potential, since hosting microorganisms with unique characteristics. Interestingly, the influence of the saline environment on the studied species, put in evidence how the surrounding habitat plays a significant role in the bacterial phenotypic plasticity, which can be exploited to select even more suitable extreme PGPB candidates, able to endure harsh conditions like high salinity, temperature, and drought, to be exploited individually or in consortia. In these extreme ecosystems, microorganisms have developed many strategies to cope with such harsh conditions, such as the production of bioactive compounds potentially valuable for biotechnological applications, for instance, antimicrobial molecules or highly efficient hydrolytic enzymes with multiple applications, from the formulation of sustainable pesticides to the production of value-added products like Polyhydroxyalkanoates (PHA) in the circular-economy sector. Finally, this Thesis proposes an advanced method to exploit spore-forming PGPB as efficient matrixes to expose bioactive molecules (functionalized-PGPB), which are often unstable or easily degraded when in the agricultural environment. It has been demonstrated that *Bacillus*' spore structure is actively shaped by the temperature of sporulation, thus affecting the heterologous molecules' display efficiency on its surface. These results suggest it is possible to take advantage of the influence of the environmental conditions on the bacterial spores' phenotype, to create an even more effective system, customizable in accordance with the features of the application soil.

In conclusion, the results obtained widely confirmed the use of spore-forming PGPB as an efficient eco-friendly alternative to agrochemicals and shed a light on the development of a “2.0 functionalized-PGPB”, as an innovative matrix to deliver agro-industrial enzymes for the promotion and protection of crops.

APPENDICES

APPENDIX I

LIST OF PUBLICATIONS

- P1)** Isticato R, Lanzilli M, **Petrillo C**, Donadio G, Baccigalupi L, Ricca E. *Bacillus subtilis builds structurally and functionally different spores in response to the temperature of growth*. 2020, Environ Microbiol, Vol. 22: 170-182. <https://doi.org/10.1111/1462-2920.14835>
- P2)** **Petrillo C**, Castaldi S, Lanzilli M, Saggese A, Donadio G, Baccigalupi L, Ricca E, Isticato R. *The temperature of growth and sporulation modulates the efficiency of spore-display in Bacillus subtilis*. 2020, Microb Cell Fact, Vol. 19: 185. <https://doi.org/10.1186/s12934-020-01446-6>.
- P3)** Castaldi S, **Petrillo C**, Donadio G, Dal Piaz F, Cimmino A, Masi M, Evidente A, Isticato R. *Plant Growth Promotion Function of Bacillus sp. Strains Isolated from Salt-Pan Rhizosphere and Their Biocontrol Potential against Macrophomina phaseolina*. 2021, Int J Mol Sci, Vol. 22: 3324. <https://doi.org/10.3390/ijms22073324>.
- P4)** **Petrillo C**¹, Castaldi S¹, Lanzilli M, Selci M, Cordone A, Giovannelli D, Isticato R. *Genomic and Physiological Characterization of Bacilli Isolated From Salt-Pans With Plant Growth Promoting Features*. 2021, Front Microbiol, Vol. 12: 715678. <https://doi.org/10.3389/fmicb.2021.715678>.
- P5)** **Petrillo C**¹, Corrado I¹, Isticato R, Casillo A, Corsaro MM, Sannia G, Pezzella C. *The power of two: An artificial microbial consortium for the conversion of inulin into Polyhydroxyalkanoates*. 2021, Int J Biol Macromol, Vol. 189: 494-502. <https://doi.org/10.1016/j.ijbiomac.2021.08.123>.
- P6)** Di Gregorio Barletta G¹, Vittoria M¹, Lanzilli M, **Petrillo C**, Ricca E, Isticato R. *CotG controls spore surface formation in response to the temperature of growth in Bacillus subtilis*. DOI: 10.1111/1462-2920.15960. Accepted 25 Feb 2022 - Environmental Microbiology.

¹ First authorship.

❖ AUTHORS' CONTRIBUTIONS

- *Bacillus subtilis* builds structurally and functionally different spores in response to the temperature of growth.
RI, ER, LB conceived and designed the experiments; ML, **CP**, GD carried out most of the experimental work RI, ER, LB wrote and revised the manuscript. All authors read and approved the final manuscript.
- The temperature of growth and sporulation modulates the efficiency of spore-display in *Bacillus subtilis*.
RI, ER, LB, conceived and designed the experiments; **CP**, SC, carried out most of the experimental work; ML, AS, GD contributed to some of the experiments; RI, ER, LB wrote and revised the manuscript. All authors read and approved the final manuscript.
- Plant Growth Promotion Function of *Bacillus* sp. Strains Isolated from Salt-Pan Rhizosphere and Their Biocontrol Potential against *Macrophomina phaseolina*.
Conceptualization, R.I.; methodology, S.C., **C.P.**, A.C., and G.D.; validation, and formal analysis, S.C. and G.D.; investigation, S.C., M.M. and F.D.P.; data curation, S.C., A.E. and R.I.; writing original draft preparation, R.I., S.C., and **C.P.**; supervision, R.I.; project administration, R.I.; funding acquisition, R.I.
- Genomic and Physiological Characterization of *Bacilli* Isolated From Salt-Pans With Plant Growth Promoting Features.
RI: conceptualization, supervision, project administration, and funding acquisition. SC and **CP**: methodology. SC, **CP**, ML, and MS: validation and formal analysis. SC, **CP**, and DG: investigation. SC, **CP**, MS, AC, and RI: data curation. RI, SC, **CP**, and DG: writing original draft preparation
- The power of two: An artificial microbial consortium for the conversion of inulin into Polyhydroxyalkanoates.
Iolanda Corrado: Methodology, Validation, Investigation; **Claudia Petrillo**: Investigation, Formal Analysis; Rachele Isticato: Conceptualization, writing original draft; Angela Casillo: Investigation; Maria Michela Corsaro: Validation; Giovanni Sannia: Funding

acquisition, Cinzia Pezzella: Conceptualization, Writing original draft, Writing - Review & Editing, Supervision.

❖ SUPPLEMENTAL MATERIAL

- *Bacillus subtilis* builds structurally and functionally different spores in response to the temperature of growth. Additional Supporting Information may be found in the online version of this article at the publisher's web-site.
- Plant Growth Promotion Function of *Bacillus* sp. Strains Isolated from Salt-Pan Rhizosphere and Their Biocontrol Potential against *Macrophomina phaseolina*. Available online at <https://www.mdpi.com/14220067/22/7/3324/s1>.
- Genomic and Physiological Characterization of *Bacilli* Isolated From Salt-Pans With Plant Growth Promoting Features. The Supplementary Material for this article can be found online at: <https://www.frontiersin.org/articles/10.3389/fmicb.2021.715678/full#supplementary-material>.
- The power of two: An artificial microbial consortium for the conversion of inulin into Polyhydroxyalkanoates. Supplementary data to this article can be found online at <https://doi.org/10.1016/j.ijbiomac.2021.08.123>.
- **CHAPTER IV**

Table S1 | Bacterial growth properties.

Strain	Colony colour	Colony morphology	*Anaerobic growth	pH range	Temperature range (°C)	PEG6000 (% range)
RHF6 ¹	Creamy white	Flat	+++	4-10	15-50	0-15
RHFS10 ²	White	Undulate	++	6-12	15-50	0-15
LS132	Milky white	Translucent	++	2-10	25-40	0-15
AGS172	Creamy white	Wrinkled	++	2-10	25-50	0-20
LMG9814	Creamy white	Flat	++	4-10	25-60	0-15
AGS84	Creamy white	Flat	++	2-12	25-60	0-20
AGS108	Creamy white	Flat	++	2-12	25-60	0-20
AGS54	Creamy white	Irregular	+	4-10	4-40	0-15

*Anaerobic growth: +: low growth; ++: moderately growth; +++: high growth. ¹ Petrillo et al., 2021; ² Castaldi et al., 2021.

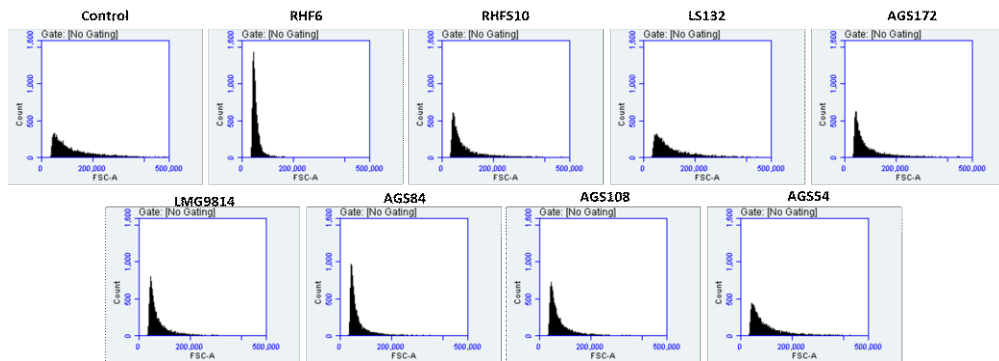


Figure S2 | Adhesion assay. Flow cytometry analysis of *S. oleracea* bioprimered-seeds. Seeds treated with individual bacterial strain were collected randomly to count bacterial cells adhering at their surface. In each panel is indicated the number of cells counted (Y-axis) against their dimension (X-axis). As control experiment 1X PBS-treated seeds were analysed.

APPENDIX II

LIST OF POSTERS

- Lanzilli MM, **Petrillo C**, Baccigalupi L, Ricca E, Isticato R. A heat-labile regulatory protein mediates spore coat formation in *Bacillus subtilis*. GIM2019, Pisa, Italy, 8-11 September 2019.
- **Petrillo C**, Corrado I, Castaldi S, Pezzella C, Isticato R. Identification of natural inulinase producing *Bacilli*, for industrial applications. GIM2019, Pisa, Italy, 8-11 September 2019
- Castaldi S, **Petrillo C**, Valkov VT, Chiurazzi M, Ricca E, Isticato R. Application of Plant Growth Promoting Rhizobacteria (PGPR) for the improvement of agricultural productivity. GIM2019, Pisa, Italy, 8-11 September 2019

❖ LIST OF ORAL PRESENTATIONS

Petrillo C. The temperature of growth modulates the efficiency of the spore-display system in *Bacillus subtilis*. Subtillery 2020, 9 June 2020.

❖ CONGRESSES ORGANIZATION

Member of the organising committee of the II Industrial Biotechnology Congress: BioID&A (Biotechnology Identity and Application) held in Naples on October 28th, 2019.

APPENDIX III

EXPERIENCE IN INDUSTRY AND FOREIGN LABORATORIES

From the 6th of October 2020 to the 6th of April 2021 I worked (in presence and remote working alternation) at Agriges s.r.l., Contrada Selva di sotto – Zona Industriale, 82035 San Salvatore Telesino (BN) – Italia, where I was tutored by Patrizia Ambrosino, PhD.

From the 7th of February to the 8th of May 2020 (in presence and remote working alternation) and from the 5th of July to the 1st of October 2021, I worked at the Laboratoire de Chimie Bactérienne, CNRS, 31 Chemin Joseph Aiguier, 13402 Marseille (France), where I was tutored by Emilia Mauriello, PhD.